

1981

BOUNDARY INTEGRAL METHODS AND FREE SURFACE PROBLEMS.

MINA BADIE. ABD-EL-MALEK

University of Windsor

Follow this and additional works at: <http://scholar.uwindsor.ca/etd>

Recommended Citation

ABD-EL-MALEK, MINA BADIE, "BOUNDARY INTEGRAL METHODS AND FREE SURFACE PROBLEMS." (1981).
Electronic Theses and Dissertations. Paper 1326.

This online database contains the full-text of PhD dissertations and Masters' theses of University of Windsor students from 1954 forward. These documents are made available for personal study and research purposes only, in accordance with the Canadian Copyright Act and the Creative Commons license—CC BY-NC-ND (Attribution, Non-Commercial, No Derivative Works). Under this license, works must always be attributed to the copyright holder (original author), cannot be used for any commercial purposes, and may not be altered. Any other use would require the permission of the copyright holder. Students may inquire about withdrawing their dissertation and/or thesis from this database. For additional inquiries, please contact the repository administrator via email (scholarship@uwindsor.ca) or by telephone at 519-253-3000ext. 3208.



National Library of Canada
Collections Development Branch

Canadian Theses on
Microfiche Service

Bibliothèque nationale du Canada
Direction du développement des collections

Service des thèses canadiennes
sur microfiche

NOTICE

The quality of this microfiche is heavily dependent upon the quality of the original thesis submitted for microfilming. Every effort has been made to ensure the highest quality of reproduction possible.

If pages are missing, contact the university which granted the degree.

Some pages may have indistinct print especially if the original pages were typed with a poor typewriter ribbon or if the university sent us a poor photocopy.

Previously copyrighted materials (journal articles, published tests, etc.) are not filmed.

Reproduction in full or in part of this film is governed by the Canadian Copyright Act, R.S.C. 1970, c. C-30. Please read the authorization forms which accompany this thesis.

THIS DISSERTATION
HAS BEEN MICROFILMED
EXACTLY AS RECEIVED

AVIS

La qualité de cette microfiche dépend grandement de la qualité de la thèse soumise au microfilmage. Nous avons tout fait pour assurer une qualité supérieure de reproduction.

S'il manque des pages, veuillez communiquer avec l'université qui a conféré le grade.

La qualité d'impression de certaines pages peut laisser à désirer, surtout si les pages originales ont été dactylographiées à l'aide d'un ruban usé ou si l'université nous a fait parvenir une photocopie de mauvaise qualité.

Les documents qui font déjà l'objet d'un droit d'auteur (articles de revue, examens publiés, etc.) ne sont pas microfilmés.

La reproduction, même partielle, de ce microfilm est soumise à la Loi canadienne sur le droit d'auteur, SRC 1970, c. C-30. Veuillez prendre connaissance des formules d'autorisation qui accompagnent cette thèse.

LA THÈSE A ÉTÉ
MICROFILMÉE TELLE QUE
NOUS L'AVONS REÇUE

**BOUNDARY INTEGRAL METHODS
AND FREE SURFACE PROBLEMS**

by



Mina Badie Abd-El-Malek

A Dissertation
Submitted to the Faculty of Graduate Studies
Through the Department of Mathematics in
Partial Fulfillment of the Requirements for
the Degree of Doctor of Philosophy at The
University of Windsor

Windsor, Ontario, Canada
1981

ERRATA

PAGE	LINE	FOR	READ
50	9	$t < 1$	$t > 1$
100 - 113	Heading of Column 3	degrees	radians
115 - 118	Heading of Column 3	degrees	radians

DEDICATION

To the soul of His Holiness the late Pope Kyrillos VI (Cyril VI),
Pope of Alexandria, and Patriarch of the see of St. Mark, the 116th,
for his warm fatherhood.

To the Souls of my beloved parents, whose main objective was
"Better Education" for their children. May their souls rest in peace
in the Paradise of Grace.

To my brothers and sister in Egypt for their continuous moral
support and encouragement.

ABSTRACT

This dissertation is a study of boundary integral methods and free surface problems. An analysis is made for three problems, flow over an uneven bottom, flow from a uniform channel over shelf, and flow from a uniform channel over a sharp-crested weir. All problems studied here include the influence of gravity, under the assumptions that the motion is irrotational, the fluid is incompressible, inviscid, and the flow is two-dimensional and steady. The solutions are obtained by using conformal mapping theory, which maps the fluid region in the normalized complex-potential plane onto an upper half-plane, and Hilbert's technique. Each problem has been programmed and run on a computer, and the computed results plotted and compared with different authors quoted in Chapter I, whenever possible.

ACKNOWLEDGEMENTS

"The God of heaven will make us prosper, and we
his servants will arise and build."

[Nehemiah 2:20]

I would like to take this opportunity to acknowledge my indebtedness to Professor Alexander Cormac Smith for directing this study with great interest and patience. His guidance and constant help broadened my horizons and understanding of mathematics. His contributions to the development of my scholarly career are deeply appreciated. I consider myself privileged and fortunate to have had the opportunity to work with Dr. Smith.

I wish to thank Dr. P.N. Kaloni for his help and personal involvement throughout my graduate studies. Thanks are also due to Dr. O.P. Chandra for his constant encouragement and to Dr. R.M. Barron for his invaluable assistance during my comprehensive examinations.

I am grateful to Dr. J.A. McCorquodale of the Civil Engineering Department who offered invaluable comments and constructive suggestions for the improvement of this work.

I would like to express my thanks to Dr. H.R. Atkinson, Chairman of the Mathematics Department, for his continuous encouragement and his personal interest.

Financial assistance from Dr. Smith's Grant (NSERC A3098), Windsor Scholarship for the University of Windsor, and a Teaching Assistantship from the Department of Mathematics are gratefully acknowledged.

It is with pleasure and gratitude that I acknowledge the help and encouragement of Dr. Yehia H. Kabil, Director of Cultural and Educational Bureau of the Egyptian Embassy in Washington, D.C., and all the members of the Embassy.

Thanks are extended to Mrs. H.M. Bunt, Mrs. A. Rowland and Mrs. V.A. Stein, of the Mathematics Department, for their invaluable help and encouragement.

Special thanks are also extended to the University of Windsor Computer Center for computational resources.

Sincere thanks are due to Mrs. Marion Campeau for her tireless efforts in typing the manuscript and for an excellent job.

TABLE OF CONTENTS

	Page
DEDICATION	(iii)
ABSTRACT	(iv)
ACKNOWLEDGEMENTS	(v)
LIST OF TABLES	(ix)
LIST OF FIGURES	(x)
LIST OF APPENDICES	(xii)
NOMENCLATURE	(xiii)
FLOW-DIAGRAM CONVENTION	(xvi)

CHAPTER

I	INTRODUCTION	1
	1.1 Free Surface Problems	2
	1.2 Open-Channel Flow	2
	1.3 Classification of Flow	3
	1.3.1 Steady Flow and Unsteady Flow	3
	1.3.2 Uniform Flow and Varied Flow	4
	1.4 Examples of Free Surface Problems	4
	1.4.1 Flow Over an Uneven Bottom	4
	1.4.2 Waterfall	6
	1.4.3 Weirs	7
	1.5 Outline of Present Work	9
II	SUMMARY OF PREVIOUS WORK	11
	2.1 Mathematical Foundations	12
	2.2 Mathematical Methods	15
	2.2.1 Hilbert's Method	15
	2.2.2 Perturbation Method	21
	2.2.3 Hodograph Method	23
	2.2.4 Relaxation Method	24

III	FLOW OVER UNEVEN BOTTOM	25
	3.1 Formulation of the Problem	26
	3.2 Solution of the Problem	33
	3.3 Numerical Solution	37
	3.4 Some Mathematical Relations	44
	3.5 Numerical Results and Discussions	45
IV	FLOW FROM UNIFORM CHANNEL OVER SHELF	46
	4.1 Formulation of the Problem	47
	4.2 Solution of the Problem	53
	4.3 Numerical Solution	57
	4.4 Numerical Results and Discussions	64
	4.5 Comparison with Previous Work	65
V	FLOW FROM UNIFORM CHANNEL OVER SHARP-CRESTED WEIR	66
	5.1 Formulation of the Problem	67
	5.2 Solution of the Problem	77
	5.3 Numerical Solution	83
	5.4 Numerical Results and Discussions	92
VI	GENERAL DISCUSSIONS, COMMENTS, AND CONCLUSIONS	93
	6.1 Some Factors Not Considered	93
	6.1.1 Surface Roughness	93
	6.1.2 Effect of Viscosity	94
	6.1.3 Cavitation Phenomena and Flow Separation	95
	6.2 Discussions on the Hilbert Method	96
	6.2.1 Bottom Configuration	96
	6.2.2 Solution Over Unit Disc	97
	6.2.3 Main Features of the Hilbert Method	98
	REFERENCES	215
	VITA AUCTORIS	219

LIST OF TABLES

TABLE		Page
3.1 - 3.4	Shape of Free Surface for a Flow Over an Uneven Bottom, for Different Values of F and α .	100
4.1 - 4.5	Shape of Lower and Upper Nappe for a Flow Over Shelf, for Different Values of F .	104
4.6	Values of C_p on the Shelf for Different Values of F .	114
5.1 - 5.2	Shape of Lower and Upper Nappe for a Flow Over Sharp-Crested Weir, for Different Values of F and α .	115

LIST OF FIGURES

FIGURE		Page
3.1	The physical-plane, Z-plane, for a flow over an uneven bottom.	119
3.2	The complex potential-plane, w-plane, for a flow over an uneven bottom.	120
3.3	The normalized complex potential-plane, w'-plane, for a flow over an uneven bottom.	121
3.4	The upper half-plane, t-plane, for a flow over an uneven bottom.	122
3.5	Relationship between F_1^2 and F_2^2 .	123
3.6 - 3.9	Shape of free surface for a flow over an uneven bottom for different values of F and α .	124
4.1	The physical-plane, Z-plane, for a flow from uniform channel over shelf.	128
4.2	The complex potential-plane, w-plane, for a flow from uniform channel over shelf.	129
4.3	The normalized complex potential-plane, w'-plane, for a flow from uniform channel over shelf.	130
4.4	The upper half-plane, t-plane, for a flow from uniform channel over shelf.	131
4.5 - 4.8	Shape of the lower and upper nappe for different values of F.	132
4.9	Shape of the free surfaces for subcritical, critical, and supercritical approaching flows.	136
4.10	Comparison with experimental data and other results.	137
4.11	Comparison with perturbation method for $F = \sqrt{20}$.	138
4.12	C_p along the flat shelf for different values of Froude number.	139

5.1	The physical-plane, Z-plane, for a flow from uniform channel over sharp-crested weir.	140
5.2	The complex potential-plane, w-plane, for a flow from uniform channel over sharp-crested weir.	141
5.3	The normalized complex potential-plane, w'-plane, for a flow from uniform channel over sharp-crested weir.	142
5.4	The upper half-plane, t-plane, for a flow from uniform channel over sharp-crested weir.	143
5.5	Calculations of the initial profile for the upper and lower nappe for a flow from uniform channel over sharp-crested weir.	144
5.6 - 5.7	Shape of lower and upper nappe for different values of F and α .	145
6.1	Nature of surface roughness.	147
6.2	The physical-plane, Z-plane, for a polygonal bottom.	148

LIST OF APPENDICES

APPENDIX		Page
A	Removing the Singularity from Singular Integral Equations.	150
B	Uniqueness of Schwartz-Christoffel Transformation by Prescribing the Mapping of Three Points on the Boundary of the Upper Half-Plane.	153
C	Proof of the Hilbert Formulae.	157
D	Computer Program for a Flow Over an Uneven Bottom.	163
E	Computer Program for a Flow From Uniform Channel Over Shelf.	178
F	Computer Program for a Flow From Uniform Channel Over Sharp-Crested Weir.	194

NOMENCLATURE

$\arg(Z)$	argument of complex coordinate Z
A_j	constant, power series j th coefficient
C_p	excess pressure coefficient
C	Chézy's constant
F	Froude number
g	gravity
h_0	fluid depth at upstream infinity
h_1	fluid depth at downstream infinity
$H(t)$	solution of the homogenous Hilbert problem in the upper half-plane
$\text{Im}(Z)$	imaginary part of complex coordinate Z
k	roughness height
k_c	critical roughness height
L	length of inclined plane
p	pressure
p_E	pressure at the point E
q	magnitude of velocity
q_1	magnitude of velocity along upper free surface
q_2	magnitude of velocity along lower free surface
$Q(t)$	solution of Hilbert problem in the upper half-plane
R	Reynolds number
$\text{Re}(Z)$	real part of complex coordinate Z

t	auxiliary half plane
t_f	real t -plane coordinate
u	x -component of vector velocity
U_0	fluid speed at upstream infinity
U_1	fluid speed at downstream infinity
$U(t)$	real part of $Q(t)$
v	y -component of vector velocity
$V(t)$	imaginary part of $Q(t)$
W	complex velocity potential
X_1	horizontal coordinate for the upper free surface in the physical plane
X_2	horizontal coordinate for the lower free surface in the physical plane
Y_1	vertical coordinate for the upper free surface in the physical plane
Y_2	vertical coordinate for the lower free surface in the physical plane
$Y_2^{(0)}$	initial value for Y_2
Z	complex coordinate in the physical plane, $= x + iy$

GREEK LETTERS

α	inclination angle
α_f	internal angle in polygon
δ	thickness of boundary layer
δ_0	thickness of laminar sublayer

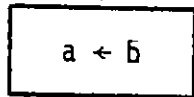
ε	dimensionless parameter used in developing the solution by perturbation method.
ζ	normalized conjugate complex velocity
θ_1	argument of complex velocity along upper free surface
θ_2	argument of complex velocity along lower free surface
μ	viscosity of water
ν	kinematic viscosity
ρ	constant density of fluid
τ	dummy variable
ϕ	velocity potential
ϕ_1, ϕ_2	velocity potential at points 1, 2
ψ	stream function
ψ_0, ψ_1	value of stream function at lower surface and upper surface
ω	$= \log \zeta$

- Note: (i) For non-dimensional variables we use "′" above the variables
(ii) We use the numbering system as follows: for example, TABLE 3.2 refers to Chapter III, and Fig. 5.3 to Chapter V.

Flow-Diagram Convention

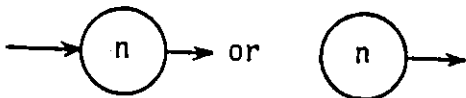
The following boxes, each of characteristic shape, are used for constructing the flow diagrams in this thesis.

Substitution

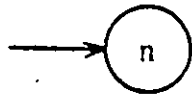


The value of the variable a is replaced by the value of the expression b.

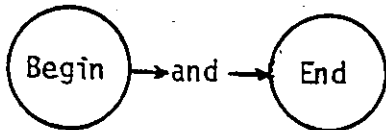
Label



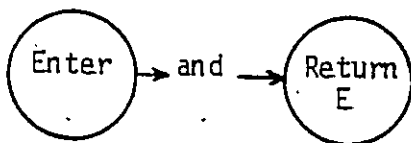
1. When a path leaves from it, the label serves merely as an identification point in the flow diagram; n is usually the same as the statement number in the corresponding program.



2. When a particular branch terminates in a label.

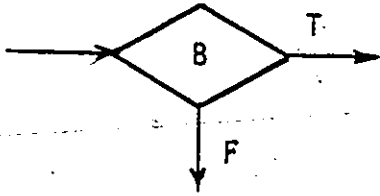


3. These special cases encompass the computations in a main program.



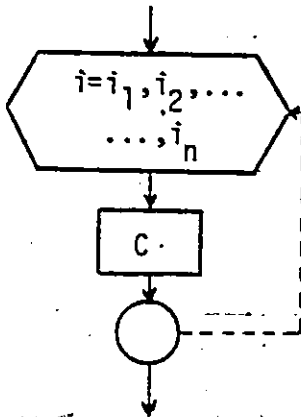
4. Indicate the start and finish of computations in a function. The value of the expression E is returned by the function.

Conditional Branching



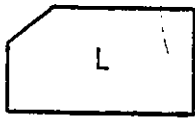
If the Boolean expression B is true, the branch marked T is followed; otherwise, the branch marked F (false) is followed.

Iteration

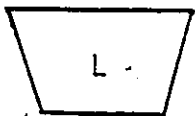


The counter i is incremented uniformly (in steps of $i_2 - i_1$) between its initial and final limits i_1 and i_n respectively. For each such value of i , the sequence of computations C is performed. The dotted line emphasizes the return for the next value of i , and the small circle, which is usually inscribed with the corresponding statement number in the program, serves as a junction box.

Input and Output



The values for the variables comprising the list L are read as input data.



The values for the variables or expressions comprising the list L are printed. A message to be printed is enclosed in quotation marks.

CHAPTER I

INTRODUCTION

- 1.1 Free surface problems.
- 1.2 Open-channel flow.
- 1.3 Classification of flow.
 - 1.3.1 Steady flow and unsteady flow.
 - 1.3.2 Uniform flow and varied flow.
- 1.4 Examples of free surface problems.
 - 1.4.1 Flow over an uneven bottom.
 - 1.4.2 Waterfall.
 - 1.4.3 Weirs.
- 1.5 Outline of present work.

1.1 Free Surface Problems

The problems of free surface theory are concerned with flows of an ideal fluid bounded in part by constant pressure surfaces, usually of unspecified shape. These boundaries are variously called free streamlines, free surfaces, free boundaries, and sometimes streamlines of discontinuity. The unspecified positions of these streamlines make the problem difficult. The principal applications of the free streamline concept are to open channel, jet, cavity and wake phenomena. Comprehensive surveys of the subject appear in Birkhoff and Zarantonello [5], Gilbarg [22], and Milne-Thomson [38]. For more complete bibliography on this subject, the reader should consult Wehausen [55] and Cryer [18].

1.2 Open-Channel Flow

The flow of water in conduit may be either open-channel flow or pipe flow. The two kinds of flow are similar in many ways but differ in one important respect. Open-channel flow must have a free surface, whereas pipe flow has none, since the water must fill the whole conduit. A free surface is subject to atmospheric pressure. Pipe flow, being confined in a closed conduit, exerts no direct atmospheric pressure but hydraulic pressure only.

Despite the similarity between the two kinds of flow, it is much more difficult to solve problems of flow in open-channels than in a pipe. Flow conditions in open channels are complicated by the fact that the position of the free surface is likely to change with respect to

space (for steady motion) and also by the fact that the depth of flow, the discharge, and the slope of the free surface are interdependent.

In pipes the cross-section of flow is fixed, since it is completely defined by the geometry of the conduit. The cross-section of a pipe is generally round, but that of an open-channel may be of any shape, from a circular to the irregular forms of natural streams.

It is important to mention that the flow in a closed conduit is not necessarily pipe flow. It must be classified as open-channel flow if it has a free surface. For more details in this subject we recommend Chow [9], Bakfmeteff [3], and Jaeger [27].

In 1868 Helmholtz first presented a two-dimensional theory of free streamlines. Kirchhoff in 1869, and others, have since elaborated a general method of dealing with such problems. It is believed that major developments in the dynamics of open-channel flow were made largely because of man's interest in the flow of water in open-channels, such as rivers and canals. This belief is evidenced by the fact that open-channel flow has been considered for a long time as an important subject in the field of civil hydraulic engineering.

1.3 Classification of Flow

Open-channel flow can be classified into many types and described in various ways. The following classification is made according to the change in flow depth with respect to time and space.

1.3.1 Steady Flow and Unsteady Flow

Flow in open-channel is said to be steady if the depth of flow does not change or if it can be assumed to be constant during the time

interval under consideration. The flow is unsteady if the depth changes with time. In most open-channel problems of steady flow, the discharge is constant throughout the length of the channel under consideration.

1.3.2 Uniform Flow and Varied Flow

Open-channel flow is said to be uniform if the depth and the cross-sectional area of flow is the same at every section of the channel. Flow is varied if the depth of flow changes along the length of the channel. A uniform and varied flow may be steady or unsteady, depending on whether or not the depth changes with time.

Varied flow may be further classified as either rapidly or gradually varied. The flow is rapidly varied if the depth changes abruptly over a comparatively short distance; otherwise, it is gradually varied.

1.4 Examples of Free Surface Problems

1.4.1 Flow Over an Uneven Bottom

Wien (1900), see Lamb [29, pp. 409], assumed a bottom of the form $y = -h + b_0 \cos kx$; by choosing the origin in the undisturbed surface. He assumed the solution as a linear combination of trigonometric functions. He chose the amplitude of unevenness, of the bottom, small compared with the depth, h , of uniform flow for the linearized theory to be applicable. Finally he found the shape of the free surface by

$$\eta(x) = \frac{kb_0 \cos(kx)}{k \cosh(kh) - \left(\frac{g}{U^2}\right) \sinh(kh)},$$

in which U = the mean stream velocity. An interesting consequence was that the free surface wave and the bed wave are in phase or out of phase if $\frac{U^2}{gh} \cong \tanh(kh)/kh$. However, when $U^2 = \left(\frac{g}{k}\right) \tanh(kh)$ the amplitude ratio of surface to bed waves becomes infinite. Lamb [29] has suggested that viscosity must be included to resolve this singular behaviour. Mei [36] has suggested that by carrying out a higher order analysis the singularity is removed by the nonlinearity of the free surface conditions. The situation is quite analogous to the forced oscillation of a non linear spring-mass system where resonance may occur when the frequency of the forcing agent coincides with the natural frequency of the vibrating system.

For an arbitrary shaped bottom, Wien applied Fourier integral theorem, i.e., for assuming $y = -h+b(x)$, by Fourier integral theorem

$$b(x) = \frac{1}{\pi} \int_0^{\infty} d\xi \int_{-\infty}^{\infty} b(\tau) \cos \xi (x-\tau) d\tau,$$

for the validity of theorem, $b(x)$ should be of bounded variation and absolutely integrable.

Various special cases of $b(x)$ have been considered. Wien assumed $b(x) = \tan^{-1}(ax)$ and took the limit $a \rightarrow \infty$ in order to find the flow over a small step. Lamb [29] replaced the unevenness by a single dipole.

The general theory of steady free surface flow about a submerged obstacle in infinitely deep fluid has been considered by Kochin (1937) for both two and three dimensions. Haskind (1945) has extended Kochin's treatment to fluid of constant finite depth.

1.4.2 Waterfall

The problem of flow from a uniform channel over shelf is such a free surface problem. It is of specific interest in that it has the simplest geometrical configuration yet it possesses the main features of the flow with gravitation. In addition, it is the limiting configuration of a sharp-crested weir which is frequently employed as a measuring device.

During the period known as the Renaissance, a gradual change from the purely philosophical science of the scholastics toward the observational science of the present day at last became perceptible. Leonardo da Vinci (1452-1519) was one of that Renaissance period who investigated that problem experimentally. He also contributed a lot of work in different subjects in the field of mechanics. For more details about his work see Rouse and Ince [43].

In 1936 Rouse carried out an experimental work and finally he concluded that the brink section has a depth of 0.715 of critical depth, y_{cr} . In 1946 Southwell and Vaisey [50] used relaxation method to plot the complete flow pattern, finding in the process a value of brink depth, y_b , of approximately 0.705 y_{cr} . In 1958 Hay and Markland [25] used the electrical analogy to determine an experimental solution in an electrolytic plotting tank. The profile they deduced was very close to Southwell and Vaisey's except near the brink, where they found $y_b = 0.676 y_{cr}$.

Early analytical work on this problem was carried out by ~~St~~Clarke [12] in 1965. Upon employing the thin jet thickness as a small parameter which is inversely proportional to F , see Eq. 2.10, of the approaching

flow, Clarke developed an asymptotic expansion, called an outer expansion, which is valid upstream and near the edge, and another asymptotic expansion, called an inner expansion, which is valid for downstream. A solution was established for the whole field after the two expansions were matched. In 1973 and later in 1979, Keller and Geer [20], [28] solved this problem more generally following the same approach as Clarke. These analyses, Clarke's; Keller and Geer's, provide valid solutions only for large Froude numbers of the approaching flow, and they give a thinner jet and the disagreement becomes worse far downstream.

In 1979, Chow and Han [10] applied a hodograph method and they came out with a good agreement with Rouse's experimental data, especially when the grid size was refined in the numerical calculation of the stream function.

For more detail of discussion of this subject, see Rouse [42], Henderson [26], and four papers of Thomson (Lord Kelvin)[52].

1.4.3 Weirs

A weir is a notch of regular form through which water flows. A weir may be a depression in the side of a tank, reservoir, or channel, or it may be an overflow dam or other similar structure. Classified in accordance with the shape of the notch, there are rectangular weirs; triangular, or V-notch, weirs; trapezoidal weirs; and parabolic weirs. The edge or surface over which the water flows is called the crest of the weir. The overflowing sheet of water is termed the nappe. A weir with a sharp upstream corner, or edge, so formed that the water springs

clear of the crest, is called a sharp-crested weir. The channel of approach is the channel leading up to the weir, and the mean velocity in this channel is the velocity of approach. If the nappe discharges into the air, the weir has free discharge. If the discharge is partially under water, the weir is said to be submerged, or drowned.

Sharp-crested weirs are useful as a means of measuring flowing water. Also the crest shape of a spillway is usually designed to fit the trajectory of a falling nappe over a sharp-crested weir.

In 1954, Blaisdell [6] derived the following empirical formulae for the lower and upper nappe from a critical analysis of a number of experimental data measurements:

For the lower nappe

$$\frac{y}{h_0} = 0.150 - 0.45 \left(\frac{h_a}{h_0}\right) + \left\{ 0.411 - 1.603 \left(\frac{h_a}{h_0}\right) - [1.568 \left(\frac{h_a}{h_0}\right)^2 - 0.892 \left(\frac{h_a}{h_0}\right) + 0.127]^{\frac{1}{2}} \right\} \left(\frac{x}{h_0}\right) + \left\{ -0.425 + 0.25 \left(\frac{h_a}{h_0}\right) \right\} \left(\frac{x}{h_0}\right)^2$$

For the upper nappe

$$\frac{y}{h_0} = 0.150 - 0.45 \left(\frac{h_a}{h_0}\right) + \left\{ 0.411 - 1.603 \left(\frac{h_a}{h_0}\right) - [1.568 \left(\frac{h_a}{h_0}\right)^2 - 0.892 \left(\frac{h_a}{h_0}\right) + 0.127]^{\frac{1}{2}} \right\} \left(\frac{x}{h_0}\right) + \left\{ -0.425 + 0.25 \left(\frac{h_a}{h_0}\right) \right\} \left(\frac{x}{h_0}\right)^2 + 0.57 - \frac{(10m)^2 e^{10m}}{50}$$

in which $h_a = \frac{U^2}{2g}$, $h_0 = h_a + h$, $m = \frac{h_a}{h_0} - 0.208$, e is the base of natural logarithms, and the other notation is as illustrated in the nomenclature. Blaisdell claimed that the equations are valid for $\frac{x}{h_0} > .50$ over the subcritical velocity range of flow.

In 1958, Hay and Markland [25] carried out experimental work for an ideal fluid over vertical sharp-crested weirs using an electrolytic tank. The shapes of the upper and lower nappes, have been obtained for weir heights in the range $0 \leq \frac{h}{L} \leq 1$, where h denotes the head on the weir and L the height of the weir above the bed of the approach channel. They found that the shapes of the nappes correspond closely to experimental results for the case of the infinitely deep weir, but as $\frac{h}{L}$ increases towards unity, experimental results diverge from the ideal solution.

Early analytical work on this kind of problem was carried out by Clarke [13] in 1966. He developed an asymptotic expansion in terms of a small parameter which is proportional to the Froude number. Thus Clarke's analysis provides valid solutions only for small Froude numbers of the approaching flow, and his results show the jet to be thinner than in reality.

For more details of discussion on this subject, see Rouse [42], Chow [9], Brater and King [7], Ginzburg [23], and Henderson [26].

1.5 Outline of Present Work

In Chapter II, we present four mathematical methods used for the solution of free surface problems, namely; Hilbert's method, Perturbation

method, hodograph method, and relaxation method with special attention to Hilbert's method; the method considered in the present work.

In Chapter III, we study the problem of flow over an uneven bottom. In Chapter IV, we solve the problem of flow from uniform channel over a shelf which is known as waterfall problem. In Chapter V, we investigate the problem of flow from uniform channel over a sharp-crested weir. In Chapter VI, we present general discussions, comments and conclusions.

All problems considered here are subject to the influence of gravity. Each problem has been programmed and run on computer, IBM 3031 at the University of Windsor, and the computed results plotted and compared with those of authors quoted in that introduction, wherever possible.

CHAPTER II

SUMMARY OF PREVIOUS WORK

2.1 Mathematical Foundations

2.2 Mathematical Methods

2.2.1 Hilbert's Method

2.2.2 Perturbation Method

2.2.3 Hodograph Method

2.2.4 Relaxation Method

2.1 Mathematical Foundations

We consider steady, two-dimensional, irrotational flow of an inviscid, incompressible fluid; for example, the flow over an uneven bottom.

Under the assumption of irrotationality, the flow of incompressible fluids governed by Laplace's equation for the velocity potential ϕ ,

$$\nabla^2 \phi = \frac{\partial^2 \phi}{\partial x^2} + \frac{\partial^2 \phi}{\partial y^2} = 0. \quad (2.1)$$

The potential and stream function of a plane flow together determine the complex potential, $W = \phi + i\psi$, which is an analytic function of $Z = x + iy$ within the region of flow and has the important property that its derivative,

$$\frac{dW(Z)}{dZ} = u(x,y) - iv(x,y) = q e^{-i\theta}, \quad (2.2)$$

is the complex conjugate of the velocity, where q is the flow speed, θ is the inclination of the velocity vector, and u, v are the x, y velocity components. The velocity components of plane flow are given by

$$\left. \begin{aligned} u &= \frac{\partial \phi}{\partial x} = \frac{\partial \psi}{\partial y} \\ v &= \frac{\partial \phi}{\partial y} = -\frac{\partial \psi}{\partial x} \end{aligned} \right\} \quad (2.3)$$

Boundary Conditions: In the boundary value problems under consideration

the flow boundaries will be either rigid, in which case they are known data of the problem, or they will be free boundaries (free streamlines), in which case their shape is unknown beforehand.

On rigid boundaries it is assumed that the motion is tangential to the surface. For steady motion this implies that the normal component of the fluid velocity is zero, or equivalently, that

$$\psi = \text{constant},$$

$$\frac{\partial \phi}{\partial n} = 0,$$

(2.4)

on the boundary.

On the free boundaries, two conditions must be satisfied which are presumably sufficient, in conjunction with the other data, to balance the incomplete knowledge of the boundary and to determine all unknowns of the flow problem. The first condition, kinematic in nature, states that the free boundary is a material surface; particles initially on the surface remain thereon. If the surface is described by the equation $S(x,y,t) = \text{constant}$ (where S might be the pressure, for example), then the velocity vector $\underline{v} = (u,v)$ and the shape are connected by the relation

$$\frac{\partial S}{\partial t} + \underline{v} \cdot \text{grad } S = 0. \quad (2.5)$$

For steady flows ($\frac{\partial S}{\partial t} = 0$) this implies that the free boundary is a stream surface, so that this boundary condition reduces again to (2.4).

The second boundary condition, which really characterizes the

free boundary problem, states that pressure is constant on the free surface. Bernoulli's equation allows this condition to be converted into one containing only the kinematic quantities. Thus, in steady motion under the influence of gravity, Bernoulli's equation states that

$$\frac{p}{\rho} + \frac{1}{2} q^2 + gy = \text{constant}, \quad (2.6)$$

throughout the fluid, where p is the pressure, ρ is the fluid density, $q (= |\mathbf{V}|)$ is the speed of the fluid, y is the vertical distance between a point on the free surface and some reference elevation, and g is the acceleration due to gravity. This would be the free surface condition.

We then map the fluid region in the physical plane onto a rectangle in the complex potential plane, the W -plane, such that the two horizontal sides correspond to $\psi = 0$ and $\psi = \psi_1 = \text{constant}$, and the two vertical sides correspond to $\phi = \phi_1$ and $\phi = \phi_2$, where ϕ_1 and ϕ_2 are constants. Bernoulli's equation (2.6) along the free surface, which lies either on $\psi = 0$ or $\psi = \psi_1$, with density $\rho = 1$, will lead to

$$q^2 + 2gy = U_1^2 + 2gh_1 = \text{constant}, \quad (2.7)$$

where U_1 is the speed at a point on the free surface at which $y = h_1$.

We introduce dimensionless variables

$$\left. \begin{aligned} y' &= \frac{y}{h_1} \\ q' &= \frac{q}{U_1} \\ W' &= \frac{W}{\psi_1} \end{aligned} \right\} \quad (2.8)$$

where $\psi_1 = h_1 U_1$. Dividing (2.7) by U_1^2 , using (2.8) and rearranging the equation we get

$$q^{-2} + \frac{2}{F^2} (y - 1) = 1, \quad (2.9)$$

where $F = \sqrt{\frac{U_1^2}{gh_1}}$, and is called the Froude number.

2.2 Mathematical Methods

In this section we summarize the principal mathematical methods involved in solving free surface problems, with special attention to Hilbert's method; the method considered in the present work.

2.2.1 Hilbert's Method

The flows considered are assumed to be inviscid, irrotational, two-dimensional, incompressible, and steady. For example, a flow over an uneven bottom subject to the influence of gravity, see Fig. 3.1.

Suppose that the stream line ABCD, $\psi = 0$ consists of two horizontal lines AB and CD and inclined line BC at an inclination angle α , and the free stream line FE, $\psi_1 = h_1 U_1$, where A is an upstream infinity and D a downstream infinity.

For convenience, we choose the origin at B, the x-axis from left to right, and y-axis upwards.

Suppose U_1 , h_1 are the speed and depth at point A respectively. We define the Froude number

$$F = \sqrt{\frac{U_1^2}{gh_1}} \quad (2.10)$$

Applying Bernoulli's equation (2.6) between points A and any other point on the downstream free surface, then results in

$$\frac{1}{2} \rho q^2 + \rho g y = \frac{1}{2} \rho U_1^2 + \rho g h_1 \quad (2.11)$$

Dividing by $\frac{1}{2} \rho U_1^2$, using the dimensionless variables in (2.8) and rearranging (2.11), we get

$$q' = \left[1 - \frac{2}{F^2} (y' - 1) \right]^{\frac{1}{2}} \quad (2.12)$$

This equation is the free surface condition in dimensionless variables.

Let $Z = x + iy$ and $W = \phi + i\psi$, then

$$\frac{dW}{dZ} = u - iv = q e^{-i\theta}$$

Now, using the dimensionless variables in (2.8), then

$$\zeta = \frac{dW'}{dZ'} = \frac{h_1}{\psi_1} \frac{dW}{dZ} = \frac{q}{U_1} e^{-i\theta} = q' e^{-i\theta} \quad (2.13)$$

Define

$$\omega = \log \zeta = \log q' + i(-\theta). \quad (2.14)$$

Equation (2.13) is the normalized conjugate complex velocity, and the ζ -plane is called the hodograph plane.

The objective of the analysis is to locate the free surface of the flow in the Z -plane (physical plane) with reasonable accuracy and to locate the pressure and velocity at any point on the boundary of the flow. Rearrangement, integration of (2.13), and use of (2.14), lead to

$$Z' = \int dZ' = \int \frac{dW'}{\zeta} = \int e^{-\omega} dW' . \quad (2.15)$$

Clearly, the integration cannot be performed until the unknowns $W'(Z')$ and $\zeta(Z')$ or $\omega(Z')$ are determined. To determine the explicit form for W' and ζ , the physical plane is first mapped onto the complex potential plane, W -plane, which can be normalized to W' -plane; and hence onto another convenient plane, upper half-plane, called the t -plane. Then Z can be expressed as a function of t and the integration of (2.15) can be carried out.

Mapping the Physical Plane to the t -plane

The analytic function W' is assumed to be a single-valued function of Z' . It is known from the Riemann mapping theorem, see Nehari [40], that there is always a mapping function which will map conformally any simply connected domain with more than one boundary point onto another simply connected domain. If W' is considered as continuous on the boundary, the uniqueness of the mapping function may be assured by prescribing the mapping of three points on the boundary of the Z' -plane onto three properly corresponding points on the W' -plane, see Appendix [B]. It follows that $Z' = F(W')$, where $F(W')$ is a single-valued function of W' , establishing a one-to-one correspondence between points in the Z' - and W' -planes.

A similar argument shows that the W' -plane can be mapped onto the upper half-plane, t -plane, by a single-valued mapping function. Hence $W' = G(t)$, where $G(t)$ is a single-valued function of t .

Since $Z' = F(W')$ and $W' = G(t)$, $Z' = F[G(t)]$. If $F[G(t)]$ is denoted by $f(t)$, the mapping function $Z' = f(t)$ establishes a one-to-one correspondence between the Z' -plane and the t -plane.

The Function $W'(t)$. The W' -, W' -planes as well as the t -plane, are shown in Fig. 3.2, Fig. 3.3, and Fig. 3.4 respectively. The W' -plane is mapped onto the upper half-plane, t -plane by a mapping function derived from the Schwarz-Christoffel transformation, see Churchill [11].

In general, the Schwarz-Christoffel transformation is of the form,

$$\frac{dW'(t)}{dt} = A \prod_i (t-t_i)^{\frac{\alpha_i}{\pi} - 1}, \quad (2.16)$$

where t_i is the t -plane coordinate related to a vertex of the polygon (the infinite strip of width unity in W' -plane may be considered as a polygon with two vertices at infinity), and α_i the corresponding internal angle in the W' -plane; A is a constant.

The conformal mapping (2.16) maps the W' -plane onto the t -plane in such a manner that the fluid region in the W' -plane corresponds to the upper half, $\text{Im}(t) > 0$ of the t -plane, and the boundary of the fluid region to the real axis, $\text{Im}(t) = 0$ of the t -plane.

Now, it is clear that the argument of the normalized conjugate complex velocity is known along the fixed boundaries, while its magnitude is known along the free surface. Then, applying the Hilbert solution to a mixed boundary value problem, we can express the function ω explicitly as a function of t .

The general solution of the Hilbert problem in the upper half-plane is well known, for example, see Mikhlín [37], Muskhelishvili [40], Tricomi [52], Larock and Street [30],[31], Larock [32],[33],[34], Agrawal [1], Lim [35], and Smith and Lim [46],[47]. If the imaginary part of an analytic function $Q(t)$ is known along $\text{Im}(t) = 0$, the real axis of the t -plane, then the value of $Q(t)$ in the upper half-plane is given by

$$Q(t) = \frac{1}{\pi} \int_{-\infty}^{\infty} \frac{\text{Im}[Q(\tau)]}{\tau - t} d\tau + \sum_{j=0}^n A_j t^j, \quad (2.17)$$

where A_j are real constants.

Note that we know either the imaginary or real part of $\omega(t)$, defined by (2.14), along the real-axis of the t -plane.

This boundary information can be converted into information about a related function $Q(t)$ so that $\text{Im}[Q(t)]$ is known on the entire real axis. In the conversion process from $\omega(t)$ to $Q(t)$ we need an auxiliary function $H(t)$, analytic for $\text{Im}(t) > 0$, which, on $\text{Im}(t) = 0$, is purely real where the imaginary part of $\omega(t)$ is known and purely imaginary where the real part of $\omega(t)$ is known. Then the imaginary part of the quotient $Q(t) = \frac{\omega(t)}{H(t)}$ known on the entire real axis.

The general solution for $H(t)$ is

$$H(t) = a \prod_i (t - b_i)^{\pm \frac{1}{2}} \quad (2.18)$$

where b_i are real constants, $a = \pm \sqrt{\pm 1}$.

Song [48] has shown that the final solution is independent of a

particular choice for $H(t)$. A branch cut is selected on the real axis to ensure that $H(t)$ is a single-valued function. Hence $\omega(t)$ can be constructed explicitly by means of Hilbert's solution, where $\omega(t) = H(t) Q(t)$.

In our problem, (the flow over an uneven bottom, see Fig. 3.1), we choose $b_1 = 1$, $a = -i$ in (2.18). The coefficients A_j , $j = 0, 1, 2, \dots, n$ in (2.17) are all zero when the upstream boundary condition is applied. Hence in this case we find

$$H(t) = -i\sqrt{t-1}, \quad (2.19)$$

$$Q(t) = \frac{1}{\pi} \int_{-\infty}^{\infty} \frac{\text{Im}[Q(\tau)]}{\tau - t} d\tau, \quad (2.20)$$

and

$$\begin{aligned} \frac{\omega(t)}{H(t)} &= \frac{1}{\pi} \int_{-\infty}^{\infty} \frac{\text{Im} \left[\frac{\omega(\tau)}{H(\tau)} \right]}{\tau - t} d\tau \\ &= U(t) + iV(t). \end{aligned} \quad (2.21)$$

Smith and Lim [47] used an equivalent form for (2.21), see Appendix [C],

$$U(t) = \frac{1}{\pi} \int_{-\infty}^{\infty} \frac{V(\tau)}{\tau - t} d\tau, \quad (2.22)$$

$$V(t) = \frac{-1}{\pi} \int_{-\infty}^{\infty} \frac{U(\tau)}{\tau - t} d\tau \quad (2.23)$$

The shape (x', y') of the free streamline DEFA can then be

calculated from (2.15] and (2.16]. In Chapter III, we will discuss the problem in detail.

2.2.2 Perturbation Method

The perturbation or small parameter method, often attributed to Poincaré [1892], is a common analytic tool for finding the approximate solutions of non-linear problems. Essentially it consists in developing the solution of a non-linear boundary or initial value problem in (usually ascending) powers of a parameter which either appears explicitly in the original problems or is introduced in some artificial manner. A perturbed system is one which differs slightly from a known standard system. The expansion in terms of the perturbation parameter provides a means for obtaining solutions to the perturbation system by utilizing the known properties of the standard system. The system has been most often used to investigate the behaviour of slightly non-linear systems.

Extensive treatments of the perturbation concept as they apply to non-linear partial differential equations may be found in Ames [2].

To apply the perturbation method, one must know a particular exact solution of the simplified problem to start with. In addition, one must be able to select a dimensionless parameter (or parameters), say ϵ , which helps to determine the exact physical problem and is such that the solutions to the exact problem associated with each value of ϵ approach (in some sense) the known exact solution when $\epsilon \rightarrow 0$. It is then assumed that the various functions entering into the problem may be expanded into power series in ϵ . The series are substituted in the equations and boundary conditions and grouped according to

powers of ϵ . The coefficients of each power then yield a sequence of equations and boundary conditions, the coefficients of ϵ giving the first-order theory, those of ϵ^2 the second-order theory, etc. As an exact initial solution it is usually most convenient to take either a state of rest or of uniform motion. Various choices of ϵ will be mentioned later.

If the order of the equations and the number of boundary conditions remains fixed in the procedure the problem is called a regular perturbation problem. However, if the order of the equations is lowered when $\epsilon = 0$ and if one or more boundary conditions have to be discarded the perturbation problem is called singular.

Expansions locally valid close to the singularity of the perturbation ϵ are called outer expansions, and those locally valid far from the singularity of the perturbation parameter ϵ are called inner expansions. The use of these terms (inner and outer expansions, or solutions) dates at least as far back as 1934 when Von Kármán and Millikan studied boundary layer separation. Then the solution for the whole field is established after the two expansions are matched.

The utility of the inner-outer expansion for the solution of singular perturbation problems has received great interest in several areas since the fundamental papers of Lagerstrom and Cole (1955), Kaplun (1957), and Proudman and Pearson (1957).

In 1965, Clarke [12] used the reciprocal of the Froude number as the parameter, ϵ , of expansion. In 1968, again Clarke [14] used a Reynolds number as ϵ . In 1973 and 1979, Keller and Geer [20],[28]

expanded the flow and its free boundaries as asymptotic series in powers of the slenderness ratio of the stream.

For more details of the discussion on this method, see Van Dyke [54], Cole [15], and Bellman [4].

2.2.3 Hodograph Method

The hodograph method began with the basic work of G. Kirchhoff [1869] for the free boundary problem and was systematized into essentially its present form by M. Planck [57] and J. Michell [56]. The basic idea of the method is to introduce the velocity as a new variable and then to exploit the fact that streamlines, unknown in shape in the physical plane, become known curves in the hodograph, or velocity plane. For plane flows of incompressible fluids the hodograph variable is $\frac{dW}{dZ} = q e^{-i\theta}$, although it is more convenient to work with the logarithmic hodograph variables, as given by (2.13), (2.14) in normalized variables.

It is clear that any flow region bounded entirely by polygonal streamlines and free stream lines is mapped into a region of the ω -plane; from (2.14)

$$\omega = \log \zeta = \log q' + i(-\theta),$$

bounded by radial segments ($\theta = \text{constant}$) and circular arcs ($q' = \text{constant}$), and is mapped into a polygonal domain in the ω -plane. Hence the hodograph image of the flow is a known region.

Since the plane of the complex potential region $W = \phi + i\psi$ is already a known polygonal region, the flow problem is essentially

solved if the mapping between the w -plane and the hodograph plane is known, with appropriate boundary correspondence, for then $W(Z)$ appears as the solution of a differential equation

$$\frac{dW}{dZ} = x(W),$$

and the flow region is determined by $Z = \int \frac{dW}{x(W)}$. Thus the flow problem is reduced to that of conformal mapping between known regions, and the difficulty raised by the unknown free boundary has been removed. This is the essence of the hodograph method.

2.2.4 Relaxation Method

The general idea of the relaxation method is well known, see Southwell [49], and requires only brief mention here. The flow field is divided into a rectangular network of appropriate fineness, and the governing equations are written in finite difference form in terms of the function values at the mesh points.

Starting from a reasonable trial solution, values at the mesh points are successively corrected until the solution is stabilized and the errors in the solution are within the limits considered acceptable in the particular problem. Additional accuracy can generally be introduced in any part of the flow by refining the network there.

CHAPTER III

FLOW OVER UNEVEN BOTTOM

- 3.1 Formulation of the Problem
- 3.2 Solution of the Problem
- 3.3 Numerical Solution
- 3.4 Some Mathematical Relations
- 3.5 Numerical Results and Discussions

3.1 Formulation of the Problem

The flows considered are assumed to be inviscid, irrotational, two-dimensional, incompressible, and steady. Hence it follows from the preceding assumptions that the stream function ψ and the velocity potential ϕ are harmonic functions of the (x,y) -coordinates in the physical plane and may be defined so that

$$\frac{\partial \phi}{\partial x} = \frac{\partial \psi}{\partial y} = u, \quad (3.1a)$$

and

$$\frac{\partial \phi}{\partial y} = -\frac{\partial \psi}{\partial x} = v, \quad (3.1b)$$

in which (u,v) are the (x,y) -components of the velocity vector, respectively. Thus ϕ and ψ are the real and imaginary parts of the complex potential

$$w = \phi + i\psi. \quad (3.2)$$

The bottom consists of a horizontal plane AB, inclined plane BC at inclination angle α and length L , and a horizontal plane CD, where it extends from $-\infty$ (point A) to $+\infty$ (point D), as shown in Fig. 3.1. The direction of flow is from the left side to right side. For convenience, we choose B to be the origin in the Z -plane, the x -axis from left to right and the y -axis upward.

Suppose U_1 , h_1 and U_2 , h_2 are the speed and depth at A and D, respectively. We have defined the Froude number F in (2.10). We have introduced the dimensionless variables Z' , q' , and W' in (2.8). In

dimensionless form, the free surface condition was expressed in (2.9). The dimensionless physical variable Z' was given in (2.15) in terms of two functions W' and ω . That is,

$$Z' = \int e^{-\omega} dW'. \quad (3.3)$$

If we can express the two functions W' and ω as functions of a single variable t , then the integral in (3.3) can be found. For the first half of the problem, to express the function W' as a function of a single variable t , we use a conformal mapping (2.16). This mapping should map the fluid region in the W' -plane, see Fig. 3.3, into the upper half-plane, the t -plane, and the boundary of the fluid region onto the real axis, the boundary of the t -plane, see Fig. 3.4. To ensure the uniqueness of the mapping, we choose three corresponding points in the following ways,

$$\left. \begin{array}{ll} B: & W' = 0, \quad t = 0, \\ D: & W' \rightarrow \infty, \quad t = 1, \\ A: & W' \rightarrow -\infty, \quad t \rightarrow \infty. \end{array} \right\} \quad (3.4)$$

The mapping is

$$W'(t) = -\frac{1}{\pi} \log (1-t), \quad (3.5)$$

for $W'(t)$ to remain single-valued function, we assume $0 \leq \arg (1-t) \leq \pi$.

For the second half of the problem, to express ω as a function of the single variable t , we introduce the Hilbert method for a mixed boundary value problem in the upper half-plane. The general solution

of the Hilbert problem for an analytic function $Q(t)$ in the upper half-plane was given in (2.17). Now, we try to relate the function $\omega(t)$ to the function $Q(t)$. From (2.17), we find that $Q(t)$ is expressed in terms of the imaginary part of $Q(t)$ along the real axis, the boundary of the t -plane. Thus, we have to examine the value of $\omega(t)$ along the real-axis of the t -plane, and we find that

$$\left. \begin{aligned} \text{Im} [\omega(t)] &= -\theta(t) & , t < 1, \\ \text{Re} [\omega(t)] &= \frac{1}{2} \log [1 - \frac{2}{F^2}(y^2 - 1)], & t > 1. \end{aligned} \right\} \quad (3.6)$$

where

$$\theta(t) = \begin{cases} 0 & , t < 0 \\ \alpha & , 0 < t < t_c \\ 0 & , t_c < t < 1 \end{cases} \quad (3.7)$$

Note that we know either the imaginary or real part of $\omega(t)$ along the real axis of the t -plane. This boundary information can be converted into information about a related function $Q(t)$ so that $\text{Im} [Q(t)]$ is known on the entire real axis. In the conversion process from $\omega(t)$ to $Q(t)$ we need an auxiliary function $H(t)$ which makes the quotient $Q(t) = \frac{\omega(t)}{H(t)}$ satisfy the above requirement. The general form of $H(t)$ was given in (2.18). One such function $H(t)$ is

$$H(t) = -i\sqrt{t-1}. \quad (3.8)$$

For $H(t)$ to remain single-valued function, we assume $0 \leq \arg [t-1] \leq \pi$.

Use of (3.6] and (3.8], we obtain

$$\operatorname{Im} [Q(t)] = \begin{cases} \frac{\theta(t)}{\sqrt{1-t}} & t < 1 \\ \frac{1}{2} \{ \log [1 - \frac{2}{F^2}(\gamma(t) - 1)] \} (t-1)^{-\frac{1}{2}}, & t > 1 \end{cases} \quad (3.9)$$

Next, we examine the upstream condition. As we approach point A along the free surface, i.e., as $t \rightarrow \infty$, $H(t) \sim -i\sqrt{t}$ and $\omega(t) \rightarrow \log 1 = 0$. Therefore, $Q(t) = \frac{\omega(t)}{H(t)} \rightarrow 0$, and from (2.17), $A_j = 0$, $j = 0, 1, \dots, n$. Thus, (2.17) takes the form

$$Q(t) = \frac{1}{\pi} \int_{-\infty}^{\infty} \frac{\operatorname{Im}[Q(\tau)]}{\tau - t} d\tau \quad (3.10)$$

Using (2.14), we get

$$\begin{aligned} Q(t) &= \frac{\omega(t)}{H(t)} = \frac{\log q^-(t) + i(-\theta(t))}{H(t)} \\ &= U(t) + iV(t) \end{aligned} \quad (3.11)$$

Writing (3.11) in details

$$\begin{array}{c}
 U(t) \\
 \hline
 \frac{\log q_1^-(t)}{\sqrt{1-t}} \quad \frac{\log q_2^-(t)}{\sqrt{1-t}} \quad \frac{\log q_3^-(t)}{\sqrt{1-t}} \quad \frac{\theta(t)}{\sqrt{t-1}} \\
 \hline
 t \\
 \hline
 V(t) \\
 \hline
 0 \quad \frac{-\alpha}{\sqrt{1-t}} \quad 0 \quad \frac{\log q^-(t)}{\sqrt{t-1}} \\
 \hline
 \end{array}
 \quad (3.12)$$

Using the Hilbert transformation relating the values on the real axis, of the real and imaginary parts of a function, analytic in the upper half-plane, given by (2.22) and (2.23), we obtain the following equations

$$\log q_1^-(t) = \frac{\sqrt{1-t}}{\pi} \left\{ \int_0^{t_c} \frac{-\alpha}{(\tau-t)\sqrt{1-\tau}} d\tau + \int_1^{\infty} \frac{\log q^-(\tau)}{(\tau-t)\sqrt{\tau-1}} d\tau \right\}, \quad t < 0 \quad (3.13)$$

$$\log q_2^-(t) = \frac{\sqrt{1-t}}{\pi} \left\{ \int_0^{t_c} \frac{-\alpha}{(\tau-t)\sqrt{1-\tau}} d\tau + \int_1^{\infty} \frac{\log q^-(\tau)}{(\tau-t)\sqrt{\tau-1}} d\tau \right\}, \quad 0 < t < t_c \quad (3.14)$$

$$\log q_3^-(t) = \frac{\sqrt{1-t}}{\pi} \left\{ \int_0^{t_c} \frac{-\alpha}{(\tau-t)\sqrt{1-\tau}} d\tau + \int_1^{\infty} \frac{\log q^-(\tau)}{(\tau-t)\sqrt{\tau-1}} d\tau \right\}, \quad t_c < t < 1 \quad (3.15)$$

$$\theta(t) = \frac{\sqrt{t-1}}{\pi} \left\{ \int_0^{t_c} \frac{-\alpha}{(\tau-t)\sqrt{1-\tau}} d\tau + \int_1^{\infty} \frac{\log q^-(\tau)}{(\tau-t)\sqrt{\tau-1}} d\tau \right\}, \quad t > 1 \quad (3.16)$$

$$\int_1^{\infty} \frac{\theta(\tau)}{(\tau-t)\sqrt{\tau-1}} d\tau = \int_{-\infty}^0 \frac{\log q_1^-(\tau)}{(\tau-t)\sqrt{1-\tau}} d\tau + \int_0^{t_c} \frac{\log q_2^-(\tau)}{(\tau-t)\sqrt{1-\tau}} d\tau + \int_{t_c}^1 \frac{\log q_3^-(\tau)}{(\tau-t)\sqrt{1-\tau}} d\tau, \quad t < 0 \quad (3.17)$$

$$\alpha = \frac{\sqrt{1-t}}{\pi} \left\{ \int_{-\infty}^0 \frac{\log q_1(\tau)}{(\tau-t)\sqrt{1-\tau}} d\tau + \int_0^{t_c} \frac{\log q_2(\tau)}{(\tau-t)\sqrt{1-\tau}} d\tau + \int_{t_c}^1 \frac{\log q_3(\tau)}{(\tau-t)\sqrt{1-\tau}} d\tau + \int_1^{\infty} \frac{\theta(\tau)}{(\tau-t)\sqrt{\tau-1}} d\tau \right\}, \quad 0 < t < t_c \quad (3.18)$$

$$- \int_1^{\infty} \frac{\theta(\tau)}{(\tau-t)\sqrt{\tau-1}} d\tau = \int_{-\infty}^0 \frac{\log q_1(\tau)}{(\tau-t)\sqrt{1-\tau}} d\tau + \int_0^{t_c} \frac{\log q_2(\tau)}{(\tau-t)\sqrt{1-\tau}} d\tau + \int_{t_c}^1 \frac{\log q_3(\tau)}{(\tau-t)\sqrt{1-\tau}} d\tau, \quad t_c < t < 1 \quad (3.19)$$

$$\log q^-(t) = \frac{-\sqrt{t-1}}{\pi} \left\{ \int_{-\infty}^0 \frac{\log q_1(\tau)}{(\tau-t)\sqrt{1-\tau}} d\tau + \int_0^{t_c} \frac{\log q_2(\tau)}{(\tau-t)\sqrt{1-\tau}} d\tau + \int_{t_c}^1 \frac{\log q_3(\tau)}{(\tau-t)\sqrt{1-\tau}} d\tau + \int_1^{\infty} \frac{\theta(\tau)}{(\tau-t)\sqrt{\tau-1}} d\tau \right\}, \quad t > 1 \quad (3.20)$$

where \int notation indicates the principal value of the integral.

The singularities in (3.13) to (3.20) may be removed by using the result of Appendix [A] and noting that

$$\int_0^{t_c} \frac{1}{(\tau-t)\sqrt{1-\tau}} d\tau = \frac{2}{\sqrt{t-1}} \tan^{-1} \left[\frac{\sqrt{t-1} (1-\sqrt{1-t_c})}{t-1 + \sqrt{1-t_c}} \right], \quad t > 1 \quad (3.21)$$

$$\int_0^{t_c} \frac{1}{(\tau-t)\sqrt{1-\tau}} d\tau = \frac{-2}{\sqrt{1-t}} \tanh^{-1} \left[\frac{\sqrt{1-t} (\sqrt{1-t_c}-1)}{1-t-\sqrt{1-t_c}} \right], \quad t < 1 \quad (3.22)$$

$$\int_1^{\infty} \frac{1}{(\tau-t)\sqrt{1-\tau}} d\tau = 0, \quad t > 1 \quad (3.23)$$

For the solution of our problem we need only the following equations; (3.13), (3.14), (3.15) and (3.16), and we use (3.20) as a numerical check. Use of (3.21) to (3.23) and the result of Appendix [A] to remove singularities from (3.13) to (3.16) and (3.20) we get,

$$\log q_1'(t) = \frac{\sqrt{1-t}}{\pi} \int_1^{\infty} \frac{\log q'(\tau)}{(\tau-t)\sqrt{\tau-1}} d\tau + \frac{2\alpha}{\pi} \tanh^{-1} \left[\frac{\sqrt{1-t} (\sqrt{1-t_c}-1)}{1-t-\sqrt{1-t_c}} \right], \quad t < 0 \quad (3.24)$$

$$\log q_2'(t) = \frac{\sqrt{1-t}}{\pi} \int_1^{\infty} \frac{\log q'(\tau)}{(\tau-t)\sqrt{\tau-1}} d\tau + \frac{2\alpha}{\pi} \tanh^{-1} \left[\frac{\sqrt{1-t} (\sqrt{1-t_c}-1)}{1-t-\sqrt{1-t_c}} \right], \quad 0 < t < t_c \quad (3.25)$$

$$\log q_3'(t) = \frac{\sqrt{1-t}}{\pi} \int_1^{\infty} \frac{\log q'(\tau)}{(\tau-t)\sqrt{\tau-1}} d\tau + \frac{2\alpha}{\pi} \tanh^{-1} \left[\frac{\sqrt{1-t} (\sqrt{1-t_c}-1)}{1-t-\sqrt{1-t_c}} \right], \quad t_c < t < 1 \quad (3.26)$$

$$\theta(t) = \frac{\sqrt{t-1}}{\pi} \int_1^{\infty} \frac{\log q'(\tau) - \log q'(t)}{(\tau-t)\sqrt{\tau-1}} d\tau - \frac{2\alpha}{\pi} \tan^{-1} \left[\frac{\sqrt{t-1} (1-\sqrt{1-t_c})}{t-1+\sqrt{1-t_c}} \right], \quad t > 1 \quad (3.27)$$

$$\log q^-(t) = \frac{-\sqrt{t-1}}{\pi} \left\{ \int_{-\infty}^0 \frac{\log q_1^-(\tau)}{(\tau-t)\sqrt{1-\tau}} d\tau + \int_0^{t_c} \frac{\log q_2^-(\tau)}{(\tau-t)\sqrt{1-\tau}} d\tau + \int_{t_c}^1 \frac{\log q_3^-(\tau)}{(\tau-t)\sqrt{1-\tau}} d\tau + \int_1^{\infty} \frac{\theta(\tau) - \theta(\tau)}{(\tau-t)\sqrt{\tau-1}} d\tau \right\}, \quad t > 1 \quad (3.28)$$

3.2 Solution of the Problem

The coordinates (x^-, y^-) of a point on the free surface can be obtained by use of (3.3) and (3.5) as follows

$$Z^-(t) = (x_0^- + i) + \int_{\infty}^t \frac{e^{i\theta(\tau)}}{q^-(\tau)} \frac{1}{\pi(1-\tau)} d\tau, \quad t > 1$$

Separating real and imaginary parts, we get

$$y^-(t) = 1 + \frac{1}{\pi} \int_{\infty}^t \frac{\sin \theta(\tau)}{(1-\tau) q^-(\tau)} d\tau, \quad t > 1 \quad (3.29)$$

$$x^-(t) = x_0^- + \frac{1}{\pi} \int_{\infty}^t \frac{\cos \theta(\tau)}{(1-\tau) q^-(\tau)} d\tau, \quad t > 1 \quad (3.30)$$

The length l^- of the inclined plane BC can be obtained by use of (3.3) and (3.5) as follows

$$Z^-(t) = Z_0^- + \frac{1}{\pi} \int_{t_0}^t \frac{e^{i\theta(\tau)}}{(1-\tau) q^-(\tau)} d\tau,$$

along BC: $\theta = \alpha$, $q^- = q_2^-$, $t_0 = 0$, $t = t_c$.

Hence,

$$\begin{aligned} z'(t) - z'_0 &= \frac{1}{\pi} \int_0^t \frac{e^{i\alpha}}{q_2'(\tau)} \frac{d\tau}{1-\tau} \\ &= z' e^{i\alpha} \end{aligned}$$

Therefore,

$$z' = \frac{1}{\pi} \int_0^t \frac{1}{(1-\tau) q_2'(\tau)} d\tau \quad (3.31)$$

To determine the pressure at a point on the bottom, use of Bernoulli's equation (2.6)

$$\begin{aligned} \frac{p}{\rho} + \frac{1}{2} q_b^2 + gy_b &= \text{constant} \\ &= \frac{1}{2} U_1^2 + gh_1, \end{aligned} \quad (3.32)$$

where q_b is the speed along the bottom.

Dividing (3.32) by $\frac{1}{2} U_1^2$ and rearranging the equation, we get

$$c_p = 1 - \frac{2}{F^2} (y_b' - 1) - q_b'^2, \quad (3.33)$$

where

$$c_p = \frac{p}{\frac{1}{2} \rho U_1^2},$$

$$\begin{aligned}
 y_B^* &= \left\{ \begin{array}{l} 0 \\ y_2^* \\ l^* \sin \alpha \end{array} \right. \left. \begin{array}{l} \text{Along AB,} \\ \text{Along BC,} \\ \text{Along CD,} \end{array} \right\} \\
 \text{and} & \\
 q_B^* &= \left\{ \begin{array}{l} q_1^* \\ q_2^* \\ q_3^* \end{array} \right. \left. \begin{array}{l} \text{Along AB,} \\ \text{Along BC,} \\ \text{Along CD.} \end{array} \right\}
 \end{aligned} \tag{3.34}$$

Now, summing up equations we need for a complete solution of our problem.

(i) Along free surface $t > 1$

$$q^*(t) = \left[1 - \frac{2}{\pi^2} (y^* - 1) \right]^{1/2} \tag{2.9}$$

$$\begin{aligned}
 \theta(t) &= \frac{\sqrt{t-1}}{\pi} \int_1^{\infty} \frac{\log q^*(\tau) - \log q^*(t)}{(\tau-t)\sqrt{\tau-1}} d\tau \\
 &\quad - \frac{2\alpha}{\pi} \tan^{-1} \left[\frac{\sqrt{t-1} (1 - \sqrt{1-t_c})}{t - 1 + \sqrt{1-t_c}} \right]
 \end{aligned} \tag{3.27}$$

$$y^*(t) = 1 + \frac{1}{\pi} \int_{\infty}^t \frac{\sin \theta(\tau) d\tau}{(1-\tau)q^*(\tau)} \tag{3.29}$$

$$x^*(t) = x_0^* + \frac{1}{\pi} \int_{\infty}^t \frac{\cos \theta(\tau) d\tau}{(1-\tau)q^*(\tau)} \tag{3.30}$$

(if) Along the boundary of the bottom

$$\log q_1^-(t) = \frac{\sqrt{1-t}}{\pi} \int_1^{\infty} \frac{\log q^-(\tau)}{(\tau-t)\sqrt{\tau-1}} d\tau + \frac{2\alpha}{\pi} \tanh^{-1} \left[\frac{\sqrt{1-t} (\sqrt{1-t_c} - 1)}{1-t - \sqrt{1-t_c}} \right],$$

$t < 0$ (3.24)

$$\log q_2^-(t) = \frac{\sqrt{1-t}}{\pi} \int_1^{\infty} \frac{\log q^-(\tau)}{(\tau-t)\sqrt{\tau-1}} d\tau + \frac{2\alpha}{\pi} \tanh^{-1} \left[\frac{\sqrt{1-t} (\sqrt{1-t_c} - 1)}{1-t - \sqrt{1-t_c}} \right],$$

$0 < t < t_c$ (3.25)

$$\log q_3^-(t) = \frac{\sqrt{1-t}}{\pi} \int_1^{\infty} \frac{\log q^-(\tau)}{(\tau-t)\sqrt{\tau-1}} d\tau + \frac{2\alpha}{\pi} \tanh^{-1} \left[\frac{\sqrt{1-t} (\sqrt{1-t_c} - 1)}{1-t - \sqrt{1-t_c}} \right],$$

$t_c < t < 1$ (3.26)

$$g^- = \frac{1}{\pi} \int_0^{t_c} \frac{1}{(1-\tau)q_2^-(\tau)} d\tau$$

(3.31)

$$c_p = \begin{cases} 1 + \frac{2}{F^2} - q_1^{-2}(t) & t < 0 \\ 1 - \frac{2}{F^2} (y_\ell^- - 1) - q_2^{-2}(t) & 0 < t < t_c \\ 1 - \frac{2}{F^2} (\ell^- \sin \alpha - 1) - q_3^{-2}(t) & t_c < t < 1 \end{cases}$$

(3.33)

(iii) For a numerical check

$$\log q'(t) = \frac{-\sqrt{t-1}}{\pi} \left\{ \int_{-\infty}^0 \frac{\log q_1'(\tau)}{(\tau-t)\sqrt{1-\tau}} d\tau + \int_0^{t_c} \frac{\log q_2'(\tau)}{(\tau-t)\sqrt{1-\tau}} d\tau \right. \\ \left. + \int_{t_c}^1 \frac{\log q_3'(\tau)}{(\tau-t)\sqrt{1-\tau}} d\tau + \int_1^{\infty} \frac{\theta(\tau) - \theta(t)}{(\tau-t)\sqrt{\tau-1}} d\tau \right\}, \quad t > 1 \quad (3.28)$$

3.3 Numerical Solution

It is more convenient to write down the free surface condition, Bernoulli's equation (2.9), in integral form, by differentiating (2.9) with respect to ϕ' , replacing $\frac{dy'}{d\phi'}$ by $\frac{V}{q'^2} = \frac{\sin\theta}{q'}$, using (3.5), and integrating we get

$$q'^3(t) = 1 - \frac{3}{\pi F^2} \int_t^{\infty} \frac{\sin\theta(\tau)}{(\tau-1)} d\tau, \quad t > 1 \quad (3.35)$$

taking into consideration that as $t \rightarrow \infty$ (upstream), $q'(t) \rightarrow 1$.

Now, consider the following transformation

$$t = \frac{1}{\sin^2(\gamma/2)}, \quad \tau = \frac{1}{\sin^2(\beta/2)}, \quad (3.36)$$

in (3.27) to (3.30) and (3.35) to overcome the difficulty arising from carrying out the integration over the infinite range, we get

$$Q^3(\gamma) = 1 - \frac{6}{\pi F^2} \int_0^\gamma \frac{\sin \theta(\beta)}{\sin \beta} d\beta, \quad 0 < \delta < \pi \quad (3.37)$$

$$\theta(\gamma) = \frac{\sin \gamma}{\pi} \int_0^\pi \frac{\log Q(\beta) - \log Q(\gamma)}{\cos \beta - \cos \gamma} d\beta + \frac{2\alpha}{\pi} \tan^{-1} \left(\frac{\sin \gamma}{\mu + \cos \gamma} \right),$$

$$0 < \gamma < \pi \quad (3.38)$$

where $\mu = \frac{2}{k} - 1$, $k = 1 - \sqrt{1 - \epsilon_c}$

$$Y(\gamma) = 1 + \frac{2}{\pi} \int_0^\gamma \frac{\sin \theta(\beta)}{\sin \beta Q(\beta)} d\beta, \quad 0 < \gamma < \pi \quad (3.39)$$

$$X(\gamma) = x_0 + \frac{2}{\pi} \int_0^\gamma \frac{\cos \theta(\beta)}{\sin \beta Q(\beta)} d\beta, \quad 0 < \gamma < \pi \quad (3.40)$$

Consider the following transformation

$$\tau = \frac{1}{\sin^2(\beta/2)}$$

in (3.24) to (3.26) and

$$t = \frac{-1}{\tan^2 \gamma}$$

in (3.24) only, we get



$$\log Q_1(\gamma) = \frac{2 \tan \gamma \sec \gamma}{\pi} \int_0^{\pi} \frac{\log Q(\beta)}{2 \tan^2 \gamma + 1 - \cos \beta} d\beta$$

$$+ \frac{2\alpha}{\pi} \tanh^{-1} \left[\frac{-k \tan \gamma \sec \gamma}{1 + k \tan^2 \gamma} \right], \quad 0 < \gamma < \frac{\pi}{2} \quad (3.41)$$

$$\log q_2^+(t) = \frac{2\sqrt{1-t}}{\pi} \int_0^{\pi} \frac{\log Q(\beta)}{2 - t(1 - \cos \beta)} d\beta + \frac{2\alpha}{\pi} \tanh^{-1} \left[\frac{k\sqrt{1-t}}{t-k} \right],$$

$$0 < t < t_c \quad (3.42)$$

$$\log q_3^-(t) = \frac{2\sqrt{1-t}}{\pi} \int_0^{\pi} \frac{\log Q(\beta)}{2 - t(1 - \cos \beta)} d\beta + \frac{2\alpha}{\pi} \tanh^{-1} \left[\frac{k\sqrt{1-t}}{t-k} \right],$$

$$t_c < t < 1 \quad (3.43)$$

Also, consider the transformation

$$\tau = \frac{-1}{\tan^2 \beta}$$

in the first term on the right side of (3.28), and

$$\tau = \frac{1}{\sin^2 (\beta/2)}$$

in the fourth term on the right side of (3.28), and

$$t = \frac{1}{\sin^2 \left(\frac{\gamma}{2} \right)}$$

in (3.28), we get

$$\begin{aligned} \log Q(\gamma) = & \frac{-\sin\gamma}{2\pi} \left\{ -4 \int_0^{\pi/2} \frac{\log Q_1(\beta)}{(1 - \cos\gamma + 2 \tan^2 \beta)} \sec\beta \, d\beta \right. \\ & + \int_0^{t_c} \frac{\log q_2^-(\tau)}{(\tau \sin^2 \frac{\gamma}{2} - 1)\sqrt{1-\tau}} \, d\tau + \int_{t_c}^1 \frac{\log q_3^-(\tau)}{(\tau \sin^2 \frac{\gamma}{2} - 1)\sqrt{1-\tau}} \, d\tau \\ & \left. + 2 \int_0^{\pi} \frac{\theta(\beta) - \theta(\gamma)}{\cos\beta - \cos\gamma} \, d\beta \right\}, \quad 0 < \gamma < \pi \end{aligned}$$

Hence, we have the following system of equations necessary to solve our problem, after dropping the dash sign, "-", and use big letters for variables:

(i) Along free surface $0 < \gamma < \pi$

$$Q(\gamma) = \left[1 - \frac{6}{\pi F^2} \int_0^{\gamma} \frac{\sin\theta(\beta)}{\sin\beta} \, d\beta \right]^{1/3} \quad (3.37)$$

$$\theta(\gamma) = \frac{\sin\gamma}{\pi} \int_0^{\pi} \frac{\log Q(\beta) - \log Q(\gamma)}{\cos\beta - \cos\gamma} \, d\beta + \frac{2\alpha}{\pi} \tan^{-1} \left(\frac{\sin\gamma}{\mu + \cos\gamma} \right) \quad (3.38)$$

$$Y(\gamma) = 1 + \frac{2}{\pi} \int_0^{\gamma} \frac{\sin\theta(\beta)}{\sin\beta Q(\beta)} \, d\beta \quad (3.39)$$

$$X(\gamma) = X_0 + \frac{2}{\pi} \int_0^\gamma \frac{\cos \beta Q(\beta)}{\sin \beta} d\beta \quad (3.40)$$

(ii) Along the boundary of the bottom

$$\log Q_1(\gamma) = \frac{2 \operatorname{sech} \gamma \tanh \gamma}{\pi} \int_0^\pi \frac{\log Q(\beta)}{2 \tan^2 \gamma + 1 - \cos \beta} d\beta + \frac{2\alpha}{\pi} \tanh^{-1} \left[\frac{-k \operatorname{sech} \gamma \tanh \gamma}{1 + k \tan^2 \gamma} \right], \quad 0 < \gamma < \pi/2 \quad (3.41)$$

$$\log Q_2(t) = \frac{2\sqrt{1-t}}{\pi} \int_0^\pi \frac{\log Q(\beta)}{2 - t(1 - \cos \beta)} d\beta + \frac{2\alpha}{\pi} \tanh^{-1} \left[\frac{k\sqrt{1-t}}{t-k} \right], \quad 0 < t < t_c \quad (3.42)$$

$$\log Q_3(t) = \frac{2\sqrt{1-t}}{\pi} \int_0^\pi \frac{\log Q(\beta)}{2 - t(1 - \cos \beta)} d\beta + \frac{2\alpha}{\pi} \tanh^{-1} \left[\frac{k\sqrt{1-t}}{t-k} \right], \quad t_c < t < 1 \quad (3.43)$$

$$e^{-\gamma} = \frac{1}{\pi} \int_0^{t_c} \frac{1}{(1-\tau) Q_2(\tau)} d\tau \quad (3.44)$$

$$c_p = \begin{cases} 1 + \frac{2}{F^2} - Q_1^2(\gamma) & , \quad 0 < \gamma < \pi/2 \\ 1 - \frac{2}{F^2} (\gamma_x - 1) - Q_2^2(t) & , \quad 0 < t < t_c \\ 1 - \frac{2}{F^2} (\alpha \sin \alpha - 1) - Q_3^2(t) & , \quad t_c < t < 1 \end{cases} \quad (3.45)$$

(iii) For a numerical check

$$\begin{aligned} \log Q(\gamma) = \frac{-\sin \gamma}{2\pi} & \left\{ -4 \int_0^{\pi/2} \frac{\log Q_1(\beta)}{(1 - \cos \gamma + 2 \tan^2 \beta)} \sec \beta \, d\beta \right. \\ & + \int_0^{t_c} \frac{\log Q_2(\tau)}{(\tau \sin^2 \frac{\gamma}{2} - 1) \sqrt{1-\tau}} \, d\tau + \int_{t_c}^1 \frac{\log Q_3(\tau)}{(\tau \sin^2 \frac{\gamma}{2} - 1) \sqrt{1-\tau}} \, d\tau \\ & \left. + 2 \int_0^{\pi} \frac{\theta(\beta) - \theta(\gamma)}{\cos \beta - \cos \gamma} \, d\beta \right\}, \quad 0 < \gamma < \pi \end{aligned} \quad (3.46)$$

Now, equation (3.38) should give values of $\theta(\gamma)$ along the free surface, but $Q(\gamma)$ appears in the numerator of the integrand on the right side of the equations. Equation (3.37) which should give values of $Q(\gamma)$ along the free surface, in turn has $\theta(\gamma)$ in the numerator of the integrand on the right side of the equation. Consequently, configuration of the free surface (Y, X) can not be found out without calculating $Q(\gamma)$

and $\theta(\gamma)$.

These two equations, (3.37) and (3.38), are of such complexity that we can not solve them analytically. Therefore, numerical methods must be introduced. Since the shape of free surface is unknown, an iterative method should be applied to solve the problem, in condition that we have to find initially a good approximation for the unknown quantities, see Scarborough [45]. The iterative method which we have used is described in detail by Larock and Street [31].

The iterative procedure works in the following manner:

- (i) We determine $Q(\gamma)$ on the free surface, initially, from the non-gravity case ($g=0$), which is, from (3.37), $Q^{(0)}(\gamma) = 1.0$.
- (ii) Using $Q^{(0)}(\gamma)$ as an input data in (3.38), we find out an expression for $\theta(\gamma)$, call it $\theta^{(1)}(\gamma)$.
- (iii) Using $\theta^{(1)}(\gamma)$ in (3.37) we will get $Q^{(1)}(\gamma)$.
- (iv) Use $Q^{(1)}(\gamma)$ and $\theta^{(1)}(\gamma)$ in (3.39) and (3.40) to find out $(\gamma^{(1)}(\gamma), x^{(1)}(\gamma))$.
- (v) Use $Q^{(1)}(\gamma)$ in (3.41) to (3.43) to find expressions for $Q_1^{(1)}$, $Q_2^{(1)}$ and $Q_3^{(1)}$, respectively.
- (vi) Use $Q_2^{(1)}$ in (3.44) to find $\lambda^{(1)}$.
- (vii) Substitute for $Q^{(1)}$, $\theta^{(1)}$, $Q_1^{(1)}$, $Q_2^{(1)}$, and $Q_3^{(1)}$ in (3.46) for a numerical check.
- (viii) Another gravity solution is obtained using the data from step (iii), $Q^{(1)}(\gamma)$.

(ix) Steps (ii) to (vii) are repeated until the results of two successive iterations differ by less than some specified small number 10^{-k} , where $k = 4$ or 6 ; at this point we stop the iterations and the gravity solution is obtained.

(x) Use Q_1 , Q_2 , and Q_3 in (3.45) to find out the pressure coefficient along the boundary of the bottom.

3.4 Some Mathematical Relations

Relationship between F_1^2 and F_2^2

Conservation of mass gives us

$$\text{Flux} = U_1 h_1 = U_2 h_2 \quad (3.47)$$

Bernoulli's equation along the free surface AD gives us

$$\frac{1}{2} U_1^2 + gh_1 = \frac{1}{2} U_2^2 + g(h_2 + d) \quad (3.48)$$

Multiplying (3.48) across by 2 and dividing by gh_1 , we get,

$$\frac{U_1^2}{gh_1} + 2 = \frac{U_2^2}{gh_2} \frac{h_2}{h_1} + 2 \left(\frac{h_2}{h_1} + \frac{d}{h_1} \right) \quad (3.49)$$

Using the definition of Froude number given by (2.10), and the dimensionless variables (2.8), we get

$$F_1^2 = h_2^2 F_2^2 + 2(h_2^2 + d^2 - 1) \quad (3.50)$$

Equation (3.50) gives a relation between F_1^2 and F_2^2 in terms of the depth far downstream and the vertical depth of the inclined plane.

It is clear from (3.50) that

- (i) when $F_1^2 > F_2^2$: the level of flow rises up
- (ii) when $F_1^2 < F_2^2$: the level of flow falls down
- (iii) when $F_1^2 = F_2^2$: no change in the level, which corresponds to $d' = 0$,

see Fig. 3.5 for illustration.

3.5 Numerical Results and Discussions

The dimensionless variables X , Y along FE are given in 3.39 and 3.40 respectively. Tables 3.1 to 3.4 show some free surfaces, which are plotted in Figs. 3.6 to 3.9.

After an initial guess, (the non-gravity case, Y along FE), we start the iterative procedure. The iterative procedure becomes stable after the second iteration, and in the fourth iteration it produces 3 significant decimal places. We need 9 iterations to produce 5 significant decimal places.

It should also be mentioned that with a 30 points of divisions, the CPU time for each iteration was approximately 0.257 minutes using an IBM 3031 computer, FORTRAN IV level G.

CHAPTER IV

FLOW FROM UNIFORM CHANNEL OVER SHELF

- 4.1 Formulation of the Problem
- 4.2 Solution of the Problem
- 4.3 Numerical Solution
- 4.4 Numerical Results and Discussions
- 4.5 Comparison with Previous Work

4.1 Formulation of the Problem

An inviscid, incompressible fluid flows over a horizontal surface until it falls over an edge under the influence of gravity. The flow is considered to be two-dimensional, steady, and irrotational. Far upstream the fluid is of depth h and has a uniform horizontal velocity U_0 , and gravity is acting vertically downwards, see Fig. 4.1. For convenience, we choose B to be the origin in the z -plane, the x -axis from left to right and the y -axis upward.

It is supposed that the two-dimensional fluid flow, taking place in the plane of a complex variable $z = x + iy$, is given by means of a velocity potential $\phi(x,y)$ and a stream function $\psi(x,y)$, both satisfy Laplace's equation. Then the complex potential $w(z) = \phi(x,y) + i\psi(x,y)$ is an analytic function of z within the region of flow and has the important property that its derivative satisfies (2.2).

Along the upper free surface, q_1 , y_1 , θ_1 are the speed of the fluid, the vertical distance between a point on the free surface and some reference elevation, and the angle of inclination of the velocity with the horizontal, respectively. Similar definitions apply for q_2 , y_2 and θ_2 along the lower free surface.

We have defined the Froude number F in (2.10). We have introduced the dimensionless variables Z' , q' and w' in (2.8), and in our problem

$$\left. \begin{aligned} Z'_i &= \frac{Z_i}{h}, \\ q'_i &= \frac{q_i}{U_0}, \\ w' &= \frac{w}{\psi_1}, \end{aligned} \right\} \quad (4.1)$$

where $i = 1, 2$ and "1" for upper free surface and "2" for lower free surface, $\psi_1 = hU_0$.

In dimensionless form, the free surface condition along the upper and lower free surfaces, respectively, are

$$q_1^2 + \frac{2}{F^2} (\psi_1 - 1) = 1, \quad (4.2a)$$

$$q_2^2 + \frac{2}{F^2} (\psi_2 - 1) = 1. \quad (4.2b)$$

The dimensionless physical variable Z' in terms of two functions w' , ω was given in (2.15), that is,

$$Z' = \int e^{-\omega} dw'. \quad (4.3)$$

If we can express the two functions w' and ω as functions of a single variable t , then the integral in (4.3) could be carried out. For the first half of the problem, to express the function w' as a function of a single variable t , we use a conformal mapping (2.16). This mapping should map the fluid region in the w' -plane (see Fig. 4.3) into the upper half-plane, the t -plane, and the boundary of the fluid region onto the real axis, the boundary of the t -plane (see Fig. 4.4). To ensure the uniqueness of the mapping, we choose three corresponding points in the following ways,

$$\left. \begin{array}{ll} B : & w' = 0 \quad t = 0, \\ C, D : & w' \rightarrow \infty \quad t = 1, \\ A, F : & w' \rightarrow -\infty, \quad t \rightarrow \infty. \end{array} \right\} \quad (4.4)$$

The mapping is

$$w(t) = \frac{-1}{\pi} \log(1-t) \quad (4.5)$$

For $w(t)$ to remain single-valued function, we assume

$$0 \leq \arg(1-t) \leq \pi. \quad (4.6)$$

For the second half of the problem, to express w as a function of the single variable t , we introduce the Hilbert method for a mixed boundary value problem in the upper half-plane. The general solution of the Hilbert problem for an analytic function $Q(t)$ in the upper half-plane was given by (2.17). Now, we try to relate the function $w(t)$ to function $Q(t)$. From (2.17), we find that $Q(t)$ is expressed in terms of the imaginary part of $Q(t)$ along the real axis, the boundary of the t -plane. Thus, we have to examine the value of $w(t)$ along the real-axis of the t -plane, and we find that

$$\begin{aligned} \operatorname{Im} [w(t)] &= 0 & t < 0 \\ \operatorname{Re} [w(t)] &= \frac{1}{2} \log \left[1 - \frac{2}{F^2} (y_2' - 1) \right], & 0 < t < 1 \\ \operatorname{Re} [w(t)] &= \frac{1}{2} \log \left[1 - \frac{2}{F^2} (y_1' - 1) \right], & t > 1 \end{aligned} \quad (4.7)$$

Note that we know either the imaginary or real part of $w(t)$ along the real axis of the t -plane.

This boundary information can be converted into information about a related function $Q(t)$ so that $\operatorname{Im} [Q(t)]$ is known on the entire real axis. In the conversion process from $w(t)$ to $Q(t)$ we need an

auxiliary function $H(t)$ which makes the quotient $Q(t) = \frac{\omega(t)}{H(t)}$ satisfy the above requirement. The general form of $H(t)$ was given in (2.18). One such function $H(t)$ is

$$H(t) = -i\sqrt{t}. \quad (4.8)$$

For $H(t)$ to remain single-valued function, we assume $0 \leq \arg(t) \leq \pi$. Use of (4.7) and (4.8), we obtain

$$\text{Im} [Q(t)] = \begin{cases} 0, & t < 0 \\ \frac{1}{2} \left\{ \log \left[1 - \frac{2}{F^2} (y_2^2 - 1) \right] \right\} t^{-\frac{1}{2}}, & 0 < t < 1 \\ \frac{1}{2} \left\{ \log \left[1 - \frac{2}{F^2} (y_1^2 - 1) \right] \right\} t^{-\frac{1}{2}}, & t < 1. \end{cases} \quad (4.9)$$

Next, we examine the upstream condition. As we approach point F along the upper free surface, i.e., as $t \rightarrow \infty$, $H(t) = -i\sqrt{t}$ and $\omega(t) \rightarrow \log 1 = 0$. Therefore $Q(t) = \frac{\omega(t)}{H(t)} \rightarrow 0$, and from (2.17), $A_j = 0$, $j = 0, 1, 2, \dots, n$. Thus, (2.17) takes the form

$$Q(t) = \frac{1}{\pi} \int_{-\infty}^{\infty} \frac{\text{Im} [Q(\tau)]}{\tau - t} d\tau \quad (4.10)$$

Use of (2.14), we get

$$\begin{aligned} Q(t) = \frac{\omega(t)}{H(t)} &= \frac{\log q(t) + i[-\theta(t)]}{H(t)} \\ &= U(t) + iV(t) \end{aligned} \quad (4.11)$$

Writing (4.11) in details

$$\begin{array}{c}
 U(t) \\
 \hline
 \frac{-\log q^-(t)}{\sqrt{-t}} \quad \frac{\theta_2(t)}{\sqrt{t}} \quad \frac{\theta_1(t)}{\sqrt{t}} \\
 \hline
 V(t) \\
 \hline
 0 \quad \frac{\log q_2^-(t)}{\sqrt{t}} \quad \frac{\log q_1^-(t)}{\sqrt{t}} \\
 \hline
 t
 \end{array}
 \quad (4.12)$$

Using the Hilbert transformation relating the values on the real axis, of the real and imaginary parts of a function, analytic in the upper half-plane, given by (2.22) and (2.23), we obtain the following equations

$$\log q^-(t) = \frac{-\sqrt{-t}}{\pi} \left\{ \int_0^1 \frac{\log q_2^-(\tau)}{(\tau-t)\sqrt{\tau}} d\tau + \int_1^\infty \frac{\log q_1^-(\tau)}{(\tau-t)\sqrt{\tau}} d\tau \right\}, \quad t < 0 \quad (4.13)$$

$$\theta_2(t) = \frac{\sqrt{t}}{\pi} \left\{ \int_0^1 \frac{\log q_2^-(\tau)}{(\tau-t)\sqrt{\tau}} d\tau + \int_1^\infty \frac{\log q_1^-(\tau)}{(\tau-t)\sqrt{\tau}} d\tau \right\}, \quad 0 < t < 1 \quad (4.14)$$

$$\theta_1(t) = \frac{\sqrt{t}}{\pi} \left\{ \int_0^1 \frac{\log q_2^-(\tau)}{(\tau-t)\sqrt{\tau}} d\tau + \int_1^\infty \frac{\log q_1^-(\tau)}{(\tau-t)\sqrt{\tau}} d\tau \right\}, \quad t > 1 \quad (4.15)$$

$$\int_{-\infty}^0 \frac{\log q^-(\tau)}{(\tau-t)\sqrt{-\tau}} d\tau = \int_0^1 \frac{\theta_2(\tau)}{(\tau-t)\sqrt{\tau}} d\tau + \int_1^\infty \frac{\theta_1(\tau)}{(\tau-t)\sqrt{\tau}} d\tau, \quad t < 0 \quad (4.16)$$

$$\log q_2^-(t) = \frac{-\sqrt{t}}{\pi} \left\{ \int_{-\infty}^0 \frac{\log q^-(\tau)}{(\tau-t)\sqrt{-\tau}} d\tau + \int_0^1 \frac{\theta_2(\tau)}{(\tau-t)\sqrt{\tau}} d\tau + \int_1^{\infty} \frac{\theta_1(\tau)}{(\tau-t)\sqrt{\tau}} d\tau \right\},$$

$0 < t < 1$ (4.17)

$$\log q_1^-(t) = \frac{-\sqrt{t}}{\pi} \left\{ \int_{-\infty}^0 \frac{\log q^-(\tau)}{(\tau-t)\sqrt{-\tau}} d\tau + \int_0^1 \frac{\theta_2(\tau)}{(\tau-t)\sqrt{\tau}} d\tau + \int_1^{\infty} \frac{\theta_1(\tau)}{(\tau-t)\sqrt{\tau}} d\tau \right\},$$

$t > 1$ (4.18)

The singularities in (4.13) to (4.18) may be removed by using the result of Appendix [A] and noting that

$$\int_0^1 \frac{1}{(\tau-t)\sqrt{\tau}} d\tau = \frac{1}{\sqrt{t}} \log \left(\frac{1-\sqrt{t}}{1+\sqrt{t}} \right), \quad 0 < t < 1 \quad (4.19)$$

$$\int_1^{\infty} \frac{1}{(\tau-t)\sqrt{\tau}} d\tau = \frac{1}{\sqrt{t}} \log \left(\frac{\sqrt{t}+1}{\sqrt{t}-1} \right), \quad t > 1 \quad (4.20)$$

$$\int_{-\infty}^0 \frac{1}{(\tau-t)\sqrt{-\tau}} d\tau = 0, \quad t < 0 \quad (4.21)$$

For the solution of our problem we need only the following equations; (4.13), (4.14) and (4.15), and use (4.16) as a numerical check. Use of (4.19) to (4.21) and the result of Appendix [A] to remove singularities from (4.13) to (4.16), we get

$$\log q^-(t) = \frac{-\sqrt{-t}}{\pi} \left\{ \int_0^1 \frac{\log q_2^-(\tau)}{(\tau-t)\sqrt{\tau}} d\tau + \int_1^\infty \frac{\log q_1^-(\tau)}{(\tau-t)\sqrt{\tau}} d\tau \right\}, \quad t < 0 \quad (4.22)$$

$$\begin{aligned} \theta_2(t) = \frac{\sqrt{t}}{\pi} & \left\{ \int_0^1 \frac{\log q_2^-(\tau) - \log q_2^-(t)}{(\tau-t)\sqrt{\tau}} d\tau + \int_1^\infty \frac{\log q_1^-(\tau)}{(\tau-t)\sqrt{\tau}} d\tau \right\} \\ & + \frac{\log q_2^-(t)}{\pi} \log \left(\frac{1-\sqrt{t}}{1+\sqrt{t}} \right), \quad 0 < t < 1 \end{aligned} \quad (4.23)$$

$$\begin{aligned} \theta_1(t) = \frac{\sqrt{t}}{\pi} & \left\{ \int_0^1 \frac{\log q_2^-(\tau)}{(\tau-t)\sqrt{\tau}} d\tau + \int_1^\infty \frac{\log q_1^-(\tau) - \log q_1^-(t)}{(\tau-t)\sqrt{\tau}} d\tau \right\} \\ & + \frac{\log q_1^-(t)}{\pi} \log \left(\frac{\sqrt{t}+1}{\sqrt{t}-1} \right), \quad t > 1 \end{aligned} \quad (4.24)$$

$$\int_{-\infty}^0 \frac{\log q^-(\tau) - \log q^-(t)}{(\tau-t)\sqrt{-\tau}} d\tau = \int_0^1 \frac{\theta_2(\tau)}{(\tau-t)\sqrt{\tau}} d\tau + \int_1^\infty \frac{\theta_1(\tau)}{(\tau-t)\sqrt{\tau}} d\tau, \quad t < 0 \quad (4.25)$$

4.2. Solution of the Problem

The coordinates (x^-, y^-) of a point on the upper and lower free surfaces can be obtained by use of (4.3) and (4.5) as follows

$$z_1^*(t) = (x_0^* + i) + \int_{\infty}^t \frac{e^{i\theta_1(\tau)}}{q_1^*(\tau)} \frac{1}{\pi(1-\tau)} d\tau, \quad t > 1$$

Separating real and imaginary parts, we get $(x_1^*(t), y_1^*(t))$ for the upper free surface

$$x_1^*(t) = x_0^* + \frac{1}{\pi} \int_{\infty}^t \frac{\cos \theta_1(\tau)}{(1-\tau)q_1^*(\tau)} d\tau, \quad t > 1 \quad (4.26)$$

$$y_1^*(t) = 1 + \frac{1}{\pi} \int_{\infty}^t \frac{\sin \theta_1(\tau)}{(1-\tau)q_1^*(\tau)} d\tau, \quad t > 1 \quad (4.27)$$

For the lower free surface,

$$z_2^*(t) = \int_0^t \frac{e^{i\theta_2(\tau)}}{q_2^*(\tau)} \frac{1}{\pi(1-\tau)} d\tau, \quad 0 < t < 1$$

Separating real and imaginary parts, we get:

$$x_2^*(t) = \frac{1}{\pi} \int_0^t \frac{\cos \theta_2(\tau)}{(1-\tau)q_2^*(\tau)} d\tau, \quad 0 < t < 1 \quad (4.28)$$

$$y_2^*(t) = \frac{1}{\pi} \int_0^t \frac{\sin \theta_2(\tau)}{(1-\tau)q_2^*(\tau)} d\tau, \quad 0 < t < 1 \quad (4.29)$$

To determine the pressure at a point on the shelf, apply

Bernoulli's equation (2.6)

$$\frac{p}{\rho} + \frac{1}{2} q^2 = \frac{1}{2} U^2 + gh, \quad (4.30)$$

where q is the speed along the shelf.

Dividing (4.30) by $\frac{1}{2} U^2$ and rearranging the equation, we get

$$c_p = 1 + \frac{2}{F^2} - q^{-2}, \quad (4.31)$$

where

$$c_p = \frac{p}{\frac{1}{2} \rho U^2} \quad (4.32)$$

Now, summing up equations we need for a complete solution of the problem

(i) Along lower free surface $0 < t < 1$

$$q_2^2(t) = \left[1 - \frac{2}{F^2} (y_2^2(t) - 1) \right]^{1/2} \quad (4.2b)$$

$$\theta_2(t) = \frac{\sqrt{t}}{\pi} \left\{ \int_0^1 \frac{\log q_2^2(\tau) - \log q_2^2(t)}{(\tau-t)\sqrt{\tau}} d\tau + \int_1^\infty \frac{\log q_1^2(\tau)}{(\tau-t)\sqrt{\tau}} d\tau \right\} + \frac{\log q_2^2(t)}{\pi} \log \left(\frac{1-\sqrt{t}}{1+\sqrt{t}} \right) \quad (4.23)$$

$$y_2'(t) = \frac{1}{\pi} \int_0^t \frac{\sin \theta_2'(\tau)}{(1-\tau)q_2'(\tau)} d\tau \quad (4.29)$$

$$x_2'(t) = \frac{1}{\pi} \int_0^t \frac{\cos \theta_2'(\tau)}{(1-\tau)q_2'(\tau)} d\tau \quad (4.28)$$

(ii) Along upper free surface $t > 1$

$$q_1'(t) = [1 - \frac{2}{\sqrt{t}} (y_1'(t) - 1)]^{\frac{1}{2}} \quad (4.2a)$$

$$\theta_1(t) = \frac{\sqrt{t}}{\pi} \left\{ \int_0^1 \frac{\log q_2'(\tau)}{(\tau-t)\sqrt{\tau}} d\tau + \int_1^{\infty} \frac{\log q_1'(\tau) - \log q_1'(t)}{(\tau-t)\sqrt{\tau}} d\tau \right\} \\ + \frac{\log q_1'(t)}{\pi} \log \left(\frac{\sqrt{t}+1}{\sqrt{t}-1} \right) \quad (4.24)$$

$$y_1'(t) = 1 + \frac{1}{\pi} \int_{\infty}^t \frac{\sin \theta_1(\tau)}{(1-\tau)q_1'(\tau)} d\tau \quad (4.27)$$

$$x_1'(t) = x_0' + \frac{1}{\pi} \int_{\infty}^t \frac{\cos \theta_1(\tau)}{(1-\tau)q_1'(\tau)} d\tau \quad (4.26)$$

(iii) Along the boundary of the open channel (solid boundary) $t < 0$

$$\log q'(t) = \frac{-\sqrt{-t}}{\pi} \left\{ \int_0^1 \frac{\log q_2'(\tau)}{(\tau-t)\sqrt{\tau}} d\tau + \int_1^{\infty} \frac{\log q_1'(\tau)}{(\tau-t)\sqrt{\tau}} d\tau \right\} \quad (4.22)$$

$$c_p = 1 + \frac{2}{p^2} - q^{-2}(t) \quad (4.31)$$

(iv) For a numerical check

$$\int_{-\infty}^0 \frac{\log q'(\tau) - \log q'(t)}{(\tau-t)\sqrt{-\tau}} d\tau = \int_0^1 \frac{\theta_2(\tau)}{(\tau-t)\sqrt{\tau}} d\tau + \int_1^{\infty} \frac{\theta_1(\tau)}{(\tau-t)\sqrt{\tau}} d\tau, \quad t < 0 \quad (4.25)$$

4.3 Numerical Solution

To overcome the difficulty which arises from carrying out the numerical integration over an infinite range, we need some transformations for that purpose.

(i) For equation (4.23), use $\tau = \frac{1}{\tau_1}$ in the second term and write τ for τ_1 , we get

$$\theta_2(t) = \frac{\sqrt{t}}{\pi} \left\{ \int_0^1 \frac{\log q_2'(\tau) - \log q_2'(t)}{(\tau-t)\sqrt{\tau}} d\tau + \int_0^1 \frac{\log q_1'(\tau)}{(1-\tau t)\sqrt{\tau}} d\tau \right\} + \frac{\log q_2'(t)}{\pi} \log \left(\frac{1-\sqrt{t}}{1+\sqrt{t}} \right), \quad 0 < t < 1$$

(ii) The necessary equations for upper free surface:

use $t = \frac{1}{t_1}$, $\tau = \frac{1}{\tau_1}$, and write t, τ for t_1, τ_1 respectively.

$$Q_1^2(t) = \left[1 - \frac{2}{F^2} (Y_1(t) - 1) \right]^2$$

$$\theta_1(t) = \frac{\sqrt{t}}{\pi} \left\{ \int_0^1 \frac{\log q_2^2(\tau)}{(\tau t - 1)\sqrt{\tau}} d\tau - \int_0^1 \frac{\log Q_1^2(\tau) - \log Q_1^2(t)}{(\tau - t)\sqrt{\tau}} d\tau \right\}$$

$$+ \frac{\log Q_1^2(t)}{\pi} \log \left(\frac{1 + \sqrt{t}}{1 - \sqrt{t}} \right)$$

$$Y_1(t) = 1 + \frac{1}{\pi} \int_0^t \frac{\sin \theta_1(\tau)}{\tau(1-\tau)Q_1^2(\tau)} d\tau$$

$$X_1(t) = x_0 + \frac{1}{\pi} \int_0^t \frac{\cos \theta_1(\tau)}{\tau(1-\tau)Q_1^2(\tau)} d\tau$$

(iii) For equations satisfied along the solid boundary:

consider

$$t = \frac{-1}{\tan^2 \gamma}$$

$\tau = \frac{1}{\tau_1}$ for the second term and write τ for τ_1 , we get

$$\log Q^-(\gamma) = \frac{-\tan \gamma}{\pi} \left\{ \int_0^1 \frac{\log q_2^-(\tau)}{(1 + \tau \tan^2 \gamma) \sqrt{\tau}} d\tau + \int_0^1 \frac{\log Q_1^-(\tau)}{(\tau + \tan^2 \gamma) \sqrt{\tau}} d\tau \right\},$$

$$0 < \gamma < \pi/2$$

(iv) For equation used in numerical check:

Consider $t = \frac{-1}{\tan^2 \gamma}$,

$$\tau = \frac{-1}{\tan^2 \beta} \text{ for left side,}$$

$$\tau = \frac{1}{\tau_1} \text{ for second term on right side, and write}$$

τ for τ_1 , we get

$$\begin{aligned} -2 \int_0^{\pi/2} \frac{\log Q^-(\beta) - \log Q^-(\gamma)}{(\tan^2 \beta - \tan^2 \gamma)} \sec^2 \beta d\beta &= \int_0^1 \frac{\theta_2(\tau)}{(1 + \tau \tan^2 \gamma) \sqrt{\tau}} d\tau \\ &+ \int_0^1 \frac{\theta_1(\tau)}{(\tau + \tan^2 \gamma) \sqrt{\tau}} d\tau, \quad 0 < \gamma < \pi/2. \end{aligned}$$

Hence we have the following system of equations necessary to solve our problem, after dropping the dash, "-", sign and use big letters for variables:

(i) Along lower free surface

$$0 < t < 1$$

$$Q_2(t) = \left[1 - \frac{2}{F^2} (\gamma_2(t) - 1) \right]^{\frac{1}{2}} \quad (4.33)$$

$$\begin{aligned} \theta_2(t) = \frac{\sqrt{t}}{\pi} & \left\{ \int_0^1 \frac{\log Q_2(\tau) - \log Q_2(t)}{(\tau-t)\sqrt{\tau}} d\tau + \int_0^1 \frac{\log Q_1(\tau)}{(1-\tau)\sqrt{\tau}} d\tau \right\} \\ & + \frac{\log Q_2(t)}{\pi} \log \left(\frac{1-\sqrt{t}}{1+\sqrt{t}} \right) \end{aligned} \quad (4.34)$$

$$\gamma_2(t) = \frac{1}{\pi} \int_0^t \frac{\sin \theta_2(\tau)}{(1-\tau)Q_2(\tau)} d\tau \quad (4.35)$$

$$\chi_2(t) = \frac{1}{\pi} \int_0^t \frac{\cos \theta_2(\tau)}{(1-\tau)Q_2(\tau)} d\tau \quad (4.36)$$

(ii) Along upper free surface

$$0 < t < 1$$

$$Q_1(t) = \left[1 - \frac{2}{F^2} (\gamma_1(t) - 1) \right]^{\frac{1}{2}} \quad (4.37)$$

$$\begin{aligned} \theta_1(t) = \frac{\sqrt{t}}{\pi} & \left\{ \int_0^1 \frac{\log Q_2(\tau)}{(\tau-1)\sqrt{\tau}} d\tau - \int_0^1 \frac{\log Q_1(\tau) - \log Q_1(t)}{(\tau-t)\sqrt{\tau}} d\tau \right\} \\ & + \frac{\log Q_1(t)}{\pi} \log \left(\frac{1+\sqrt{t}}{1-\sqrt{t}} \right) \end{aligned} \quad (4.38)$$

$$Y_1(t) = 1 + \frac{1}{\pi} \int_0^t \frac{\sin \theta_1(\tau)}{\tau(1-\tau)Q_1(\tau)} d\tau \quad (4.39)$$

$$X_1 = x_0 + \frac{1}{\pi} \int_0^t \frac{\cos \theta_1(\tau)}{\tau(1-\tau)Q_1(\tau)} d\tau \quad (4.40)$$

(iii) Along the solid boundary $0 < \gamma < \pi/2$

$$\log Q(\gamma) = \frac{-\tan \gamma}{\pi} \left\{ \int_0^1 \frac{\log Q_2(\tau)}{(1+\tau \tan^2 \gamma)\sqrt{\tau}} d\tau + \int_0^1 \frac{\log Q_1(\tau)}{(\tau + \tan^2 \gamma)\sqrt{\tau}} d\tau \right\} \quad (4.41)$$

$$c_p = 1 + \frac{2}{Fz} - Q^2(\gamma) \quad (4.42)$$

(iv) For a numerical check $0 < \gamma < \pi/2$

$$\begin{aligned} -2 \int_0^{\pi/2} \frac{\log Q(\beta) - \log Q(\gamma)}{(\tan^2 \beta - \tan^2 \gamma)} \sec^2 \beta d\beta &= \int_0^1 \frac{\theta_2(\tau)}{(1+\tau \tan^2 \gamma)\sqrt{\tau}} d\tau \\ &+ \int_0^1 \frac{\theta_1(\tau)}{(\tau + \tan^2 \gamma)\sqrt{\tau}} d\tau \end{aligned} \quad (4.43)$$

Now, equation (4.33) should give an expression for $\theta_2(t)$, which found on the left side of the equation. But $Q_1(t)$ and $Q_2(t)$ appear in the numerator of the integrand on the right side of the equation. Equations (4.33) and (4.37) which should give expressions for $Q_2(t)$

and $Q_1(t)$, respectively, in turn are functions in $Y_2(t)$ and $Y_1(t)$ which are originally unknowns. Equations (4.35), (4.36), (4.39) and (4.40) can not give an expression for the free surfaces profile unless an expression for $\theta_2(t)$, $Q_2(t)$, $\theta_1(t)$, and $Q_1(t)$ are determined. Finally knowing $Q_1(t)$ and $Q_2(t)$ are essential for equation (4.41).

These equations are of such complexity that most analytical methods of integral equations theory are not useful. Our way to solve these equations is to apply iteration method, on condition that we have to find initially a good approximation for the unknown quantities, since the successive-approximation scheme often converges only if the initial approximation is sufficiently close to the final solution, see Scarborough [45].

Then, if the problem has been properly formulated, and the initial approximation has been correctly chosen, it should be possible successively to improve upon the initial approximation until, after a sufficient number of improvements, the correct solution, for a specific degree of accuracy, to the gravity problem is indeed found. In our iteration method the complete solution is computed in each cycle.

The iterative procedure works in the following manner:

(i) Initial approximation will be found from non-gravity case, $g = 0$, which gives

$$Y_1^{(0)} = 1.0, \quad Y_2^{(0)} = 0$$

following the same starting as Southwell and Vaisey [50].

(ii) Using the input data from step (i), $\gamma_2^{(0)}$ in equation (4.33) and $\gamma_1^{(0)}$ in equation (4.37), we find an expression for $Q_2^{(1)}$ and $Q_1^{(1)}$ respectively.

(iii) Use $Q_1^{(1)}$ and $Q_2^{(1)}$ in (4.34) and (4.38) to find out $\theta_2^{(1)}$ and $\theta_1^{(1)}$.

(iv) Use $Q_2^{(1)}$ and $\theta_2^{(1)}$ in (4.35) and (4.36) to find out $\gamma_2^{(1)}$ and $x_2^{(1)}$ respectively.

(v) Use $Q_1^{(1)}$ and $\theta_1^{(1)}$ in (4.39) to (4.40) to calculate $\gamma_1^{(1)}$ and $x_1^{(1)}$ respectively.

(vi) Another gravity solution is obtained using the data from steps (iv) and (v), $\gamma_1^{(1)}$ and $\gamma_2^{(1)}$.

(vii) Steps (iii) to (v) are repeated until the results to two successive iterations differ by less than some specified small number 10^{-k} , where $k = 4$ or 6 , at this point we stop the iterations and the gravity solution is obtained.

(viii) At each iteration check the validity of equation (4.43) to be satisfied by the numerical figures.

(ix) Use final solution of Q_1 and Q_2 in equation (4.41) to find Q along the solid boundary.

(x) Apply Q in equation (4.42) to find out the pressure coefficient on the solid boundary.

4.4 Numerical Results and Discussions

The dimensionless variables X_1 , Y_1 along FD and X_2 , Y_2 along BC are given in 4.40, 4.39, 4.36 and 4.35 respectively. Tables 4.1 to 4.5 show some free surfaces, which are plotted in Figs. 4.5 to 4.8, keeping the Froude number F fixed. Table 4.5 shows the distribution of the values of C_p along the shelf for different values of F , and is plotted in Fig. 4.12.

After an initial guess, (the non-gravity case, Y_1 along FD and Y_2 along BC), we start the iterative procedure. The iterative procedure becomes stable after the third iteration, and in the fourth iteration it produces 3 significant decimal places for the lower free surface and 2 significant decimal places for the upper one. We need 7 iterations to produce 5 significant decimal places for the lower free surface and 4 significant decimal places for the upper one.

It is found that when the numerical check is carried out, equation 4.43 is satisfied with error between 0.015 to 0.041.

It should also be mentioned that with a 300 points of divisions. The CPU time for each iteration was approximately 1.774 minutes using an IBM 3031 computer, FORTRAN IV level G.

Finally we conclude that the solution can be improved by using more points and/or double precision arithmetic in the computer. However, both of these would involve substantial increases in time and cost.

4.5 Comparison with Previous Work

In order to compare our results with experimental data produced by Rouse, it is necessary that the numerical results for the critical approach flow must be employed. This comparison is shown in Fig. 4.10 where results by Chow and Han [10] from hodograph method and results by Southwell and Vaisey [50] from relaxational calculations are also presented. It is obvious that the present numerical results yield a very good result when compared with Rouse's experimental data.

It has been mentioned previously that Clarke [12] has obtained solutions of this problem for flows with large approaching Froude numbers. In order to see how his solution relates to the present numerical calculations, Fig. 4.11 presents his results obtained for the condition of $F = \sqrt{20}$ and the corresponding numerical results from the present scheme. It is apparent that these results agree closely with each other near the crest. Further downstream, however, Clarke's solution seems to give a thinner jet and the disagreement is expected to become worse far downstream. This may suggest that higher-order terms are needed in Clarke's solution to achieve better agreement in the downstream flow region.

CHAPTER V

FLOW FROM UNIFORM CHANNEL OVER

SHARP-CRESTED WEIR

- 5.1 Formulation of the Problem
- 5.2 Solution of the Problem
- 5.3 Numerical Solution
- 5.4 Numerical Results and Discussions

5.1 Formulation of the Problem

An inviscid, incompressible fluid in two-dimensions flows along a flat shelf AB at a depth h with uniform velocity U_0 . It then encounters an inclined plane BC at inclination angle α and its length is L . The fluid then flows down the sharp edge of the weir under the influence of gravity. See Fig. 5.1.

As the flow far upstream is supposed uniform and hence irrotational, and viscosity is absent then it is always irrotational and so there exists a velocity potential ϕ . Also as the fluid is incompressible there exists a stream function ψ . Accordingly the equations of motion are well-known

$$\nabla^2 \phi = 0 ; \quad \nabla^2 \psi = 0 . \quad (5.1)$$

Unfortunately we do not know the location of the free surfaces a priori, but the fact that along the streamline, ψ is constant allows us to denote the upper free surface FE by $\psi = \text{constant}$; similarly ψ is also a constant on the solid boundary ABC and lower free surface CD. See Fig. 5.1.

The flow domain in (ϕ, ψ) -plane, as it is shown in Fig. 5.2 is the infinite strip $-\infty \leq \phi \leq \infty$; $U_0 h \leq \psi \leq 0$. Here we have designated the upper free surface $\psi = U_0 h$, as $U_0 h$ is the flux, the solid boundary and the lower free surface becoming $\psi = 0$. For convenience, we choose B to be the origin in the Z -plane, the x -axis from left to right and the y -axis upward.

Along the upper free surface q_1 , y_1 , θ_1 are the speed of the fluid, the vertical distance between a point on the free surface and some reference elevation, and the angle of inclination of the velocity with the horizontal, respectively. Similar definitions apply to q_2 , y_2 , and θ_2 along the lower free surface.

The boundary conditions are that the normal velocity vanishes on the solid surface and that the pressure is continuous across the free surfaces. As we shall measure the pressure relative to that outside the fluid region, the condition on the free surface becomes that the pressure, p , vanishes.

As the flow is irrotational we have the Bernoulli equation (2.6). Non-dimensional variables are defined in (2.8), and in our problem

$$\left. \begin{aligned} z_i' &= \frac{z_i}{h} , \\ q_i' &= \frac{q_i}{U_0} , \\ w' &= \frac{w}{\psi_1} , \end{aligned} \right\} \quad (5.2)$$

where $i = 1, 2$, and "1" for upper free surface and "2" for lower free surface, $\psi_1 = hU_0$.

In dimensionless form, the free surface condition along the upper and lower free surfaces, respectively, are

$$q_1'^2 + \frac{2}{F^2} (y_1' - 1) = 1 , \quad (5.3a)$$

$$q_2^2 + \frac{2}{F^2} (y_2 - 1) = 1, \quad (5.3b)$$

where the Froude number F was defined in (2.10).

The upper free surface, in dimensionless variables is denoted by $\psi_1 = 1$, while the lower free surface by $\psi_0 = 0$, as shown in Fig. 5.3.

The dimensionless physical variable Z' in terms of two function W' , ω was given in (2.15), that is

$$Z' = \int e^{-\omega} dW'. \quad (5.4)$$

If we can express the two functions W' and ω as functions of a single variable t , then the integral in (5.4) could be carried out.

(i) To express the function W' as a function of t :

Conformal mapping given by (2.16) helps us to find out that expression for W' . This mapping maps the fluid region in the W' -plane into the upper half-plane, the t -plane, and the boundary of the fluid region onto the real axis, the boundary of the t -plane (see Fig. 5.4). To ensure the uniqueness of the mapping, we choose three corresponding points in the following ways,

$$\left. \begin{array}{l} B: \quad W' = 0, \quad t = 0, \\ A, F: \quad W' \rightarrow -\infty, \quad t = -1, \\ D, E: \quad W' \rightarrow \infty, \quad t \rightarrow \infty. \end{array} \right\} \quad (5.5)$$

The mapping is

$$W' (t) = \frac{1}{\pi} \log (1+t). \quad (5.6)$$

For $W(t)$ to remain single-valued function, we assume

$$0 \leq \arg(1+t) \leq \pi \quad (5.7)$$

(ii) To express the function ω as a function of t :

Hilbert's method for a mixed boundary value problem in the upper half-plane enables us to find out that expression.

The general solution of the Hilbert problem for an analytic function $Q(t)$ in the upper-half plane was given by (2.17).

Now, we try to relate the function $\omega(t)$ to the function $Q(t)$. From (2.17), we find that $Q(t)$ is expressed in terms of the imaginary part of $Q(t)$ along the boundary of the t -plane.

Thus, we have to examine the value of $\omega(t)$ along the boundary of the t -plane, we find that

$$\left. \begin{aligned} \operatorname{Re} [\omega(t)] &= \frac{1}{2} \log \left[1 - \frac{2}{F^2} (y_1^2(t) - 1) \right], & t < -1 \\ \operatorname{Im} [\omega(t)] &= 0, & -1 < t < 0 \\ \operatorname{Im} [\omega(t)] &= -\alpha, & 0 < t < 1 \\ \operatorname{Re} [\omega(t)] &= \frac{1}{2} \log \left[1 - \frac{2}{F^2} (y_2^2(t) - 1) \right], & t > 1 \end{aligned} \right\} \quad (5.8)$$

This boundary information can be converted into information about a related function $Q(t)$ so that $\operatorname{Im} [Q(t)]$ is known on the entire real axis. In the conversion process from $\omega(t)$ to $Q(t)$ we need an auxiliary function $H(t)$ which makes the quotient $Q(t) = \frac{\omega(t)}{H(t)}$ satisfies the above requirement.

The general form of $H(t)$ was given in (2.18).

One such function $H(t)$ is

$$H(t) = -i [(t+1)(t-1)]^{-\frac{1}{2}}. \quad (5.9)$$

A branch cut on the real axis interval $(-1, 1)$ insures that $H(t)$ is single-valued.

Use of (5.8) and (5.9), we obtain

$$\text{Im}[Q(t)] = \begin{cases} \frac{1}{2} \left\{ \log \left[1 - \frac{2}{F^2} (y_1'(t)-1) \right] \right\} [-(t+1)(1-t)]^{-\frac{1}{2}}, & t < -1 \\ 0 & -1 < t < 0 \\ -\alpha [(t+1)(1-t)]^{-\frac{1}{2}} & 0 < t < 1 \\ \frac{1}{2} \left\{ \log \left[1 - \frac{2}{F^2} (y_2'(t)-1) \right] \right\} [(t+1)(t-1)]^{-\frac{1}{2}}, & t > 1 \end{cases} \quad (5.10)$$

Now, let us examine the behaviour of $Q(t)$ as $t \rightarrow \infty$. As $t \rightarrow \infty$, $H(t) \sim -it$ and $q(t) \sim [\log(1+t)]^{1/3}$, $\theta(t)$ is bounded, therefore $\omega(t) \sim [\log(1+t)]^{1/3} + i \text{ constant}$. Hence $Q(t) = \frac{\omega(t)}{H(t)} \rightarrow 0$ and $t \rightarrow \infty$, and from (2.17), $A_j = 0$, $j = 0, 1, \dots, n$. Thus (2.17) takes the form

$$Q(t) = \frac{1}{\pi} \int_{-\infty}^{\infty} \frac{\text{Im}[Q(\tau)]}{\tau-t} d\tau. \quad (5.11)$$

Use of (2.14), we get

$$\begin{aligned} Q(t) &= \frac{\omega(t)}{H(t)} = \frac{\log q^-(t) + i[-\theta(t)]}{H(t)} \\ &= U(t) + iV(t) \end{aligned} \quad (5.12)$$

Writing (5.12) in details

$$\begin{array}{c|ccc}
 U(t) & \frac{-\theta_1(t)}{\sqrt{-(t+1)(1-t)}} & \frac{\log q_1(t)}{\sqrt{(t+1)(1-t)}} & \frac{\theta_2(t)}{\sqrt{(t+1)(t-1)}} \\
 \hline
 V(t) & \frac{-\log q_1(t)}{\sqrt{-(t+1)(1-t)}} & \frac{-\theta(t)}{\sqrt{(t+1)(1-t)}} & \frac{\log q_2(t)}{\sqrt{(t+1)(t-1)}}
 \end{array} \quad t \quad (5.13)$$

where

$$q(t) = \begin{cases} q_H(t)^* & , -1 < t < 0 , \\ q_W(t)^{**} & , 0 < t < 1 , \end{cases}$$

and

$$\theta(t) = \begin{cases} 0 & , -1 < t < 0 , \\ \alpha & , 0 < t < 1 . \end{cases}$$

Using the Hilbert transformation relating the values on the real axis, of the real and imaginary parts of a function, analytic in the upper half-plane, given by (2.22) and (2.23), we obtain the following equations

* q_H : speed of the flow along the flat plane AB.

** q_W : speed of the flow along the weir BC.

$$\theta_1(t) = \frac{\sqrt{t^2-1}}{\pi} \left\{ \int_{-\infty}^{-1} \frac{-\log q_1^*(\tau)}{(\tau-t)\sqrt{\tau^2-1}} d\tau + \int_0^1 \frac{-\alpha}{(\tau-t)\sqrt{1-\tau^2}} d\tau \right. \\ \left. + \int_1^{\infty} \frac{\log q_2^*(\tau)}{(\tau-t)\sqrt{\tau^2-1}} d\tau \right\}, \quad t < -1 \quad (5.14)$$

$$\log q_H^*(t) = \frac{\sqrt{1-t^2}}{\pi} \left\{ \int_{-\infty}^{-1} \frac{-\log q_1^*(\tau)}{(\tau-t)\sqrt{\tau^2-1}} d\tau + \int_0^1 \frac{-\alpha}{(\tau-t)\sqrt{1-\tau^2}} d\tau \right. \\ \left. + \int_1^{\infty} \frac{\log q_2^*(\tau)}{(\tau-t)\sqrt{\tau^2-1}} d\tau \right\}, \quad -1 < t < 0 \quad (5.15)$$

$$\log q_W^*(t) = \frac{\sqrt{1-t^2}}{\pi} \left\{ \int_{-\infty}^{-1} \frac{-\log q_1^*(\tau)}{(\tau-t)\sqrt{\tau^2-1}} d\tau + \int_0^1 \frac{-\alpha}{(\tau-t)\sqrt{1-\tau^2}} d\tau \right. \\ \left. + \int_1^{\infty} \frac{\log q_2^*(\tau)}{(\tau-t)\sqrt{\tau^2-1}} d\tau \right\}, \quad 0 < t < 1 \quad (5.16)$$

$$\theta_2(t) = \frac{\sqrt{t^2-1}}{\pi} \left\{ \int_{-\infty}^{-1} \frac{-\log q_1^*(\tau)}{(\tau-t)\sqrt{\tau^2-1}} d\tau + \int_0^1 \frac{-\alpha}{(\tau-t)\sqrt{1-\tau^2}} d\tau \right. \\ \left. + \int_1^{\infty} \frac{\log q_2^*(\tau)}{(\tau-t)\sqrt{\tau^2-1}} d\tau \right\}; \quad t > 1 \quad (5.17)$$

$$\log q_1^*(\tau) = \frac{\sqrt{t^2-1}}{\pi} \left\{ \int_{-\infty}^{-1} \frac{-\theta_1(\tau)}{(\tau-t)\sqrt{\tau^2-1}} d\tau + \int_{-1}^0 \frac{\log q_H^*(\tau)}{(\tau-t)\sqrt{1-\tau^2}} d\tau + \int_0^1 \frac{\log q_W^*(\tau)}{(\tau-t)\sqrt{1-\tau^2}} d\tau + \int_1^{\infty} \frac{\theta_2(\tau)}{(\tau-t)\sqrt{\tau^2-1}} d\tau \right\}, t < -1 \quad (5.18)$$

$$0 = \int_{-\infty}^{-1} \frac{-\theta_2(\tau)}{(\tau-t)\sqrt{\tau^2-1}} d\tau + \int_{-1}^0 \frac{\log q_H^*(\tau)}{(\tau-t)\sqrt{1-\tau^2}} d\tau + \int_0^1 \frac{\log q_W^*(\tau)}{(\tau-t)\sqrt{1-\tau^2}} d\tau + \int_1^{\infty} \frac{\theta_2(\tau)}{(\tau-t)\sqrt{\tau^2-1}} d\tau, -1 < t < 0 \quad (5.19)$$

$$\alpha = \frac{\sqrt{1-t^2}}{\pi} \left\{ \int_{-\infty}^{-1} \frac{-\theta_1(\tau)}{(\tau-t)\sqrt{\tau^2-1}} d\tau + \int_{-1}^0 \frac{\log q_H^*(\tau)}{(\tau-t)\sqrt{1-\tau^2}} d\tau + \int_0^1 \frac{\log q_W^*(\tau)}{(\tau-t)\sqrt{1-\tau^2}} d\tau + \int_1^{\infty} \frac{-\theta_2(\tau)}{(\tau-t)\sqrt{\tau^2-1}} d\tau \right\}, 0 < t < 1 \quad (5.20)$$

$$\log q_2^*(t) = \frac{-\sqrt{t^2-1}}{\pi} \left\{ \int_{-\infty}^{-1} \frac{-\theta_1(\tau)}{(\tau-t)\sqrt{\tau^2-1}} d\tau + \int_{-1}^0 \frac{\log q_H^*(\tau)}{(\tau-t)\sqrt{1-\tau^2}} d\tau + \int_0^1 \frac{\log q_W^*(\tau)}{(\tau-t)\sqrt{1-\tau^2}} d\tau + \int_1^{\infty} \frac{\theta_2(\tau)}{(\tau-t)\sqrt{\tau^2-1}} d\tau \right\}, t > 1 \quad (5.21)$$

The singularities in (5.14) to (5.21) may be removed by using the result of Appendix [A] and the following identities

$$\int_{-\infty}^{-1} \frac{1}{(\tau-t)\sqrt{\tau^2-1}} d\tau = \frac{-1}{\sqrt{t^2-1}} \log \left(\frac{\sqrt{\frac{t-1}{t+1}} - 1}{\sqrt{\frac{t-1}{t+1}} + 1} \right), \quad t < -1 \quad (5.22)$$

$$\int_0^1 \frac{1}{(\tau-t)\sqrt{1-\tau^2}} d\tau = \frac{-1}{\sqrt{1-t^2}} \log \left(\frac{\sqrt{\frac{1+t}{1-t}} - 1}{\sqrt{\frac{1+t}{1-t}} + 1} \right), \quad 0 < t < 1 \quad (5.23)$$

$$\int_1^{\infty} \frac{1}{(\tau-t)\sqrt{\tau^2-1}} d\tau = \frac{1}{\sqrt{t^2-1}} \log \left(\frac{\sqrt{\frac{t+1}{t-1}} - 1}{\sqrt{\frac{t+1}{t-1}} + 1} \right), \quad t > 1 \quad (5.24)$$

$$\int_0^1 \frac{1}{(\tau-t)\sqrt{1-\tau^2}} d\tau = \frac{2}{\sqrt{t^2-1}} \tan^{-1} \left(\sqrt{\frac{-(t+1)}{1-t}} \right), \quad t < -1 \quad (5.25)$$

$$\int_0^1 \frac{1}{(\tau-t)\sqrt{1-\tau^2}} d\tau = \frac{-1}{\sqrt{1-t^2}} \log \left(\frac{-1 + \sqrt{\frac{1-t}{1+t}}}{1 + \sqrt{\frac{1-t}{1+t}}} \right), \quad -1 < t < 0 \quad (5.26)$$

$$\int_{-1}^0 \frac{1}{(\tau-t)\sqrt{1-\tau^2}} d\tau = \frac{1}{\sqrt{1-t^2}} \log \left(\frac{-1 + \sqrt{\frac{1+t}{1-t}}}{1 + \sqrt{\frac{1+t}{1-t}}} \right), \quad -1 < t < 0 \quad (5.27)$$

For the solution of our problem we need only the following equations; (5.14) to (5.17) and use (5.19) as a numerical check.

Use of (5.22) to (5.27) and the result of Appendix [A] in (5.14) to (5.17) and (5.19) we get

$$\begin{aligned} \theta_1(t) &= \frac{\sqrt{t^2-1}}{\pi} \left\{ \int_{-\infty}^{-1} \frac{\log q_1^-(\tau) - \log q_1^-(t)}{(\tau-t)\sqrt{\tau^2-1}} d\tau - \int_1^{\infty} \frac{\log q_2^-(\tau)}{(\tau-t)\sqrt{\tau^2-1}} d\tau \right\} \\ &= \frac{\log q_1^-(t)}{\pi} \log \left(\frac{\sqrt{\frac{t-1}{t+1}} - 1}{\sqrt{\frac{t-1}{t+1}} + 1} \right) + \frac{2\alpha}{\pi} \tan^{-1} \sqrt{\frac{-(1+t)}{1-t}}, \quad t < -1 \end{aligned} \quad (5.28)$$

$$\begin{aligned} \log q_H^+(t) &= \frac{\sqrt{1-t^2}}{\pi} \left\{ - \int_{-\infty}^{-1} \frac{\log q_1^+(\tau)}{(\tau-t)\sqrt{\tau^2-1}} d\tau + \int_1^{\infty} \frac{\log q_2^+(\tau)}{(\tau-t)\sqrt{\tau^2-1}} d\tau \right\} \\ &+ \frac{\alpha}{\pi} \log \left(\frac{-1 + \sqrt{\frac{1-t}{1+t}}}{1 + \sqrt{\frac{1-t}{1+t}}} \right), \quad -1 < t < 0 \end{aligned} \quad (5.29)$$

$$\begin{aligned} \log q_W^+(t) &= \frac{\sqrt{1-t^2}}{\pi} \left\{ - \int_{-\infty}^{-1} \frac{\log q_1^+(\tau)}{(\tau-t)\sqrt{\tau^2-1}} d\tau + \int_1^{\infty} \frac{\log q_2^+(\tau)}{(\tau-t)\sqrt{\tau^2-1}} d\tau \right\} + \frac{\alpha}{\pi} \log \left(\frac{\sqrt{\frac{1+t}{1-t}} - 1}{\sqrt{\frac{1+t}{1-t}} + 1} \right), \\ &0 < t < 1 \end{aligned} \quad (5.30)$$

$$\theta_2(t) = \frac{\sqrt{t^2-1}}{\pi} \left\{ - \int_{-\infty}^{-1} \frac{\log q_1^*(\tau)}{(\tau-t)\sqrt{\tau^2-1}} d\tau + \int_1^{\infty} \frac{\log q_2^*(\tau) - \log q_2^*(t)}{(\tau-t)\sqrt{\tau^2-1}} d\tau \right\} \\ + \frac{2\alpha}{\pi} \tan^{-1} \sqrt{\frac{t+1}{t-1}} + \frac{\log q_2^*(t)}{\pi} \log \left(\frac{\sqrt{\frac{t+1}{t-1}} - 1}{\sqrt{\frac{t+1}{t-1}} + 1} \right), \quad t > 1 \quad (5.31)$$

$$0 = - \int_{-\infty}^{-1} \frac{\theta_1(\tau)}{(\tau-t)\sqrt{\tau^2-1}} d\tau + \int_{-1}^0 \frac{\log q_H^*(\tau) - \log q_H^*(t)}{(\tau-t)\sqrt{1-\tau^2}} d\tau + \int_0^1 \frac{\log q_W^*(\tau)}{(\tau-t)\sqrt{1-\tau^2}} d\tau \\ + \int_1^{\infty} \frac{\theta_2(\tau)}{(\tau-t)\sqrt{\tau^2-1}} d\tau + \log q_H^*(t) \log \left(\frac{1 + \sqrt{\frac{1+t}{1-t}}}{1 + \sqrt{\frac{1-t}{1+t}}} \right), \quad -1 < t < 0 \quad (5.32)$$

5.2 Solution of the Problem

The coordinates (x', y') of a point on the upper and lower free surfaces can be obtained by use of (5.4) and (5.6) as follows

$$Z_1^*(t) = (x_0' + i) + \frac{1}{\pi} \int_{-1}^t \frac{e^{i\theta_1(\tau)}}{(\tau+1)q_1^*(\tau)} d\tau, \quad t < -1$$

Separating real and imaginary parts, we get $(x_1^*(t), y_1^*(t))$ for the upper free surface

$$x_1'(t) = x_0' + \frac{1}{\pi} \int_{-1}^t \frac{\cos \theta_1(\tau)}{(\tau+1)q_1'(\tau)} d\tau, \quad t < -1 \quad (5.33)$$

$$y_1'(t) = 1 + \frac{1}{\pi} \int_{-1}^t \frac{\sin \theta_1(\tau)}{(\tau+1)q_1'(\tau)} d\tau, \quad t < -1 \quad (5.34)$$

For the lower free surface,

$$Z_2'(t) = \ell' e^{i\alpha} + \frac{1}{\pi} \int_1^t \frac{e^{i\theta_2(\tau)}}{(\tau+1)q_2'(\tau)} d\tau, \quad t > 1$$

Separating real and imaginary parts, we get $\{x_2'(t), y_2'(t)\}$ for the lower free surface

$$x_2'(t) = \ell' \cos \alpha + \frac{1}{\pi} \int_1^t \frac{\cos \theta_2(\tau)}{(\tau+1)q_2'(\tau)} d\tau, \quad t > 1 \quad (5.35)$$

$$y_2'(t) = \ell' \sin \alpha + \frac{1}{\pi} \int_1^t \frac{\sin \theta_2(\tau)}{(\tau+1)q_2'(\tau)} d\tau, \quad t > 1 \quad (5.36)$$

The length ℓ' of the inclined plane BC can be obtained by use of (5.4) and (5.6) as follows

$$Z'(t) = Z_0' + \frac{1}{\pi} \int_{t_0}^t \frac{e^{i\theta(\tau)}}{(\tau+1)q'(\tau)} d\tau,$$

along BC: $\theta = \alpha$, $q' = q_w'$, $t_0 = 0$, $t = 1$,

Hence,

$$\begin{aligned} Z'(t) - Z_0' &= \frac{1}{\pi} \int_0^1 \frac{e^{i\alpha}}{(\tau+1)q_w'(\tau)} d\tau \\ &= \varepsilon' e^{i\alpha} \end{aligned}$$

Therefore

$$\varepsilon' = \frac{1}{\pi} \int_0^1 \frac{1}{(\tau+1)q_w'(\tau)} d\tau \quad (5.37)$$

To determine the pressure at points along the flat shelf and the inclined plane BC using Bernoulli's equation (2.6)

$$\begin{aligned} \frac{p}{\rho} + \frac{1}{2} q_b^2 + g y_b &= \text{constant} \\ &= \frac{1}{2} U_0^2 + g h, \end{aligned} \quad (5.38)$$

where q_b is the speed of the flow along the bottom.

Dividing (5.38) by $\frac{1}{2} U_0^2$ and rearranging the equation, we get

$$c_p = 1 - \frac{2}{F^2} (y_b' - 1) - q_b'^2, \quad (5.39)$$

where $c_p = \frac{p}{\frac{1}{2} \rho U_0^2}$,

$$y_b^- = \begin{cases} 0 & \text{along AB,} \\ y_l^- & \text{along BC,} \end{cases}$$

and

$$q_b^- = \begin{cases} q_H^- & \text{along AB,} \\ q_W^- & \text{along BC.} \end{cases}$$

(5.40)

Now, summing up equations we need for a complete solution for our problem

(i) Along lower free surface $t > 1$

$$q_2^-(t) = \left[1 - \frac{2}{F^2} (y_2^-(t) - 1) \right]^{3/2} \quad (5.3b)$$

$$\theta_2(t) = \frac{\sqrt{t^2-1}}{\pi} \left\{ - \int_{-\infty}^{-1} \frac{\log q_1^-(\tau)}{(\tau-t)\sqrt{\tau^2-1}} d\tau + \int_1^{\infty} \frac{\log q_2^-(\tau) - \log q_2^-(t)}{(\tau-t)\sqrt{\tau^2-1}} d\tau \right\} \\ + \frac{2\alpha}{\pi} \tan^{-1} \sqrt{\frac{t+1}{t-1}} + \frac{\log q_2^-(t)}{\pi} \log \left(\frac{\sqrt{\frac{t+1}{t-1}} - 1}{\sqrt{\frac{t+1}{t-1}} + 1} \right) \quad (5.31)$$

$$y_2^*(t) = \varepsilon' \sin \alpha + \frac{1}{\pi} \int_1^t \frac{\sin \theta_2(\tau)}{(\tau+1)q_2^*(\tau)} d\tau \quad (5.36)$$

$$x_2(t) = \varepsilon' \cos \alpha + \frac{1}{\pi} \int_1^t \frac{\cos \theta_2(\tau)}{(\tau+1)q_2^*(\tau)} d\tau \quad (5.35)$$

(ii) Along upper free surface $t < -1$

$$q_1^*(t) = [1 - \frac{2}{\beta^2} (y_1^*(t) - 1)]^{\frac{1}{2}} \quad (5.3a)$$

$$\theta_1(t) = \frac{\sqrt{t^2+1}}{\pi} \left\{ \int_{-\infty}^{-1} \frac{\log q_1^*(\tau) - \log q_1^*(t)}{(\tau-t)\sqrt{\tau^2-1}} d\tau - \int_1^{\infty} \frac{\log q_2^*(\tau)}{(\tau-t)\sqrt{\tau^2-1}} d\tau \right\} \\ - \frac{\log q_1^*(t)}{\pi} \log \left(\frac{\sqrt{\frac{t-1}{t+1}} - 1}{\sqrt{\frac{t-1}{t+1}} + 1} \right) + \frac{2\alpha}{\pi} \tan^{-1} \sqrt{\frac{t+1}{t-1}} \quad (5.28)$$

$$y_1^*(t) = 1 + \frac{1}{\pi} \int_{-1}^t \frac{\sin \theta_1(\tau)}{(\tau+1)q_1^*(\tau)} d\tau \quad (5.34)$$

$$x_1^*(t) = x_0 + \frac{1}{\pi} \int_{-1}^t \frac{\cos \theta_1(\tau)}{(\tau+1)q_1^*(\tau)} d\tau \quad (5.33)$$

(iii) Along the flat shelf

$$-1 < t < 0$$

$$\log q_H^-(t) = \frac{\sqrt{1-t^2}}{\pi} \left\{ - \int_{-\infty}^{-1} \frac{\log q_1^-(\tau)}{(\tau-t)\sqrt{\tau^2-1}} d\tau + \int_1^{\infty} \frac{\log q_2^-(\tau)}{(\tau-t)\sqrt{\tau^2-1}} d\tau \right\}$$

$$+ \frac{\alpha}{\pi} \log \left(\frac{-1 + \sqrt{\frac{1-t}{1+t}}}{1 + \sqrt{\frac{1-t}{1+t}}} \right) \quad (5.29)$$

$$c_p = 1 + \frac{2}{F^2} - q_H^{-2}(t) \quad (5.41)$$

(iv) Along the inclined plane

$$0 < t < 1$$

$$\log q_W^-(t) = \frac{\sqrt{1-t^2}}{\pi} \left\{ - \int_{-\infty}^{-1} \frac{\log q_1^-(\tau)}{(\tau-t)\sqrt{\tau^2-1}} d\tau + \int_1^{\infty} \frac{\log q_2^-(\tau)}{(\tau-t)\sqrt{\tau^2-1}} d\tau \right\}$$

$$+ \frac{\alpha}{\pi} \log \left(\frac{\sqrt{\frac{1+t}{1-t}} - 1}{\sqrt{\frac{1+t}{1-t}} + 1} \right) \quad (5.30)$$

$$g^- = \frac{1}{\pi} \int_0^1 \frac{1}{(\tau+1)q_W^-(\tau)} d\tau \quad (5.37)$$

$$c_p = 1 - \frac{2}{F^2} (g^-(t) - 1) - q_W^{-2}(t) \quad (5.42)$$

(iv) For a numerical check

$$\begin{aligned}
 0 = & - \int_{-\infty}^{-1} \frac{\theta_1(\tau)}{(\tau-t)\sqrt{\tau^2-1}} d\tau + \int_{-1}^0 \frac{\log q_H^+(\tau) - \log q_H^+(t)}{(\tau-t)\sqrt{1-\tau^2}} d\tau \\
 & + \int_0^1 \frac{\log q_W^+(\tau)}{(\tau-t)\sqrt{1-\tau^2}} d\tau + \int_1^{\infty} \frac{\theta_2(\tau)}{(\tau-t)\sqrt{\tau^2-1}} d\tau \\
 & + \log q_H^+(t) \log \left(\frac{-1 + \sqrt{\frac{1+t}{1-t}}}{1 + \sqrt{\frac{1+t}{1-t}}} \right), \quad -1 < t < 0
 \end{aligned} \tag{5.32}$$

5.3 Numerical Solution

To overcome the difficulty which arises from carrying out the numerical integration over an infinite range, we need some transformations for that purpose.

Use $\tau = \frac{1}{\sin \beta}$, $t = \frac{1}{\sin \gamma}$ we get the following equations,

after dropping the dash, " ", sign and using big letters:

(i) Along lower free surface $0 < \gamma < \frac{\pi}{2}$

$$Q_2(\gamma) = \left[1 - \frac{2}{F^2} (\gamma_2(\gamma) - 1) \right]^{\frac{1}{2}} \tag{5.43}$$

$$\theta_2(\gamma) = \frac{\cos \gamma}{\pi} \left\{ \int_0^{-\pi/2} \frac{\log Q_1(\beta)}{\sin \gamma - \sin \beta} d\beta - \int_0^{\pi/2} \frac{\log Q_2(\beta) - \log Q_2(\gamma)}{\sin \beta - \sin \gamma} d\beta \right\} \\ + \frac{\alpha}{\pi} \left(\frac{\pi}{2} + \gamma \right) + \frac{\log Q_2(\gamma)}{\pi} \log \left(\tan \frac{\gamma}{2} \right) \quad (5.44)$$

$$\gamma_2(\gamma) = \lambda \sin \alpha + \frac{1}{\pi} \int_0^{\pi/2} \frac{\sin \theta_2(\beta)}{\sin \beta (1 + \sin \beta) Q_2(\beta)} \cos \beta d\beta \quad (5.45)$$

$$\chi_2(\gamma) = \lambda \cos \alpha + \frac{1}{\pi} \int_{-\gamma}^{\pi/2} \frac{\cos \theta_2(\beta)}{\sin \beta (1 + \sin \beta) Q_2(\beta)} \cos \beta d\beta \quad (5.46)$$

(ii) Along upper free surface $-\frac{\pi}{2} < \gamma < 0$

$$Q_1(\gamma) = \left[1 - \frac{2}{F^2} (\gamma_1(\gamma) - 1) \right]^{1/2} \quad (5.47)$$

$$\theta_1(\gamma) = \frac{\cos \gamma}{\pi} \left\{ \int_0^{-\pi/2} \frac{\log Q_1(\beta) - \log Q_1(\gamma)}{\sin \beta - \sin \gamma} d\beta - \int_0^{\pi/2} \frac{\log Q_2(\beta)}{\sin \beta - \sin \gamma} d\beta \right\} \\ + \frac{\alpha}{\pi} \left(\frac{\pi}{2} + \gamma \right) + \frac{\log Q_1(\gamma)}{\pi} \log \left(\tan \left(\frac{\pi}{2} + \frac{\gamma}{2} \right) \right) \quad (5.48)$$

$$Y_1(\gamma) = 1 - \frac{1}{\pi} \int_{-\pi/2}^{\pi} \frac{\sin \theta_1(\beta)}{\sin \beta (1 + \sin \beta) Q_1(\beta)} \cos \beta \, d\beta \quad (5.49)$$

$$X_1(\gamma) = x_0 - \frac{1}{\pi} \int_{-\pi/2}^{\gamma} \frac{\cos \theta_1(\beta)}{\sin \beta (1 + \sin \beta) Q_1(\beta)} \cos \beta \, d\beta \quad (5.50)$$

For the equations satisfied along the flat shelf and along the inclined plane, and for that one used for a numerical check use the following transformations $t = \sin \delta$, $\tau = \frac{1}{\sin \beta}$, we get the following equations

(iii) Along the flat shelf $-\frac{\pi}{2} < \delta < 0$

$$\log Q_H(\delta) = \frac{\cos \delta}{\pi} \left\{ - \int_{-\pi/2}^0 \frac{\log Q_1(\beta)}{(1 - \sin \beta \sin \delta)} d\beta + \int_0^{\pi/2} \frac{\log Q_2(\beta)}{(1 - \sin \beta \sin \delta)} d\beta \right\} + \frac{\alpha}{\pi} \log \left(\tan \left(\frac{\pi}{2} + \frac{\delta}{2} \right) \right) \quad (5.51)$$

$$c_p = 1 + \frac{2}{F^2} - Q_H^2(\delta) \quad (5.52)$$

(iv) Along the inclined plane $0 < \delta < \frac{\pi}{2}$

$$\log Q_W(\delta) = \frac{\cos \delta}{\pi} \left\{ - \int_{-\pi/2}^0 \frac{\log Q_2(\beta)}{1 - \sin \beta \sin \delta} d\beta + \int_0^{\pi/2} \frac{\log Q_2(\beta)}{1 - \sin \beta \sin \delta} d\beta \right\}$$

$$+ \frac{\alpha}{\pi} \log\left(\tan \frac{\delta}{2}\right) \quad (5.53)$$

$$L = \frac{1}{\pi} \int_0^{\pi/2} \frac{\cos \beta}{(1 + \sin \beta) Q_W(\beta)} d\beta \quad (5.54)$$

$$c_p = 1 - \frac{2}{F^2} (Y_L(\delta) - 1) - Q_W^2(\delta) \quad (5.55)$$

Now, use $\tau = \frac{1}{\sin \beta}$ in the first and fourth terms, and $\tau = \sin \beta$

in the second and third terms on the right side of (5.32), we get

(v) For a numerical check

$$0 = \int_{-\pi/2}^0 \frac{\theta_1(\beta)}{1 - \sin \beta \sin \delta} d\beta + \int_{-\pi/2}^0 \frac{\log Q_H(\beta) - \log Q_H(\delta)}{\sin \beta - \sin \delta} d\beta + \int_0^{\pi/2} \frac{\log Q_W(\beta)}{\sin \beta - \sin \delta} d\beta$$

$$+ \int_0^{\pi/2} \frac{\theta_2(\beta)}{1 - \sin \beta \sin \delta} d\beta + \log Q_H(\delta) \log\left(\tan\left(\frac{\pi}{2} + \frac{\delta}{2}\right)\right)$$

$$-\frac{\pi}{2} < \delta < 0 \quad (5.56)$$

Now, equation (5.44) should give values for $\theta_2(\gamma)$, which appears on the left side of the equation, but $Q_1(\gamma)$ and $Q_2(\gamma)$ appear in the

numerator of the integrands on the right side of the same equation. Equations (5.43) and (5.47) should give values of $Q_2(r)$ and $Q_1(r)$, respectively, but they are in terms of $Y_2(r)$ and $Y_1(r)$ which are originally unknowns. Equations (5.45), (5.46), (5.49), and (5.50) can not give an expression for the free surfaces profile unless values of $\theta_2(r)$, $Q_2(r)$, $\theta_1(r)$, and $Q_1(r)$ are determined. Finally $Q_1(r)$ and $Q_2(r)$ are essential for (5.51) and (5.52) to determine the speed of the flow at the flat shelf and the inclined plane respectively.

These equations are complicated enough such that most analytical methods of integral equations theory are not useful. Our way to solve these equations is to apply iteration method, in condition that we have to find initially a good approximation for the unknown quantities. Since the successive approximation scheme often converges only if the initial approximation is sufficiently close to the final solution, see Scarborough [45].

Then, if the problem has been properly formulated, and the initial approximation has been correctly chosen, it should be possible successively to improve upon the initial approximation until, after a sufficient number of improvements, the correct solution, for a specific degree of accuracy, to the problem is indeed found. In our iteration method the complete solution is computed in each cycle.

Initial Approximation

We make the reasonable assumption that the internal pressure, between the free surfaces, approaches zero. That assumption does the

acceleration become independent of any pressure action and hence dependent upon weight alone, see Rouse and Howe [44]. From this region on, the elements behave as though they were freely falling particles accelerating downwards at the rate g , and the one-dimensional method of analysis becomes generally applicable. A particle of water in the lower nappe will, in time t , travel a horizontal distance x from the edge of the weir of

$$x = (q_c \cos \alpha) t + \ell \cos \alpha. \quad (5.57)$$

In the same time the particle will travel a vertical distance y of

$$y = \frac{-1}{2} g t^2 + (q_c \sin \alpha) t + \ell \sin \alpha. \quad (5.58)$$

In equations (5.57) and (5.58) q_c is the velocity of the particle at the edge point c .

Solving equation (5.57) for t , substituting in equation (5.58) and simplifying

$$y = \frac{-g}{2q_c^2 \cos^2 \alpha} x^2 + \left(\frac{g \ell}{q_c^2 \cos \alpha} + \tan \alpha \right) x - \frac{g \ell^2}{2q_c^2}, \quad (5.59)$$

which gives the initial form of the lower nappe.

To find out the initial profile for the upper nappe, Blaisdell [6] assumed that the horizontal velocity is constant and hence he concluded that the vertical thickness of the nappe must also be constant. The equation of the upper nappe, according to Blaisdell's approach, is

$$y_{\text{upper}} = y_{\text{lower}} + \text{constant.}$$

and he found out the value of that constant using data of the U.S. Bureau of Reclamation, of Hinds, Creager, and Justin, and of Ippen.

We mentioned his empirical formulae in Chapter I.

Our way of approach to find out the initial profile for the upper nappe, from equation (5.59)

$$\theta_2^{(0)} = \tan^{-1} \left\{ \frac{-g}{q_c^2 \cos^2 \alpha} x + \frac{g \ell}{q_c^2 \cos \alpha} + \tan \alpha \right\} \quad (5.60)$$

Referring to Fig. 5.5, we see that

$$T = \frac{1}{Q_2^{(0)} \cos \theta_2^{(0)}}, \quad (5.61)$$

where T is the vertical thickness of the nappe. Notice that the above script, (0) , refers to initial approximation.

Therefore, for initial approximation we have

(i) Along lower free surface

$$x_2^{(0)} = \phi$$

$$y_2^{(0)} = \frac{-g}{2Q_c^2 \cos^2 \alpha} x_2^{(0)} + \left(\frac{g \ell^{(0)}}{Q_c^2 \cos \alpha} + \tan \alpha \right) x_2^{(0)} - \frac{g \ell^{(0)}}{2Q_c^2}$$

$$\theta_2^{(0)} = \tan^{-1} \left\{ \frac{-g}{Q_c^2 \cos^2 \alpha} x_2^{(0)} + \frac{g \ell^{(0)}}{Q_c^2 \cos \alpha} + \tan \alpha \right\}$$

$$Q_2^{(0)} = \left[1 - \frac{2}{F^2} (Y_2^{(0)} - 1) \right]^{\frac{1}{2}},$$

where

$$\phi = \frac{1}{\pi} \log \left| \frac{1 + \sin \gamma}{\sin \gamma} \right|, \quad 0 < \gamma < \frac{\pi}{2}$$

$$Q_c = \left[1 - \frac{2}{F^2} (l^{(0)} \sin \alpha - 1) \right]^{\frac{1}{2}}$$

(ii) Along upper free surface

$$Y_1^{(0)} = \begin{cases} 1.0 & -\infty < X < l^{(0)} \cos \alpha \\ Y_2^{(0)} + \frac{1}{Q_2^{(0)} \cos \theta_2^{(0)}} & l^{(0)} \cos \alpha < X < \infty \end{cases}$$

$$Q_1^{(0)} = \left[1 - \frac{2}{F^2} (Y_1^{(0)} - 1) \right]^{\frac{1}{2}}$$

The iteration procedure works in the following manner:

(i) Use $Q_1^{(0)}$ and $Q_2^{(0)}$ in (5.44), (5.48), and (5.53) to get $\theta_2^{(1)}$, $\theta_1^{(1)}$, and $Q_w^{(1)}$ respectively.

(ii) Use $Q_w^{(1)}$ in (5.54) to find out $l^{(1)}$.

(iii) Use $\theta_2^{(0)}$ and $Q_2^{(0)}$ in (5.45) and (5.46) to find out $Y_2^{(1)}$ and $X_2^{(1)}$ respectively.

(iv) Use $\theta_1^{(0)}$ and $Q_1^{(0)}$ in (5.49) and (5.50) to find out $Y_1^{(1)}$

and $x_1^{(1)}$ respectively.

(v) Substitute $\gamma_2^{(1)}$ in (5.43) for $Q_2^{(1)}$ and $\gamma_1^{(1)}$ in (5.47) for $Q_1^{(1)}$.

(vi) Use $Q_1^{(1)}$ and $Q_2^{(1)}$ in (5.51) to find Q_H along the flat shelf.

(vii) Another solution is obtained by using the data from Step (v), i.e., $Q_1^{(1)}$ and $Q_2^{(1)}$.

(viii) Steps (i) to (vi) are repeated until the results of two successive iterations differ by less than some specified small number 10^{-k} , where $k = 4$ or 6 , at this point we stop the iterations and the appropriate solution is obtained.

(ix) At each iteration check the validity of equation (5.56) to be satisfied by the numerical figures.

(x) Substitute Q_H and Q_w in (5.52) and (5.53) respectively to find out the pressure distribution along the solid boundary.

5.4 Numerical Results and Discussions

The dimensionless variables X_1, Y_1 along FE and X_2, Y_2 along CD are given in 5.50, 5.49, 5.46 and 5.45 respectively. Tables 5.1 and 5.2 show some free surfaces, which are plotted in Figs. 5.6 and 5.7.

After an initial guess we start the iterative procedure which is accurate to four decimal places after 2 iterations for the problem of supercritical flow but for the subcritical one it needs 13 iterations. In the fifth iteration it produces 6 significant decimal places for the problem of subcritical flow.

We used throughout our numerical work 200 points of divisions. The CPU time found for each iteration was approximately 1.586 minutes using an IBM 3031 computer, FORTRAN IV level G. When 160 points of divisions are used, the CPU time found for each iteration was approximately 1.187 minutes.

CHAPTER VI

GENERAL DISCUSSIONS, COMMENTS,

AND CONCLUSIONS.

- 6.1 Some Factors Not Considered.
 - 6.1.1 Surface Roughness
 - 6.1.2 Effect of Viscosity
 - 6.1.3 Cavitation Phenomena and Flow Separation
- 6.2 Discussions on the Hilbert Method
 - 6.2.1 Bottom Configuration
 - 6.2.2 Solution Over Unit Disc
 - 6.2.3 Main Features of the Hilbert Method

6.1 Some Factors Not Considered

Throughout our present work, we considered an inviscid flow and neglected the effect of surface roughness of the conduits. Now, we summarize the effect of both these factors.

6.1.1 Surface Roughness

When the surface profile of a channel is enlarged, see Fig. 6.1, it can be seen that the surface is composed of irregular peaks and valleys. The effective height of the irregularities forming the roughness elements is called the roughness height k . The ratio k/L of the roughness height to the hydraulic radius is known as the relative roughness.

We use the Chézy formula, namely

$$k_c = \frac{5C}{\sqrt{g}} \cdot \frac{\nu}{U}, \quad (6.1)$$

where C is Chézy's constant, ν is the kinematic viscosity, U is the mean velocity, and k_c is called the critical roughness. Then

(i) If $k < k_c$: the surface irregularities will be so small that all roughness elements will be entirely submerged in the laminar sublayer. In this case the roughness has no effect upon the flow outside the laminar sublayer, and the surface is said to be hydraulically smooth.

(ii) If $k > k_c$: the roughness elements will have sufficient magnitude and angularity to extend their effects beyond the laminar sublayer and thus to disturb the flow in the channel. The surface is therefore said to be rough.

In 1955, Morris [39], studied the roughness in conduit and he assumed that the loss of energy in turbulent flow over a rough surface is due largely to the formation of wakes behind each roughness element.

6.1.2 Effect of Viscosity

The state or behaviour of open-channel flow is governed basically by the effects of viscosity and gravity relative to the inertial forces of the flow. The surface tension of water does not play a significant role in almost all open-channel problems except in small models.

Depending on the effect of viscosity relative to inertia, the flow may be laminar, turbulent, or transitional. The flow is laminar if the viscous forces are so strong relative to the inertial forces that viscosity plays a significant part in determining the flow behaviour. The flow is turbulent if the viscous forces are weak relative to the inertial forces. Between the laminar and turbulent states there is a mixed, or transitional, state.

The effect of viscosity relative to inertia can be represented by the Reynolds number, defined as

$$R = \frac{UL\rho}{\mu} , \quad (6.2)$$

where U is the velocity of flow, L is a characteristic length (here considered equal to the hydraulic radius of a conduit), μ is the viscosity of water, and ρ is the mass density of water.

For more details of the discussion on this subject, see Chow [9].

6.1.3 Cavitation Phenomena and Flow Separation

Cavitation Phenomena: Formation of vapor bubbles within a flowing liquid, at zones of sufficiently low pressure, together with the abrupt collapse of these bubbles as they are carried into zones of higher pressure, is known as cavitation. The occurrence of cavitation is to be avoided for a number of pertinent reasons. First, the change in the flow pattern which such discontinuities produce represents a reduction in flow efficiency. Second, the extremely high intensities of stress resulting from the rapidly repeated collapse of the vapor bubbles may produce eventual failure of the boundary material in the immediate vicinity. Conduit inlets, turbine blades, and ship propellers have been severely damaged in this manner. Insurance against the cavitation phenomenon is to be sought by any means, that is, by careful streamlining of boundary profiles, reduction of mean velocities through enlargement of flow passages, or increase of the overall hydrostatic load upon the system.

Flow Separation: In applying the stream-function and velocity-potential concepts to particular boundary conditions, it is usually assumed that the boundaries determine the form of the limiting stream surfaces; in other words, that the flow follows the boundaries throughout. It is well known, however, that a fluid having an appreciable velocity will be guided by divergent boundaries only if the angle of divergence is relatively small.

As a general rule, therefore, in any locality for which the flow pattern obtained by analytical means indicates a rapid reduction in boundary velocity (ie, a local divergence of stream lines), separation is to be expected, and the analytical results cannot be considered fully applicable. For more detail of discussion of this subject, see Rouse [42], Birkhoff and Zarantonello [5], and Milne-Thomson [38].

6.2 Discussions on the Hilbert Method

6.2.1 Bottom Configuration

Throughout all problems we presented, we considered only the case of simple configuration of bottom composed of a finite number of linear segments; one segment in each of problem I and III, connected at arbitrary angle, denoted by α . Since that arbitrary angle is constant along the related segment, it is easy to carry out the integration analytically, i.e.,

$$\int_{t_1}^{t_2} \frac{1}{(\tau-t) H(\tau)} d\tau \quad (6.3)$$

where $H(\tau)$ is a known function.

Using that simple idea, it is possible to apply the Hilbert method for problems of flow over polygonal bottom, as shown in Fig. 6.2, and analytical integration over each segment is easy to evaluate.

For the case of problems with arbitrary shape of bottom, ideally it is reasonable to prescribe the inclination $\theta(Z)$ at each point on the bottom boundary so the shape of the bottom is known a priori. Due to the non-linear nature of the Hilbert solution, however, this is not directly possible since here θ must be initially prescribed as a function of t , not Z . One of the possible ways to prescribe $\theta(t)$ is to represent it as a piecewise continuous, n th degree polynomial, i.e.,

$$\theta(t) = \sum_{i=1}^n a_i t^i. \quad (6.4)$$

The coefficients a_j can be chosen so that $\theta(t)$ will assume a specified value θ_k at each particular juncture point t_j and also at the end points. So, the selection of m intermediate points t_j requires evaluation of integrals in (6.3) over the intervals (t_0, t_{j1}) , (t_{j1}, t_{j2}) , ..., (t_{jm}, t_∞) , rather than integrating directly over the range (t_0, t_∞) , where t_0 and t_∞ correspond to the end points. For more discussions see Larock [33], [34]. It is clear that as the number of subdivisions, n , of the bottom increases we approach to the real form of bottom configuration, but in this case calculations will be more bulky.

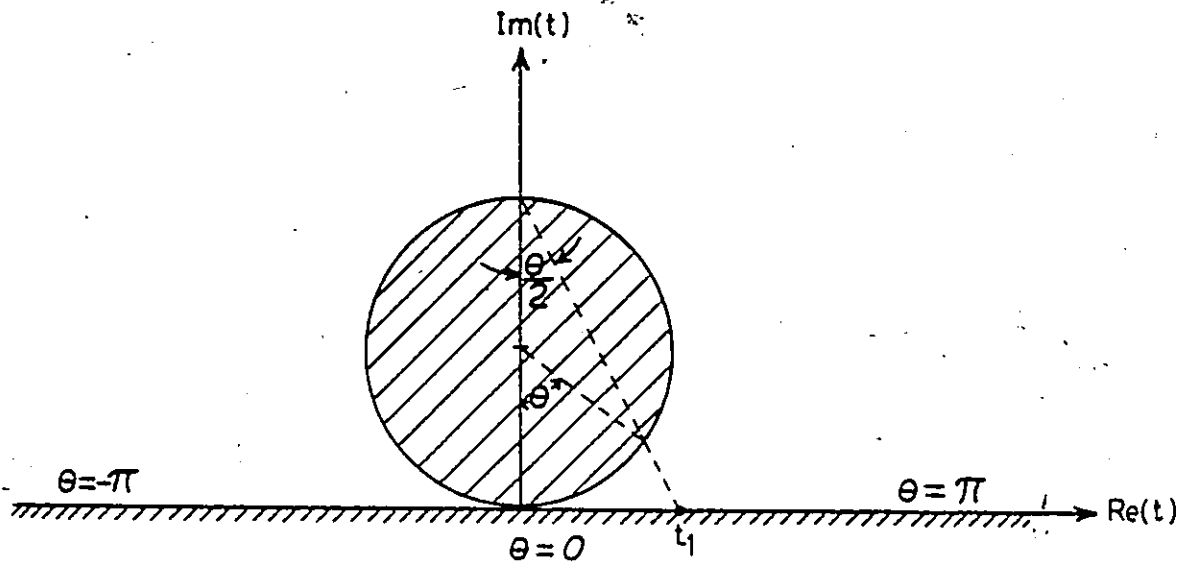
Therefore we conclude that Hilbert's method can be applied successfully to any flow over arbitrary bottom configuration.

6.2.2 Solution Over Unit Disc

We carried out our problems through Hilbert's transformation over upper half-plane, and one of the major problems encountered in that case during the numerical work is the infinite limit for some integrals. But it is possible to transform the upper half-plane to a unit disc, using the transformation

$$t_1 = \tan \frac{1}{2} \theta; \quad (6.5)$$

where θ is the angle subtended at the center of the unit disc, as shown in the figure, and t_1 is the real t -plane coordinate.



Then it is possible to apply the Hilbert transformation over the boundary of the unit disc, i.e.,

$$u(\theta) = \frac{1}{2\pi} \int_{-\pi}^{\pi} \cot \frac{\gamma - \theta}{2} v(\gamma) d\gamma, \quad (6.6)$$

$$v(\theta) = \frac{-1}{2\pi} \int_{-\pi}^{\pi} \cot \frac{\gamma - \theta}{2} u(\gamma) d\gamma, \quad (6.7)$$

provided that

$$\int_{-\pi}^{\pi} u(\theta) d\theta = \int_{-\pi}^{\pi} v(\theta) d\theta = 0. \quad (6.8)$$

For more details see Tricomi [53].

6.2.3 Main Features of the Hilbert Method

The Hilbert method characterizes by the following features:

(i) It normally requires two or three iterations for the solution to be stable up to the second or third decimal place, and more iterations are required for more accurate solution.

(ii) CPU time required for each iteration is a fraction of minute, and for some simple problems it is a fraction of second.

(iii) This method provides us with an extra integral equations which can be used for a numerical check.

(iv) It is restricted to steady, two-dimensional problems.

TABLE 3.1

Shape of Free Surface for a Flow
Over An Uneven Bottom

$F = 0.6$, $\alpha = \pi/4$, $N = 30$

x	q	θ (degrees)	y
-0.809 418	1.001 857	0.000 642	0.999 331
-0.640 885	1.003 715	0.000 410	0.998 660
-0.533 708	1.005 573	-0.004 493	0.997 988
-0.388 584	1.009 287	-0.011 931	0.996 641
-0.285 337	1.013 004	-0.020 132	0.995 288
-0.202 226	1.016 721	-0.028 230	0.993 930
-0.130 050	1.020 438	-0.035 567	0.992 567
-0.063 768	1.024 155	-0.041 572	0.991 199
-0.000 000	1.027 875	-0.045 739	0.989 825
0.064 022	1.032 796	-0.047 637	0.988 445
0.129 611	1.035 321	-0.046 970	0.987 060
0.166 830	1.039 046	-0.043 689	0.985 669
0.202 186	1.042 774	-0.038 183	0.984 272
0.208 739	1.046 505	-0.031 652	0.982 869
0.268 230	1.050 238	-0.027 227	0.981 460
0.303 383	1.054 267	-0.000 002	0.979 335

$L = 1.070$

TABLE 3.2

Shape of Free Surface for a Flow
Over An Uneven Bottom

$F = 0.894$, $\alpha = \pi/6$, $N = 30$

x	q	θ (degrees)	y
-0.808 519	1.001 722	-0.003 181	0.998 621
-0.640 053	1.003 444	-0.006 582	0.997 240
-0.532 940	1.005 165	-0.011 178	0.995 857
-0.452 761	1.006 887	-0.014 337	0.994 471
-0.387 937	1.008 610	-0.019 538	0.993 082
-0.332 977	1.010 332	-0.022 121	0.991 691
-0.284 808	1.012 055	-0.027 674	0.990 298
-0.241 515	1.013 778	-0.029 457	0.988 902
-0.201 816	1.015 500	-0.035 168	0.987 504
-0.164 795	1.017 223	-0.035 955	0.986 103
-0.129 766	1.018 945	-0.041 644	0.984 700
-0.063 619	1.022 393	-0.046 739	0.981 885
-0.000 000	1.025 841	-0.050 092	0.979 060
0.063 852	1.029 290	-0.051 361	0.976 225
0.096 720	1.032 740	-0.050 254	0.973 379
0.156 948	1.036 192	-0.046 577	0.970 522
0.171 093	1.039 648	-0.040 323	0.967 653
0.220 665	1.043 103	-0.031 791	0.964 774
0.246 580	1.046 562	-0.021 828	0.961 883
0.272 768	1.048 293	-0.009 136	0.960 433
0.294 183	1.051 754	-0.000 001	0.957 525

$L = 1.065$

TABLE 3.3

Shape of Free Surface for a Flow
Over An Uneven Bottom

$$F = 1.1, \alpha = \pi/4, N = 30$$

x	q	θ (degrees)	y
-0.812 257	0.997 228	0.011 203	1.003 349
-0.643 748	0.994 440	0.021 948	1.006 709
-0.536 527	0.991 636	0.030 554	1.010 077
-0.456 197	0.988 816	0.041 158	1.013 456
-0.391 188	0.985 981	0.048 032	1.016 844
-0.336 016	0.983 128	0.058 599	1.020 242
-0.287 609	0.980 260	0.063 688	1.023 650
-0.244 057	0.977 374	0.074 120	1.027 067
-0.204 074	0.974 471	0.077 257	1.030 496
-0.166 746	0.971 551	0.087 385	1.033 934
-0.131 385	0.968 613	0.088 349	1.037 382
-0.097 450	0.965 657	0.097 966	1.040 841
-0.032 128	0.959 690	0.105 375	1.047 791
0.032 227	0.953 649	0.109 092	1.054 785
0.098 364	0.947 529	0.108 599	1.061 823
0.169 397	0.941 330	0.103 433	1.068 908
0.215 224	0.935 048	0.093 267	1.076 039
0.225 044	0.928 680	0.077 981	1.083 220
0.251 895	0.922 224	0.057 655	1.090 448
0.253 550	0.918 962	0.032 993	1.094 083
0.257 602	0.915 676	0.031 929	1.097 730
0.742 615	0.912 367	0.000 394	1.101 390

$$L = 1.034$$

TABLE 3.4

Shape of Free Surface for a Flow
Over An Uneven Bottom

$$F = 1.2, \alpha = \pi/6, N = 30$$

x	q	θ (degrees)	y
-0.806 769	0.998 527	0.006 972	1.002 118
-0.638 447	0.997 051	0.013 693	1.004 240
-0.531 465	0.995 569	0.019 266	1.006 366
-0.451 408	0.994 084	0.025 873	1.008 493
-0.386 702	0.992 594	0.030 483	1.010 625
-0.331 858	0.991 099	0.037 000	1.012 760
-0.283 802	0.989 600	0.040 593	1.014 898
-0.201 040	0.986 588	0.049 396	1.019 183
-0.164 137	0.985 075	0.055 436	1.021 332
-0.122 160	0.982 035	0.062 215	1.025 637
-0.063 337	0.978 976	0.066 943	1.029 956
-0.000 000	0.975 898	0.069 275	1.034 288
0.063 533	0.972 801	0.068 874	1.038 634
0.107 515	0.969 683	0.065 441	1.042 994
0.165 410	0.966 546	0.058 778	1.047 368
0.207 002	0.964 969	0.048 953	1.049 561
0.208 749	0.963 387	0.048 838	1.051 757
0.228 987	0.961 801	0.036 916	1.053 956
0.241 912	0.960 208	0.035 747	1.056 159
0.262 233	0.958 611	0.021 766	1.058 366
0.270 084	0.957 008	0.019 502	1.060 576
0.314 405	0.955 400	0.002 003	1.062 791

$$L = 1.036$$

TABLE 4.1(a)
 Lower nappe for a flow over shelf
 $F = .8, N = 300$

x	q	θ (degrees)	y
0.000 000	2.031 010	0.000 000	0.000 000
0.010 244	2.032 856	-0.064 936	-0.002 404
0.020 091	2.034 666	-0.091 287	-0.004 765
0.030 013	2.036 528	-0.112 012	-0.007 192
0.040 627	2.038 558	-0.130 869	-0.009 843
0.050 651	2.040 513	-0.146 705	-0.012 399
0.060 642	2.042 500	-0.161 164	-0.014 998
0.070 549	2.044 506	-0.174 519	-0.017 627
0.080 307	2.046 519	-0.186 925	-0.020 266
0.090 738	2.048 711	-0.199 527	-0.023 142
0.100 016	2.050 695	-0.210 263	-0.025 749
0.150 740	2.062 127	-0.263 472	-0.040 819
0.201 344	2.074 516	-0.310 818	-0.057 249
0.252 643	2.088 056	-0.355 501	-0.075 322
0.303 187	2.102 302	-0.397 513	-0.094 470
0.352 276	2.116 894	-0.437 065	-0.114 225
0.402 985	2.132 580	-0.477 014	-0.135 621
0.458 604	2.150 198	-0.519 897	-0.159 852
0.483 623	2.158 150	-0.538 783	-0.170 857
0.514 372	2.167 845	-0.561 460	-0.184 336
0.532 897	2.173 605	-0.574 724	-0.192 375
0.554 466	2.180 197	-0.589 548	-0.201 606
0.580 348	2.187 895	-0.606 201	-0.212 422
0.612 852	2.197 136	-0.624 137	-0.225 463
0.657 033	2.208 714	-0.639 422	-0.241 892

TABLE 4.1(b)

Upper nappe for a flow over shelf

F = .8, N = 300

105

x	q	θ (degrees)	y
-1.600 000	1.145 644	0.000 000	0.900 000
-0.311 304	1.332 308	-0.016 788	0.752 048
-0.300 230	1.335 821	-0.068 339	0.749 051
-0.290 188	1.339 050	-0.093 346	0.746 290
-0.280 465	1.342 200	-0.112 529	0.743 588
-0.270 329	1.345 531	-0.129 772	0.740 725
-0.250 500	1.352 171	-0.158 670	0.734 998
-0.200 025	1.369 772	-0.217 441	0.719 680
-0.150 018	1.388 218	-0.265 305	0.703 415
-0.100 636	1.407 445	-0.307 110	0.686 231
-0.051 164	1.427 732	-0.345 441	0.667 846
0.000 907	1.450 218	-0.383 028	0.647 163
0.009 933	1.454 235	-0.389 306	0.643 435
0.032 602	1.464 486	-0.404 813	0.633 875
0.050 423	1.472 701	-0.416 747	0.626 164
0.061 885	1.478 060	-0.424 317	0.621 112
0.082 496	1.487 847	-0.437 724	0.611 838
0.100 587	1.496 597	-0.449 293	0.603 495
0.125 678	1.508 981	-0.465 055	0.591 606
0.154 260	1.523 449	-0.482 630	0.577 593
0.202 539	1.548 782	-0.511 540	0.552 740
0.301 778	1.604 645	-0.568 811	0.496 524
0.401 929	1.667 103	-0.628 487	0.431 406
0.484 738	1.724 765	-0.706 284	0.369 323
0.524 062	1.754 072	-0.819 427	0.337 343

TABLE 4.2(a)
 Lower nappe for a flow over shelf
 $F = 1.00$, $N = 300$

x	q	θ (degrees)	y
0.000 000	1.732 051	0.000 000	0.000 000
0.010 269	1.733 214	-0.050 011	-0.002 022
0.020 500	1.734 394	-0.070 914	-0.004 074
0.030 651	1.735 585	-0.087 022	-0.006 145
0.040 672	1.736 779	-0.100 601	-0.008 226
0.050 505	1.737 971	-0.112 499	-0.010 303
0.060 087	1.739 151	-0.123 127	-0.012 360
0.070 210	1.740 417	-0.133 578	-0.014 569
0.080 019	1.741 663	-0.143 106	-0.016 746
0.090 397	1.743 002	-0.152 671	-0.019 087
0.100 384	1.744 311	-0.161 461	-0.021 378
0.151 121	1.751 275	-0.201 755	-0.033 592
0.201 259	1.758 670	-0.237 069	-0.046 624
0.251 149	1.766 535	-0.269 616	-0.060 548
0.300 822	1.774 854	-0.300 368	-0.075 353
0.352 464	1.783 995	-0.331 158	-0.091 711
0.401 882	1.793 174	-0.359 836	-0.108 234
0.455 212	1.803 491	-0.390 158	-0.126 921
0.510 256	1.814 489	-0.420 906	-0.146 983
0.560 523	1.824 739	-0.448 467	-0.165 808
0.611 688	1.835 246	-0.475 727	-0.185 245
0.657 516	1.844 620	-0.498 855	-0.202 704
0.686 341	1.850 459	-0.512 236	-0.213 642
0.721 306	1.857 467	-0.526 076	-0.226 829
0.765 519	1.866 238	-0.536 146	-0.243 441

TABLE 4.2(b)
Upper nappe for a flow over shelf
F = 1.00, N = 300

x	q	θ (degrees)	y
-1.600 000	1.095 445	0.000 000	0.900 000
-0.176 978	1.215 178	-0.014 033	0.761 769
-0.159 390	1.218 508	-0.067 322	0.757 722
-0.125 005	1.225 199	-0.115 269	0.749 553
-0.101 023	1.230 027	-0.140 078	0.743 632
-0.075 712	1.235 259	-0.162 789	0.737 190
-0.050 251	1.240 667	-0.183 354	0.730 500
-0.024 880	1.246 204	-0.202 253	0.723 623
-0.001 564	1.251 422	-0.218 566	0.717 113
0.000 072	1.251 793	-0.219 678	0.716 650
0.010 112	1.254 083	-0.226 427	0.713 784
0.050 869	1.263 620	-0.252 557	0.701 789
0.102 193	1.276 194	-0.283 211	0.685 837
0.151 539	1.288 884	-0.310 916	0.669 577
0.202 050	1.302 497	-0.337 894	0.651 953
0.251 834	1.316 544	-0.363 387	0.633 571
0.303 135	1.331 686	-0.388 726	0.613 526
0.354 144	1.347 437	-0.413 153	0.592 426
0.401 425	1.362 675	-0.435 241	0.571 764
0.461 055	1.382 811	-0.462 564	0.544 073
0.511 843	1.400 826	-0.485 637	0.518 910
0.620 109	1.442 251	-0.536 738	0.459 493
0.672 844	1.464 206	-0.566 087	0.426 916
0.743 263	1.495 813	-0.627 098	0.377 784
0.790 114	1.518 362	-0.735 708	0.338 606

TABLE 4.3(a)
 - Lower nappe for a flow over shelf
 $F = 1.2, N = 300$

x	q	θ (degrees)	y
0.000 000	1.545 603	00.000 000	0.000 000
0.010 230	1.546 367	-0.039 679	-0.001 699
0.020 269	1.547 129	-0.056 029	-0.003 392
0.030 058	1.547 881	-0.068 446	-0.005 067
0.040 344	1.548 685	-0.079 561	-0.006 854
0.050 327	1.549 476	-0.089 148	-0.008 615
0.060 828	1.550 320	-0.098 342	-0.010 496
0.070 016	1.551 068	-0.105 823	-0.012 165
0.080 630	1.551 946	-0.113 951	-0.014 120
0.090 789	1.552 797	-0.121 314	-0.016 020
0.100 390	1.553 613	-0.127 964	-0.017 841
0.151 054	1.558 092	-0.159 544	-0.027 856
0.200 152	1.562 716	-0.186 541	-0.038 222
0.250 948	1.567 788	-0.212 224	-0.049 628
0.300 609	1.573 024	-0.235 839	-0.061 437
0.351 048	1.578 609	-0.258 724	-0.074 073
0.403 377	1.584 662	-0.281 547	-0.087 820
0.454 454	1.590 797	-0.303 059	-0.101 800
0.506 149	1.597 192	-0.324 114	-0.116 423
0.553 901	1.603 216	-0.342 889	-0.130 250
0.603 044	1.609 479	-0.361 436	-0.144 674
0.714 112	1.623 506	-0.399 143	-0.177 160
0.772 974	1.630 621	-0.415 236	-0.193 733
0.811 385	1.635 053	-0.423 346	-0.204 086
0.860 158	1.640 368	-0.429 520	-0.216 531

TABLE 4.3(b)
 Upper nappe for a flow over shelf
 $F = 1.2$, $N = 300$

x	q	θ (degrees)	y
-1.600 000	1.067 187	0.000 000	0.900 000
-0.082 323	1.145 602	-0.011 698	0.775 079
-0.059 540	1.148 310	-0.061 463	0.770 609
-0.029 323	1.152 000	-0.093 630	0.764 501
-0.019 572	1.153 219	-0.102 077	0.762 479
-0.010 599	1.154 352	-0.109 357	0.760 597
-0.005 997	1.154 938	-0.112 937	0.759 625
-0.000 134	1.155 687	-0.117 369	0.758 378
0.001 056	1.155 841	-0.118 250	0.758 124
0.005 863	1.156 459	-0.121 763	0.757 094
0.010 757	1.157 093	-0.125 259	0.756 040
0.050 612	1.162 374	-0.151 350	0.747 226
0.100 870	1.169 353	-0.180 210	0.735 520
0.150 050	1.176 535	-0.205 770	0.723 405
0.200 192	1.184 223	-0.230 016	0.710 354
0.252 746	1.192 688	-0.254 024	0.695 891
0.303 195	1.201 217	-0.276 063	0.681 220
0.351 976	1.209 847	-0.296 650	0.666 276
0.401 037	1.218 916	-0.316 796	0.650 464
0.506 385	1.239 772	-0.358 760	0.613 700
0.604 782	1.261 075	-0.397 301	0.575 595
0.707 865	1.285 543	-0.438 810	0.531 230
0.822 673	1.316 028	-0.492 691	0.475 380
0.890 310	1.336 200	-0.538 326	0.438 564
0.985 671	1.369 845	-0.715 159	0.381 689

TABLE 4.4(a)
 Lower nappe for a flow over shelf
 $F = 2.0, N = 300$

x	q	θ (degrees)	y
0.000 000	1.224 745	0.000 000	-0.000 000
0.101 453	1.224 940	-0.019 588	-0.000 971
0.020 422	1.225 130	-0.027 456	-0.001 909
0.030 792	1.225 328	-0.033 814	-0.002 896
0.040 595	1.225 519	-0.038 934	-0.003 841
0.050 785	1.225 719	-0.043 674	-0.004 834
0.060 313	1.225 908	-0.047 725	-0.005 774
0.070 207	1.226 107	-0.051 638	-0.006 760
0.080 495	1.226 315	-0.055 455	-0.007 798
0.091 211	1.226 536	-0.059 212	-0.008 892
0.101 125	1.226 742	-0.062 524	-0.009 916
0.151 165	1.227 814	-0.077 539	-0.015 257
0.200 002	1.228 915	-0.090 426	-0.020 753
0.251 113	1.230 125	-0.102 777	-0.026 806
0.300 859	1.231 359	-0.114 046	-0.032 993
0.352 341	1.232 693	-0.125 147	-0.039 700
0.400 114	1.233 980	-0.135 060	-0.046 196
0.503 129	1.236 913	-0.155 481	-0.061 059
0.605 801	1.240 022	-0.174 815	-0.076 935
0.703 650	1.243 119	-0.192 367	-0.092 887
0.819 113	1.246 877	-0.211 712	-0.112 445
0.920 361	1.250 192	-0.226 731	-0.129 924
0.991 576	1.252 499	-0.235 338	-0.142 237
1.036 237	1.253 926	-0.239 338	-0.149 933
1.090 037	1.255 626	-0.241 721	-0.159 185

TABLE 4.4(b)
 Upper nappe for a flow over shelf
 $F = 2.00$, $N = 300$

x	q	θ (degrees)	y
-1.600 000	1.024 694	0.000 000	0.900 000
0.085 934	1.042 520	-0.005 977	0.826 761
0.100 242	1.042 880	-0.023 555	0.825 274
0.125 286	1.043 525	-0.038 599	0.822 610
0.150 207	1.044 182	-0.049 482	0.819 896
0.175 958	1.044 880	-0.058 944	0.817 010
0.201 164	1.045 583	-0.067 170	0.814 107
0.250 208	1.047 004	-0.081 394	0.808 234
0.300 542	1.048 537	-0.094 480	0.801 890
0.351 211	1.050 161	-0.106 686	0.795 170
0.400 610	1.051 824	-0.117 952	0.788 285
0.452 908	1.053 672	-0.129 396	0.780 626
0.500 075	1.055 419	-0.319 408	0.773 381
0.551 335	1.057 407	-0.150 044	0.765 134
0.601 928	1.059 464	-0.160 366	0.756 599
0.656 131	1.061 773	-0.171 293	0.747 005
0.706 309	1.064 014	-0.181 351	0.737 690
0.757 237	1.066 394	-0.191 551	0.727 793
0.807 510	1.068 851	-0.201 669	0.717 564
0.854 894	1.071 272	-0.211 313	0.707 485
0.911 278	1.074 291	-0.223 020	0.694 899
1.001 270	1.079 454	-0.242 636	0.673 353
1.100 283	1.085 699	-0.266 820	0.647 230
1.250 263	1.096 667	-0.319 307	0.601 026
1.367 850	1.107 450	-0.441 748	0.554 139

TABLE 4.5(a)
Lower nappe for a flow over shelf

$F = \sqrt{20}$, $N = 300$

x	q	θ (degrees)	y
0.000 000	1.048 809	0.000 000	0.000 000
0.010 259	1.048 820	-0.004 719	-0.000 232
0.020 877	1.048 832	-0.006 747	-0.000 474
0.030 763	1.048 843	-0.008 206	-0.000 702
0.040 983	1.048 855	-0.009 491	-0.000 939
0.050 366	1.048 866	-0.010 541	-0.001 159
0.060 049	1.048 877	-0.011 532	-0.001 387
0.070 052	1.048 889	-0.012 479	-0.001 625
0.080 397	1.048 902	-0.013 396	-0.001 873
0.091 107	1.048 914	-0.014 289	-0.002 132
0.100 800	1.048 925	-0.015 058	-0.002 368
0.151 206	1.048 988	-0.018 612	-0.003 623
0.201 726	1.049 053	-0.021 683	-0.004 928
0.300 692	1.049 188	-0.026 860	-0.007 607
0.403 381	1.049 335	-0.031 455	-0.010 540
0.501 793	1.049 484	-0.035 274	-0.013 463
0.553 534	1.049 565	-0.037 058	-0.015 030
0.600 941	1.049 641	-0.038 546	-0.016 477
0.657 161	1.049 730	-0.040 113	-0.018 197
0.704 851	1.049 808	-0.041 253	-0.019 651
0.761 476	1.049 899	-0.042 344	-0.021 363
0.801 346	1.049 963	-0.042 918	-0.022 551
0.847 272	1.050 036	-0.043 347	-0.023 869
0.864 272	1.050 063	-0.043 436	-0.024 385
0.882 282	1.050 092	-0.043 484	-0.024 898

TABLE 4.5(b)
Lower nappe for a flow over shelf

$$F = \sqrt{20.}, N = 300$$

x	q	θ (degrees)	y
-1.600 000	1.004 987	0.000 000	0.900 000
0.154 441	1.005 967	-0.001 496	0.879 871
0.200 682	1.006 032	-0.010 239	0.878 516
0.226 028	1.006 069	-0.012 811	0.877 744
0.250 666	1.006 105	-0.014 972	0.876 969
0.275 836	1.006 149	-0.016 969	0.876 155
0.301 511	1.006 185	-0.018 856	0.875 299
0.350 200	1.006 266	-0.022 167	0.873 606
0.400 819	1.006 353	-0.025 373	0.871 744
0.502 390	1.006 545	-0.031 443	0.867 670
0.601 413	1.006 752	-0.037 215	0.863 229
0.657 784	1.006 879	-0.040 537	0.860 474
0.701 824	1.006 983	-0.043 184	0.858 198
0.752 974	1.007 110	-0.046 347	0.855 413
0.805 676	1.007 247	-0.049 740	0.852 373
0.859 053	1.007 394	-0.053 363	0.849 105
0.900 380	1.007 512	-0.056 334	0.846 437
0.960 979	1.007 694	-0.061 027	0.842 290
1.003 798	1.007 829	-0.064 651	0.839 179
1.053 297	1.007 992	-0.069 254	0.835 382
1.111 957	1.008 193	-0.075 459	0.830 576
1.242 960	1.008 678	-0.094 140	0.818 440
1.358 977	1.009 135	-0.122 490	0.805 602
1.469 095	1.009 521	-0.181 601	0.790 645
1.542 162	1.009 523	-0.293 529	0.777 905

TABLE 4.6

Values of C_p on the shelf for different
values of Froude number F .

X \ F		0.80		1.00		1.20		2.00	
-1.600	000	3.125	000	2.000	000	1.388	888	0.500	000
-1.503	999	3.125	000	2.000	000	1.388	888	0.500	000
-1.402	666	3.125	000	2.000	000	1.388	888	0.500	000
-1.201	000	3.068	334	1.932	703	1.282	788	0.347	446
-1.002	665	2.557	170	1.616	908	1.042	066	0.211	591
-0.704	000	1.635	283	1.200	000	0.761	981	0.209	248
-0.501	334	1.346	494	0.897	393	0.602	800	0.225	015
-0.304	001	0.760	000	0.480	000	0.340	000	0.140	000
0.000	000	0.000	000	0.000	000	0.000	000	0.000	000

TABLE 5.1(a)

Lower Nappe for a Flow Over Sharp-
Crested Weir

$$F = 0.9, \alpha = \pi/3, N = 200$$

x	ζ	θ (degrees)	y
0.249 329	1.551 016	1.042 083	0.430 712
0.249 503	1.550 826	0.919 009	0.430 950
0.250 002	1.550 364	0.793 818	0.431 530
0.250 511	1.550 065	0.718 864	0.431 905
0.251 011	1.549 890	0.658 483	0.432 125
0.251 509	1.549 841	0.607 817	0.432 187
0.252 028	1.549 918	0.561 601	0.432 089
0.253 523	1.550 839	0.452 251	0.430 933
0.254 036	1.551 384	0.420 179	0.430 250
0.255 091	1.552 857	0.360 002	0.428 396
0.256 050	1.554 602	0.310 534	0.426 201
0.257 154	1.557 078	0.258 110	0.423 080
0.259 042	1.562 466	0.176 445	0.416 273
0.260 154	1.566 326	0.131 656	0.411 382
0.270 371	1.628 773	-0.246 547	0.330 575
0.280 654	1.772 661	-0.739 521	0.132 357
0.286 638	1.959 604	-1.166 973	-0.150 220

TABLE 5.1(b)

Upper Nappe for a Flow Over Sharp-
Crested Weir

$F = 0.9$, $\alpha = \pi/3$, $N = 200$

x	q	θ (degrees)	y
-0.430 839	1.074 901	-0.006 948	0.937 058
-0.282 663	1.075 327	-0.013 906	0.936 687
-0.017 436	1.088 688	-0.049 218	0.924 977
-0.012 755	1.088 775	-0.056 461	0.924 901
0.130 033	1.093 678	-0.173 743	0.920 566
0.134 612	1.104 580	-0.513 950	0.910 861
0.167 087	1.167 377	-0.799 231	0.853 078
0.197 582	1.227 309	-0.800 687	0.794 953
0.224 751	1.273 531	-0.833 681	0.748 138
0.251 232	1.317 545	-0.871 158	0.701 951
0.292 757	1.386 724	-0.933 071	0.626 183
0.303 049	1.404 013	-0.948 604	0.606 643
0.356 966	1.493 090	-1.027 430	0.502 126
0.405 226	1.574 133	-1.096 713	0.401 453
0.504 358	1.746 615	-1.235 362	0.169 481
0.560 357	1.849 719	-1.311 360	0.019 308
0.604 324	1.933 299	-1.366 836	-0.108 748

TABLE 5.2(a)

Lower Nappe for a Flow Over Sharp-Crested Weir.

$$F = 5.916, \alpha = \pi/4, N = 200$$

x	q	θ (degrees)	y
0.262 690	1.020 848	0.783 377	0.262 690
0.265 065	1.020 772	0.724 765	0.265 417
0.270 746	1.020 596	0.676 235	0.271 736
0.280 272	1.020 315	0.629 690	0.281 734
0.290 133	1.020 045	0.597 285	0.291 372
0.300 858	1.019 773	0.570 940	0.301 114
0.350 659	1.018 739	0.500 030	0.337 979
0.400 352	1.018 018	0.463 827	0.363 678
0.454 740	1.017 521	0.440 233	0.381 411
0.486 772	1.017 355	0.430 777	0.387 298
0.501 937	1.017 308	0.427 118	0.388 969
0.527 998	1.017 273	0.421 841	0.390 208
0.571 032	1.017 340	0.415 461	0.387 821
0.612 321	1.017 549	0.411 614	0.380 402
0.711 755	1.018 635	0.410 347	0.341 698

TABLE 5.2(b)

Upper Nappe for a Flow Over Sharp-
Crested Weir

$F = 5.916$, $\alpha = \pi/4$, $N = 200$

x	q	θ (degrees)	y
-0.851 330	0.999 810	-0.013 992	1.006 642
0.240 444	0.998 832	-0.017 852	1.040 867
0.252 245	0.998 861	-0.096 407	1.039 832
0.332 013	1.000 321	-0.307 266	0.988 731
0.408 473	1.001 618	-0.404 433	0.943 291
0.501 669	1.003 333	-0.501 295	0.883 127
0.557 249	1.004 443	-0.554 309	0.844 151
0.603 036	1.005 403	-0.596 437	0.810 389
0.704 695	1.007 690	-0.687 679	0.729 778
0.759 333	1.009 029	-0.736 889	0.682 538
0.809 045	1.010 318	-0.782 106	0.637 023
0.848 138	1.011 379	-0.818 032	0.599 468
0.921 175	1.013 450	-0.884 876	0.526 087
0.983 530	1.015 354	-0.942 140	0.458 457
1.118 887	1.019 920	-1.044 050	0.295 841

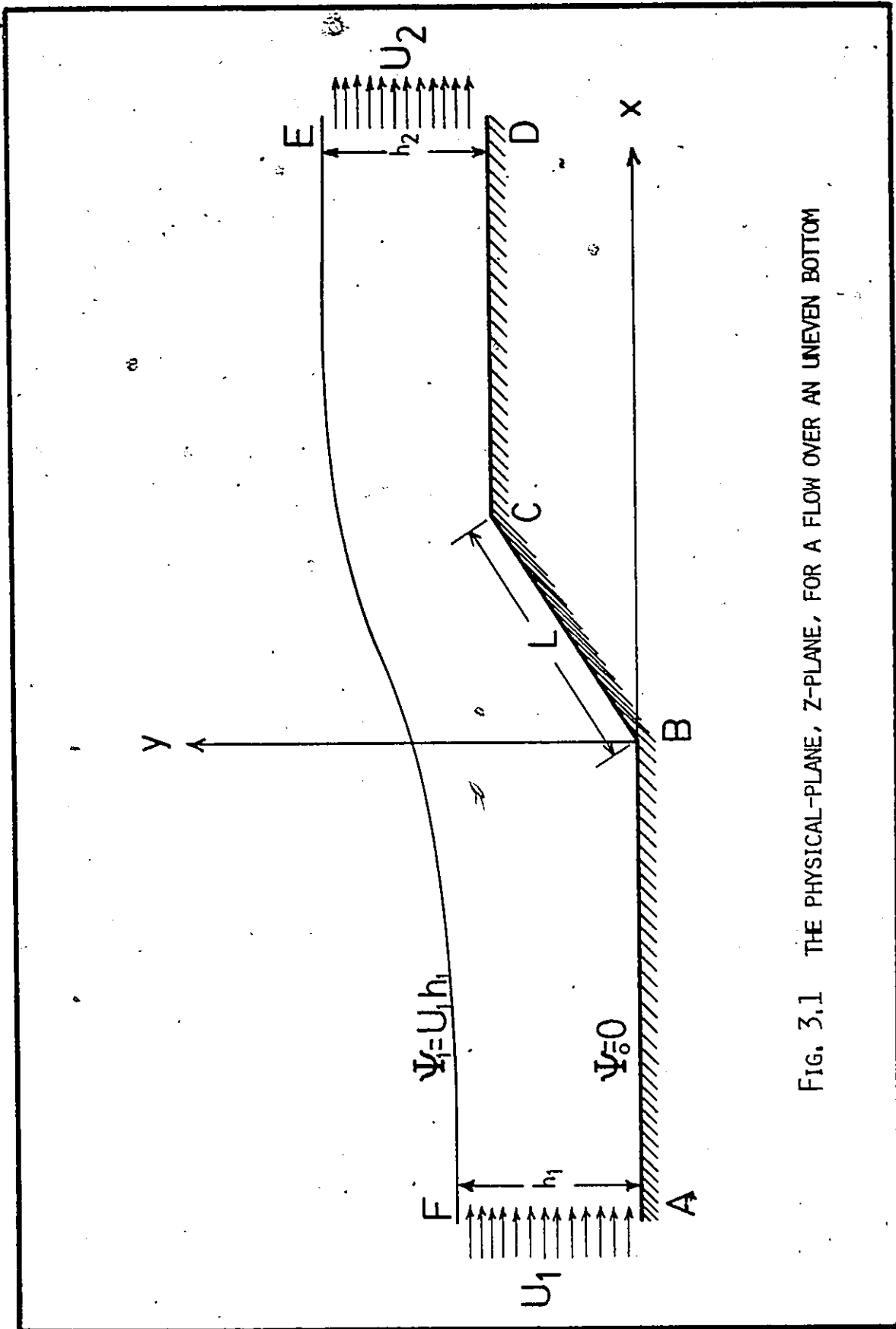


FIG. 3.1 THE PHYSICAL-PLANE, Z-PLANE, FOR A FLOW OVER AN UNEVEN BOTTOM

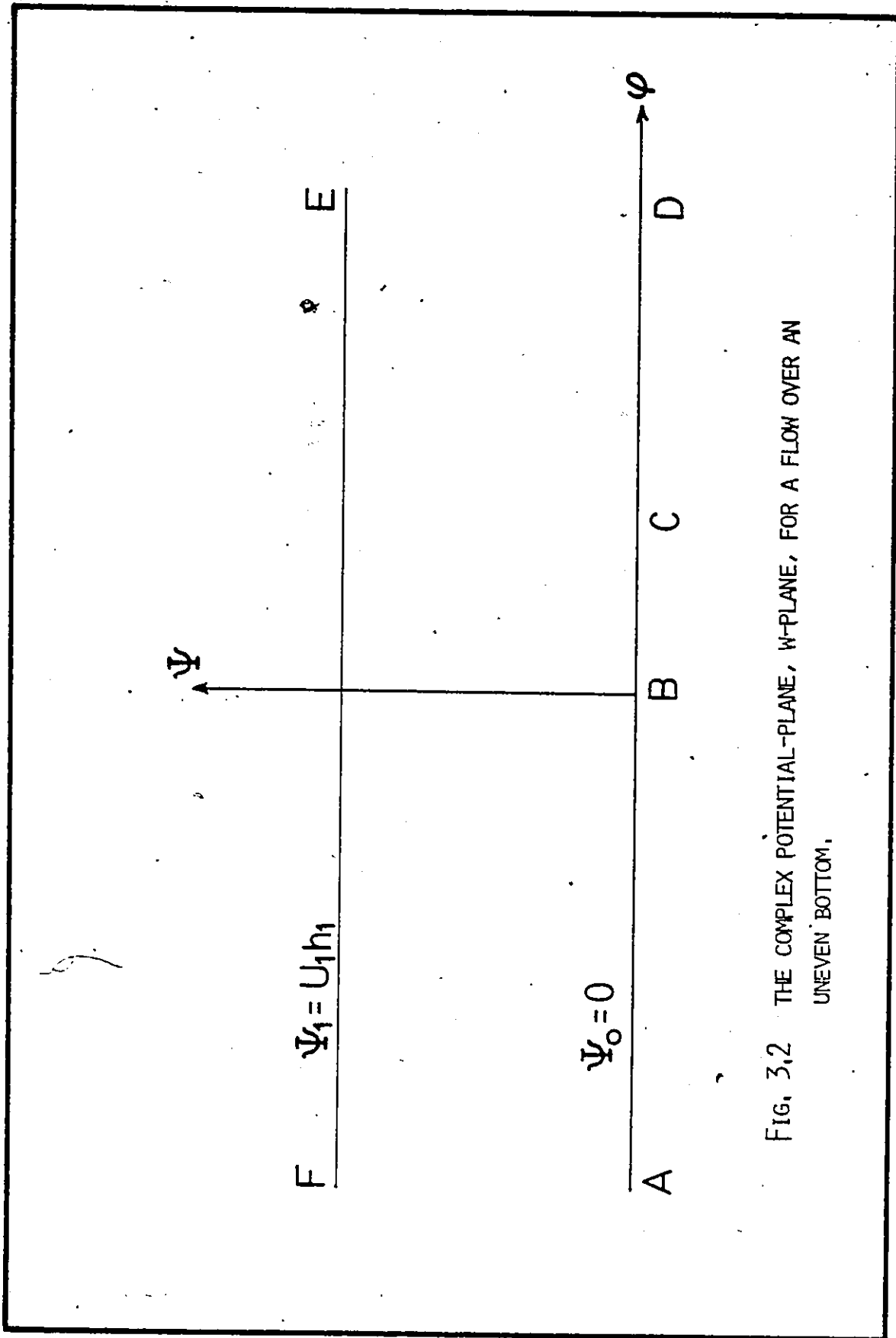


FIG. 3.2 THE COMPLEX POTENTIAL-PLANE, w -PLANE, FOR A FLOW OVER AN UNEVEN BOTTOM.

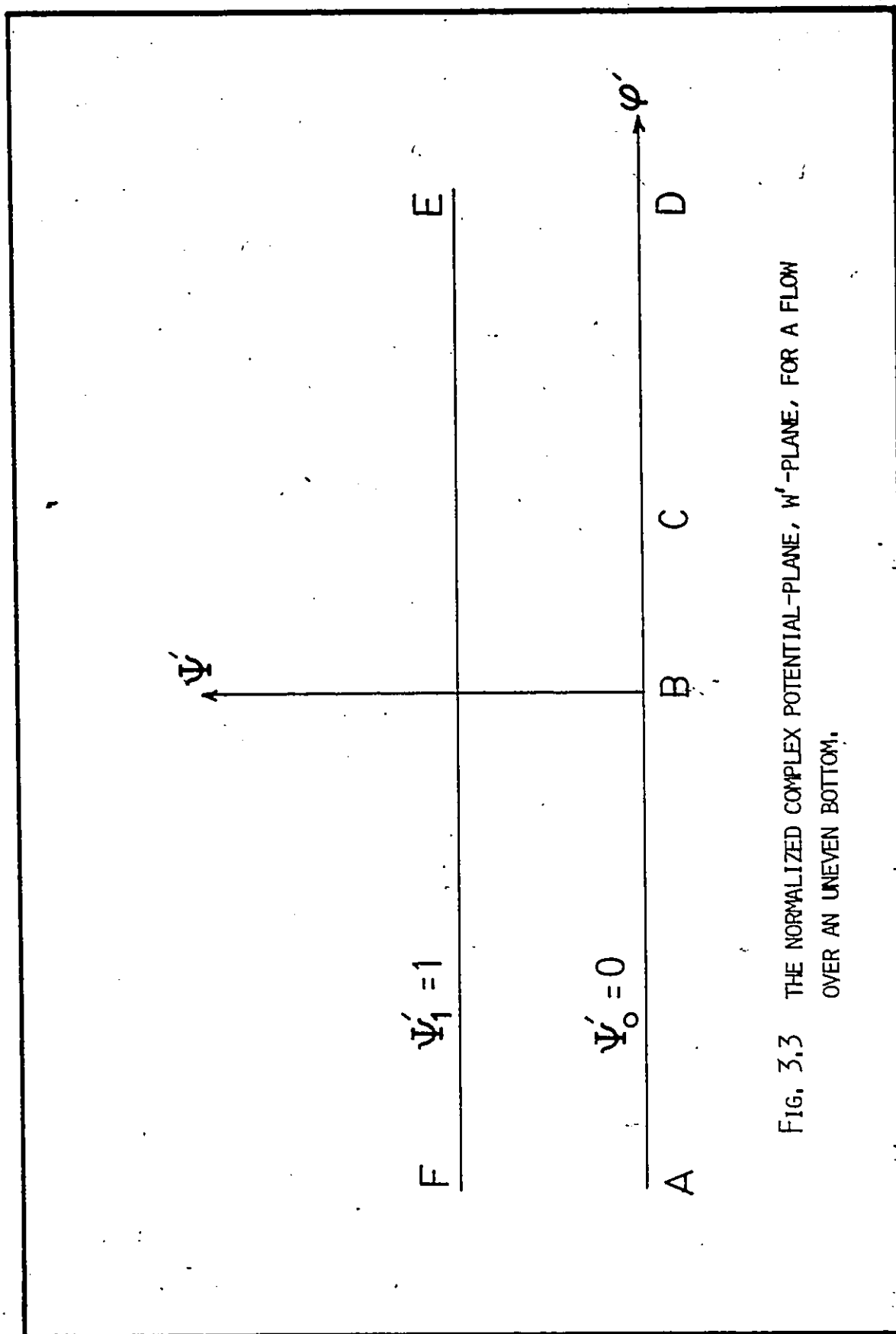


FIG. 3.3 THE NORMALIZED COMPLEX POTENTIAL-PLANE, w' -PLANE, FOR A FLOW OVER AN UNEVEN BOTTOM.

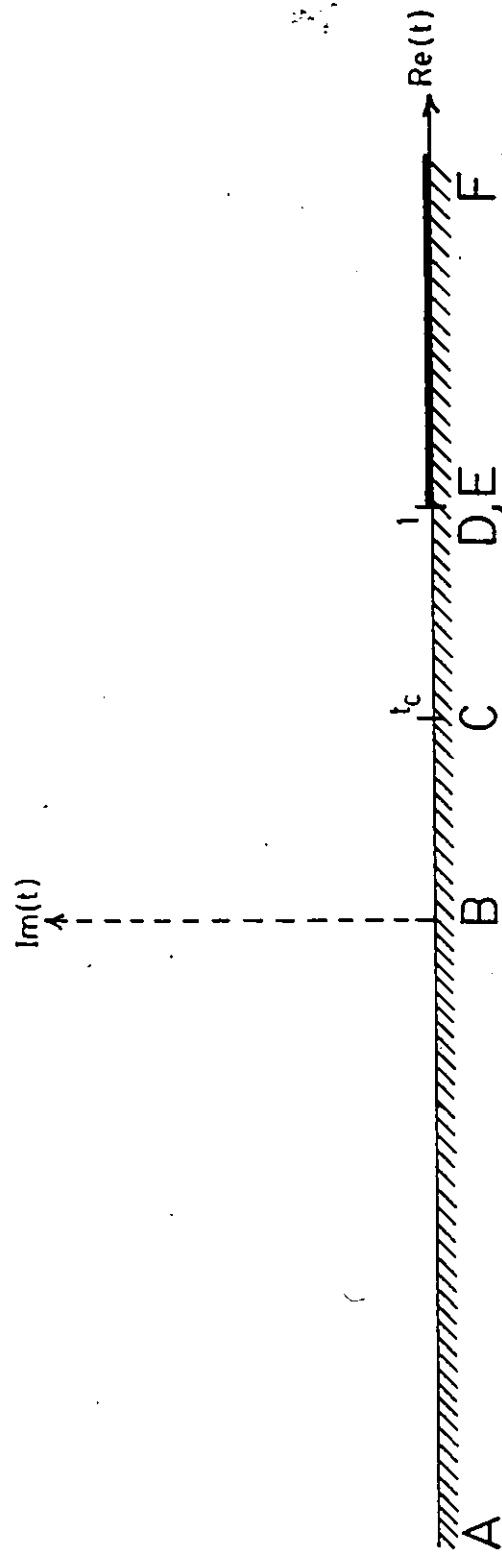


FIG. 3.4 THE UPPER HALF-PLANE, t -PLANE, FOR A FLOW OVER AN UNEVEN BOTTOM.

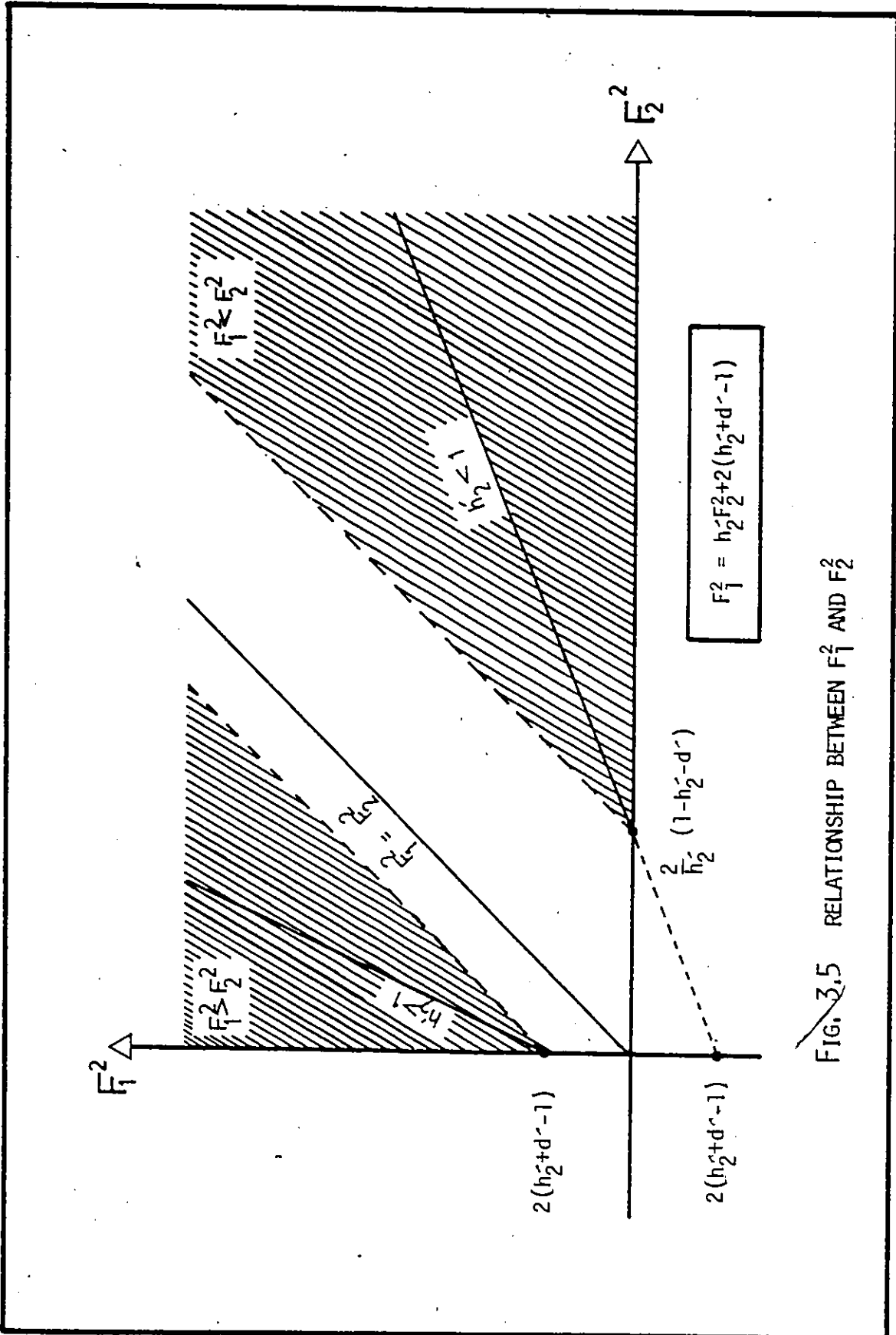
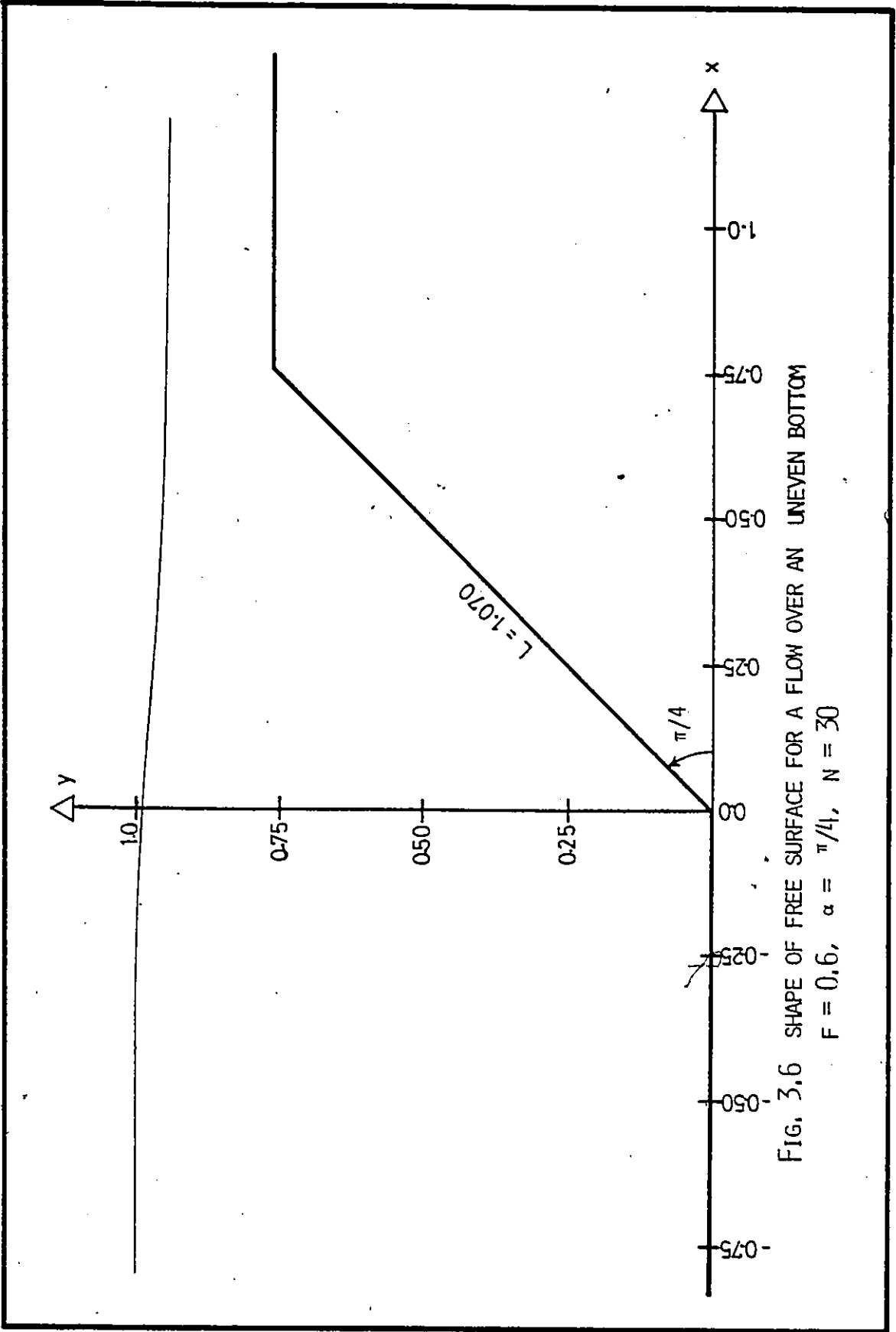


FIG. 3.5 RELATIONSHIP BETWEEN F_1^2 AND F_2^2



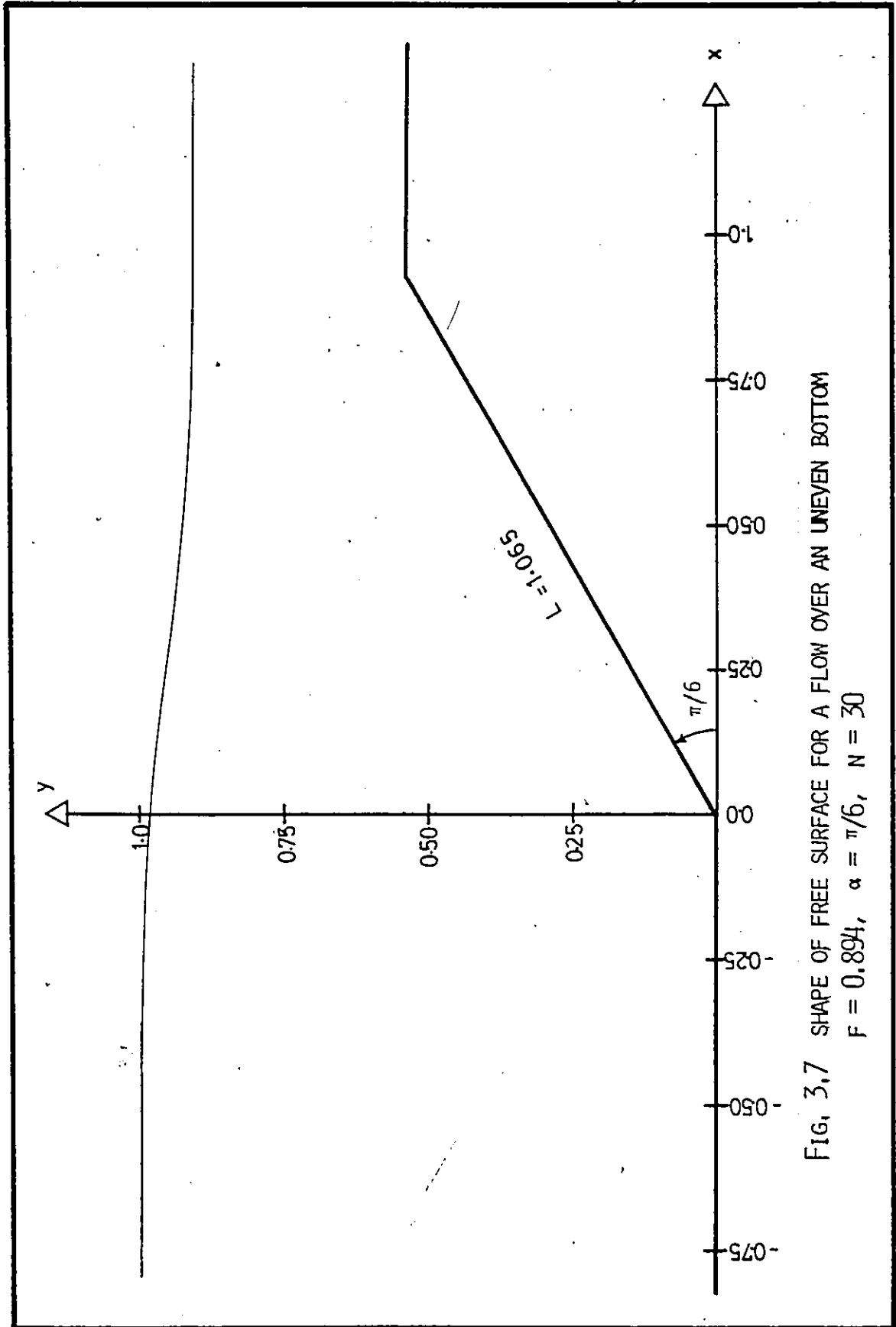


FIG. 3.7 SHAPE OF FREE SURFACE FOR A FLOW OVER AN UNEVEN BOTTOM
 $F = 0.894$, $\alpha = \pi/6$, $N = 30$

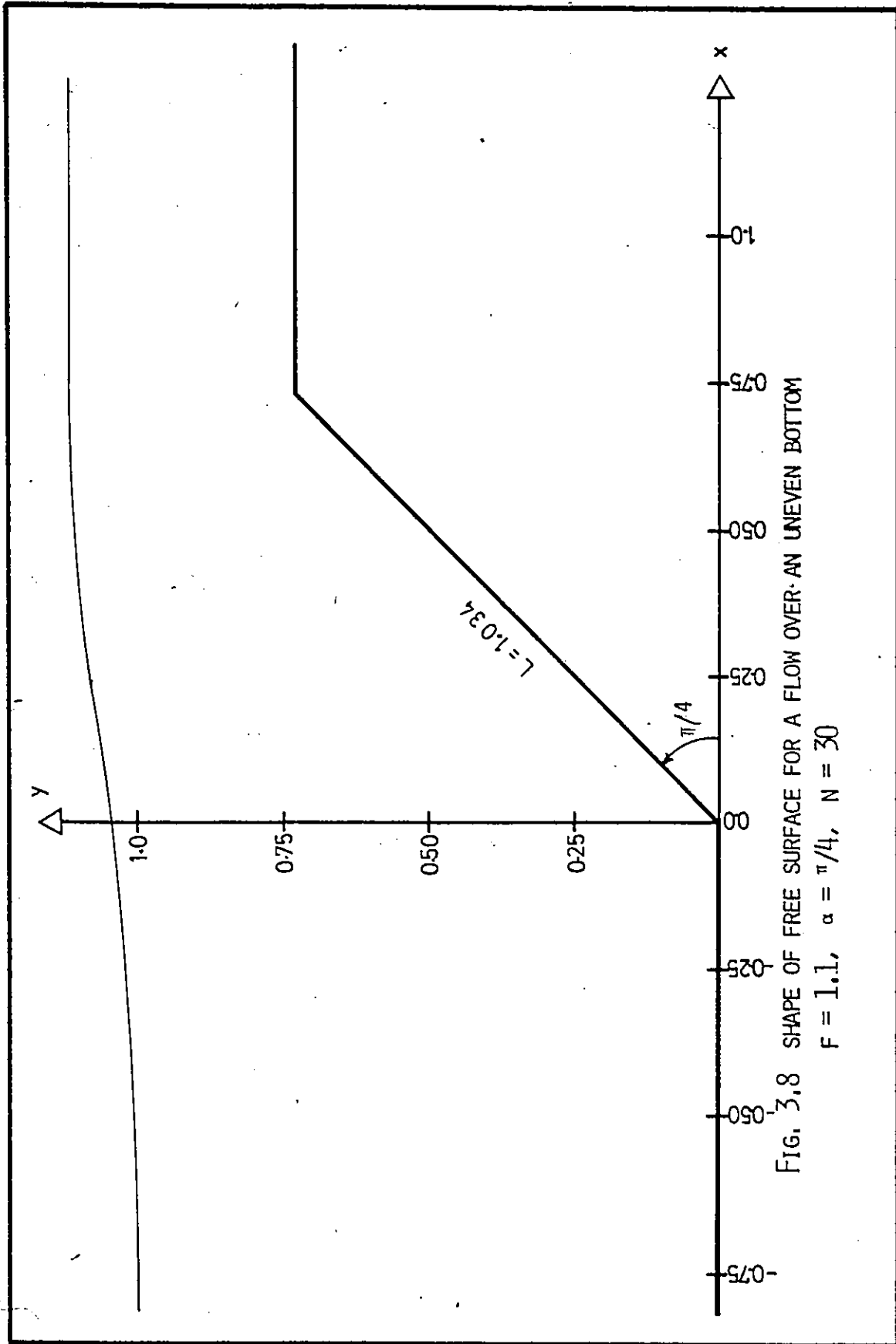


FIG. 3.8 SHAPE OF FREE SURFACE FOR A FLOW OVER AN UNEVEN BOTTOM
 $F = 1.1$, $\alpha = \pi/4$, $N = 30$

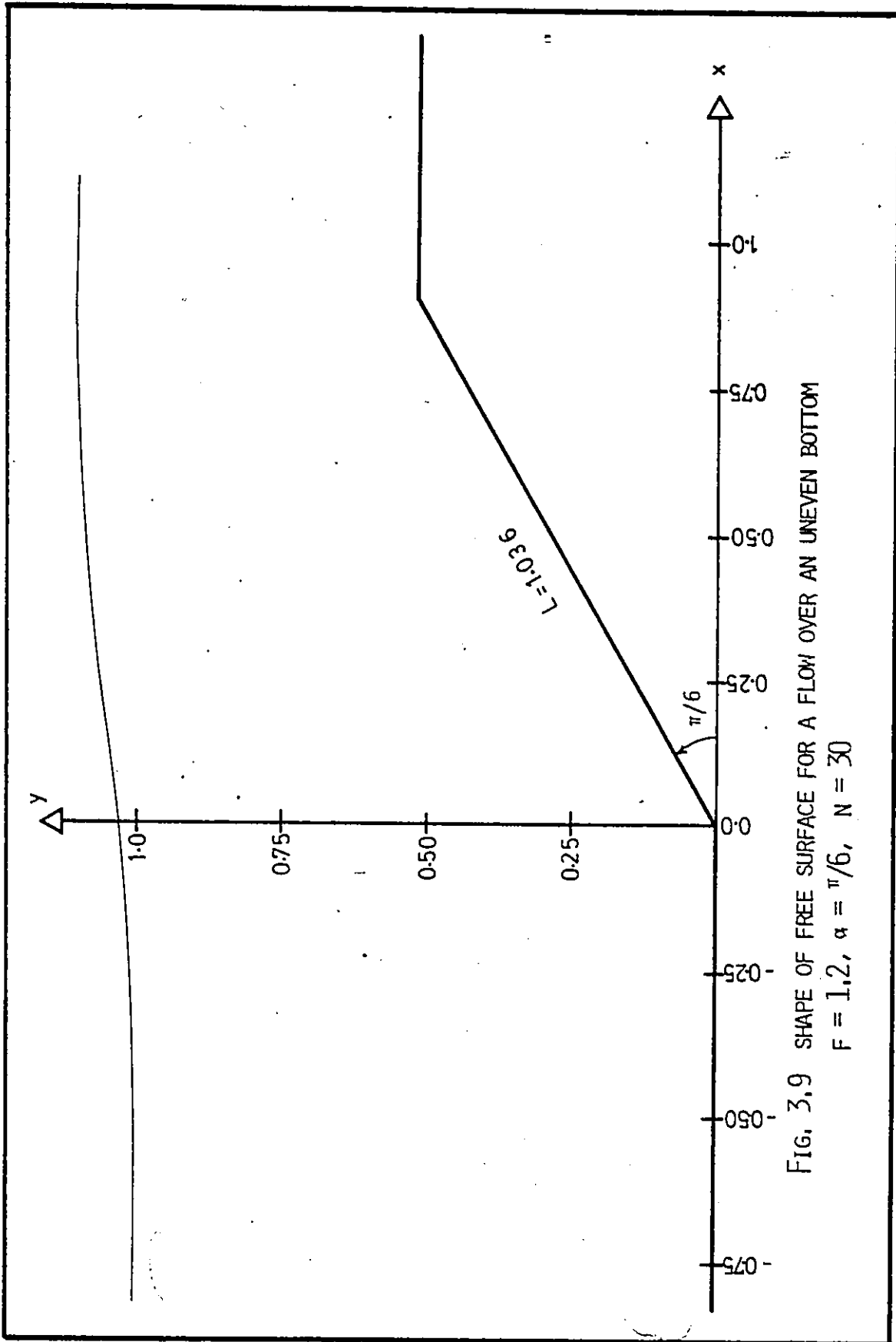


FIG. 3.9 SHAPE OF FREE SURFACE FOR A FLOW OVER AN UNEVEN BOTTOM
 $F = 1.2, \alpha = \pi/6, N = 30$

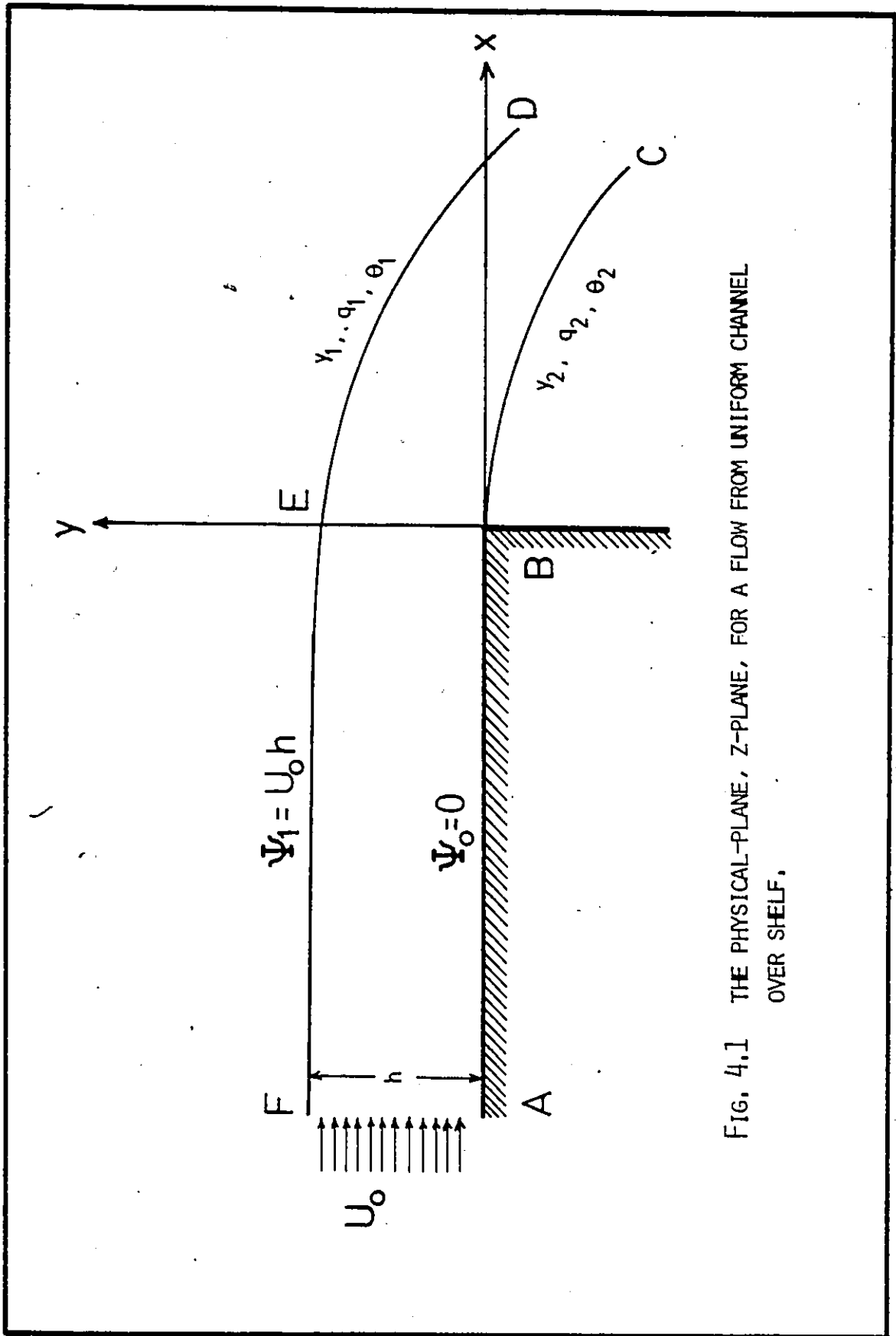


FIG. 4.1.1 THE PHYSICAL-PLANE, Z-PLANE, FOR A FLOW FROM UNIFORM CHANNEL OVER SHELF.

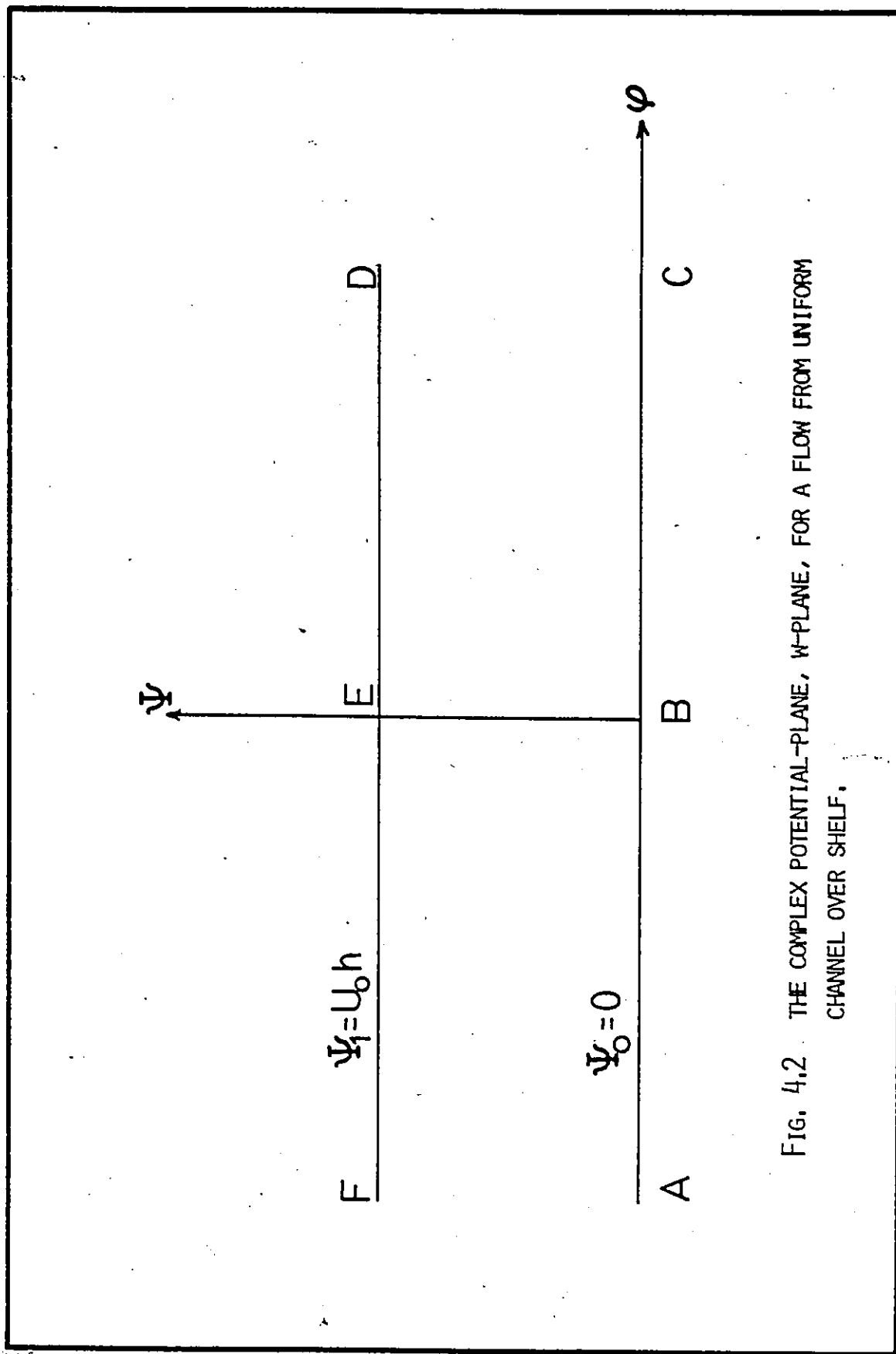


FIG. 4.2 THE COMPLEX POTENTIAL-PLANE, w -PLANE, FOR A FLOW FROM UNIFORM CHANNEL OVER SHELF.

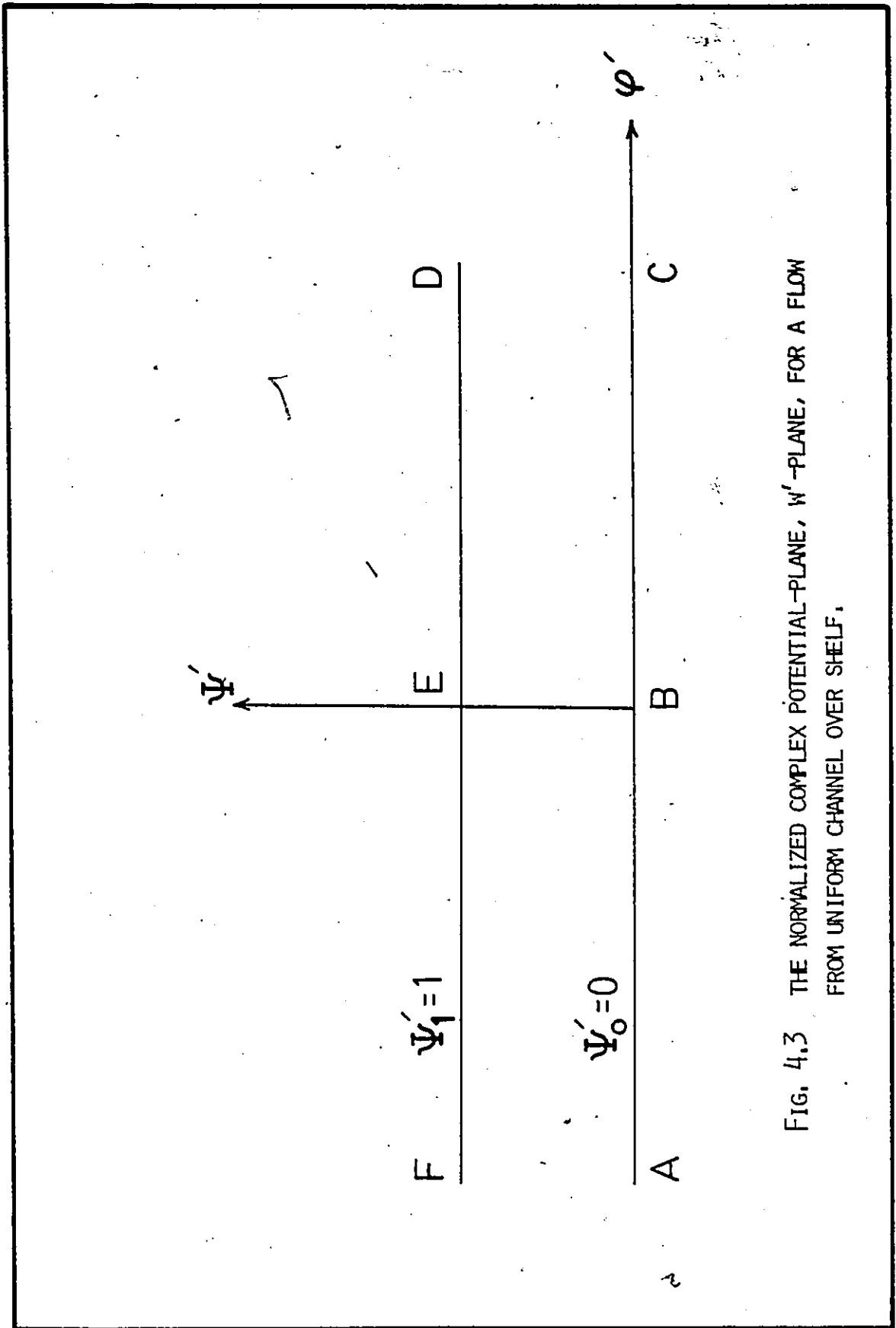


FIG. 4.3 THE NORMALIZED COMPLEX POTENTIAL-PLANE, w' -PLANE, FOR A FLOW FROM UNIFORM CHANNEL OVER SHELF.

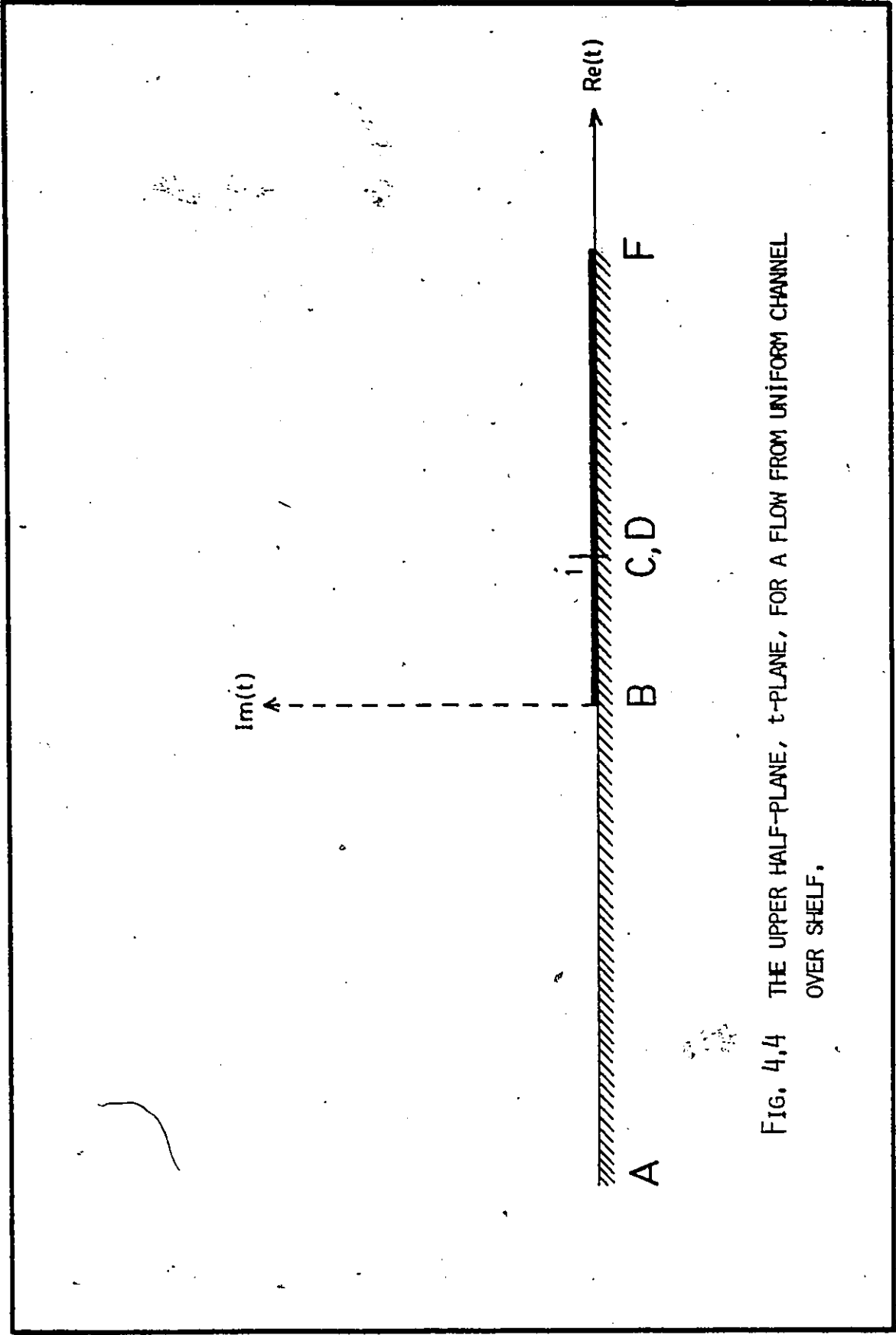


FIG. 4.4 THE UPPER HALF-PLANE, t -PLANE, FOR A FLOW FROM UNIFORM CHANNEL OVER SHELF.

re

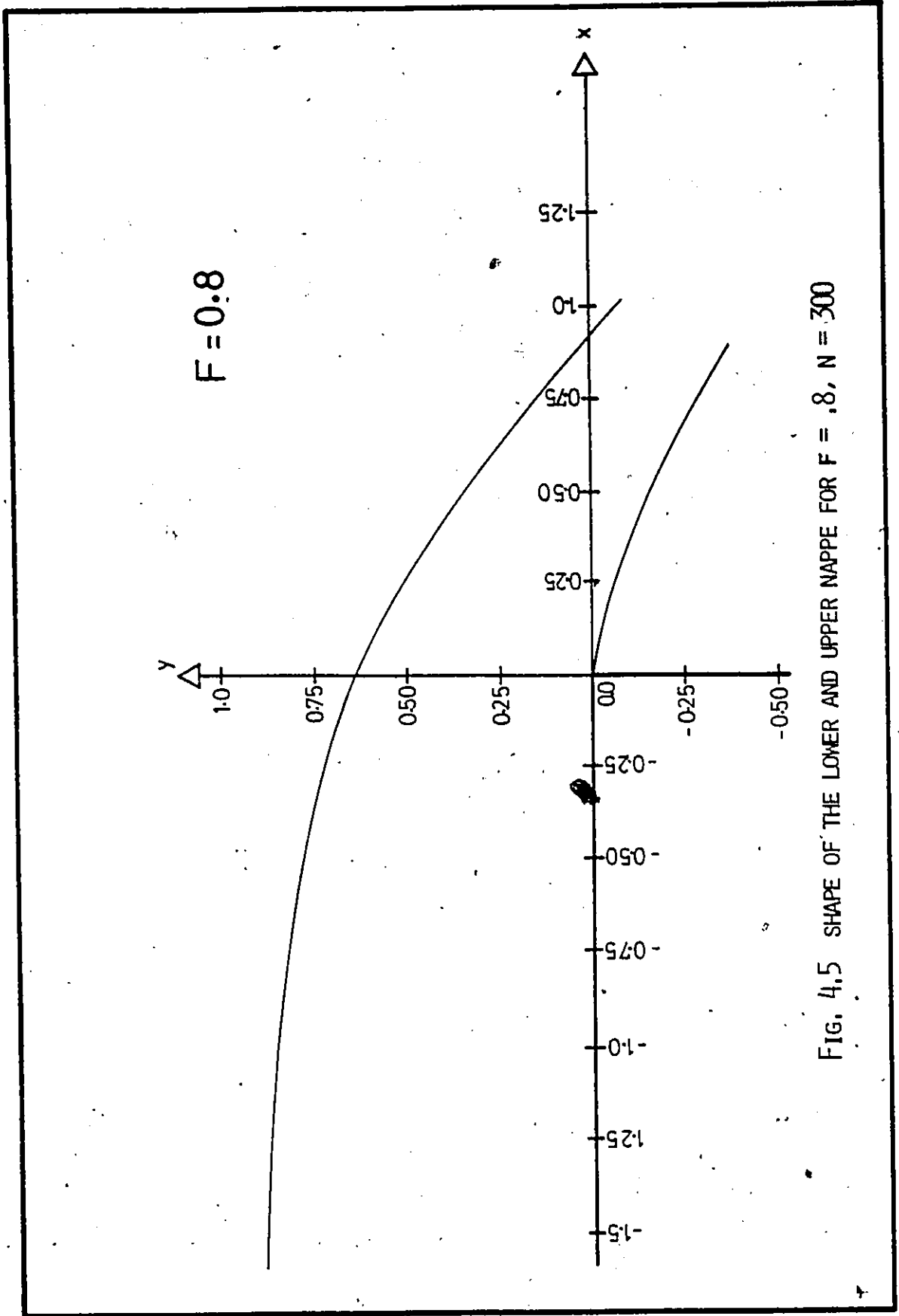
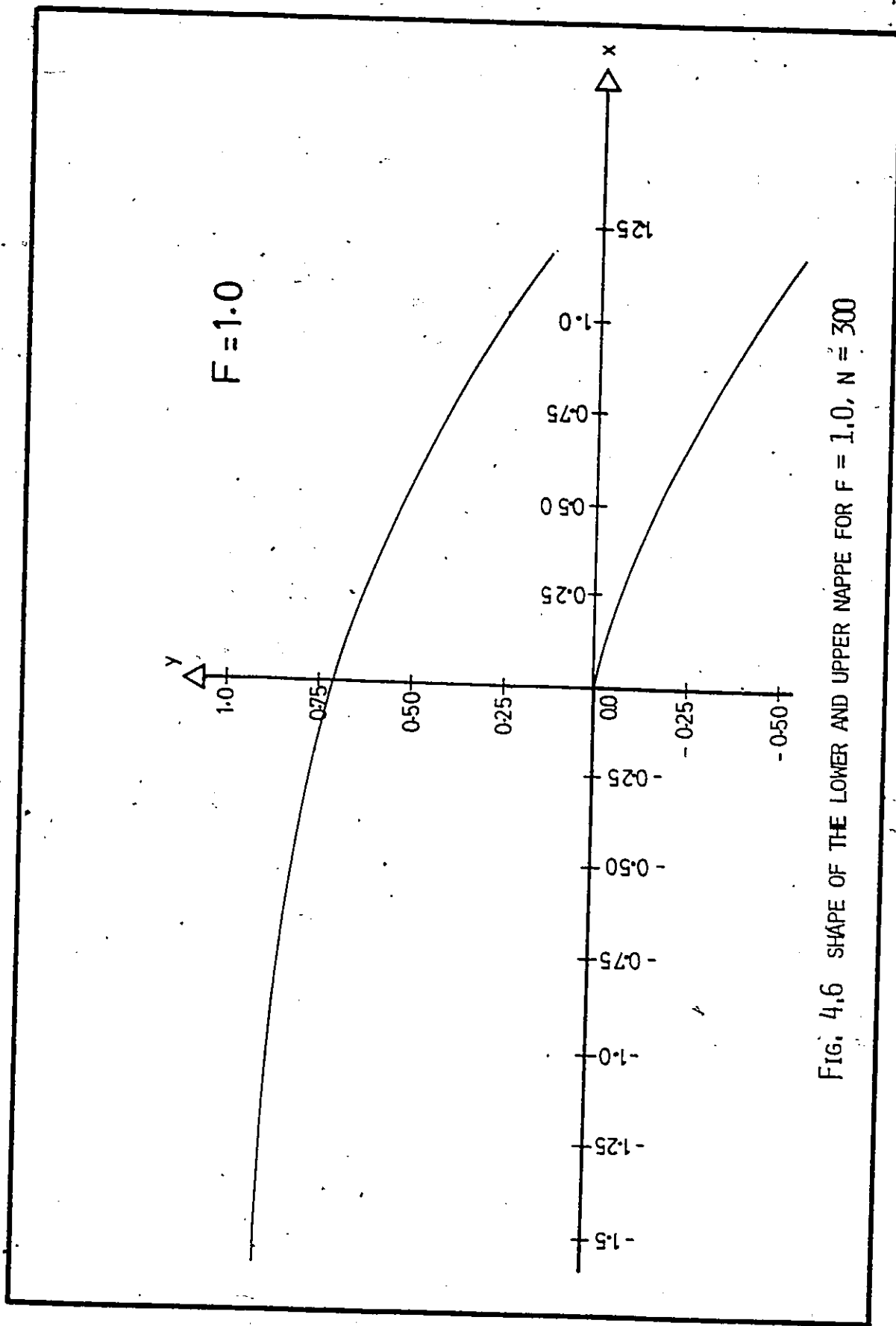


FIG. 4.5 SHAPE OF THE LOWER AND UPPER NAPPE FOR $F = .8$, $N = 300$



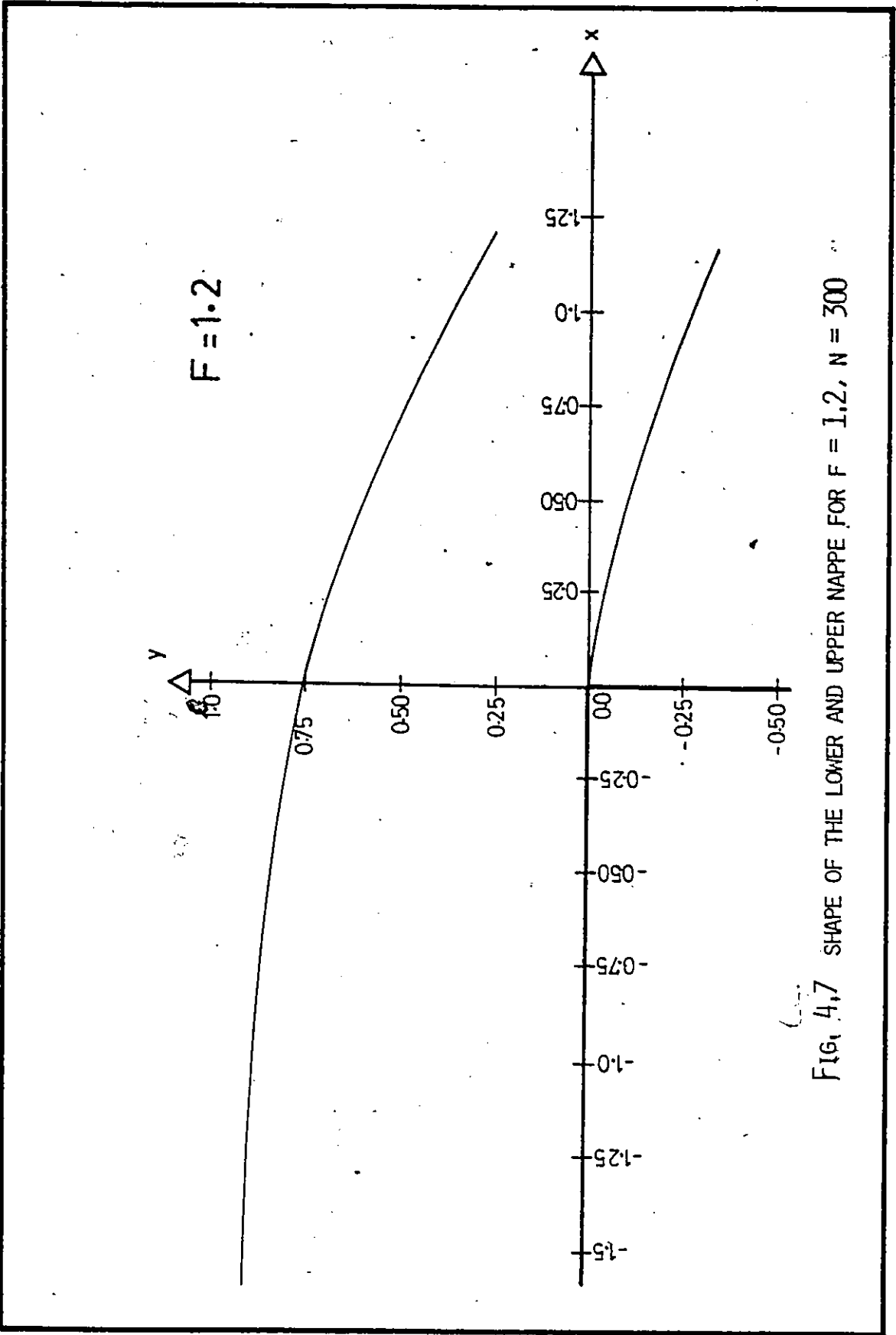


FIG. 4.7 SHAPE OF THE LOWER AND UPPER NAPPE FOR $F = 1.2$, $N = 300$

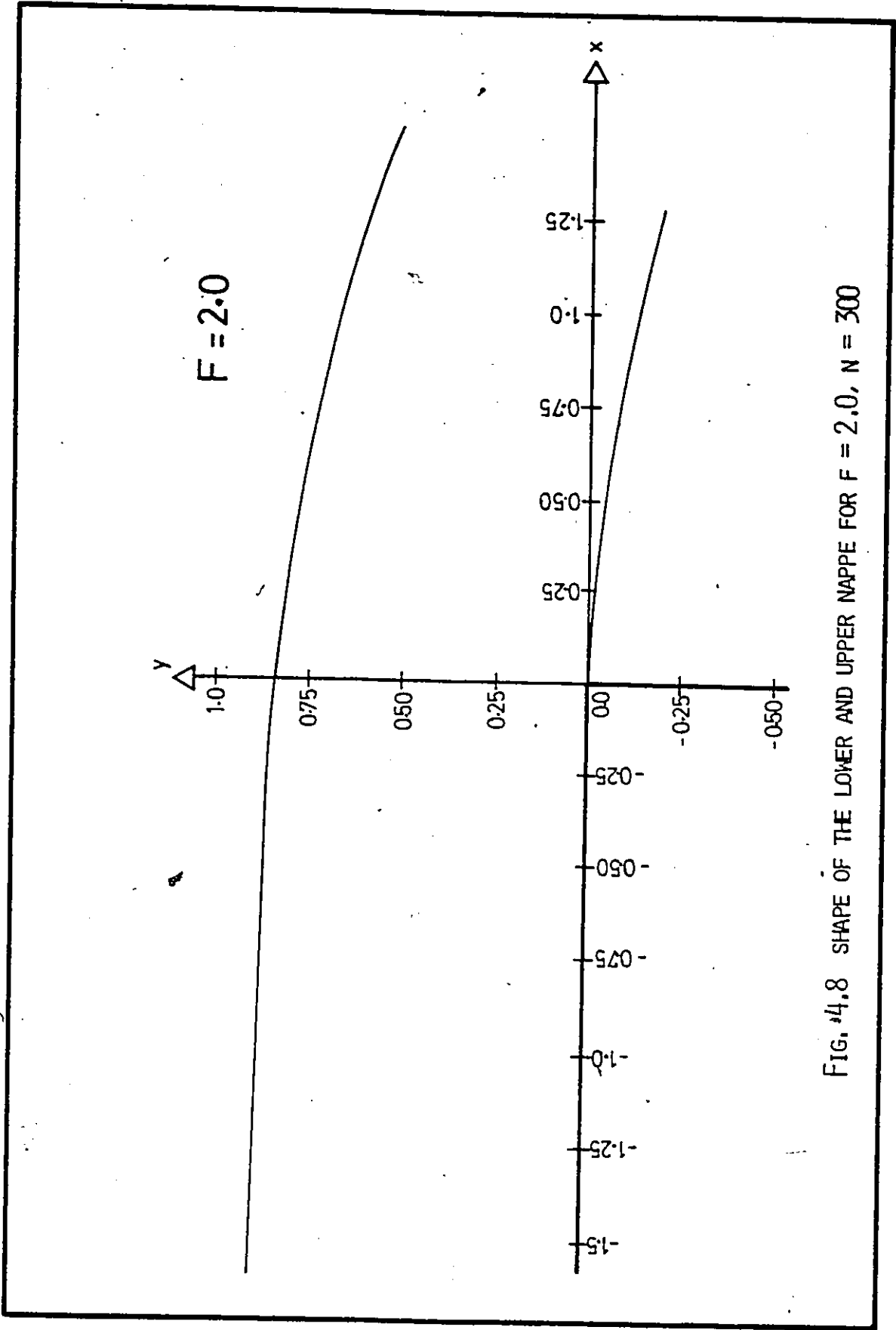


FIG. 4.8 SHAPE OF THE LOWER AND UPPER NAPPE FOR $F = 2.0$, $N = 300$

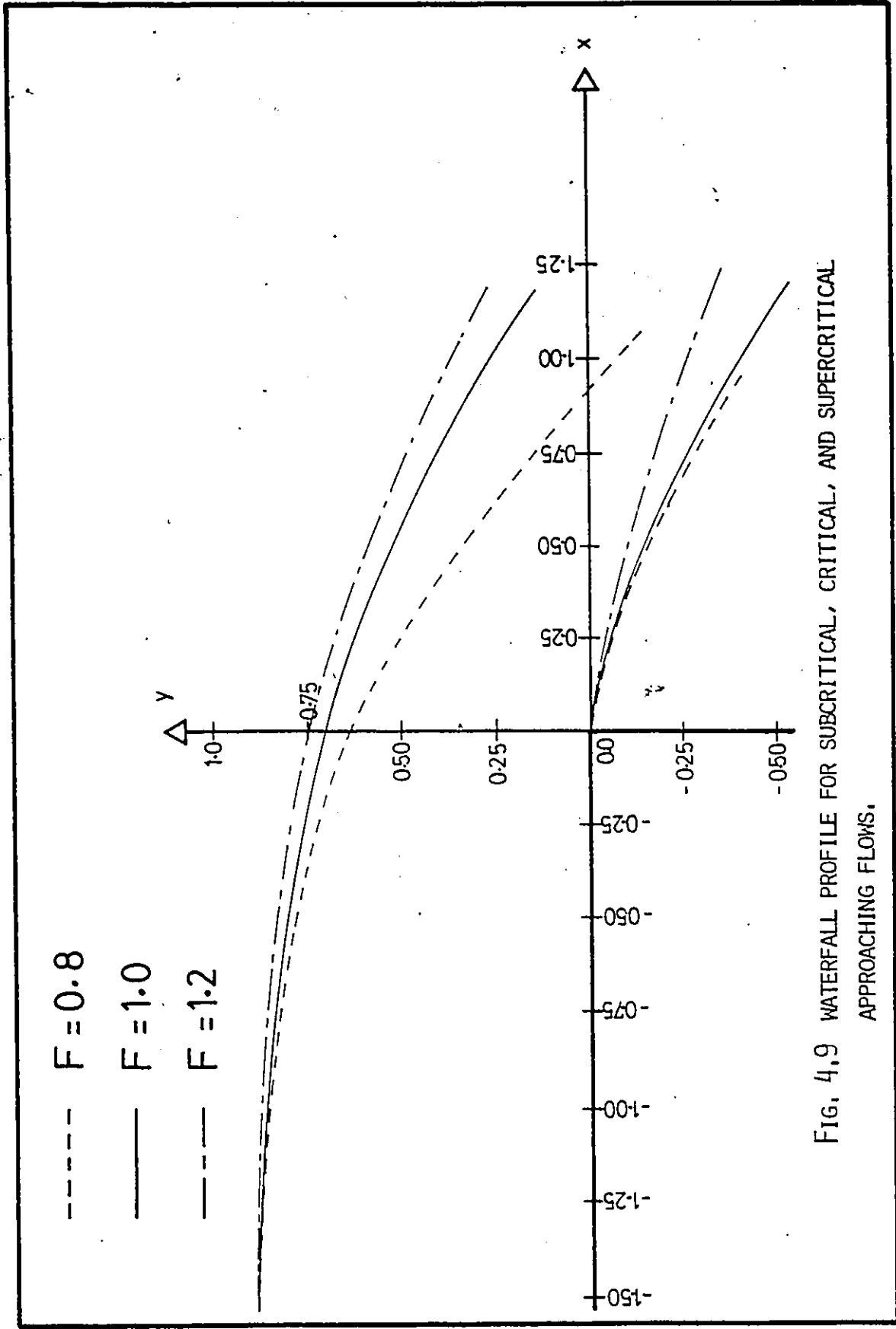


FIG. 4.9 WATERFALL PROFILE FOR SUBCRITICAL, CRITICAL, AND SUPERCRITICAL APPROACHING FLOWS.

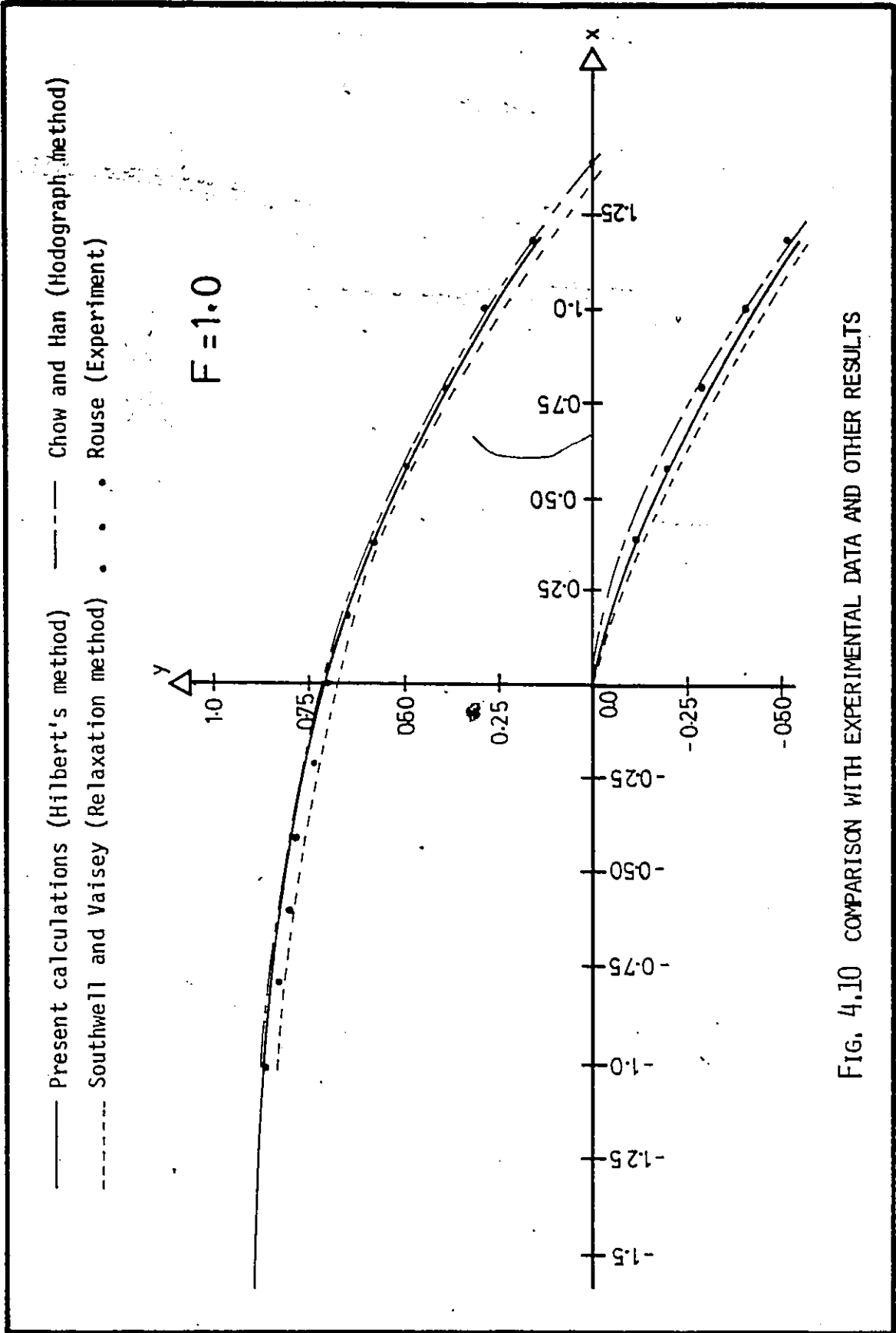


FIG. 4.10 COMPARISON WITH EXPERIMENTAL DATA AND OTHER RESULTS

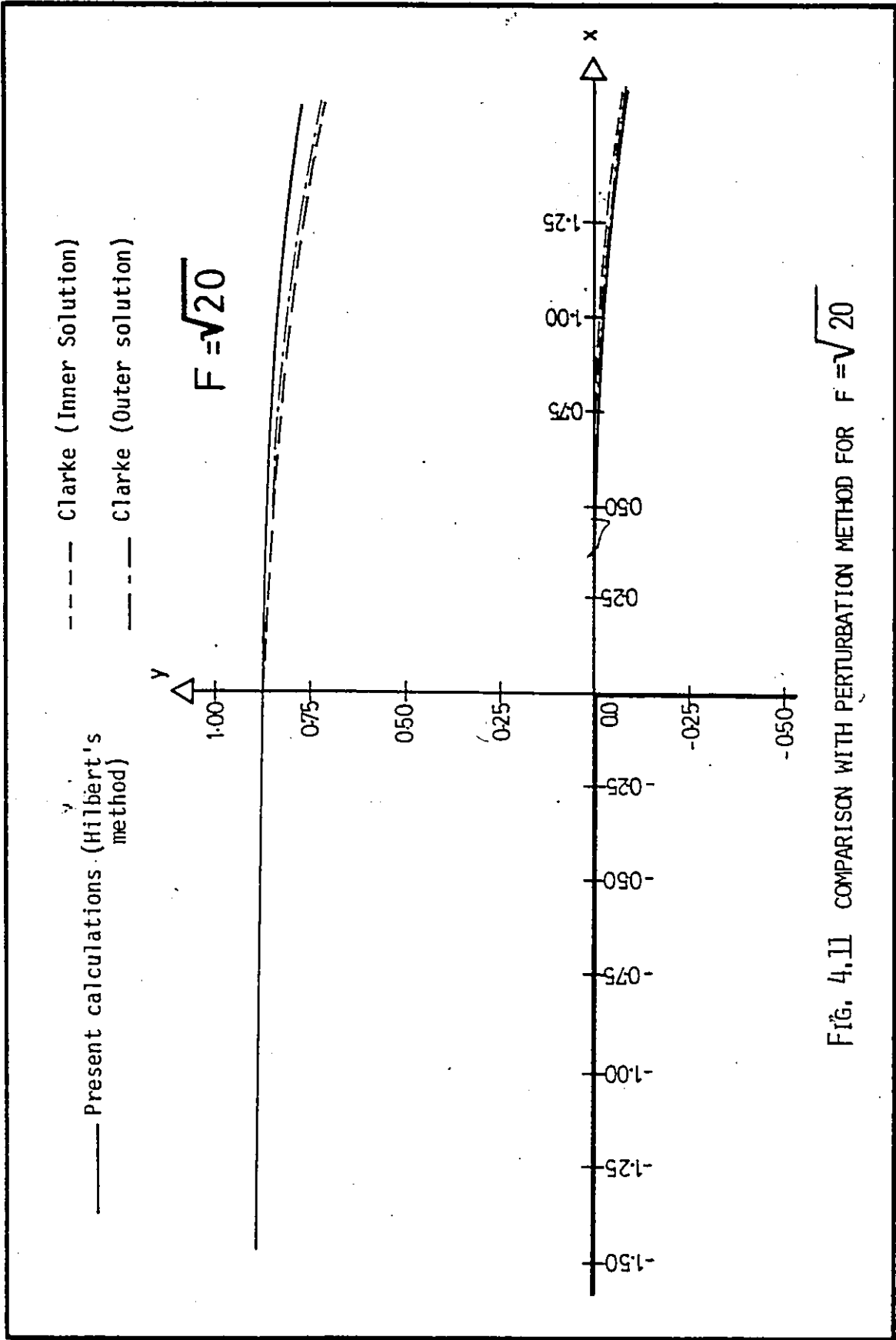


FIG. 4.11 COMPARISON WITH PERTURBATION METHOD FOR $F = \sqrt{20}$

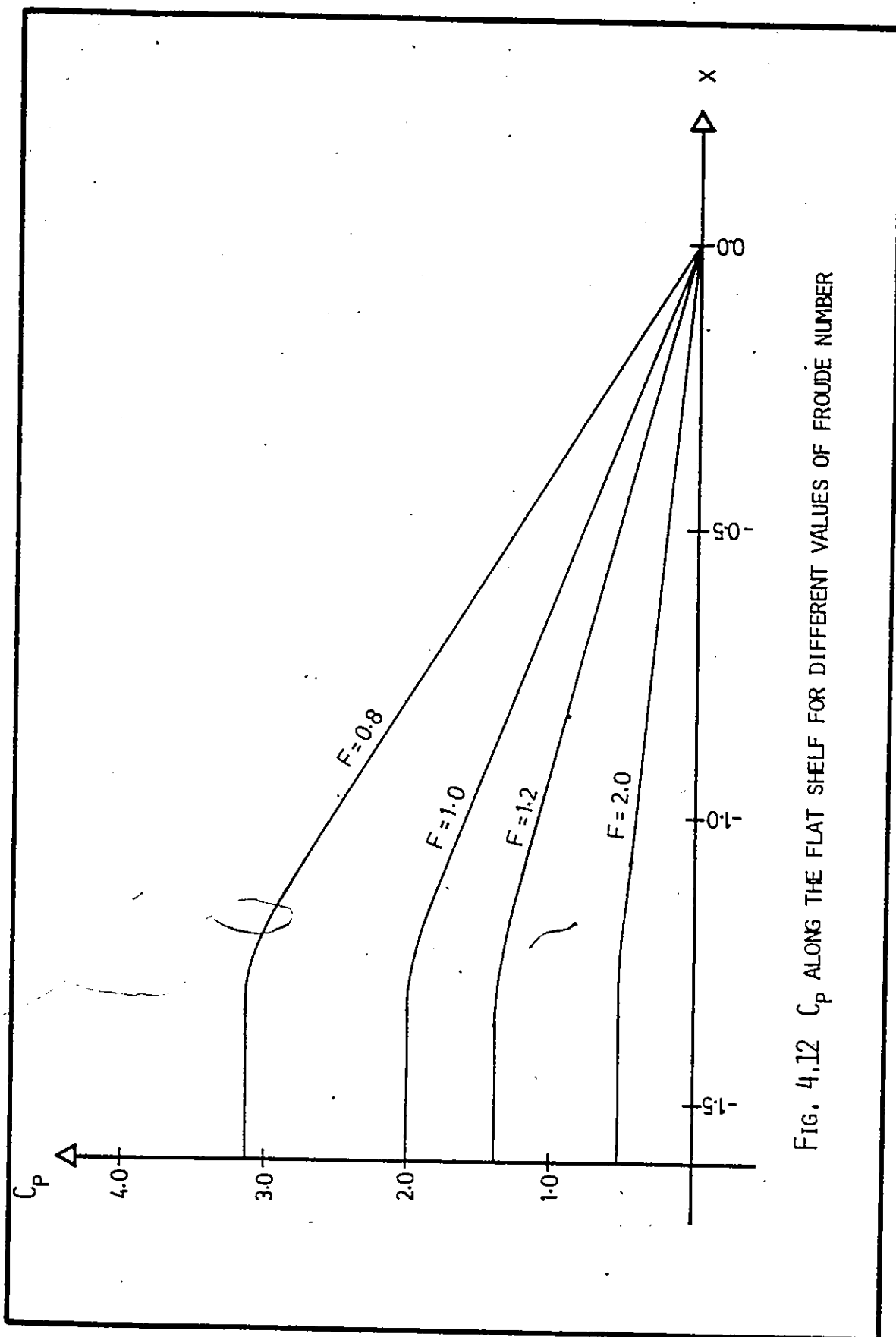


FIG. 4.12 C_p ALONG THE FLAT SHELF FOR DIFFERENT VALUES OF FROUDE NUMBER

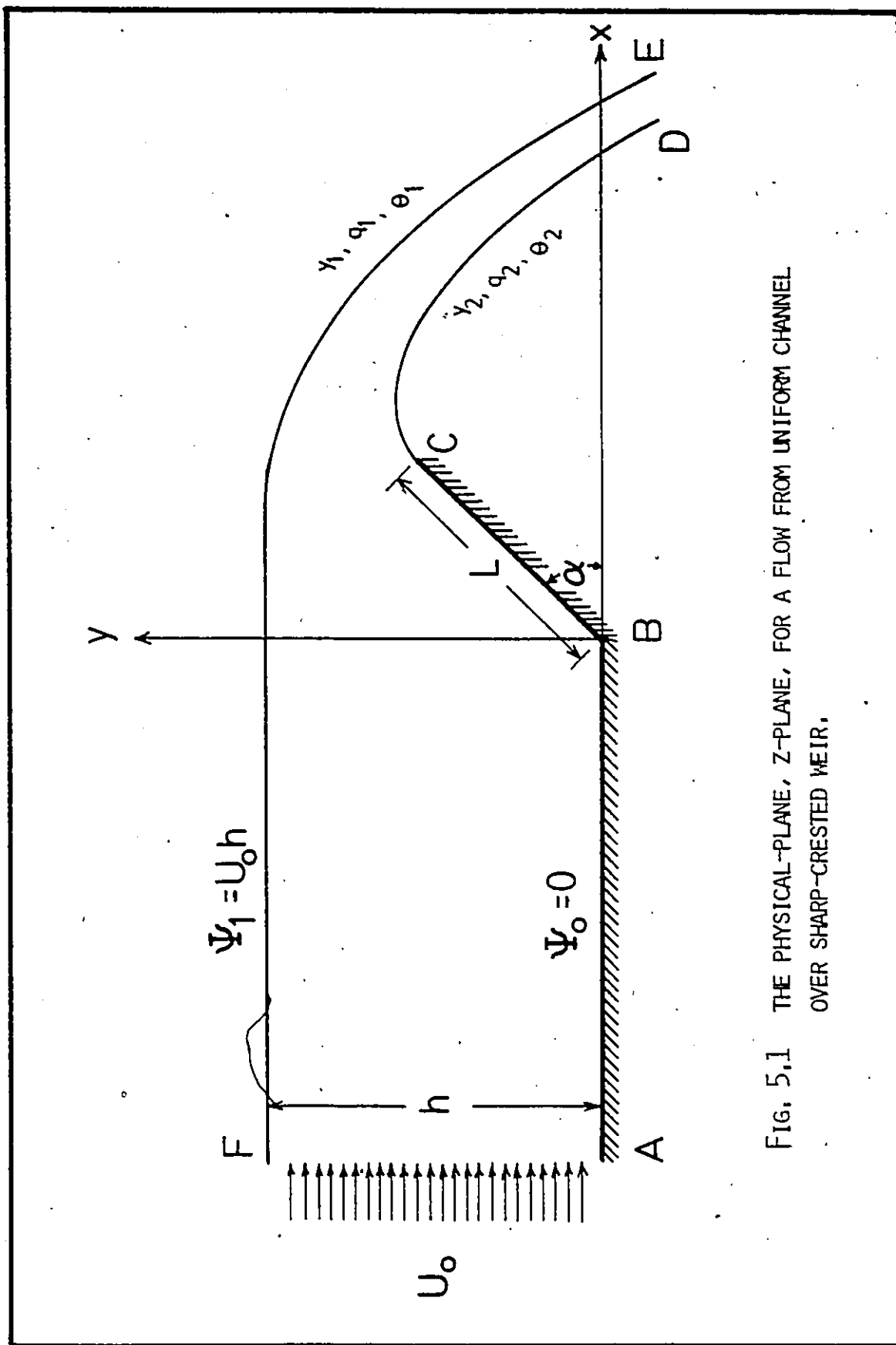


FIG. 5.1 THE PHYSICAL-PLANE, Z-PLANE, FOR A FLOW FROM UNIFORM CHANNEL OVER SHARP-CRESTED WEIR.

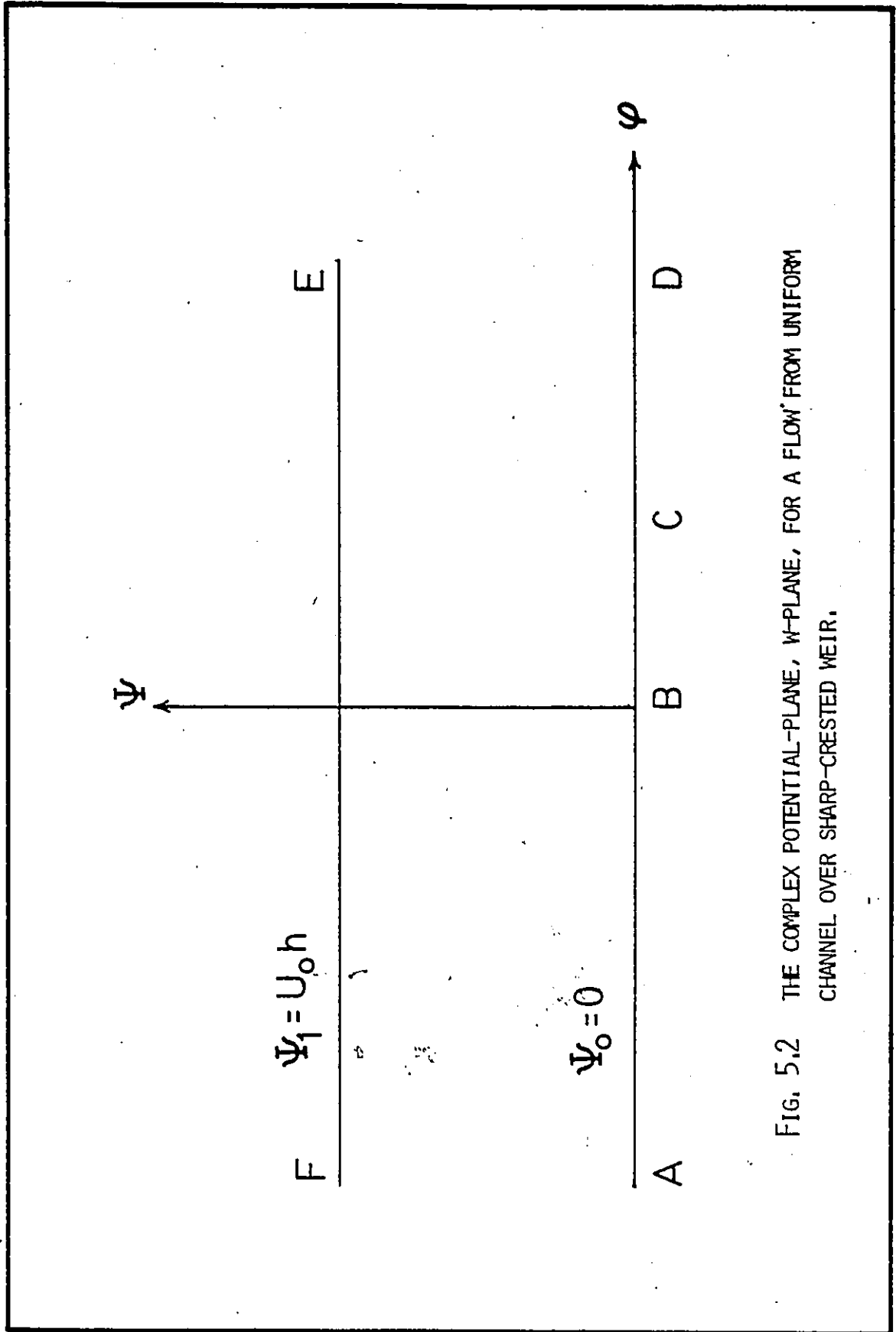


FIG. 5.2 THE COMPLEX POTENTIAL-PLANE, w -PLANE, FOR A FLOW FROM UNIFORM CHANNEL OVER SHARP-CRESTED WEIR.

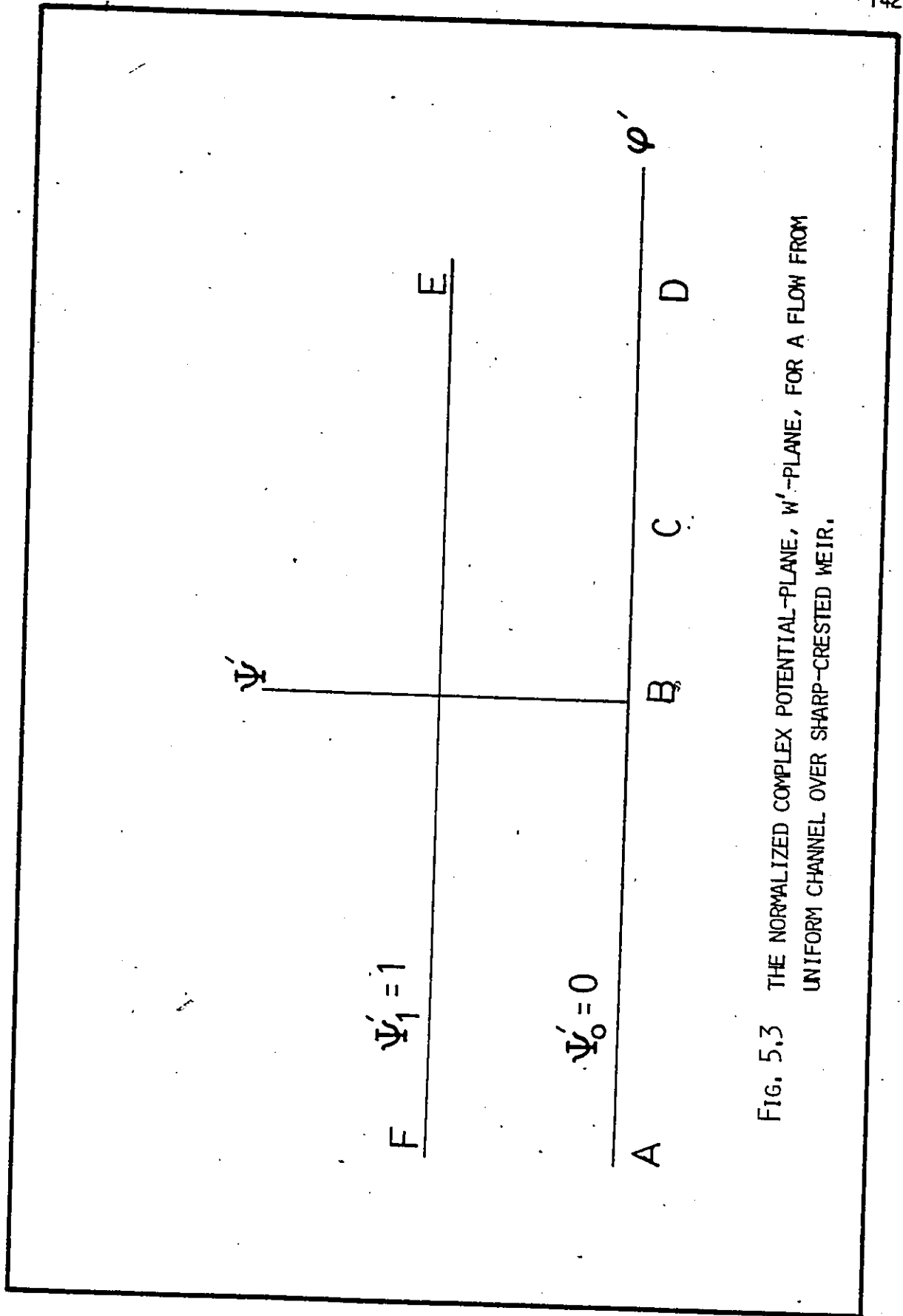


FIG. 5.3 THE NORMALIZED COMPLEX POTENTIAL-PLANE, w' -PLANE, FOR A FLOW FROM UNIFORM CHANNEL OVER SHARP-CRESTED WEIR.

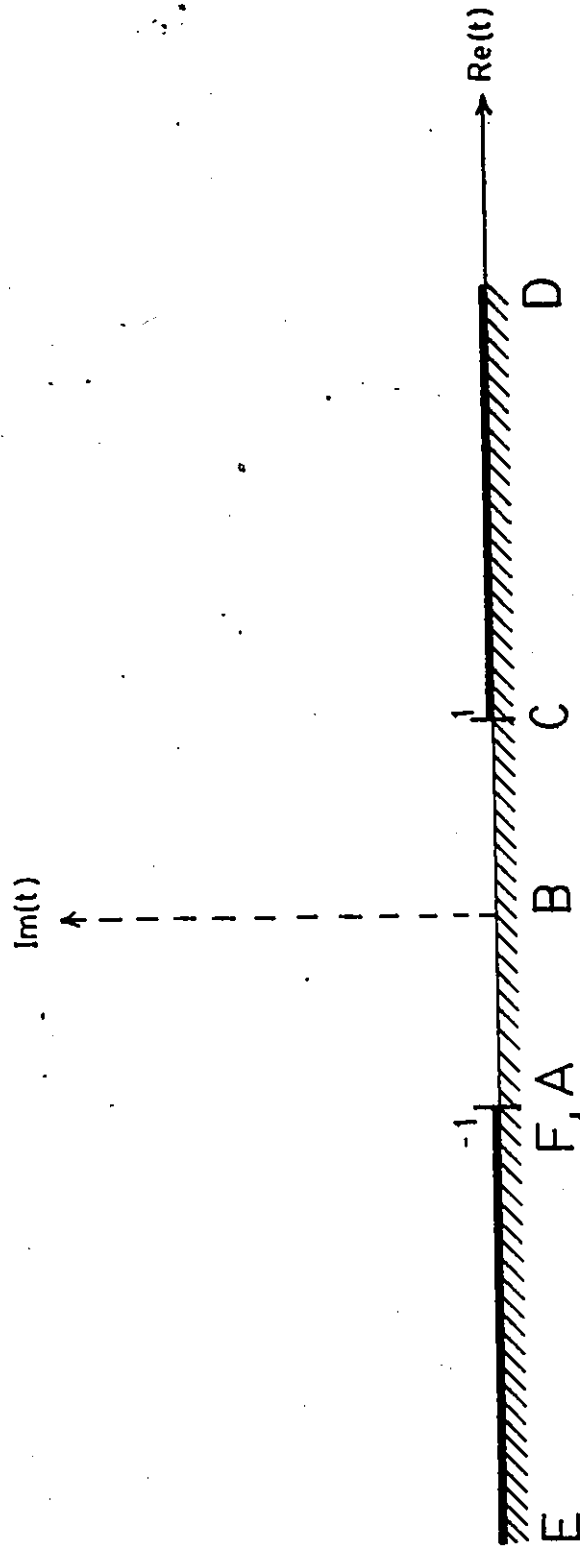
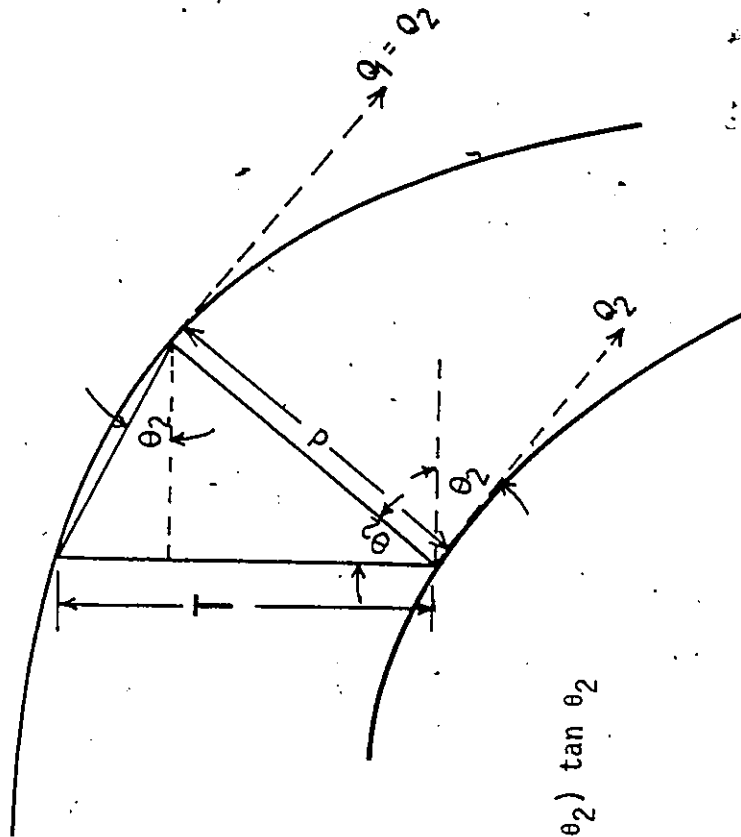


FIG. 5.4 THE UPPER HALF-PLANE, t -PLANE, FOR A FLOW FROM UNIFORM CHANNEL OVER SHARP-CRESTED WEIR.



$$d = 1/Q_2$$

$$T = d \cos \theta_2 + (d \sin \theta_2) \tan \theta_2$$

$$= 1/(Q_2 \cos \theta_2)$$

FIG. 5.5 CALCULATIONS OF THE INITIAL PROFILE FOR THE UPPER AND LOWER NAPPE FOR A FLOW FROM UNIFORM CHANNEL OVER SHARP-CRESTED WEIR.

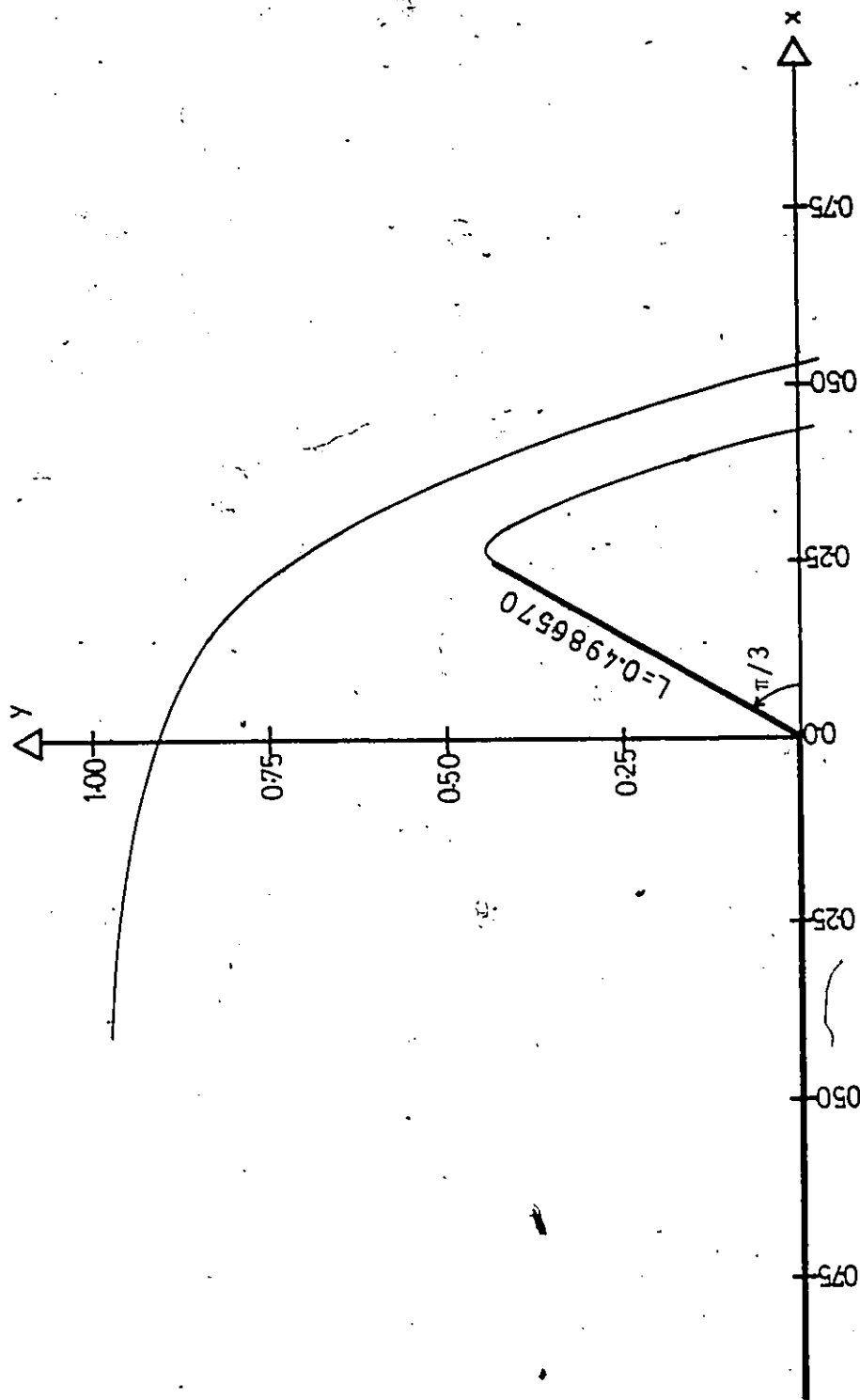


FIG. 5.6 SHAPE OF THE LOWER AND UPPER NAPPE FOR A FLOW FROM UNIFORM CHANNEL OVER SHARP-CRESTED WEIR. $F = .9$; $\alpha = \pi/3$

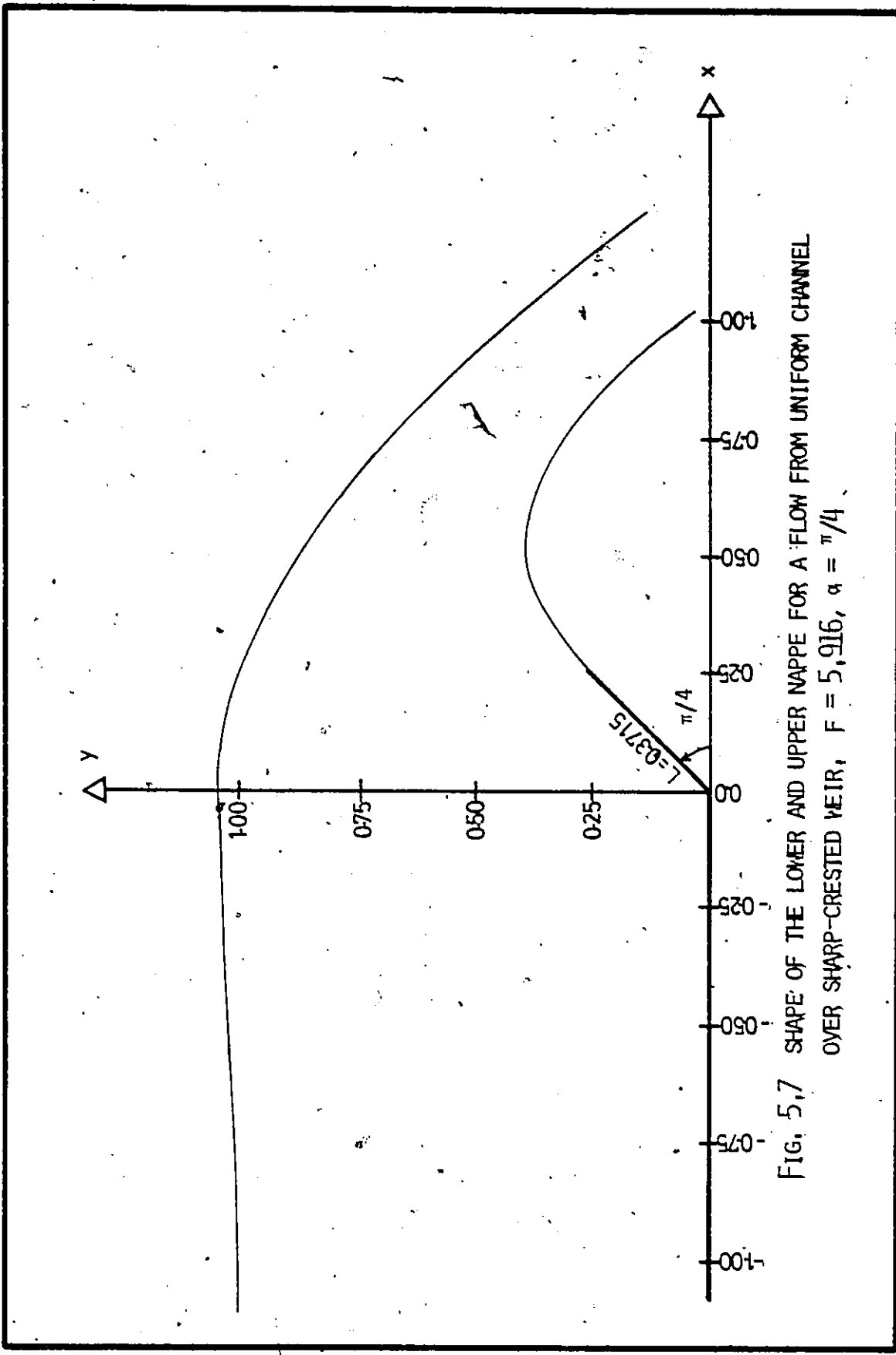


FIG. 5.7 SHAPE OF THE LOWER AND UPPER NAPPE FOR A FLOW FROM UNIFORM CHANNEL OVER SHARP-CRESTED WEIR, $F = 5.916$, $\alpha = \pi/4$.

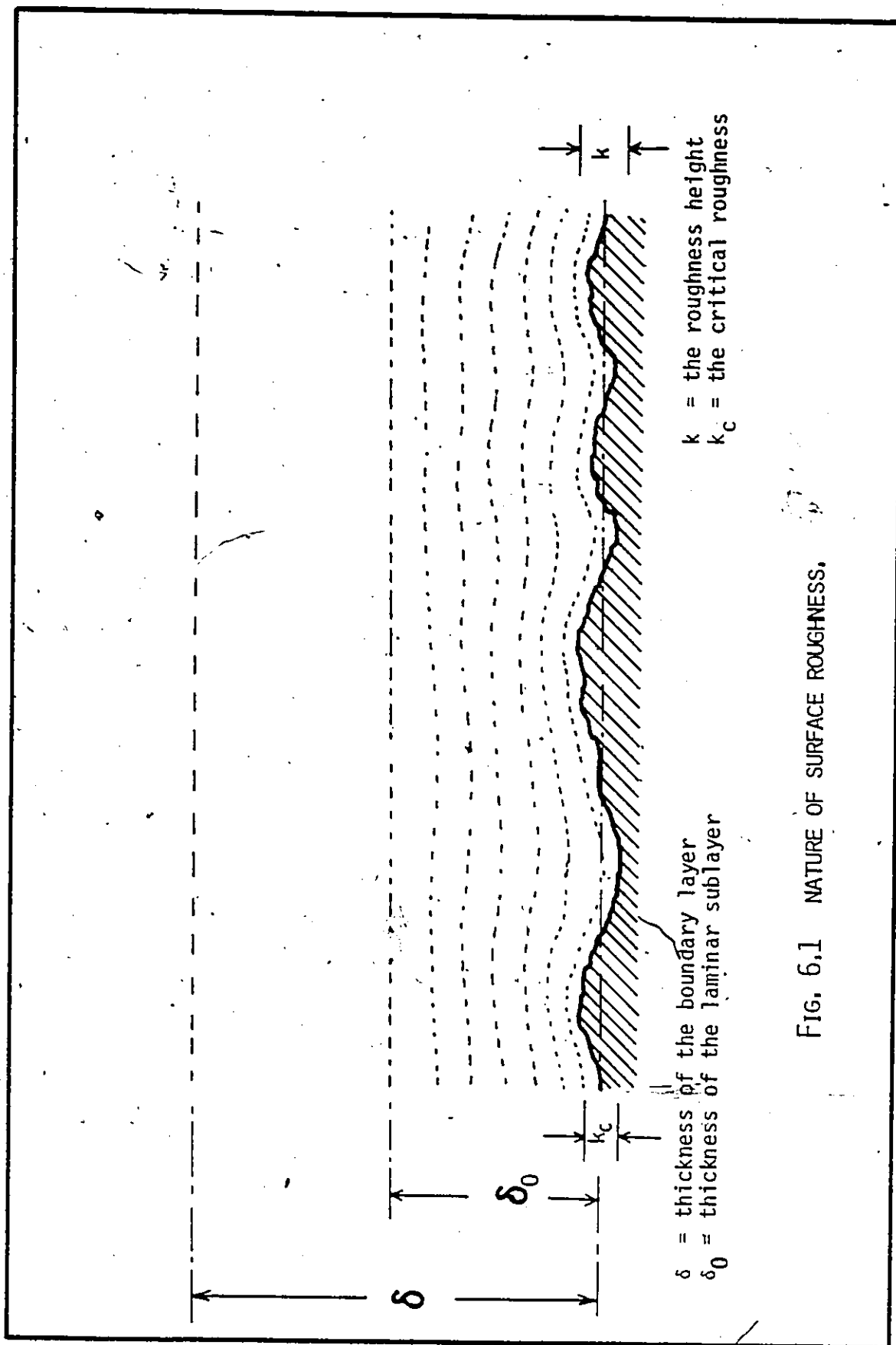


FIG. 6.1 NATURE OF SURFACE ROUGHNESS.

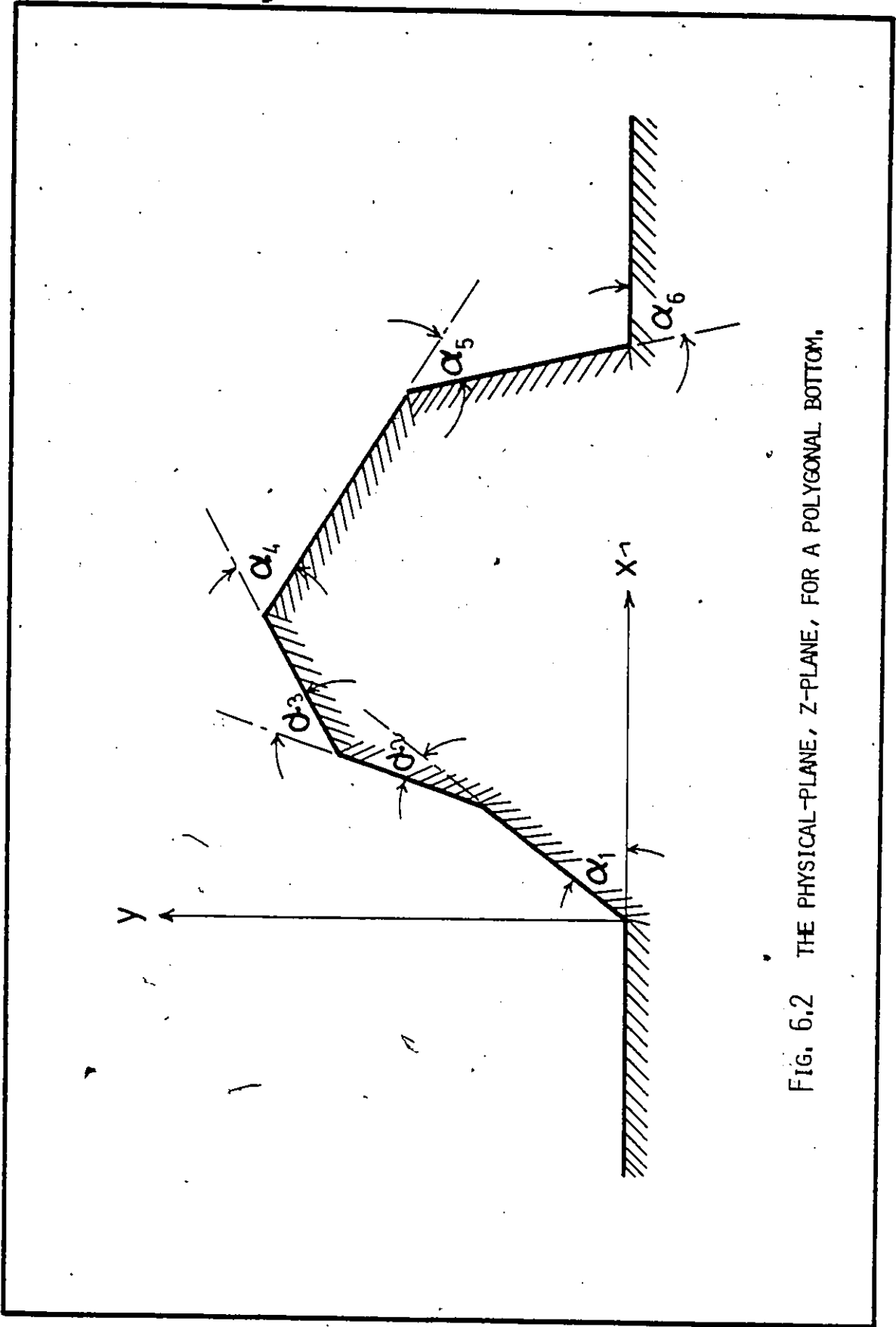


FIG. 6.2 THE PHYSICAL-PLANE, Z-PLANE, FOR A POLYGONAL BOTTOM.

APPENDICES

- [A] REMOVING THE SINGULARITY FROM SINGULAR INTEGRAL EQUATIONS.
- [B] UNIQUENESS OF SCHWARTZ-CHRISTOFFEL TRANSFORMATION BY PRESCRIBING THE MAPPING OF THREE POINTS ON THE BOUNDARY OF THE UPPER HALF-PLANE.
- [C] PROOF OF THE HILBERT FORMULAE.
- [D] COMPUTER PROGRAM FOR A FLOW OVER AN UNEVEN BOTTOM.
- [E] COMPUTER PROGRAM FOR A FLOW FROM UNIFORM CHANNEL OVER SHELF.
- [F] COMPUTER PROGRAM FOR A FLOW FROM UNIFORM CHANNEL OVER SHARP-CRESTED WEIR.

APPENDIX [A]

REMOVING THE SINGULARITY FROM SINGULAR INTEGRAL EQUATION

Consider the following integral equation

$$\frac{1}{\pi} \int_{-a}^b \frac{g(y)}{y-x} dy = f(x), \quad -a \leq x \leq b \quad (A.1)$$

In the case of $a = 1, b = 1$, (A.1) is of Carleman's type.

The left-hand member of (A.1) is the finite Hilbert transform of the unknown $g(x)$. The \int notation, denotes a singular integral in the sense of Cauchy which we define as

$$\int_{-a}^b \frac{g(y)}{y-x} dy = \lim_{\epsilon \rightarrow 0} \left\{ \int_{-a}^{x-\epsilon} \frac{g(y)}{y-x} dy + \int_{x+\epsilon}^b \frac{g(y)}{y-x} dy \right\}, \quad (A.2)$$

provided that this limit exists. A sufficient condition, which turns out to be convenient in applications, is that $g(x)$ satisfies a Lipschitz condition

$$|g(x_1) - g(x_0)| < c|x_1 - x_0|^\alpha, \quad 0 < \alpha < 1 \quad (A.3)$$

where c is fixed. In particular, (A.3) ensures that $g(x)$ is a continuous function. Then (A.2) may be replaced by

$$\int_{-a}^b \frac{g(y)}{y-x} dy = \lim_{\epsilon \rightarrow 0} \left\{ \int_{-a}^{x-\epsilon} \frac{g(y) - g(x)}{y-x} dy + \int_{x+\epsilon}^b \frac{g(y) - g(x)}{y-x} dy \right\}$$

$$+ g(x) \int_{-a}^b \frac{1}{y-x} dy$$

$$= \lim_{\epsilon \rightarrow 0} \left\{ \int_{-a}^{x-\epsilon} \frac{g(y) - g(x)}{y-x} dy + \int_{x+\epsilon}^b \frac{g(y) - g(x)}{y-x} dy \right\}$$

$$+ g(x) \left[\log|y-x| \right]_{-a}^b$$

$$= \lim_{\epsilon \rightarrow 0} \left\{ \int_{-a}^{x-\epsilon} \frac{g(y) - g(x)}{y-x} dy + \int_{x+\epsilon}^b \frac{g(y) - g(x)}{y-x} dy \right\}$$

$$+ g(x) \log \left(\frac{b-x}{a+x} \right),$$

and here the integrand is continuous for any $\epsilon > 0$.

Since

$$\left| \int_{x-\epsilon}^{x+\epsilon} \frac{g(y) - g(x)}{y-x} dy \right| \leq \frac{2c}{\alpha} \epsilon^\alpha$$

We may allow $\epsilon \rightarrow 0$ and write

$$\int_{-a}^b \frac{g(y)}{y-x} dy = g(x) \log \left(\frac{b-x}{a+x} \right) + \int_{-a}^b \frac{g(y) - g(x)}{y-x} dy, \quad (\text{A.4})$$

where the integral on the right side of (A.4) converges at $y=x$ in the ordinary sense.

APPENDIX [B]

UNIQUENESS OF SCHWARTZ-CHRISTOFFEL TRANSFORMATIONBY PRESCRIBING THE MAPPING OF THREE POINTS ONTHE BOUNDARY OF THE UPPER HALF-PLANE

Consider the bilinear (or linear fractional or Möbius) transformation

$$w = \frac{az+b}{cz+d} \quad , \quad (B.1)$$

where a, b, c and d , in general, are complex numbers such that $bc-ad \neq 0$.

To show that the bilinear transformation can be expressed as a succession of transformations:

(i) If $c \neq 0$, division of (B.1) yields

$$\begin{aligned} w &= \frac{az+b}{cz+d} = \left(\frac{bc-ad}{c}\right) \frac{1}{cz+d} + \frac{a}{c} \\ &= \frac{1}{\left(\frac{c^2}{bc-ad}\right)z + \left(\frac{cd}{bc-ad}\right)} + \frac{a}{c} \\ &= \frac{1}{Ae^{ik}z + \beta} + \gamma \quad , \quad (B.2) \end{aligned}$$

where

$$A = \left| \frac{c^2}{bc-ad} \right|,$$

$$K = -\arg\left(\frac{c^2}{bc-ad}\right),$$

$$B = \frac{cd}{bc-ad}, \text{ and}$$

$$\gamma = \frac{a}{c}$$

Hence, the bilinear transformation is equivalent to the following transformations

$$\zeta_1 = e^{ik}z \quad (\text{rotation}),$$

$$\zeta_2 = A\zeta_1 \quad (\text{scale rotation}),$$

$$\zeta_3 = \zeta_2 + B \quad (\text{translation}),$$

$$\zeta_4 = 1/\zeta_3 \quad (\text{inverse and reflection}), \text{ and}$$

$$w = \zeta_4 + \gamma \quad (\text{translation})$$

(ii) If $c = 0$, then $w = \frac{az+b}{d}$ and $d \neq 0$ since $bc-ad = -ad \neq 0$. Hence, the transformation w can be written as $w = \left(\frac{a}{d}\right)z + \left(\frac{b}{d}\right) = \alpha z + \beta$ which is equivalent to rotation, scale change, and translation.

Since the transformation of the type $w = \frac{1}{z}$ carries circles and straight lines (not necessarily respectively) into circles and straight lines, and since rotations, scale change, and translation preserve straight line and circles, the bilinear transformation carries straight lines and circles into straight line and circles (not necessarily

respectively],

Now, consider the Schwarz-Christoffel transformation in the differential form

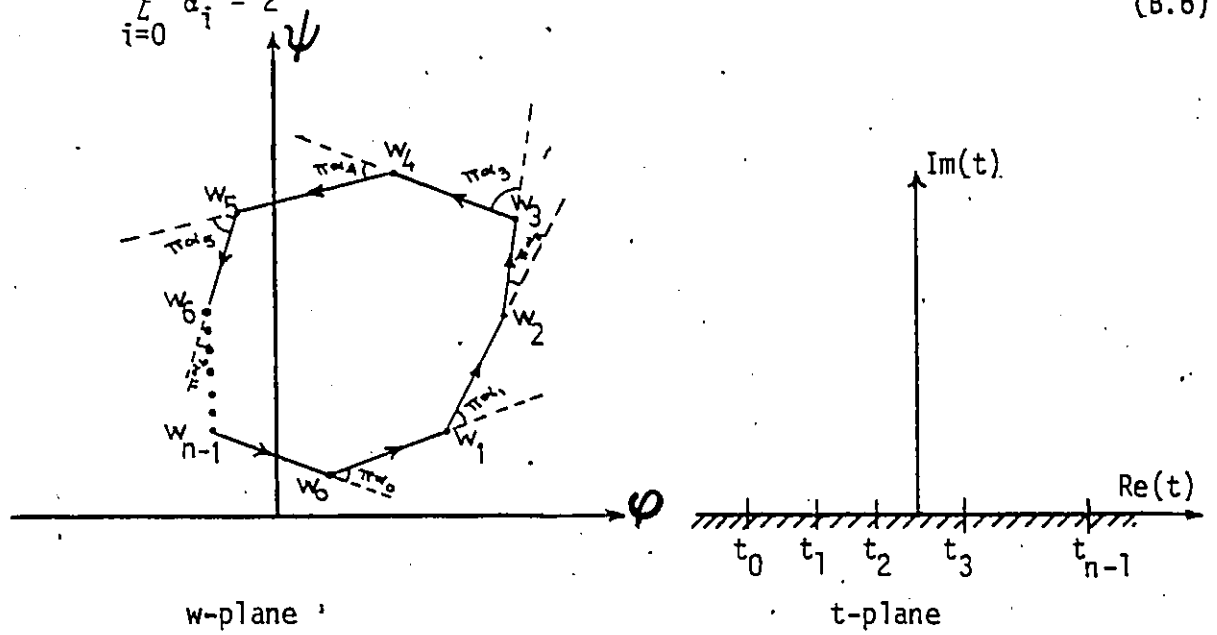
$$\frac{dw(t)}{dt} = A (t - t_1)^{-\alpha_1} (t - t_2)^{-\alpha_2} \dots (t - t_{n-1})^{-\alpha_{n-1}}, \quad (B.3)$$

where A is a complex constant, t_1, t_2, \dots, t_{n-1} and $\alpha_1, \alpha_2, \dots, \alpha_{n-1}$ are real numbers satisfying

$$t_1 < t_2 < t_3 < \dots < t_{n-1}, \quad (B.4)$$

$$-1 < \alpha_i < 1, \quad i=1,2,\dots,n-1, \quad (B.5)$$

and
$$\sum_{i=0}^{n-1} \alpha_i = 2 \quad (B.6)$$



Now, to prove that any three of the real numbers t_1, t_2, t_3, \dots can be chosen arbitrary, satisfying condition (B.4) to ensure uniqueness of the mapping

proof:

Consider any three definite points, say t_1, t_2 , and t_3 . The bilinear transformation

$$t = \frac{a\zeta + b}{c\zeta + d},$$

where a, b, c and d are real quantities satisfying $ad - bc = 1$, will change (t_1, t_2, t_3) to (t'_1, t'_2, t'_3) say.

Substituting

$$t - r = \frac{a - rc}{c\zeta + d} (\zeta - r), \quad (B.7)$$

and using (B.6) in (B.3), we have

$$\frac{dw}{d\zeta} = B(\zeta - t'_1)^{-\alpha_1} (\zeta - t'_2)^{-\alpha_2} \dots (\zeta - t'_{n-1})^{-\alpha_{n-1}}, \quad (B.8)$$

where B is a new constant. By the real substitution, the axis of real quantities, $\text{Im}(t) = 0$, is preserved, and thus the new form equally effects the conformal representation of the polygon.

It is worth to remark that when three of the points on the real axis of t -plane are thus chosen, the remainder are then determinate in terms of them and of the constants of the polygon.

The given proof is summarized from Forsyth [19], and Hauser [24].

APPENDIX [C]

PROOF OF THE HILBERT FORMULAE

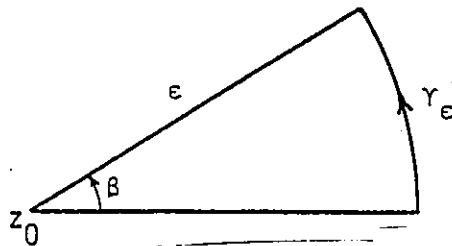
To prove the Hilbert formulae we need the following theorem:

Theorem: Let $f(z) = u(x,y) + iv(x,y)$ be an analytic function for $\text{Im}(z) \geq 0$, and $f(z) \rightarrow 0$ uniformly as $|z| \rightarrow \infty$, $0 < \arg(z) < \pi$ (which can be written as $f(z) = O(z^{-\alpha})$, $\text{Re } \alpha > 0$), then $f(z)$ satisfies

$$f(z_0) = \frac{1}{\pi i} \int_{-\infty}^{\infty} \frac{f(x,0)}{x-x_0} dx ; \quad \text{Im}(z_0) = 0.$$

To prove that theorem, we need the following two lemmas.

Lemma 1: Let $g(z)$ have a simple pole at z_0 and let γ_ϵ be a portion of a circular arc of radius ϵ and angle β . Then



$$\lim_{\epsilon \rightarrow 0} \int_{\gamma_\epsilon} g(z) dz = i\beta \text{Res}(g(z); z_0)$$

where $\text{Res}(g(z); z_0)$ means residue of the given function $g(z)$ evaluated at the point z_0 .

Proof: Near z_0 we can write

$$g(z) = \frac{b_1}{z-z_0} + g_1(z),$$

where $g_1(z)$ is analytic function and $b_1 = \text{Res}(g(z); z_0)$.

Thus

$$\int_{\gamma_\epsilon} g(z) dz = \int_{\gamma_\epsilon} \frac{b_1}{z-z_0} dz + \int_{\gamma_\epsilon} g_1(z) dz$$

Therefore

$$\int_{\gamma_\epsilon} \frac{b_1}{z-z_0} dz = b_1 \int_{\beta_0}^{\beta_0 + \beta} \frac{1}{\epsilon e^{i\theta}} i\epsilon e^{i\theta} d\theta = i\beta b_1$$

Here, $\gamma_\epsilon(\theta): z = z_0 + \epsilon e^{i\theta}; \beta_0 \leq \theta \leq \beta_0 + \beta$.

Also, since $g_1(z)$ is analytic, it is bounded near z_0 , say by a constant M , so

$$\left| \int_{\gamma_\epsilon} g_1(z) dz \right| \leq M \ell(\gamma_\epsilon) = M \beta \epsilon \rightarrow 0 \text{ as } \epsilon \rightarrow 0.$$

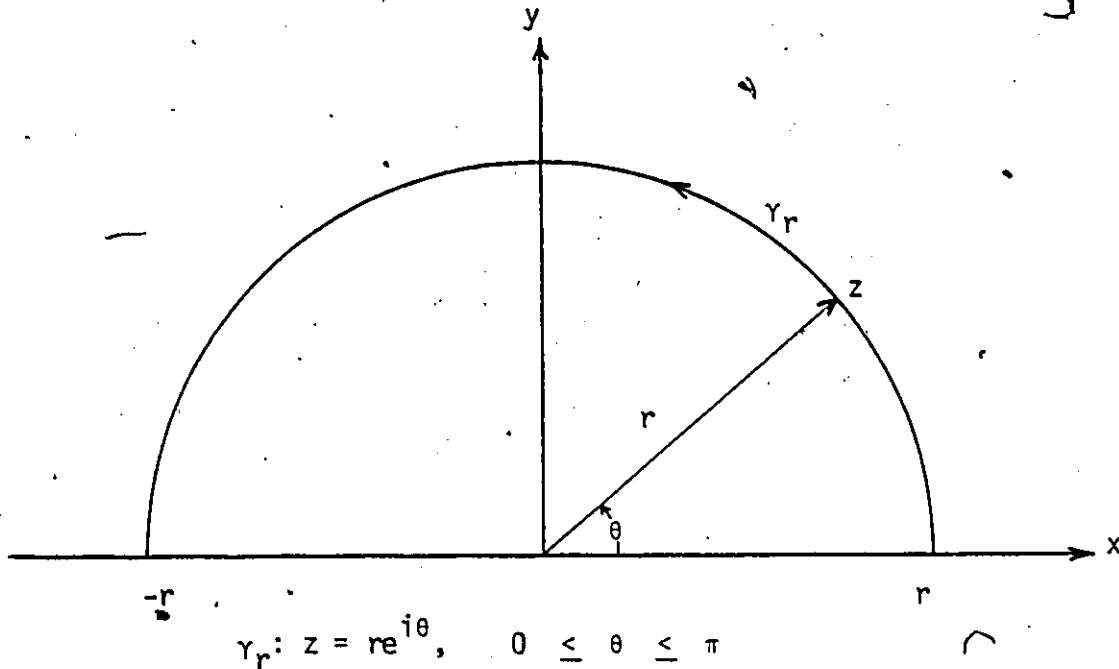
Then

$$\lim_{\epsilon \rightarrow 0} \int_{\gamma_\epsilon} g(z) dz = i\beta \text{Res}(g(z); z_0)$$

Lemma 2: Let $K(z)$ be an analytic function for $\text{Im}(z) \geq 0$ except for a finite number of poles, none of which is on the real axis. Suppose that $K(z) = O(z^{-\alpha_1})$, $\text{Re } \alpha_1 > 1$ for $|z| > R$, where R is a number, then

$$\int_{\gamma_r} K(z) dz \rightarrow 0 \text{ as } r \rightarrow \infty$$

Proof:



Assume there exists a constant M , say, such that $K(z) = \frac{M}{z^{\alpha_1}}$, where $\text{Re } \alpha_1 > 1$. Therefore

$$\begin{aligned} \left| \int_{\gamma_r} K(z) dz \right| &= \left| \int_0^\pi K(re^{i\theta}) r e^{i\theta} d\theta \right| < \pi r |K(re^{i\theta})| \\ &= \frac{\pi M}{r^{\alpha_1 - 1}} \rightarrow 0 \text{ as } r \rightarrow \infty \end{aligned}$$

Therefore,

$$\int_{\gamma_r} K(z) dz \rightarrow 0 \text{ as } r \rightarrow \infty.$$

Proof of the Theorem:

Let $F(z)$ be an analytic function except for a simple pole x_0 lying on the real axis. Then $F(z)$ can be written as $F(z) = \frac{f(z)}{z - z_0}$; $\text{Im}(z_0) = 0$, where $f(z)$ is analytic function for $\text{Im}(z) \geq 0$.

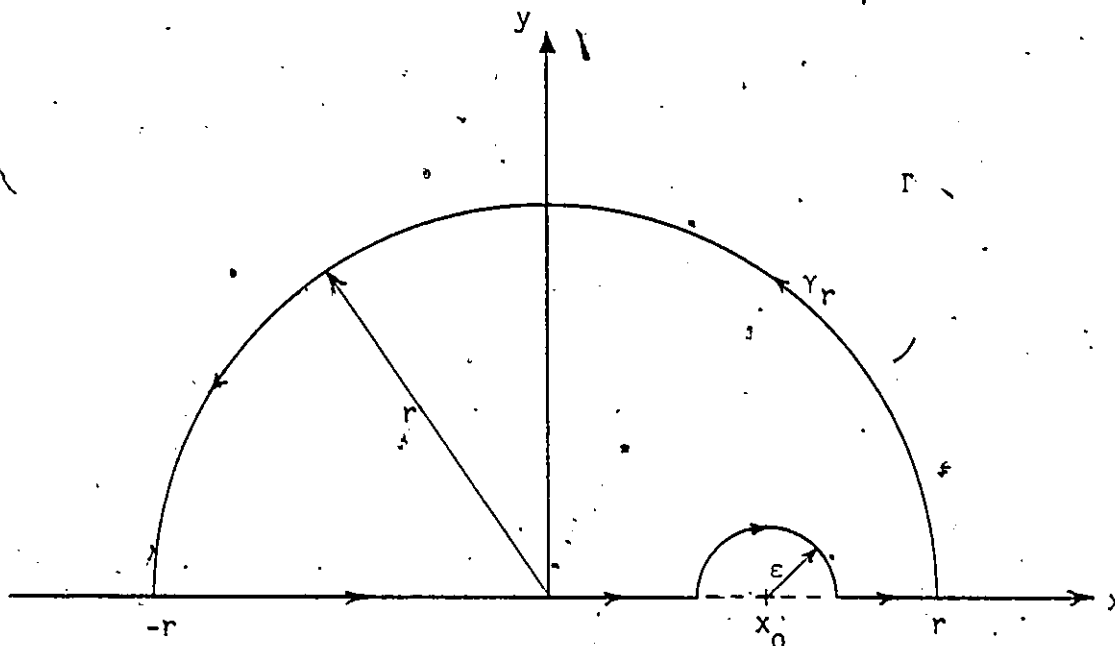
$$\text{Let } \Gamma = \gamma_r \cup \gamma_\epsilon \cup \gamma,$$

where

γ_r : is the semicircular portion of radius r ,

γ_ϵ : " " " " " " ϵ around the point x_0

γ : straight line portions of Γ along the real axis.



$$\begin{aligned}
 \int_{\Gamma} F(z) dz &= \int_{\Gamma} \frac{f(z)}{z-z_0} dz \\
 &= \int_{-r}^{x_0-\epsilon} \frac{f(x,0)}{x-x_0} dx + \int_{\gamma_\epsilon} \frac{f(z)}{z-z_0} dz \\
 &\quad + \int_{x_0+\epsilon}^r \frac{f(x,0)}{x-x_0} dx + \int_{\gamma_r} \frac{f(z)}{z-z_0} dz
 \end{aligned} \tag{C.1}$$

By lemma 1: $\int_{\gamma_\epsilon} \frac{f(z)}{z-z_0} dz = -i\pi f(z_0)$ as $\epsilon \rightarrow 0$.

$$\tag{C.2}$$

By lemma 2: $\int_{\gamma_r} \frac{f(z)}{z-z_0} dz \rightarrow 0$ as $r \rightarrow \infty$

$$\tag{C.3}$$

Both of integrals $\int_{-r}^{x_0-\epsilon} \frac{f(x,0)}{x-x_0} dx$, $\int_{x_0+\epsilon}^r \frac{f(x,0)}{x-x_0} dx$ converges for

every $\epsilon > 0$ and their sum equal to principle value of:

$$\int_{-\infty}^{\infty} \frac{f(x,0)}{x-x_0} dx \text{ which we denote by } \int_{-\infty}^{\infty} \frac{f(x,0)}{x-x_0} dx. \tag{C.4}$$

By residue theorem

$$\int_{\Gamma} F(z) dz = 2\pi i \sum \{\text{residue in upper half plane}\}.$$

Since $F(z)$ is analytic function in the upper half-plane, $\text{Im}(z) > 0$, therefore its residue is 0.

$\tag{C.5}$

Substitute from (C.2) to (C.5) in (C.1), we get

$$0 = \int_{-\infty}^{\infty} \frac{f(x,0)}{x-x_0} dx - \pi i f(z_0)$$

or

$$f(z_0) = \frac{1}{\pi i} \int_{-\infty}^{\infty} \frac{f(x,0)}{x-x_0} dx ; \quad \text{Im}(z_0) = 0 \quad (\text{C.6})$$

Using $f(z) = u(x,y) + iv(x,y)$, (C.6) can be written as

$$u(x_0,0) + iv(x_0,0) = \frac{1}{\pi i} \int_{-\infty}^{\infty} \frac{u(x,0) + iv(x,0)}{x-x_0} dx$$

Equating real and imaginary parts, we get

$$u(x_0,0) = \frac{1}{\pi} \int_{-\infty}^{\infty} \frac{v(x,0)}{x-x_0} dx , \quad (\text{C.7})$$

$$v(x_0,0) = \frac{-1}{\pi} \int_{-\infty}^{\infty} \frac{u(x,0)}{x-x_0} dx . \quad (\text{C.8})$$

(C.7) and (C.8) are the Hilbert formulae.

APPENDIX [D]

COMPUTER PROGRAM FOR A FLOWOVER AN UNEVEN BOTTOM

FORTRAN Implementation

List of Principal Variables

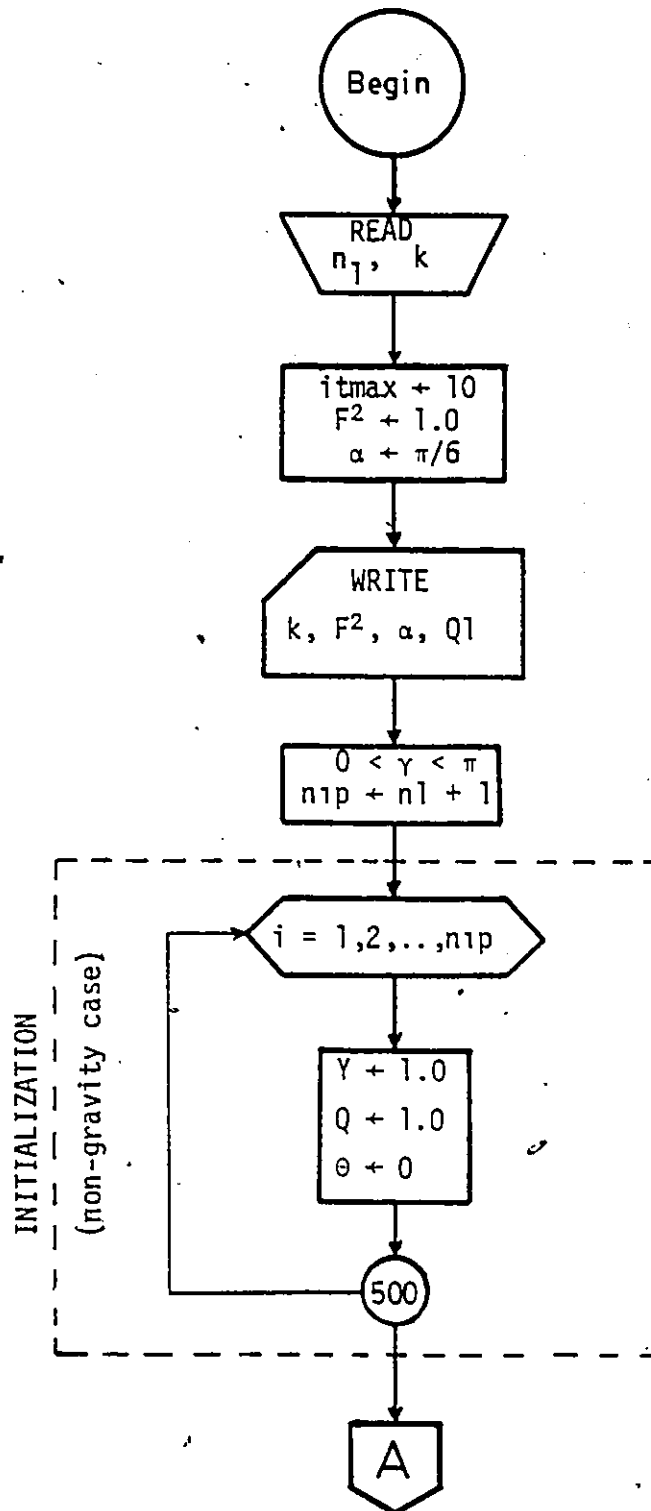
Program Symbol	Definition
(Main)	
ALPHA	inclination angle, α .
CP1	excess pressure coefficient along AB, Cp_1 .
CP2	excess pressure coefficient along BC, Cp_2 .
CP3	excess pressure coefficient along CD, Cp_3 .
DR	length of BC, l .
F2	Froude number square, F^2 .
FLAGR	function of implementing Lagrange's interpolation formula.
ITER	counter on the number of iterations, iter.
ITMAX	maximum number of iterations allowed, itmax.
NI	number of increments, $n1$.
PI	π

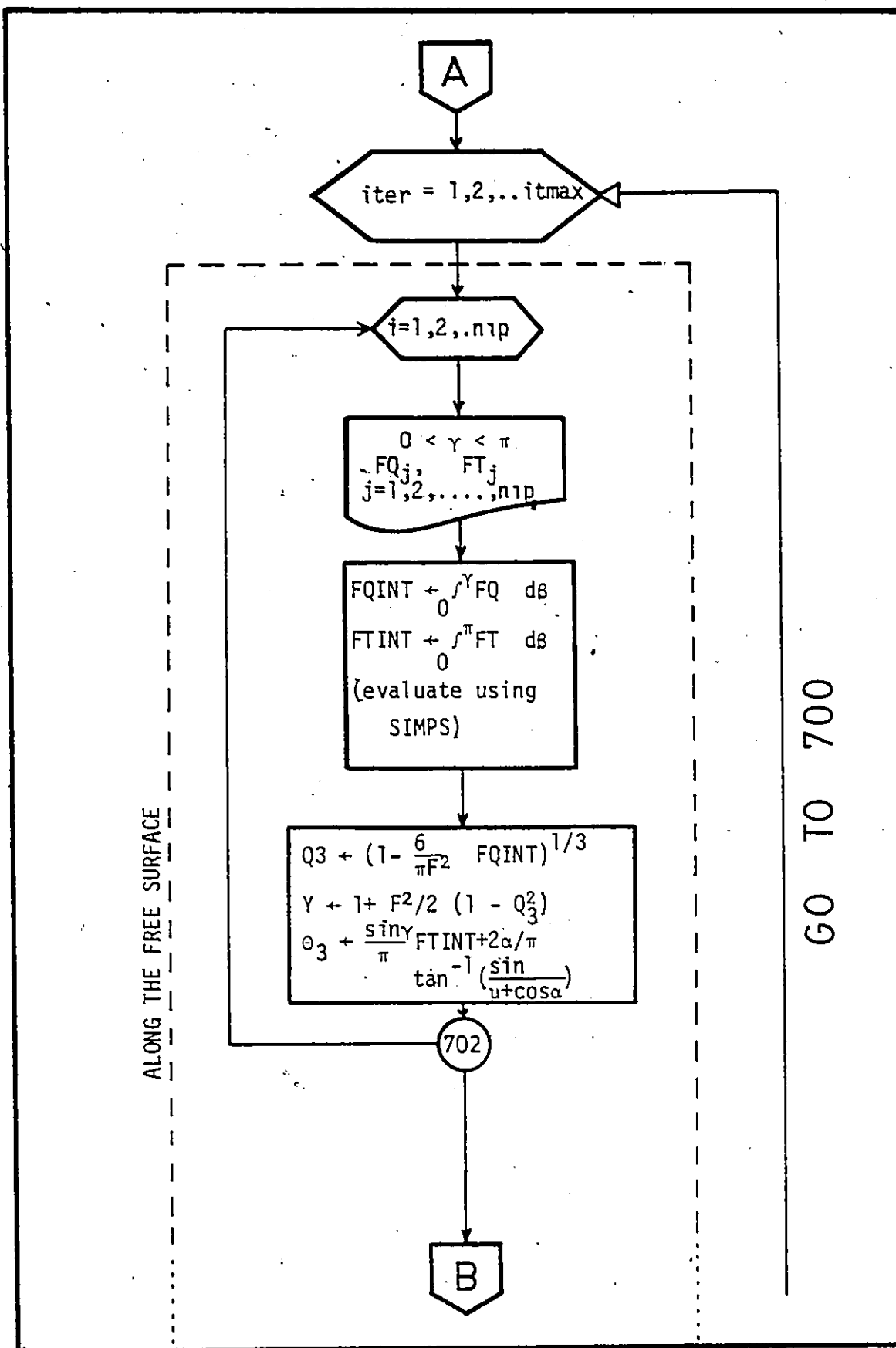
Program Symbol

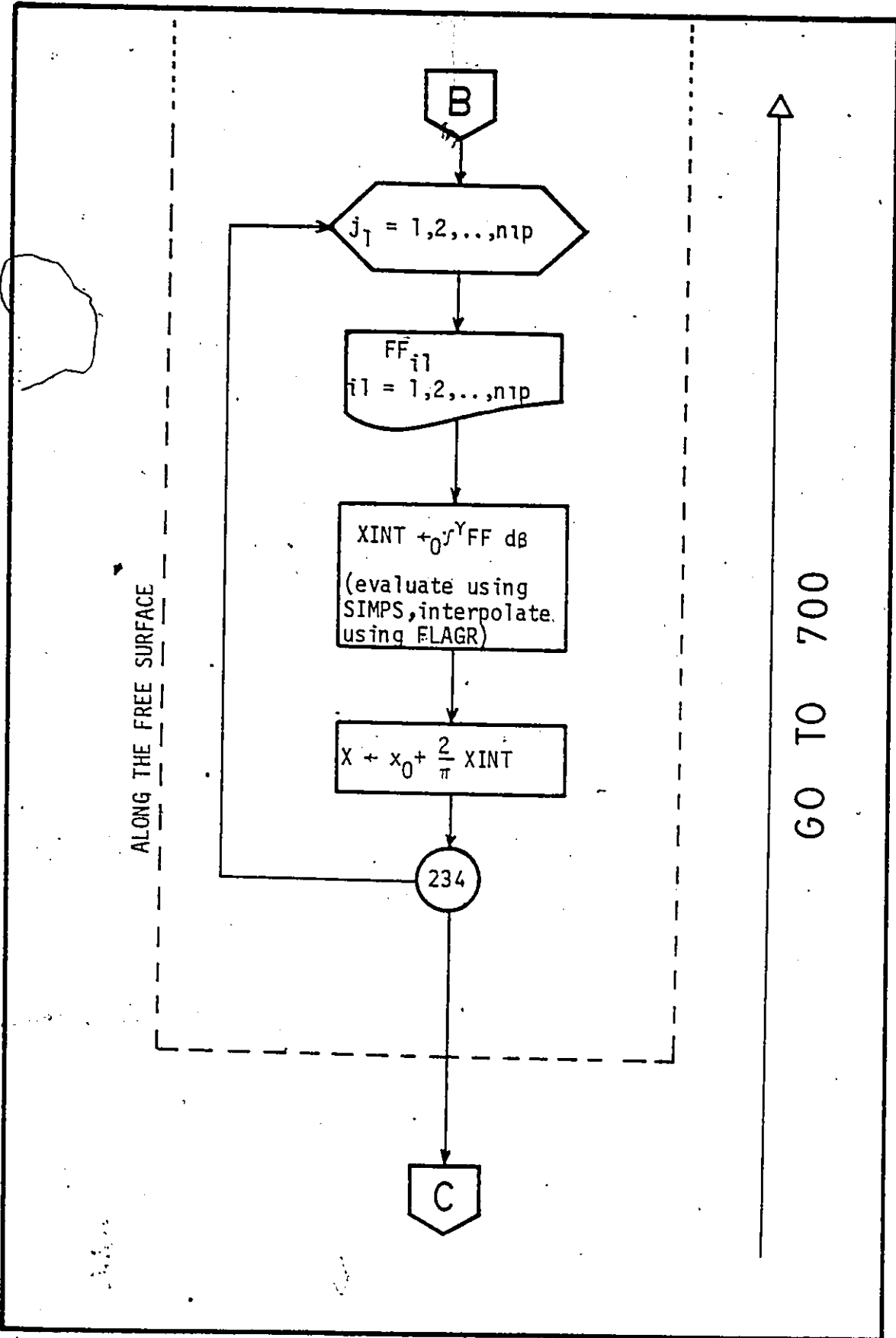
Definition

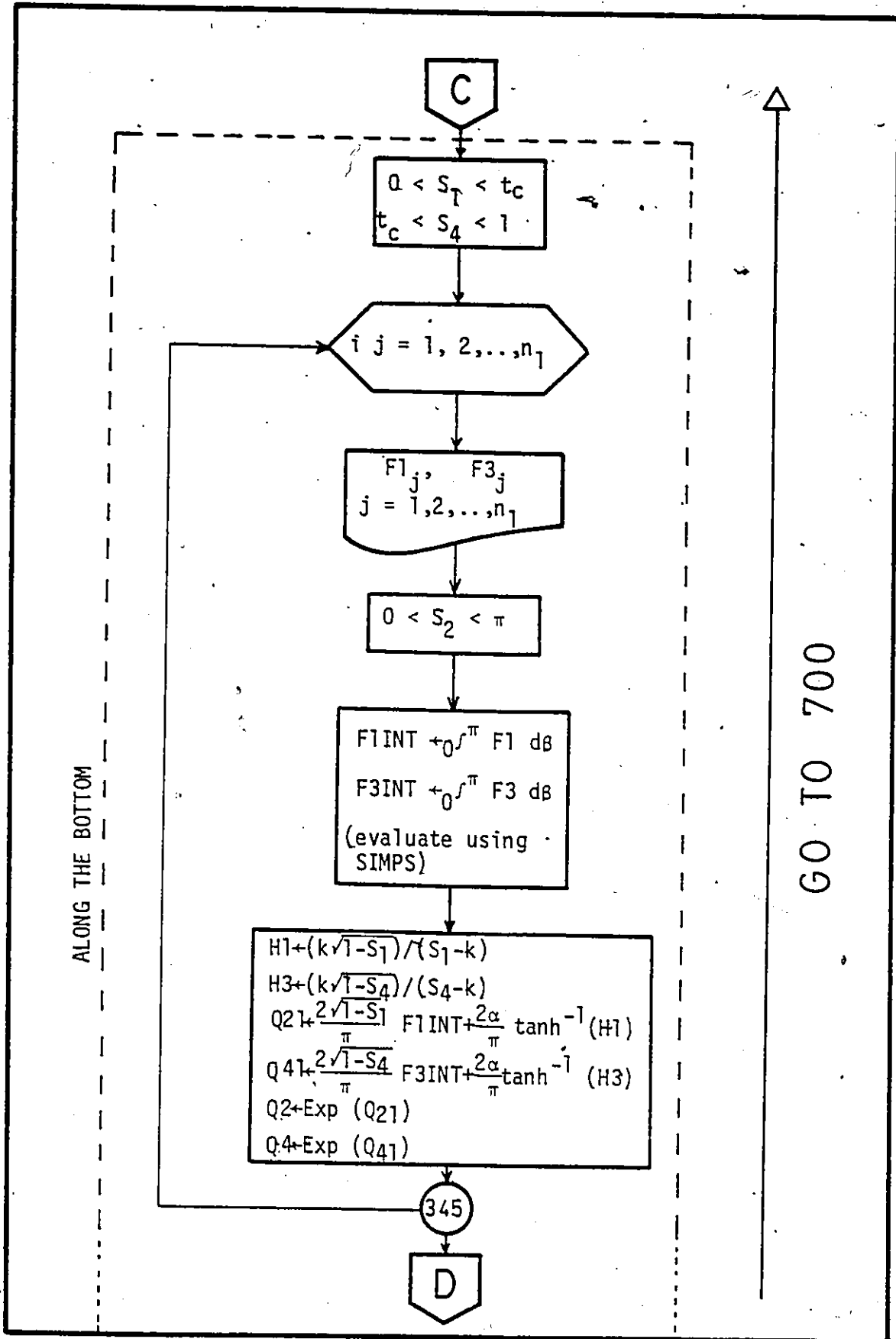
Q	magnitude of velocity along free surface, Q.
Q1	magnitude of velocity along AB, Q1.
Q2	magnitude of velocity along BC, Q2.
Q3	magnitude of velocity along CD, Q3.
s	$1 - \sqrt{1-t_c}$, k; where t_c is the position of point C on the upper half plane.
SIMPS	function of implementing Simpson's rule.
T	argument of complex velocity along the free surface, θ .
X	dummy variable, γ .
XTA	horizontal coordinate for the free surface.
Y	vertical coordinate for the free surface.

Flow Diagram - 1



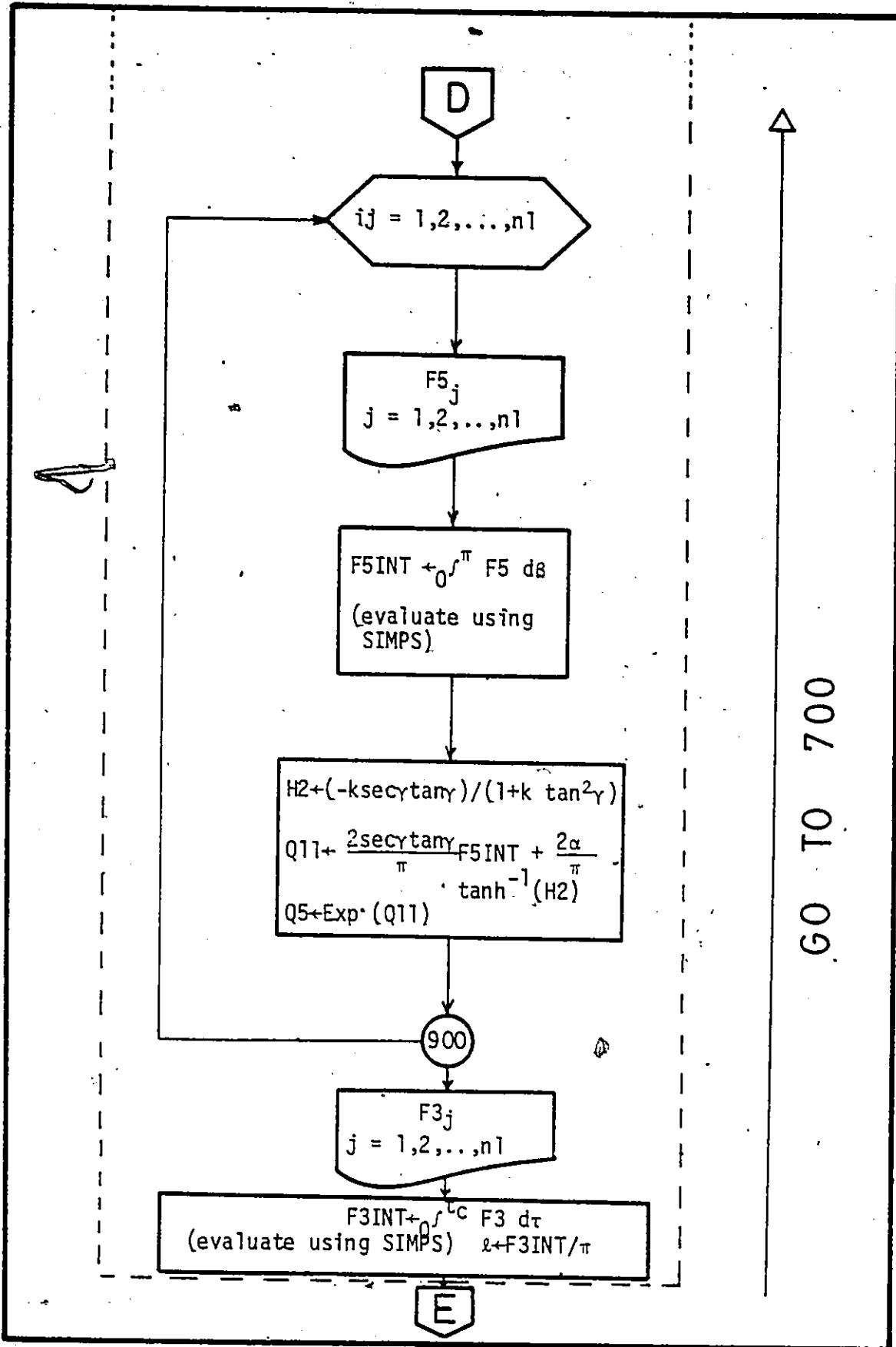


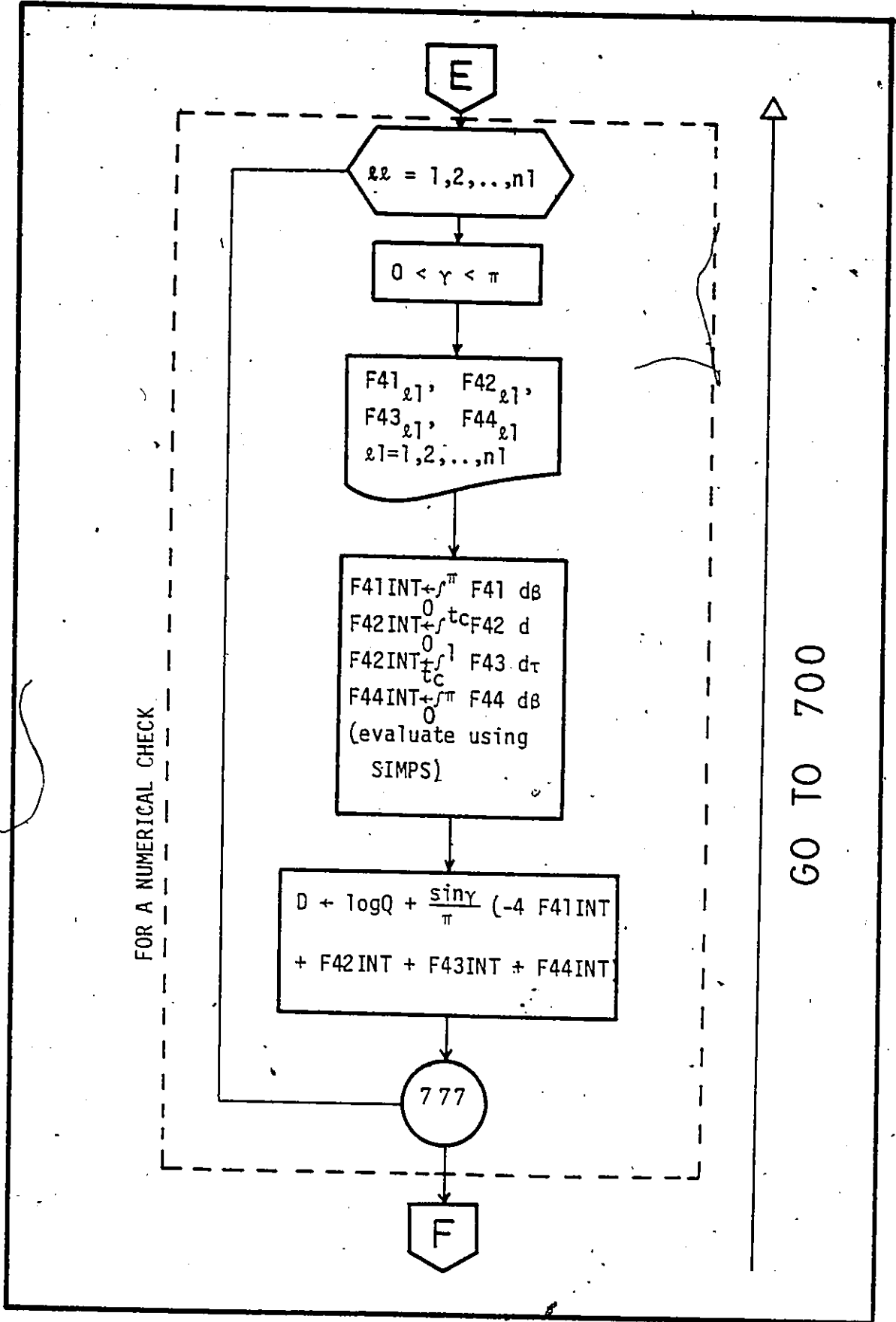




ALONG THE BOTTOM

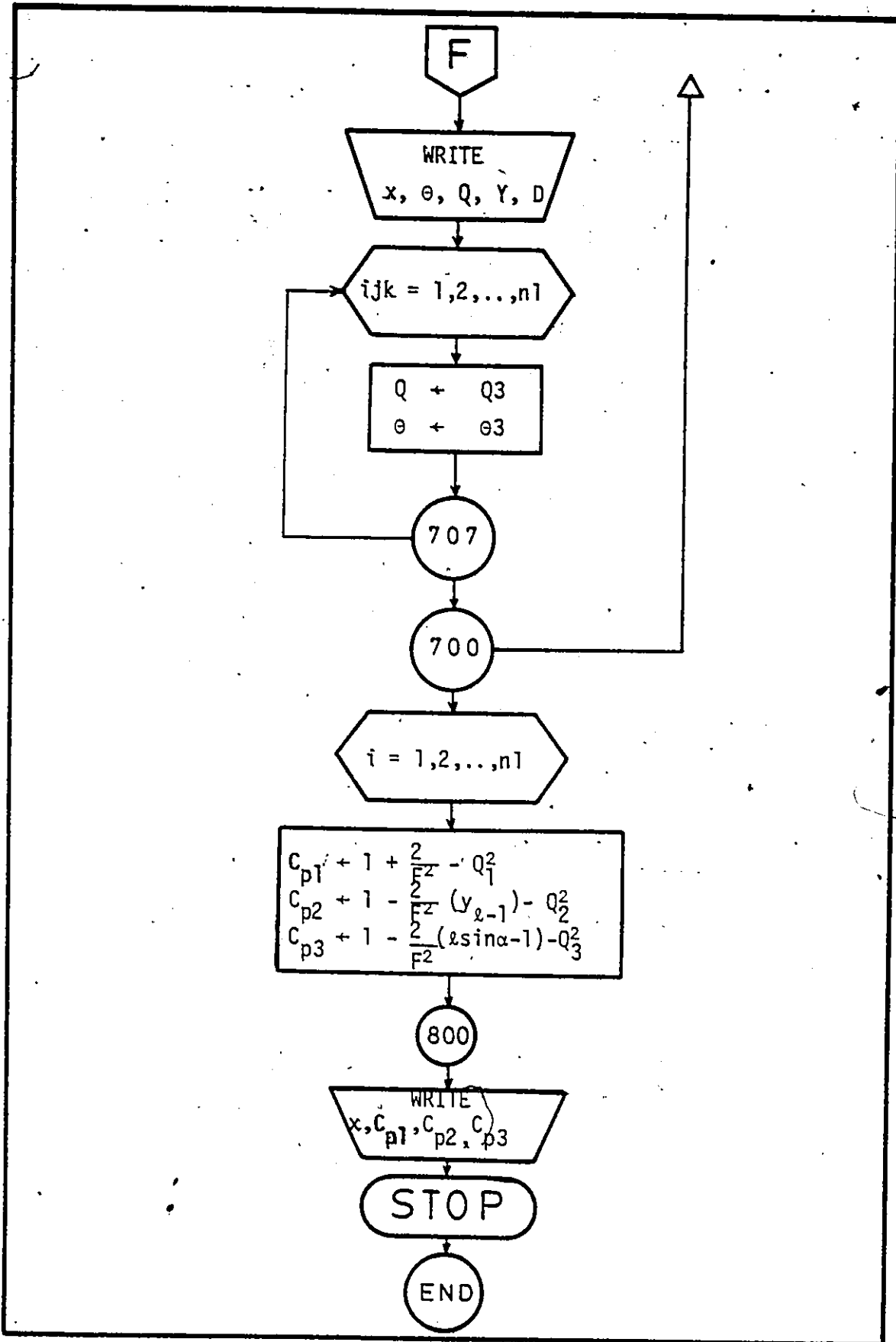
GO TO 700





FOR A NUMERICAL CHECK

GO TO 700




```

*****
*
* .. SUCCESSIVE APPROXIMATIONS .. *
*
*****
0041 DO 700 ITER=1,ITMAX
0042 WRITE(6,701) ITER
0043 701 FORMAT(///10X,'ITER=',I4/)

*****
*
* .. ALONG THE FREE SURFACE .. *
*
*****
0044 DO 702 I=1,N1P
0045 XLOW3=0
0046 XHIGH3=X(I)
0047 DO 703 J=1,N1P
0048 UQ(J)=SIN(T(J))
0049 VQ(J)=SIN(X(J))
0050 IF(VQ(J).EQ.0) GO TO 713
0051 IF(X(J).GT.3.1415) GO TO 714
0052 FQ(J)=UQ(J)/VQ(J)
0053 GO TO 703
0054 713 FQ(J)=1.
0055 GO TO 703
0056 714 FQ(J)=-1.
0057 703 CONTINUE
0058 FQINT=SIMPS(XLOW3,XHIGH3,N1P,FQ)
0059 Q3(I)=(1.-(6./(PI*F2))*FQINT)**(1./3.)
0060 524 Y(I)=1.+(.5*F2)*(1.-(Q3(I))**2)
0061 702 CONTINUE
0062 DO 704 I1=1,N1P
0063 HT(I1)=SIN(X(I1))/(G+COS(X(I1)))
0064 XLOW1=0
0065 XHIGH1=PI
0066 DP=(XHIGH1-XLOW1)/FLOAT(N1)
0067 IIK=0
0068 DO 705 K=1,N1P
0069 UT(K)=ALOG(Q(K))
0070 VT(K)=COS(X(K))-COS(X(I1))
0071 IF(VT(K).EQ.0.) GO TO 705
0072 FT(K)=UT(K)/VT(K)
0073 IIK=IIK+1
0074 FT(IIK)=FT(K)
0075 705 CONTINUE
0076 FTINT=SIMPS(XLOW1,XHIGH1,IIK,FT)
0077 T3(I1)=(SIN(X(I1))/PI)*FTINT+(2*ALPHA/PI)*ATAN(HT(I1))
0078 704 CONTINUE
0079 DO 707 IJK=1,N1P
0080 Q(IJK)=Q3(IJK)
0081 T(IJK)=T3(IJK)
0082 707 CONTINUE
0083 DO 234 J1=1,N1P
0084 XLOW=2*ARSIN(RO)

```

```

0085      XHIGH=X(J1)
0086      DXX=(XHIGH-XLOW)/N1
0087      DO 235 I1=1,N1P
0088      XX=XLOW+DXX*(I1-1)
0089      T1(I1)=FLAGR(X,T,XX,20,1,N1P)
0090      QQ(I1)=FLAGR(X,Q,XX,20,1,N1P)
0091      FF(I1)=COS(T1(I1))/(QQ(I1)*SIN(XX))
0092      235  CONTINUE
0093      XINT=SIHPS(XLOW,XHIGH,N1P,FF)
0094      XTA(J1)=X0+(2./PI)*XINT
0095      234  CONTINUE
C
C      *****
C      *
C      * ... ALONG THE BOTTOM ... *
C      *
C      *****
C
0096      XLOW1=0
0097      XHIGH1=PI *
0098      HX=4.
0099      DS1=S*(2.-S)/N1
0100      DS4=(1./N1)-DS1
0101      S1=DS1
0102      S4=DS4
0103      DO 345 IJ=1,N1
0104      H1(IJ)=- (S1-S+S*SQRT(1.-S1))/(S1-S-S*SQRT(1.-S1))
0105      H3(IJ)=(S4-S+S*SQRT(1.-S4))/(S4-S-S*SQRT(1.-S4))
0106      IF(H3(IJ).LE.0) GO TO 345
0107      S2=0.
0108      DO 456 J=1,N1
0109      DS2=PI/N1
0110      U1(J)=ALOG(Q(J))
0111      V1(J)=2.-S1*(1.-COS(S2))
0112      V3(J)=2.-S4*(1.-COS(S2))
0113      F1(J)=U1(J)/V1(J)
0114      F3(J)=U1(J)/V3(J)
0115      S2=S2+DS2
0116      456  CONTINUE
C
0117      F1INT=SIMPS(XLOW1,XHIGH1,N1,F1)
0118      F3INT=SIMPS(XLOW1,XHIGH1,N1,F3)
0119      Q21(IJ)=(2*SQRT(1.-S1)*F1INT)/PI+(ALPHA/PI)*ALOG(H1(IJ))
0120      Q41(IJ)=(2*SQRT(1.-S4)*F3INT)/PI+(ALPHA/PI)*ALOG(H3(IJ))
0121      Q2(IJ)=EXP(Q21(IJ))
0122      Q4(IJ)=EXP(Q41(IJ))
0123      S1=S1+DS1
0124      S4=S4+DS4
0125      345  CONTINUE
0126      S5=0
0127      DO 900 IJ=1,N1
0128      DS5=PI/(2*N1)
0129      H2(IJ)=(1.+S*(TAN(S5)**2-S*(TAN(S5)/COS(S5)))/
* (1.+S*(TAN(S5)**2+S*(TAN(S5)/COS(S5)))
0130      S2=0
0131      DO 901 J=1,N1
0132      DS2=PI/N1
0133      U5(J)=1.+2*(TAN(S5)**2)-COS(S2)
0134      F5(J)=ALOG(Q(J))/V5(J)

```

```

0135          901 CONTINUE
0136             F5INT=SIMPS(XLOW1,XHIGH1,N1,F5)
0137             Q11(IJ)=((2*TAN(SS)*F5INT)/(PI*COS(SS)**2))
                *(ALPHA/PI)*ALOG(H2(IJ))
0138             Q5(IJ)=EXP(Q11(IJ))
0139             S5=S5+DS5
0140          900 CONTINUE
0141             XLOW2=0
0142             XHIGH2=1.-(1.-S)*(1.-S)
0143             DS3=(XHIGH2-XLOW2)/N1
0144             S3=XLOW2
0145             DO 89 J=1,N1
0146                 U2(J)=1.
0147                 V2(J)=(1.-S3)*Q2(J)
0148                 F3(J)=U2(J)*V2(J)
0149                 S3=S3+DS3
0150          89 CONTINUE
0151             F3INT=SIMPS(XLOW2,XHIGH2,N1,F3)
0152             DR=F3INT/PI

C
C *****
C *
C * .. FOR A NUMERICAL CHECK .. *
C *
C *****
C

0153             S2=0
0154             DS2=PI/N1
0155             DO 777 LL=1,N1
0156                 S5=0
0157                 DS5=PI/(2*N1)
0158                 DO 751 L1=1,N1
0159                     F71(L1)=ALOG(Q11(L1))/(1-COS(S2)+2*TAN(SS)**2)
0160                     S5=S5+DS5
0161          751 CONTINUE
0162                     F71INT=SIMPS(XLOW1,XHIGH1,N1,F71)
0163                     S6=0
0164                     DS6=S*(2-S)/N1
0165                     DO 752 L2=1,N1
0166                         F72(L2)=ALOG(Q2(L2))/((S6*SIN(S2/2)**2-1.)
                *SQRT(1.-S2))
0167                         S6=S6+DS6
0168          752 CONTINUE
0169                         F72INT=SIMPS(XLOW2,XHIGH2,N1,F72)
0170                         XLOW3=XHIGH2
0171                         XHIGH3=1.
0172                         S7=0
0173                         DS7=(1./N)-DS6
0174                         DO 753 L3=1,N1
0175                             F73(L3)=ALOG(Q3(L3))/((S7*SIN(S2/2)**2-1.)
                *SQRT(1.-S7))
0176                             S7=S7+DS7
0177          753 F73INT=SIMPS(XLOW3,XHIGH3,N1,F73)
0178                             S8=0
0179                             DS8=PI/N1
0180                             DO 754 L4=1,N1
0181                                 IF(S8.EQ.S2) GO TO 754
0182                                 F74(L4)=(ALOG(T(L4))-ALOG(T(LL)))/(COS(S8)-COS(S2))
0183          754 CONTINUE

```

```

0184      F74INT=SIMPS(XLOW1,XHIGH1,N1,F74)
0185      ERR(LL)=ALOG(Q(LL))+{SIN(S2)/2*PI)*(-4*F71INT+
          *F72INT+F73INT+2*F74INT)
0186      777 CONTINUE
0187      WRITE(6,600) (XTA(I),T(I),Q(I),Y(I),ERR(I),I=1,N1P)
0188      700 CONTINUE
0189      DO 800 I=1,N1P
0190      YL(I)=(DR/N1)*(I-1)
0191      CP1(I)=1.+(2./F2)-Q5(I)*Q5(I)
0192      CP2(I)=1.-(2./F2)*(YL(I)-1.)-Q2(I)*Q2(I)
0193      CP3(I)=1.-(2./F2)*(DR*SIN(ALPHA)-1.)-Q4(I)*Q4(I)
0194      800 CONTINUE
0195      WRITE(6,99)
0196      WRITE(6,991) (XTA(I),CP1(I),CP2(I),CP3(I),I=1,N1P)
0197      99  FORMAT(//10X,'PRESSURE DIST. ALONG THE BOTTOM'//17X,' X
          $',14X,'CP1',14X,'CP2',16X,'CP3',100('*'))
0198      991 FORMAT(4X,F20.6)
0199      600 FORMAT(4X,5F20.6)
0200      100 FORMAT(I4,F5.3)
0201      STOP
0202      END

```

Function SIMPS

```

C
C
0001      FUNCTION SIMPS(U,V,N,F)
0002      REAL F(110)
C
C      ./. INITIALIZATION ...
0003      H=(V-U)/(6*FLOAT(N))
0004      S1=0
0005      S2=0
0006      N2=(N/2.)-1.
C
C      ... EVALUATE SUM1 & SUM2 ...
0007      DO 109 I=1,N2
0008      J=2*I+1
0009      K=2*I
0010      S1=S1+F(J)
0011      S2=S2+F(K)
0012      109 CONTINUE
C
C      ... RETURN ESTIMATED VALUE OF THE INTEGRAL ...
C
0013      SIMPS=(2*S2+4*S1-F(1)+F(N))*H
0014      RETURN
0015      END

```

Function FLAGR

```

C
C
0001      FUNCTION FLAGR(X,Y,XARG,IDEG,MIN,N)
C
0002      REAL X(110),Y(110)
C          ... COMPUTE VALUE OF FACTOR ...
C
0003      FACTOR=1.
0004      MAX=MIN+IDEG
0005      DO 2 J=MIN,MAX
0006      IF(XARG.NE.X(J)) GO TO 2
0007      FLAGR=Y(J)
0008      RETURN
0009      2 FACTOR=FACTOR*(XARG-X(J))
C
C          ... EVALUATE INTERPOLATING POLYNOMIAL ...
C
0010      YEST=0
0011      DO 5 I=MIN,MAX
0012      TERM=Y(I)*FACTOR/(XARG-X(I))
0013      DO 4 J=MIN,MAX
0014      4 IF(I.NE.J) TERM=TERM/(X(I)-X(J))
0015      5 YEST=YEST+TERM
0016      FLAGR=YEST
0017      RETURN
0018      END

```

APPENDIX [E]

COMPUTER PROGRAM FOR A FLOWFROM UNIFORM CHANNEL OVER SHELF

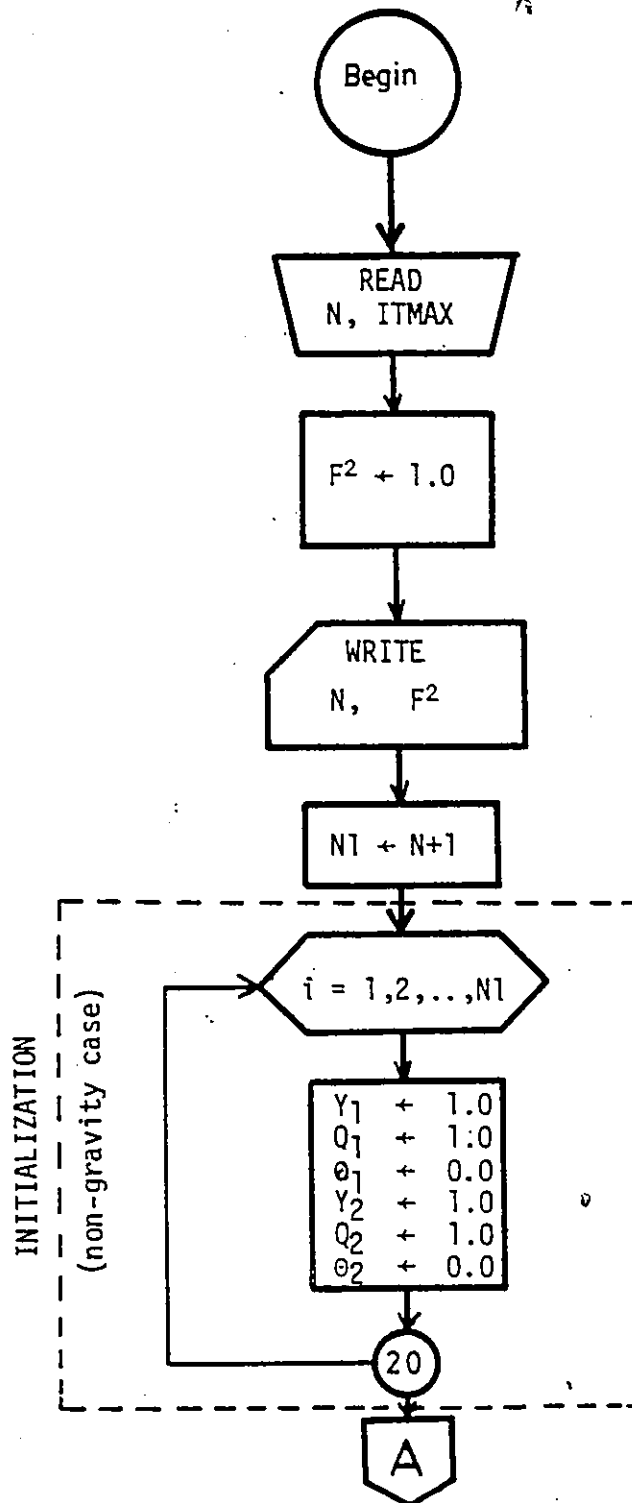
FORTRAN Implementation

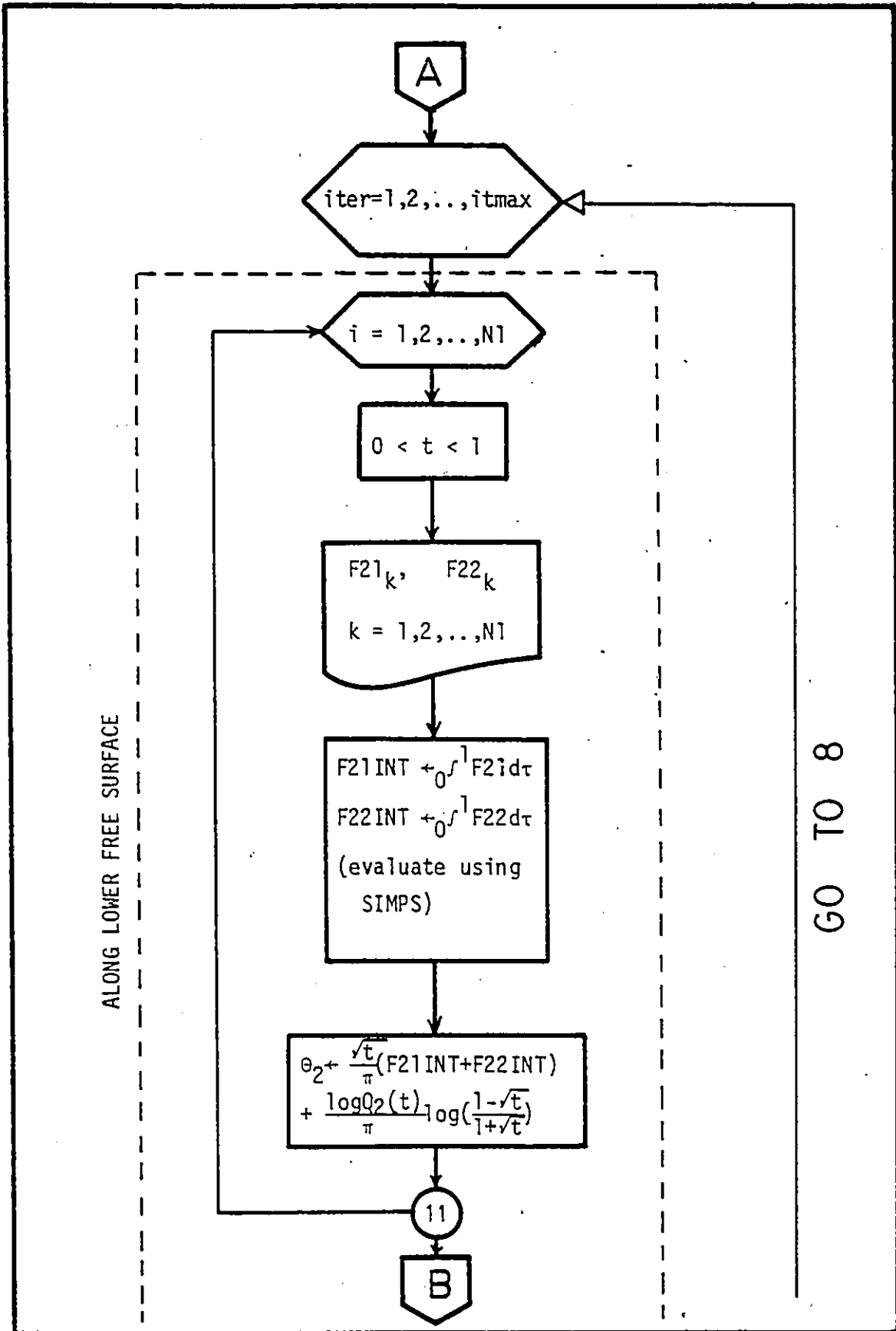
List of Principal Variables

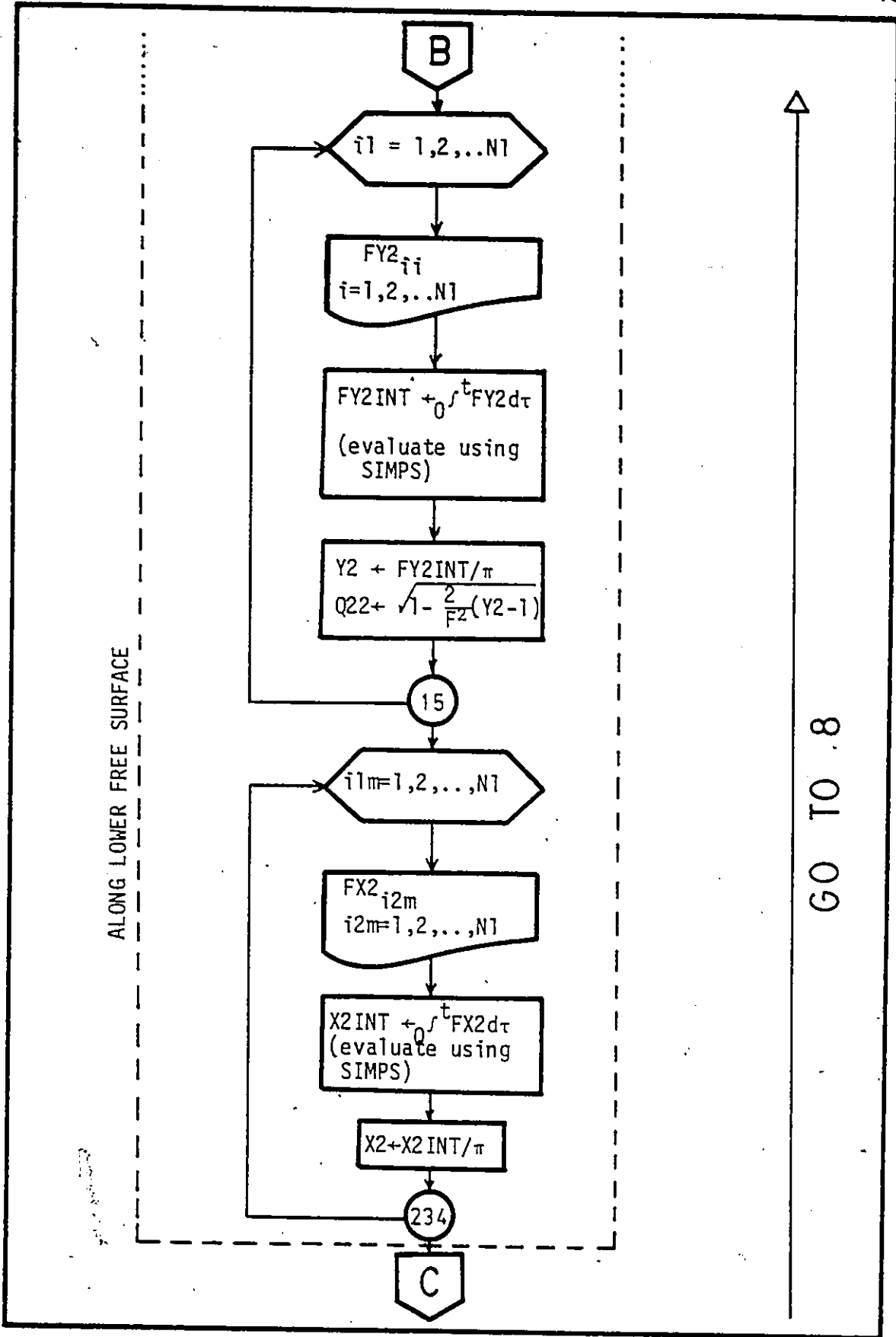
Program Symbol	Definition
(Main)	
CP	excess pressure coefficient along the shelf, C_p .
F2	Froude number square, F^2 .
ITER	counter on the number of iterations, iter.
ITMAX	maximum number of iterations allowed, itmax.
N	number of increments, n.
PI	π
Q	magnitude of velocity along the shelf, Q.
Q1	magnitude of velocity along the upper free surface, Q1.

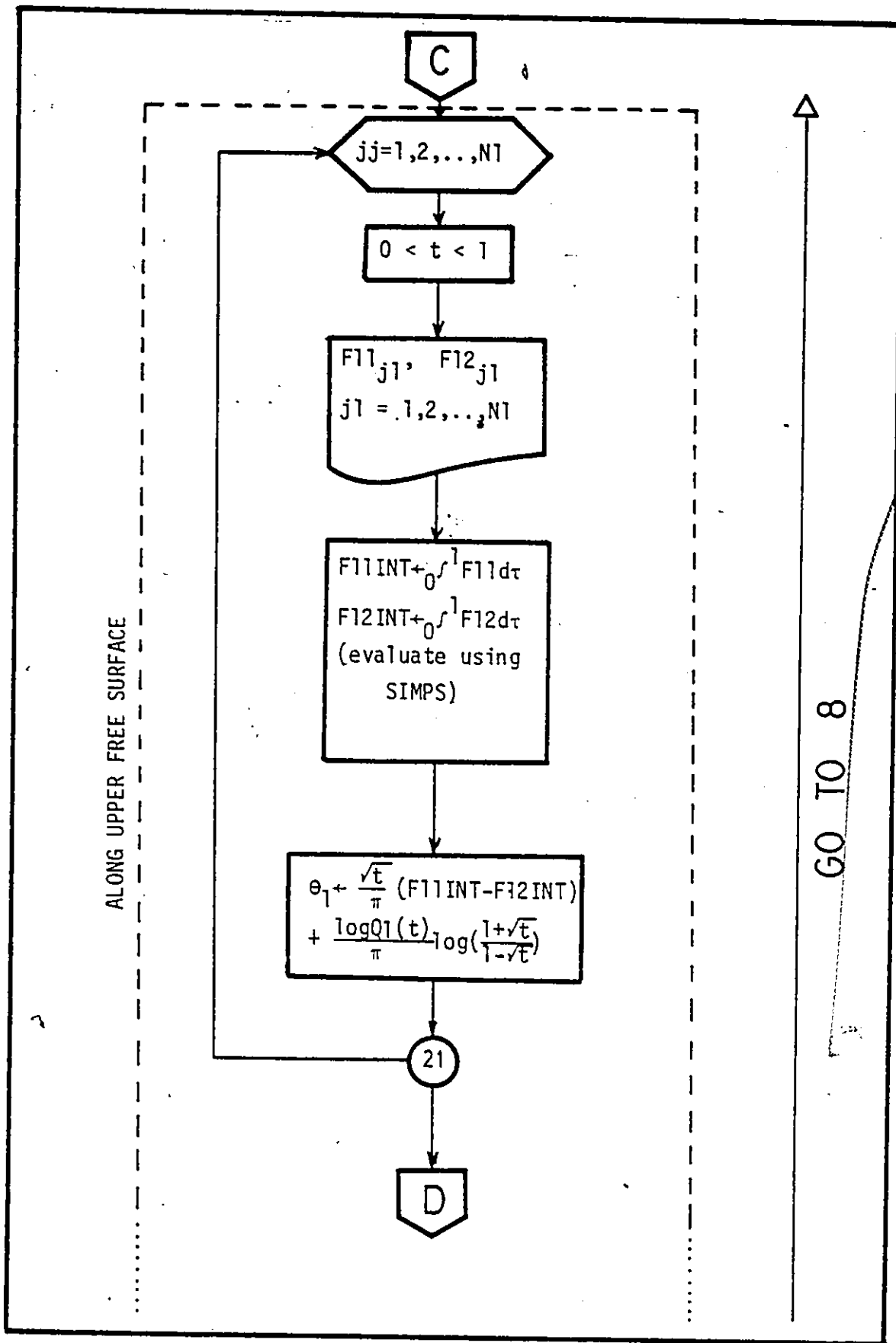
Q2	magnitude of velocity along the lower free surface, Q_2 .
SIMPS	function of implementing Simpson's rule.
TH1	argument of complex velocity along the upper free surface, θ_1 .
TH2	argument of complex velocity along the lower free surface, θ_2 .
t	real t-plane coordinate.
X1	horizontal coordinate for the upper free surface, x_1 .
X2	horizontal coordinate for the lower free surface, x_2 .
Y1	vertical coordinate for the upper free surface, y_1 .
Y2	vertical coordinate for the lower free surface, y_2 .

Flow Diagram - 2









C

jj=1,2,...,NT

0 < t < 1

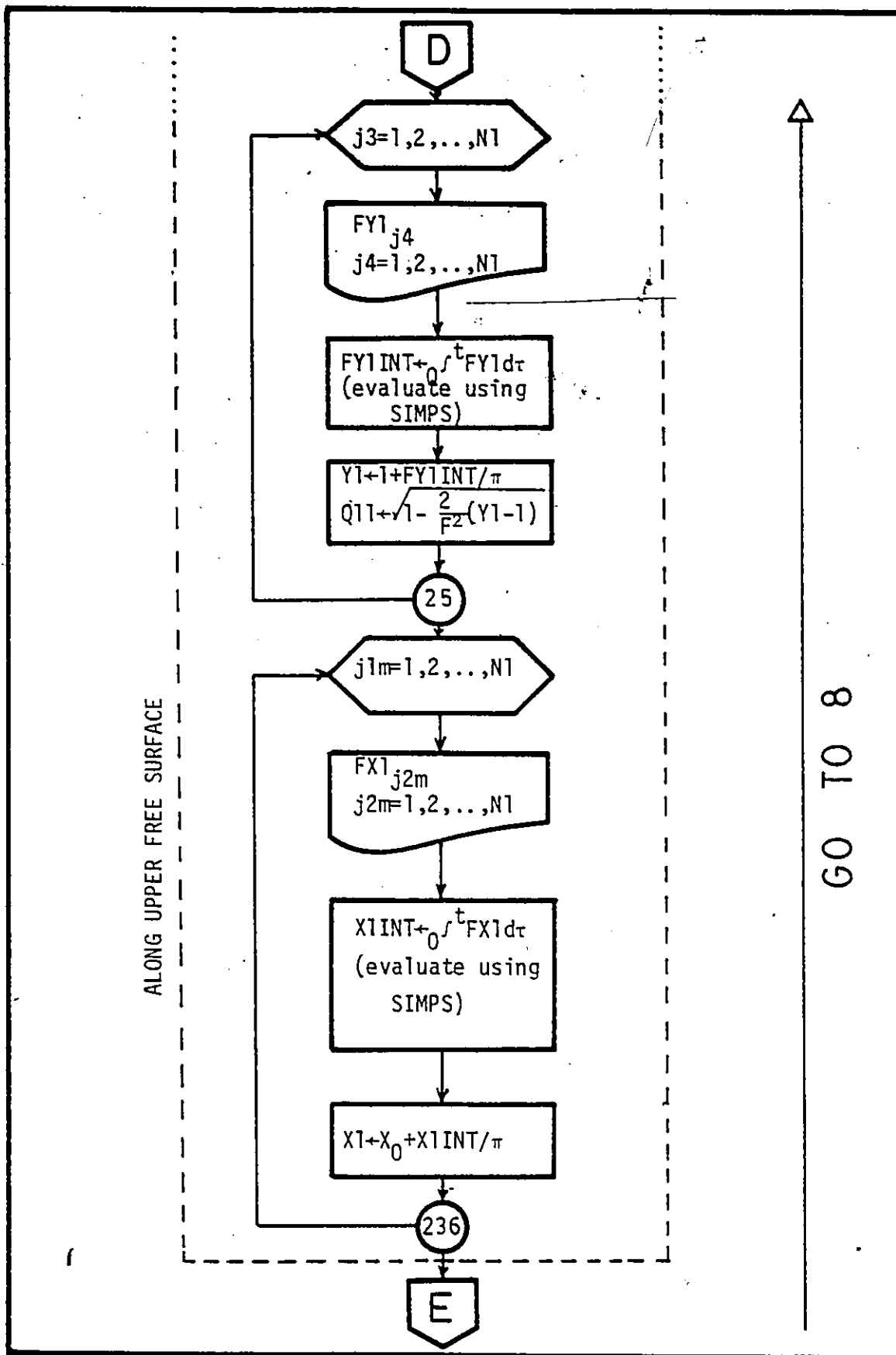
F11_{j1}, F12_{j1}
j1 = 1,2,...,NT

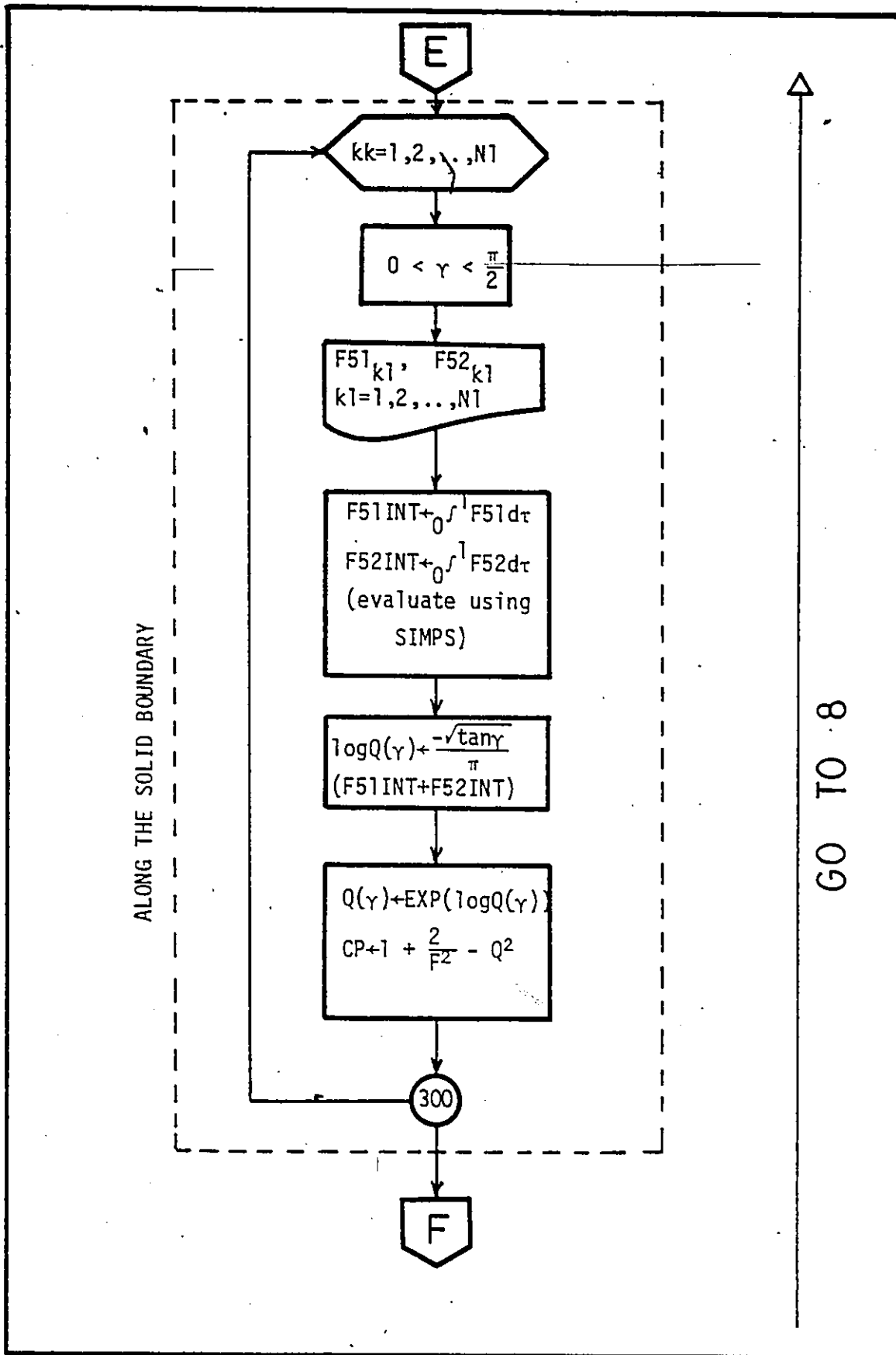
F11INT + ∫₀¹ F11 dτ
F12INT + ∫₀¹ F12 dτ
(evaluate using SIMPS)

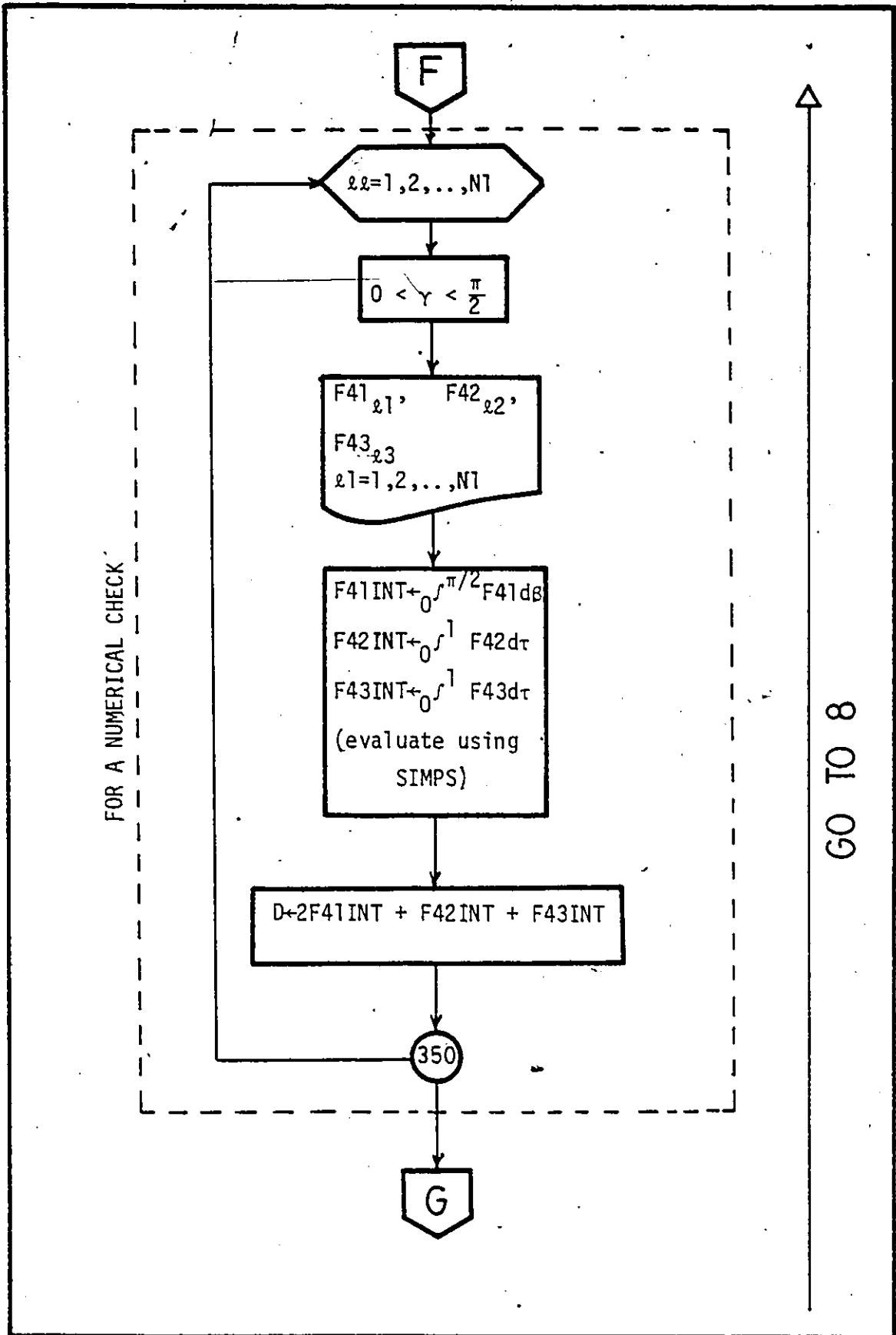
$\theta_1 + \frac{\sqrt{t}}{\pi} (F11INT - F12INT)$
 $+ \frac{\log Q1(t)}{\pi} \log \left(\frac{1+\sqrt{t}}{1-\sqrt{t}} \right)$

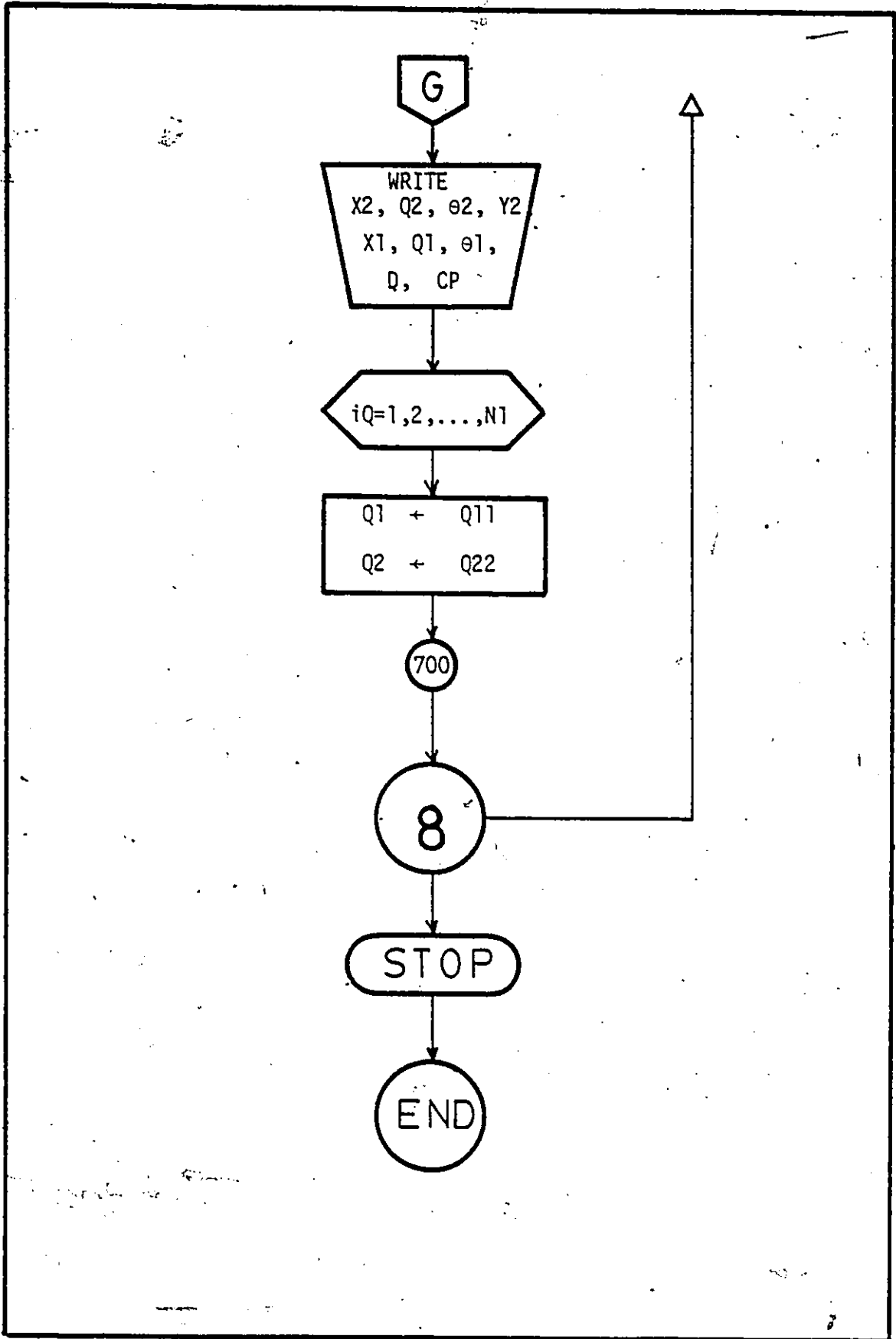
21

D









Program Listing

Main Program,

```

C      WRITTEN BY MINA B. ABD-EL-MALEK , FEB.12,1980
C
C *****
C *
C * .. FLOW FROM UNIFORM CHANNEL OVER SHELF .. *
C *
C *****
C
0001 REAL TH1(310),TH2(310),Q1(310),Q2(310),Y1(310),Y2(310)
0002 REAL T(310),U21(310),F21(310),U22(310),T1(310)
0003 REAL F22(310),FY2(310),GAMMA(310),U51(310),F51(310)
0004 REAL V11(310),F11(310),U12(310),F12(310),Q(310)
0005 REAL VY1(310),FY1(310),Q11(310),Q22(310),F41(310)
0006 REAL UX2(310),FX2(310),X2(310),U52(41),F52(310)
0007 REAL UX1(310),FX1(310),X1(310),CP(310),U41(310)
0008 REAL U42(310),F42(310),U43(310),F43(310),D(310)
C
C *****
C *
C * ...NUMERICAL VALUES FOR CONSTANTS... *
C *
C *****
C
0009 READ(5,50) N,ITMAX
0010 F2=1.
0011 N1=N+1
0012 DX=1./FLOAT(N)
0013 XLOW=0.
0014 XHIGH=1.
0015 PHIO=0
0016 X0=-1.6
0017 PI=3.141592654
0018 TO=1.+EXP(-PHIO*PI)
0019 WRITE(6,500) N,F2
C
C ...INITIALIZATION...
C
0020 DO 20 I=1,N1
0021 X=DX*(I-1)
0022 Q1(I)=1.
0023 Q2(I)=1.
0024 20 CONTINUE
C
C ...PERFORM SUCCESSIVE APPROXIMATION...
C
0025 WRITE(6,400)
0026 400 FORMAT(/10X,'X2',13X,'Q2',12X,'TH2',12X,'Y2',13X,
0027 $'X1',13X,'Q1',12X,'TH1',12X,'Y1'/120(' '))
0027 DO 8 ITER=1,ITMAX
0028 WRITE(6,217) ITER
0029 217 FORMAT(/5X,'ITER=',I4)
0030 DT=1./N
C *****
C *
C * ... ALONG LOWER FREE SURFACE ... *
C *
C *****
0031 DO 11 I=1,N1
0032 T(I)=DT*(I-1)

```

```

0033      DS=(XHIGH-XLOW)/N
0034      IK=0
0035      DO 13 K=1,N1
0036      S=DS*(K-1)
0037      V21(K)=SQRT(S)*(S-T(I))
0038      IF(V21(K).EQ.0) GO TO 13
0039      F21(K)=(ALOG(Q2(K))-ALOG(Q2(I)))/V21(K)
0040      IK=IK+1
0041      F21(IK)=F21(K)
0042      13 CONTINUE
0043      F21INT=SIMPS(XLOW,XHIGH,IK,F21)
0044      IN=0
0045      DO 14 K1=1,N1
0046      S=DS*(K1-1)
0047      V22(K1)=SQRT(S)*(1.-S*T(I))
0048      IF(V22(K1).EQ.0) GO TO 14
0049      F22(K1)=ALOG(Q1(K1))/V22(K1)
0050      IN=IN+1
0051      F22(IN)=F22(K1)

0052      14 CONTINUE
0053      F22INT=SIMPS(XLOW,XHIGH,IN,F22)
0054      TH2(I)=(SQRT(T(I))/PI)*(F21INT+F22INT)+(ALOG(Q2(I))/PI)*
*ALOG((1.-SQRT(T(I)))/(1.+SQRT(T(I))))

0055      11 CONTINUE
0056      DO 15 I1=1,N1
0057      XLOW2=0
0058      XHIGH2=T(I1)
0059      DS2=(XHIGH2-XLOW2)/N
0060      DO 16 II=1,N1
0061      S2=DS2*(II-1)
0062      FY2(II)=SIN(TH2(II))/((1.-S2)*Q2(II))
0063      16 CONTINUE
0064      FY2INT=SIMPS(XLOW2,XHIGH2,N,FY2)
0065      Y2(I1)=FY2INT/PI
0066      Q22(I1)=SQRT(1.-(2./F2)*(Y2(I1)-1.))
0067      15 CONTINUE
0068      DO 234 I1M=1,N1
0069      XLOW4=0
0070      XHIGH4=T(I1M)
0071      DXX=(XHIGH4-XLOW4)/N
0072      KL=0
0073      DO 235 I2M=1,N1
0074      XX=XLOW4+DXX*(I2M-1)
0075      VX2(I2M)=(1.-XX)*Q2(I2M)
0076      IF(VX2(I2M).EQ.0) GO TO 235
0077      FX2(I2M)=COS(TH2(I2M))/VX2(I2M)
0078      KL=KL+1
0079      FX2(KL)=FX2(I2M)
0080      235 CONTINUE
0081      X2INT=SIMPS(XLOW4,XHIGH4,KL,FX2)
0082      X2(I1M)=X2INT/PI
0083      234 CONTINUE
C *****
C *
C * ... ALONG UPPER FREE SURFACE ... *
C *
C *****
0084      DT1=1./FLOAT(N)
0085      DO 30 IJK=1,N1

```

```

0086      T1(IJK)=DT1*(IJK-1)
0087      30  CONTINUE
0088      DO 21 JJ=1,N1
0089      IJ=0
0090      DO 22 J1=1,N1
0091      S=DS*(J1-1)
0092      V11(J1)=SQRT(S)*(S*T(JJ)-1.)
0093      IF(V11(J1).EQ.0) GO TO 22
0094      F11(J1)=ALOG(Q2(J1))/V11(J1)
0095      IJ=IJ+1
0096      F11(IJ)=F11(J1)
0097      22  CONTINUE
0098      F11INT=SIMPS(XLOW,XHIGH,IJ,F11)
0099      JK=0
0100      DO 24 J2=1,N1
0101      S=DS*(J2-1)
0102      V12(J2)=SQRT(S)*(S-T(JJ))
0103      IF(V12(J2).EQ.0) GO TO 24
0104      F12(J2)=(ALOG(Q1(J2))-ALOG(Q1(JJ)))/V12(J2)
0105      JK=JK+1
0106      F12(JK)=F12(J2)
0107      24  CONTINUE
0108      F12INT=SIMPS(XLOW,XHIGH,JK,F12)
0109      TH1(JJ)=(SQRT(T(JJ))/PI)*(F11INT-F12INT)+(ALOG(Q1(JJ))/PI)*
0110      21  *ALOG((1.+SQRT(T(JJ)))/(1.-SQRT(T(JJ))))
0111      CONTINUE
0112      IC=0
0113      DO 25 J3=1,N1
0114      XLOW3=0
0115      XHIGH3=T1(J3)
0116      DS3=(XHIGH3-XLOW3)/N
0117      IF(XHIGH3.EQ.XLOW3) GO TO 75
0118      IIK=0
0119      DO 26 J4=1,N1
0120      S3=DS3*(J4-1)
0121      VY1(J4)=S3*(1.-S3)*Q1(J4)
0122      IF(VY1(J4).EQ.0) GO TO 26
0123      FY1(J4)=SIN(TH1(J4))/VY1(J4)
0124      IIK=IIK+1
0125      FY1(IIK)=FY1(J4)
0126      26  CONTINUE
0127      FY1INT=SIMPS(XLOW3,XHIGH3,IIK,FY1)
0128      GO TO 85
0129      75  FY1INT=0
0130      85  Y1(J3)=(FY1INT/PI)+1.
0131      Q11(J3)=SQRT(1.-(2./F2)*(Y1(J3)-1.))
0132      IC=IC+1
0133      Q11(IC)=Q11(J3)
0134      25  CONTINUE
0135      JX=0
0136      DO 236 J1M=1,N1
0137      XLOW5=0
0138      XHIGH5=T1(J1M)
0139      IF(XHIGH5.EQ.XLOW5) GO TO 232
0140      DX1=(XHIGH5-XLOW5)/N1
0141      KLL=0
0142      DO 237 J2M=1,N1
0143      XX1=XLOW5+DX1*(J2M-1)

```

```

0143          VX1(J2M)=XX1*(1.-XX1)*Q1(J2M)
0144          IF(VX1(J2M).EQ.0) GO TO 237
0145          FX1(J2M)=COS(TH1(J2M))/VX1(J2M)
0146          KLL=KLL+1
0147          FX1(KLL)=FX1(J2M)
0148          237 CONTINUE
0149          X1INT=SIMPS(XLW5,XHIGH5,KLL,FX1)
0150          GO TO 233
0151          232 X1INT=0
0152          233 X1(J1M)=X0+(X1INT/PI)
0153          JX=JX+1
0154          X1(JX)=X1(J1M)
0155          234 CONTINUE
C
C
C *****
C *
C * ... ALONG THE SOLID BOUNDRY ... *
C *
C *****
C
0156          DO 300 KK=1,N
0157          GAMMA(KK)=(PI/(2*N))*(KK-1)
0158          IR=0
0159          DO 301 K1=1,N1
0160          V51(K1)=(1.+T(K1)*TAN(GAMMA(KK))**2)*SQRT(T(K1))
0161          IF(V51(K1).EQ.0) GO TO 301
0162          F51(K1)=ALOG(Q2(K1))/V51(K1)
0163          IR=IR+1
0164          F51(IR)=F51(K1)
0165          301 CONTINUE
0166          F51INT=SIMPS(XLOW,XHIGH,IR,F51)
0167          IS=0
0168          DO 302 K1=1,N1
0169          V52(K1)=(T(K1)+TAN(GAMMA(KK))**2)*SQRT(T(K1))
0170          IF(V52(K1).EQ.0) GO TO 302
0171          F52(K1)=ALOG(Q1(K1))/V52(K1)
0172          IS=IS+1
0173          F52(IS)=F52(K1)
0174          302 CONTINUE
0175          F52INT=SIMPS(XLOW,XHIGH,IS,F52)
0176          Q(KK)=EXP((-TAN(GAMMA(KK))/PI)*(F51INT+F52INT))
0177          CP(KK)=1.+(2./F2)-Q(KK)*Q(KK)
0178          300 CONTINUE
C
C *****
C *
C * ...FOR A NUMERICAL CHECK .. *
C *
C *****
C
0179          DO 350 LL=1,N
0180          IF(Q(LL).EQ.0) GO TO 350
0181          XHIGH6=PI/2.
0182          XLOW6=0
0183          DL=(XHIGH6-XLOW6)/N
0184          IL=0
0185          DO 351 L1=1,N

```

```

0186      HL=DL*(L1-1)
0187      IF(Q(L1).EQ.0) GO TO 351
0188      V41(L1)=(TAN(HL)**2-TAN(GAMMA(LL))**2)*(COS(HL)**2)
0189      IF(V41(L1).EQ.0) GO TO 351
0190      F41(L1)=(ALOG(Q(L1))-ALOG(Q(LL)))/V41(L1)
0191      IL=IL+1
0192      F41(IL)=F41(L1)
0193      351 CONTINUE
0194      F41INT=SIMPS(XLOW6,XHIGH6,IL,F41)
0195      IM=0
0196      DO 352 L1=1,N1
0197      V42(L1)=(1.+T(L1)*TAN(GAMMA(LL))**2)*SQRT(T(L1))
0198      IF(V42(L1).EQ.0) GO TO 352
0199      F42(L1)=TH2(L1)/V42(L1)
0200      IM=IM+1
0201      F42(IM)=F42(L1)
0202      352 CONTINUE
0203      F42INT=SIMPS(XLOW,XHIGH,IM,F42)
0204      IN=0
0205      DO 353 L1=1,N1
0206      V43(L1)=(T(L1)+TAN(GAMMA(LL))**2)*SQRT(T(L1))
0207      IF(V43(L1).EQ.0) GO TO 353
0208      F43(L1)=TH1(L1)/V43(L1)
0209      IN=IN+1
0210      F43(IN)=F43(L1)
0211      353 CONTINUE
0212      F43INT=SIMPS(XLOW,XHIGH,IN,F43)
0213      D(LL)=2*F41INT+F42INT+F43INT
0214      350 CONTINUE
C
0215      WRITE(6,600) (X2(I),Q2(I),TH2(I),Y2(I),X1(I),Q1(I),
0216      *TH1(I),Y1(I),D(I),I=1,N)
0217      600 FORMAT(9F13.6)
0218      DO 700 IQ=1,N1
0219      Q1(IQ)=Q11(IQ)
0220      Q2(IQ)=Q22(IQ)
0221      700 CONTINUE
0222      8 CONTINUE
0223      WRITE(6,801)
0224      801 FORMAT(///10X,'PRESSURE DIST. ALONG THE SOLID BOUNDARY
0225      *...CP... '/')
0226      WRITE(6,800) (CP(I),I=1,N)
0227      800 FORMAT(25X,F20.10)
C
C      ..PRINT OUTPUT...
C
0226      50 FORMAT(I4,I4)
0227      500 FORMAT(//10X,'N      =',I4/10X,'F2      =',F10.5/)
0228      STOP
0229      END

```

Function SIMPS

```
      C
      C
0001      FUNCTION SIMPS(U,V,N,F)
0002      REAL F(310)
0003      NN=N-1
0004      H=(V-U)/(3*FLOAT(NN))
0005      S1=0
0006      S2=0
0007      N2=NN/2
0008      DO 109 I=1,N2
0009      K=2*I
0010      IF(I.EQ.N2) GO TO 108
0011      J=2*I+1
0012      S1=S1+F(J)
0013      S2=S2+F(K)
0014      109 CONTINUE
0015      SIMPS=(2*S2+4*S1+F(1)+F(N))*H
0016      RETURN
0017      END
```

APPENDIX [F]


COMPUTER PROGRAM FOR A FLOW
FROM UNIFORM CHANNEL OVER SHARP-
CRESTED WEIR

FORTRAN Implementation

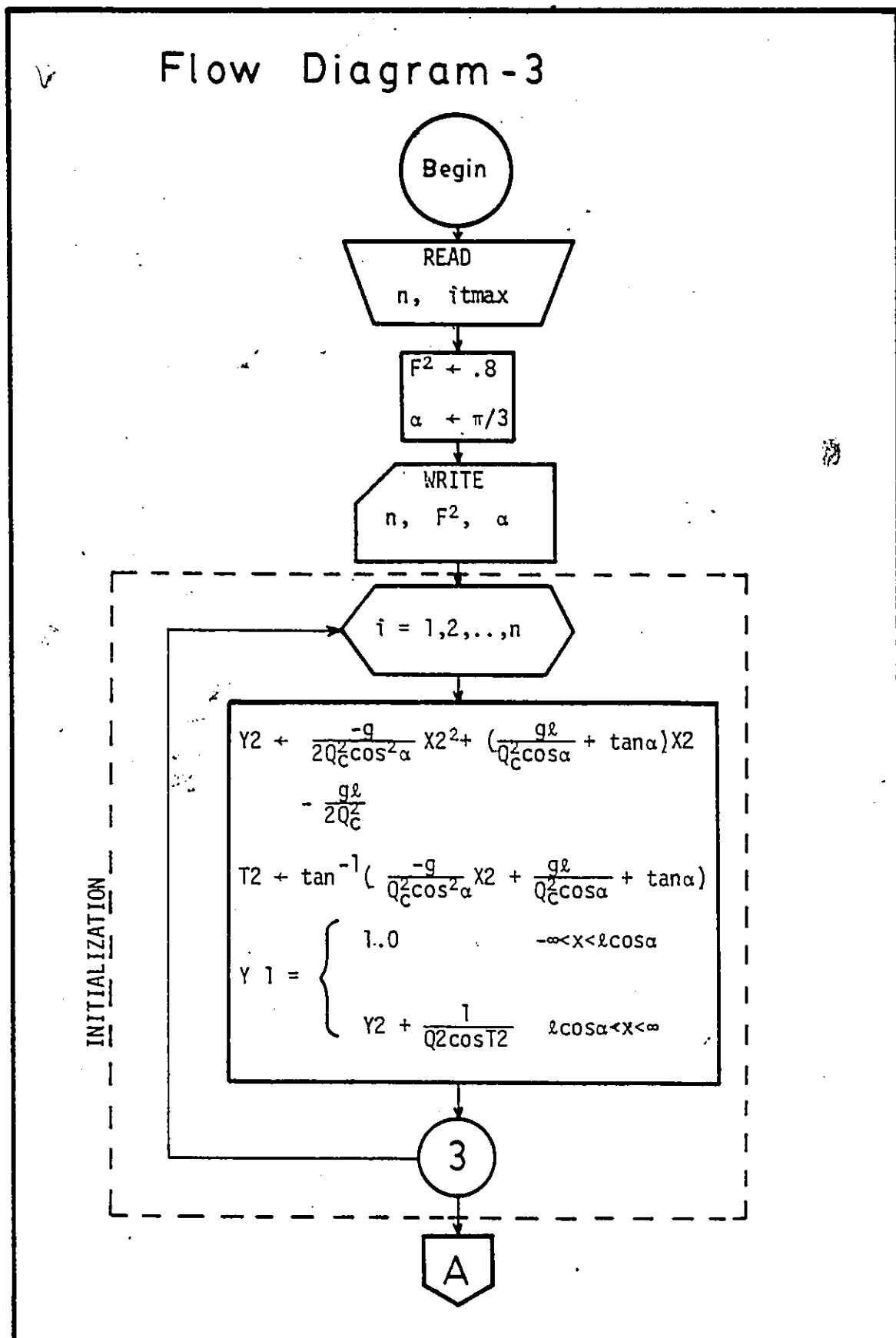
List of Principal Variables

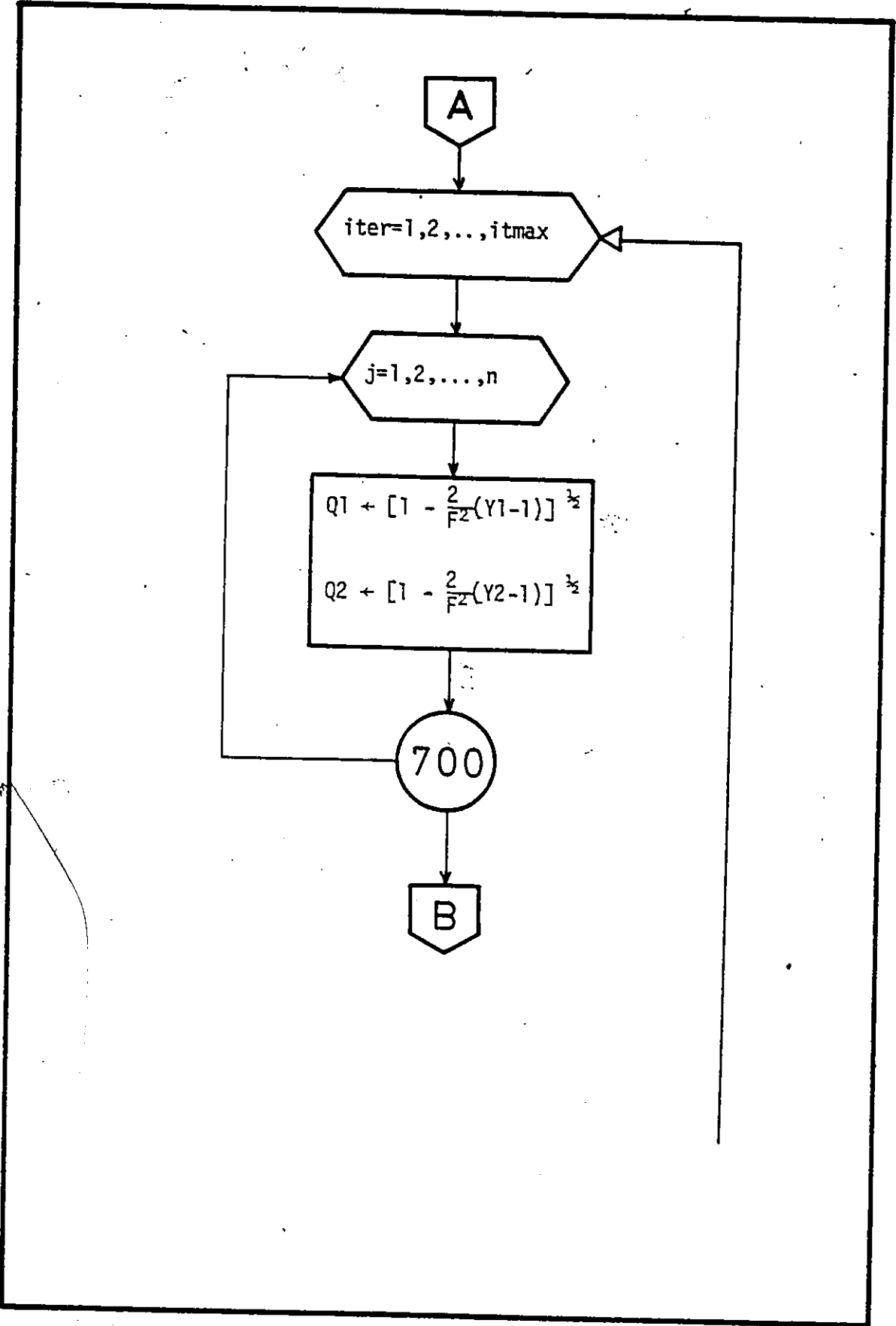
Program Symbol	Definition
F2	Froude number square, F^2 .
ITER	counter on the number of iterations, iter.
ITMAX	maximum number of iterations allowed, itmax.
L	length of inclined plane.
N	number of increments, n.
Q 1	magnitude of velocity along upper free surface, q_1 .
Q 2	magnitude of velocity along lower free surface, q_2 .
Q H	magnitude of velocity along horizontal plane AB, q_H .

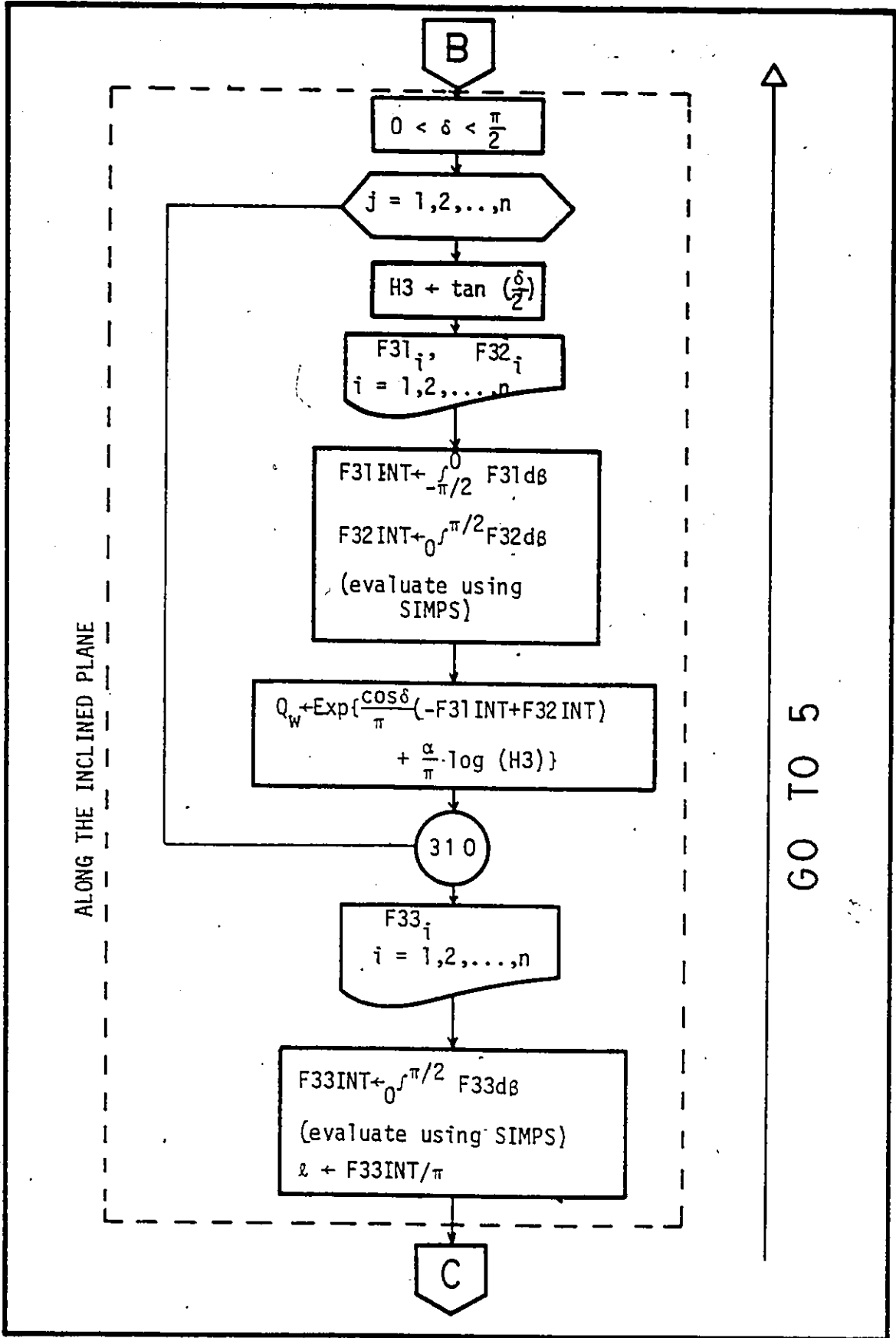
Q_w	magnitude of velocity along the weir, q_w .
SIMPS	function of implementing Simpson's rule.
t	real t -plane coordinate.
T_1	argument of complex velocity along the upper free surface, θ_1 .
T_2	argument of complex velocity along the lower free surface, θ_2 .
X_1	horizontal coordinate for the upper free surface.
X_2	horizontal coordinate for the lower free surface.
Y_1	vertical coordinate for the upper free surface.
Y_2	vertical coordinate for the lower free surface.

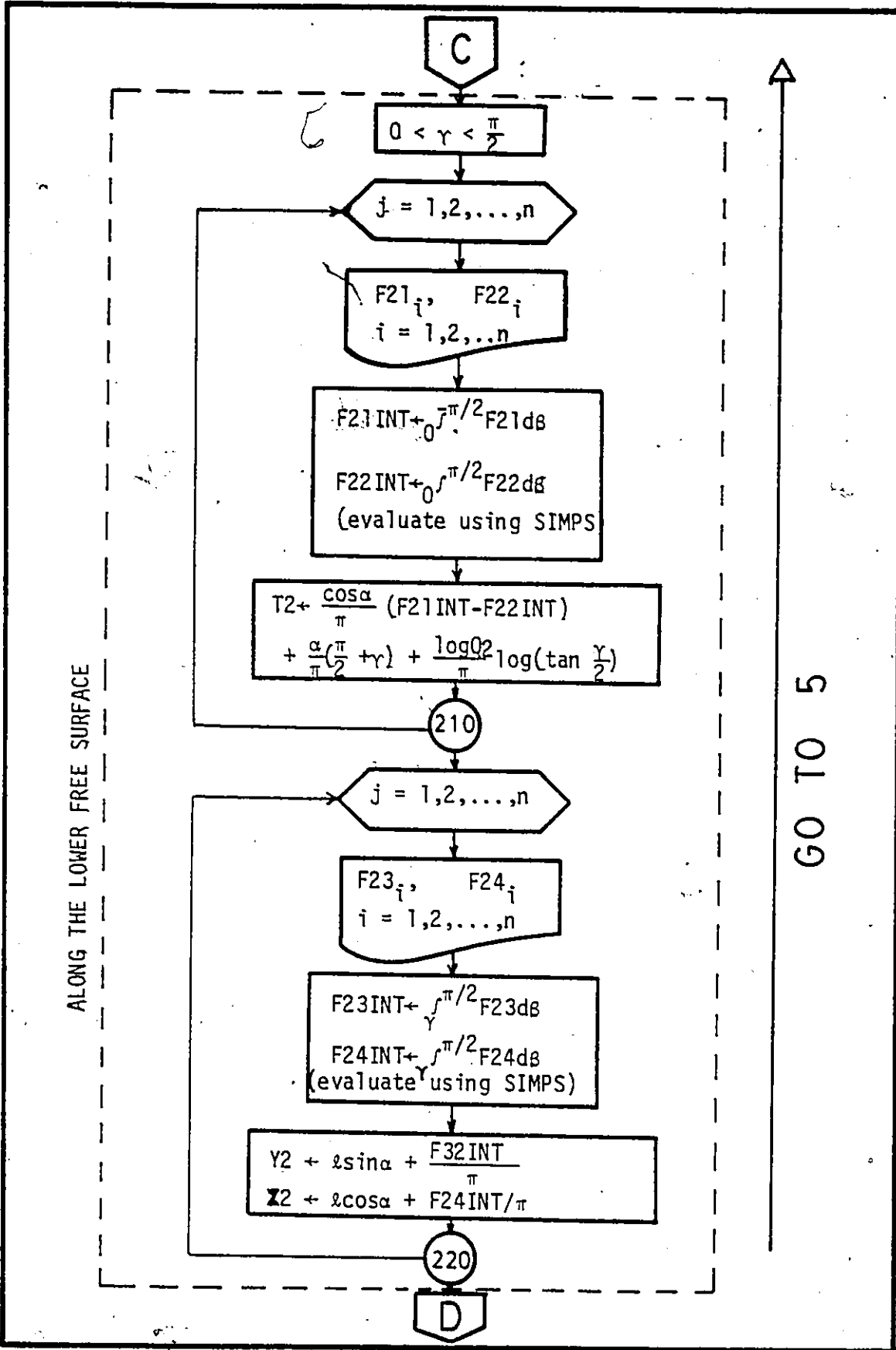


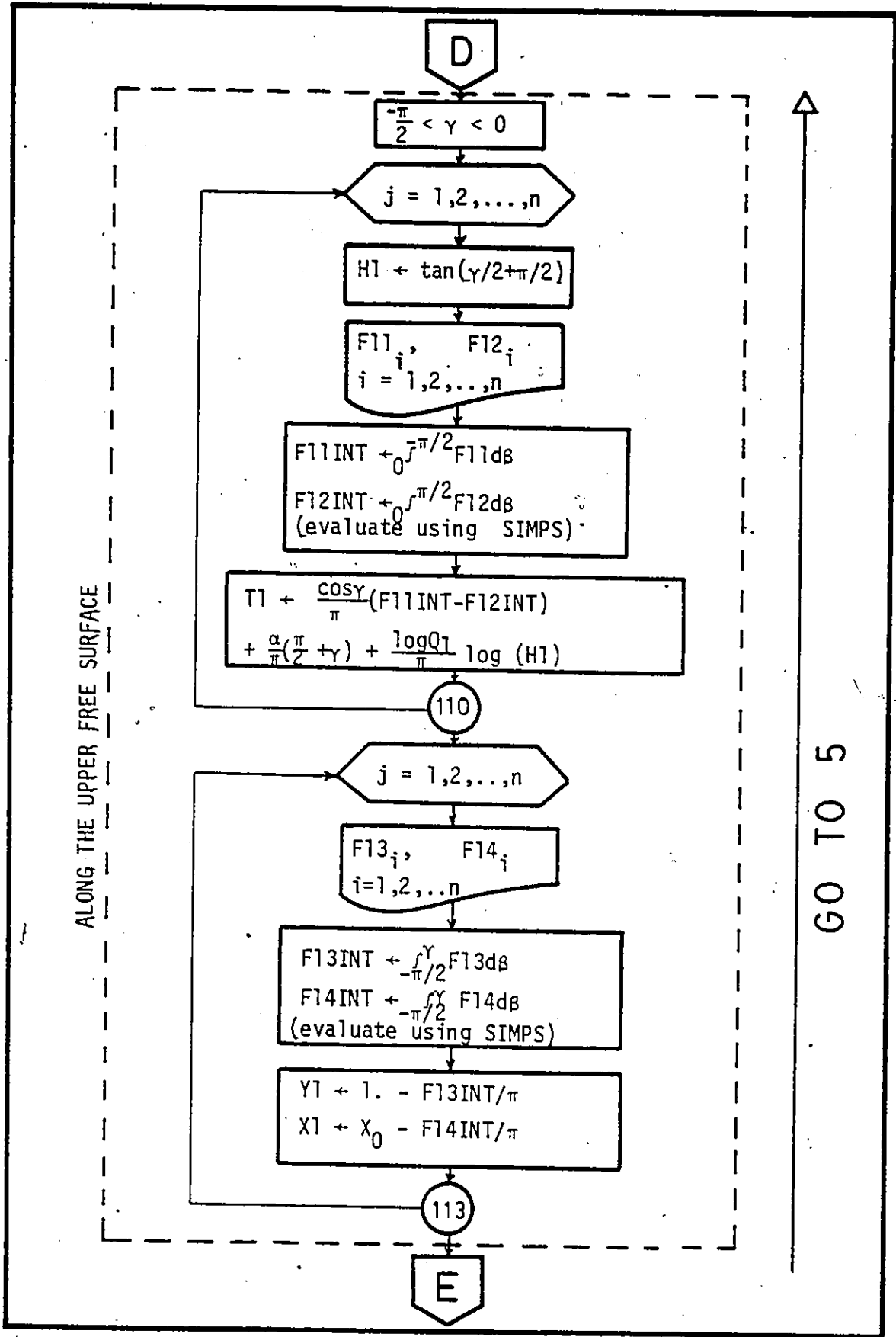
Flow Diagram - 3





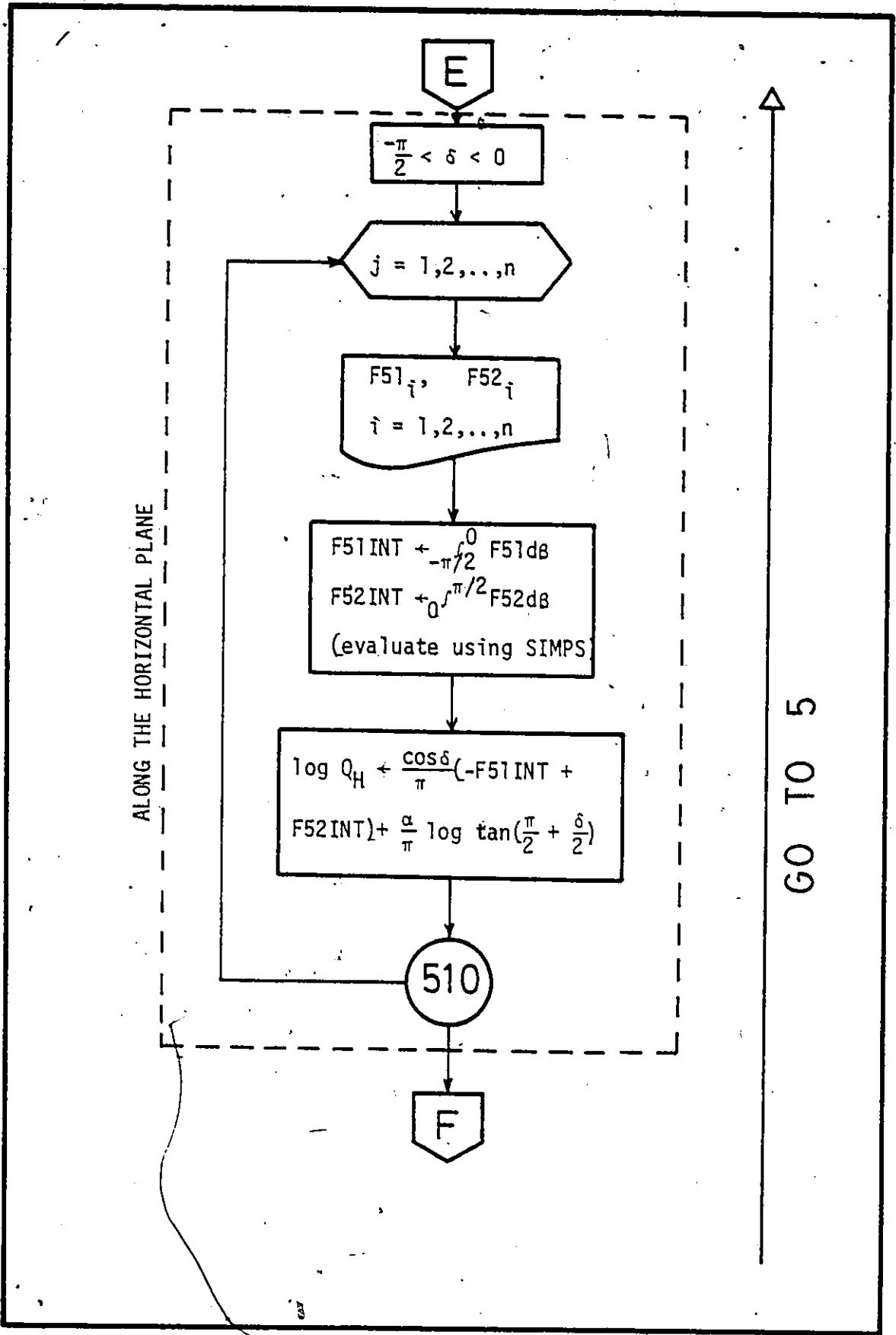


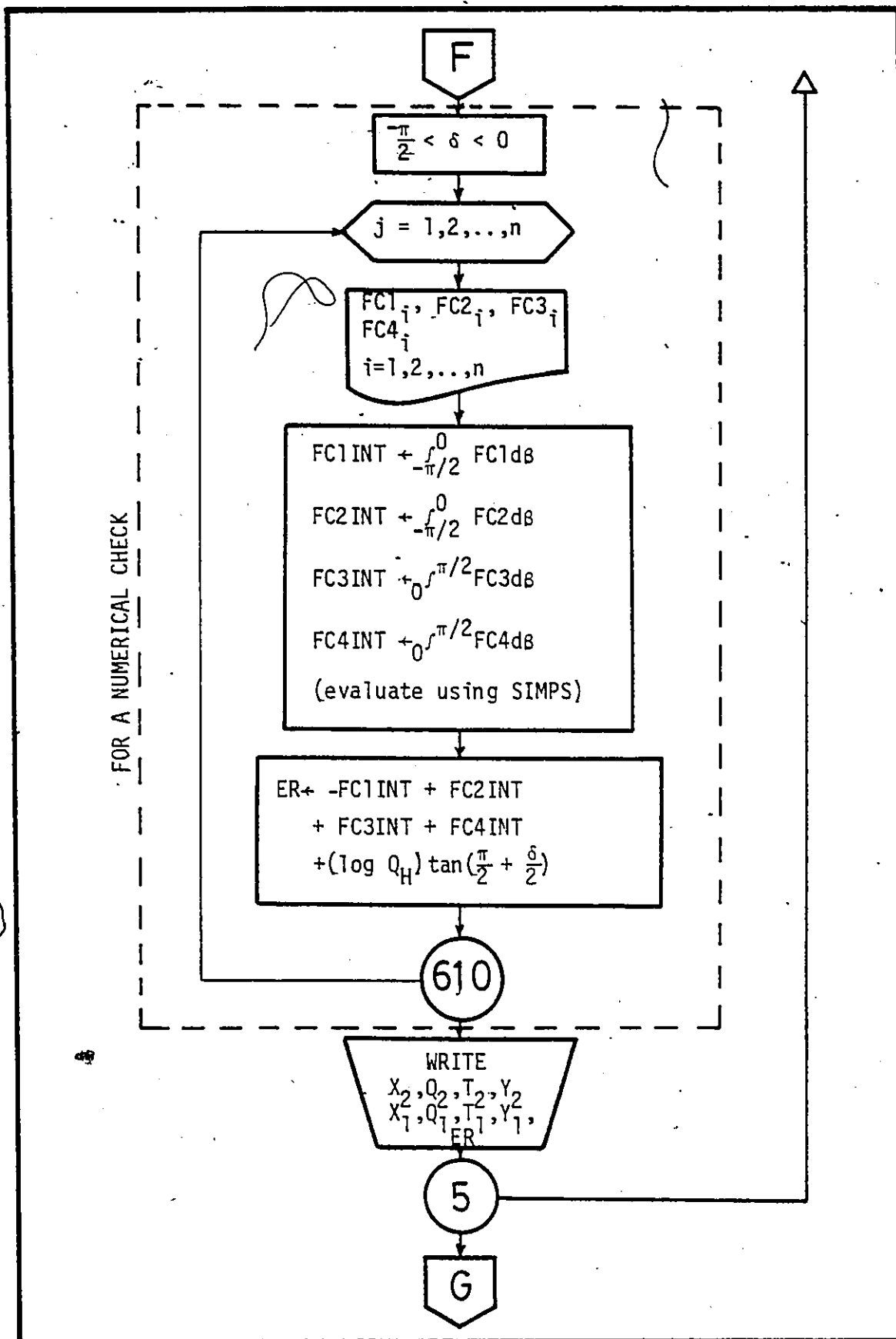


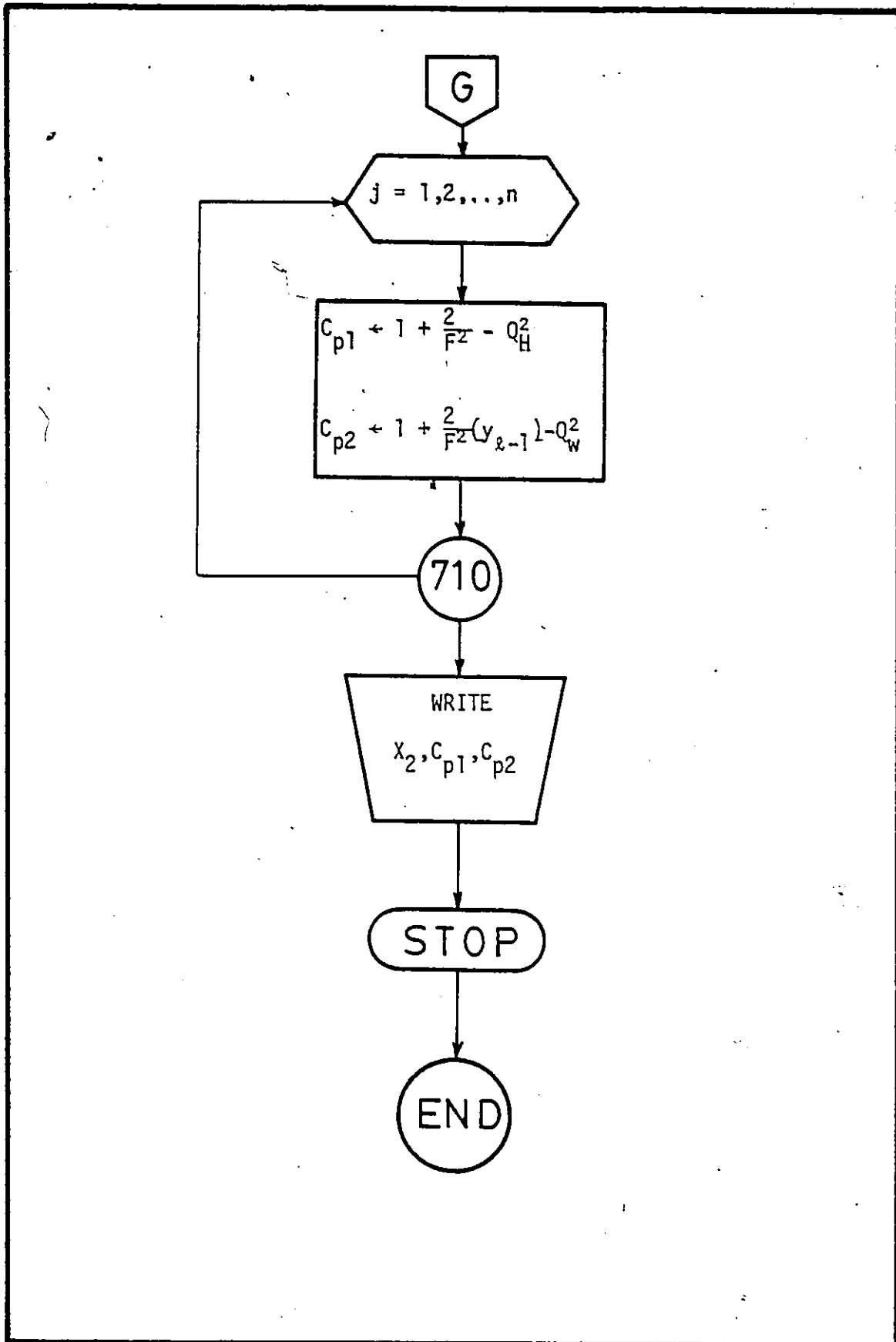


ALONG THE UPPER FREE SURFACE

GO TO 5







Program Listing

Main Program

```

C
C
C      WRITTEN BY MINA B. ABD-EL-MALEK , MARCH 9 , 1980 .
C
C      *****
C      *
C      *.. FLOW FROM UNIFORM CHANNEL OVER SHARP-CRESTED WEIR ...*
C      *
C      *****
C
0001      REAL Q1(210),Q2(210),R(210),S(210),H3(210),HA3(210)
0002      REAL U31(210),V31(210),F31(210),U32(210),V32(210)
0003      REAL F32(210),Q(210),U33(210),V33(210),F33(210)
0004      REAL V21(210),F21(210),U22(210),V22(210),T2(210)
0005      REAL U23(210),V23(210),U24(210),F23(210),F24(210)
0006      REAL X2(210),H1(210),HA1(210),U11(210),V11(210)
0007      REAL U12(210),V12(210),F12(210),T1(210),S1(210)
0008      REAL V13(210),U14(210),F13(210),F14(210),Y1(210)
0009      REAL SP(210),Y3(210),Q3(210),V51(210),F51(210)
0010      REAL Y22(210),F52(210),QHL(210),QH(210),CP2(210)
0011      REAL F41(210),F42(210),F43(210),F44(210),ERR(210)
0012      REAL F22(210),QG(210),U21(210),S2(210),Y2(210)
0013      REAL F11(210),U13(210),T11(210),X1(210),T22(210)
0014      REAL U52(210),CP1(210)
C
0015      READ(5,1) N,ITMAX
0016      PI=3.141592654
0017      H=1.5
0018      F2=.8
0019      G2=1.+5*F2
0020      GRA=1.
0021      N1=N
0022      ALPHA=PI/3.
0023      Q(N1)=1.-(2./F2)*(H*SIN(ALPHA)-1.)
0024      X0=-2.5
0025      GS=GRA*SIN(ALPHA)/(Q(N1)**3)
0026      C=SQRT(2*GS)
0027      K=1
0028      NY=N-1
0029      XLR=-1.570796327
0030      XHR=0
0031      XLS=0
0032      XHS=1.570796327
0033      DR=(XHR-XLR)/FLOAT(N)
0034      DS=(XHS-XLS)/FLOAT(N)
0035      GQ=GRA/((Q(N1)**2)*COS(ALPHA))
0036      WRITE(6,2) N,F2,X0,ALPHA
C
C      ...INITIALIZATION...
C
0037      DO 3 I=1,N1
0038      R(I)=XLR+DR*I
0039      S(I)=XHS-DS*I
0040      SP(I)=(1./PI)*ALOG(SIN(S(I)))/(1.-SIN(S(I)))
0041      Y2(I)=-(.5*GQ/COS(ALPHA))*(SP(I)**2)+(GQ*H+TAN
      (ALPHA))*SP(I)-.5*GRA*((H/Q(N1))**2)
0042      Q2(I)=SQRT(1.-(2./F2)*(Y2(I)-1.))
0043      T2(I)=ATAN(-(GQ*SP(I)/COS(ALPHA))+GQ*H+TAN(ALPHA))
0044      IF(I.GT.30) Y1(I)=Y2(I)+1./(Q2(I)*COS(T2(I)))

```

```

0045      Y1(I)=1.
0046      Y3(I)=Y1(I)
0047      Q1(I)=SQRT(1.-(2./F2)*(Y1(I)-1.))
0048      CONTINUE
          3
C
C      ... PERFORM SUCCESSIVE APPROXIMATION ...
C
0049      WRITE(6,4)
0050      4  FORMAT(//10X,'X2',13X,'Q2',12X,'T2',12X,'Y2',13X,
0051      *'X1',13X,'Q1',12X,'T1',12X,'Y1'/120('*'))
0052      DO 5 ITER=1,ITMAX
0053      6  WRITE(6,6) ITER
          6  FORMAT(//5X,'ITER=',I4)
          C
          C
0054      IR=0
0055      DO 700 J=1,N1
0056      XR=S(J)
0057      H3(J)=TAN(S(J)/2.)

0058      HA3(J)=ABS(H3(J))
0059      IF(HA3(J).EQ.0) GO TO 700
0060      IR1=0
0061      K=J-1
0062      IF(Y1(J).GT.G2) Y1(J)=Y1(K)
0063      Q1(J)=SQRT(1.-(2./F2)*(Y1(J)-1.))
0064      Q2(J)=SQRT(1.-(2./F2)*(Y2(J)-1.))
0065      IR=IR+1
0066      Q2(IR)=Q2(J)
0067      700 CONTINUE
          C
          C      *****
          C      *
          C      * ..ALONG THE INCLINED PLANE.. *
          C      *
          C      *****
          C
0068      IK=0
0069      DO 310 J=1,N1
0070      H3(J)=TAN(S(J)/2.)
0071      HA3(J)=ABS(H3(J))
0072      IF(HA3(J).EQ.0) GO TO 310
0073      IC1=0
0074      DO 311 I=1,N1
0075      U31(I)=ALOG(Q1(I))
0076      V31(I)=1.-SIN(S(J))*SIN(R(I))
0077      IF(V31(I).EQ.0) GO TO 311
0078      F31(I)=U31(I)/V31(I)
0079      IC1=IC1+1
0080      F31(IC1)=F31(I)
0081      311 CONTINUE
0082      F31INT=SIMPS(XLR,XHR,IC1,F31)
0083      IC2=0
0084      DO 312 I=1,N1
0085      U32(I)=ALOG(Q2(I))
0086      V32(I)=1.-SIN(S(J))*SIN(S(I))
0087      IF(V32(I).EQ.0) GO TO 312
0088      F32(I)=U32(I)/V32(I)

```

```

0089          IC2=IC2+1
0090          F32(IC2)=F32(I)
0091          312 CONTINUE
0092          F32INT=SIMPS(XLS,XHS,IC2,F32)
0093          IK=IK+1
0094          QG(J)=(COS(S(J))/PI)*(-F31INT+F32INT)+(ALPHA/PI)
          *ALOG(HA3(J))
0095          Q(J)=EXP(QG(J))
0096          QG(IK)=QG(J)
0097          Q(IK)=Q(J)
0098          310 CONTINUE
0099          IC3=0
0100          DO 313 I=1,N1
0101          U33(I)=COS(S(I))
0102          V33(I)=(1.+SIN(S(I)))*Q(I)
0103          IF(V33(I).EQ.0) GO TO 313
0104          F33(I)=U33(I)/V33(I)
0105          IC3=IC3+1
0106          F33(IC3)=F33(I)
0107          313 CONTINUE
0108          F33INT=SIMPS(XLS,XHS,IC3,F33)
0109          D=F33INT/PI

C
C *****
C *
C * ..ALONG LOWER FREE SURFACE.. *
C *
C *****
C

0110          IN=0
0111          DO 210 J=1,N1
0112          IF(HA3(J).EQ.0) GO TO 210
0113          IC4=0
0114          DO 211 I=1,N1
0115          U21(I)=ALOG(Q1(I))
0116          V21(I)=SIN(R(I))-SIN(S(J))
0117          IF(V21(I).EQ.0) GO TO 211
0118          F21(I)=U21(I)/V21(I)
0119          IC4=IC4+1
0120          F21(IC4)=F21(I)

0121          211 CONTINUE
0122          F21INT=SIMPS(XLR,XHR,IC4,F21)
0123          IC5=0
0124          DO 212 I=1,N1
0125          U22(I)=ALOG(Q2(I))-ALOG(Q2(J))
0126          V22(I)=SIN(S(I))-SIN(S(J))
0127          IF(V22(I).EQ.0) GO TO 212
0128          F22(I)=U22(I)/V22(I)
0129          IC5=IC5+1
0130          F22(IC5)=F22(I)
0131          212 CONTINUE
0132          F22INT=SIMPS(XLS,XHS,IC5,F22)
0133          IN=IN+1
0134          T22(J)=(COS(S(J))/PI)*(F21INT-F22INT)+(1./PI)*
          *ALPHA*(PI/2.+S(J))
          *+ALOG(Q2(J))*ALOG(HA3(J))
0135          T22(IN)=T22(J)
0136          210 CONTINUE

```

```

0137          DO 215 I=1,N1
0138          Y1(I)=Y2(I)+1./(Q2(I)*COS(T2(I)))
0139          K=I-1
0140          IF(Y1(I).GT.G2) Y1(I)=Y1(K)
0141          Q1(I)=SQRT(1.-(2./F2)*(Y1(I)-1.))
0142          215 CONTINUE
0143          DO 220 J=1,N1
0144          XL2=S(J)
0145          XH2=1.570796327
0146          IC6=0
0147          DO 221 I=1,N1
0148          DS2=(XH2-XL2)/FLOAT(N)
0149          S2(I)=XL2+DS2*(I-1)
0150          U23(I)=COS(S2(I))*SIN(T2(I))
0151          U24(I)=COS(S2(I))*COS(T2(I))
0152          V23(I)=SIN(S2(I))*(1.+SIN(S2(I)))
0153          IF(V23(I).EQ.0) GO TO 221
0154          F23(I)=U23(I)/V23(I)
0155          F24(I)=U24(I)/V23(I)
0156          IC6=IC6+1
0157          F23(IC6)=F23(I)
0158          F24(IC6)=F24(I)
0159          221 CONTINUE
0160          F23INT=SIMPS(XL2,XH2,IC6,F23)
0161          F24INT=SIMPS(XL2,XH2,IC6,F24)
0162          Y2(J)=D*SIN(ALPHA)+(F23INT/PI)
0163          X2(J)=D*COS(ALPHA)+(F24INT/PI)
0164          220 CONTINUE
C
C
C *****
C *
C * ..ALONG UPPER FREE SURFACE.. *
C *
C *****
C
0165          IL=0
0166          DO 110 J=1,N1
0167          H1(J)=TAN(R(J)/2.)
0168          HA1(J)=ABS(H1(J))
0169          IF(HA1(J).EQ.0) GO TO 110
0170          IC7=0
0171          DO 111 I=1,N1
0172          U11(I)=ALOG(Q1(I))-ALOG(Q1(J))
0173          V11(I)=SIN(R(I))-SIN(R(J))
0174          IF(V11(I).EQ.0) GO TO 111
0175          F11(I)=U11(I)/V11(I)
0176          IC7=IC7+1
0177          F11(IC7)=F11(I)
0178          111 CONTINUE
0179          F11INT=SIMPS(XLR,XHR,IC7,F11)
0180          IC8=0
0181          DO 112 I=1,N1
0182          U12(I)=ALOG(Q2(I))
0183          V12(I)=SIN(S(I))-SIN(R(J))
0184          IF(V12(I).EQ.0) GO TO 112
0185          F12(I)=U12(I)/V12(I)
0186          IC8=IC8+1
0187          F12(IC8)=F12(I)

```

```

0188          112 CONTINUE
0189          F12INT=SIMPS(XLS,XHS,IC8,F12)
0190          IL=IL+1
0191          T1(J)=(COS(R(J))/PI)*(F11INT-F12INT)+((1./PI)*(
          $ALPHA*(PI/2.)+R(J))
          $+ALOG(Q1(J))*ALOG(HA1(J)))
0192          110 CONTINUE
0193          IM=0
0194          DO 113 J=1,N1
0195          XL1=-1.570796327
0196          XH1=R(J)
0197          IC9=0
0198          DS1=(XH1-XL1)/FLOAT(N)
0199          IF(DS1.EQ.0) GO TO 113
0200          DO 114 I=1,N1
0201          S1(I)=XL1+DS1*(I-1)
0202          U13(I)=COS(S1(I))*SIN(T1(I))
0203          U14(I)=COS(S1(I))*COS(T1(I))
0204          V13(I)=SIN(S1(I))*(1.+SIN(S1(I)))*Q1(I)
0205          IF(V13(I).EQ.0) GO TO 114
0206          F13(I)=U13(I)/V13(I)
0207          F14(I)=U14(I)/V13(I)
0208          IC9=IC9+1
0209          F13(IC9)=F13(I)
0210          F14(IC9)=F14(I)
0211          114 CONTINUE
0212          F13INT=SIMPS(XL1,XH1,IC9,F13)
0213          IM=IM+1
0214          Y1(J)=1.-(F13INT/PI)
0215          F14INT=SIMPS(XL1,XH1,IC9,F14)
0216          X1(J)=X0-(F14INT/PI)
0217          113 CONTINUE
          C
          C *****
          C *
          C * ... ALONG THE FLAT SHELF ... *
          C *
          C *****
          C
0218          DO 510 J=1,N1
0219          DO 509 I=1,N1
0220          V51(I)=1.-SIN(R(I))*SIN(R(J))
0221          F51(I)=ALOG(Q1(I))/V51(I)
0222          V52(I)=1.-SIN(S(I))*SIN(R(J))
0223          F52(I)=ALOG(Q2(I))/V52(I)
0224          509 CONTINUE
0225          F51INT=SIMPS(XLR,XHR,N1,F51)
0226          F52INT=SIMPS(XLS,XHS,N1,F52)
0227          QHL(J)=(COS(R(J))/PI)*(-F51INT+F52INT)+(ALPHA/PI)
          $*ALOG(TAN((XHS+R(J)/2.))
0228          QH(J)=EXP(QHL(J))
0229          510 CONTINUE
          C
          C *****
          C *
          C * ... FOR A NUMERICAL CHECK ... *
          C *
          C *****
          C
0230          DO 610 J=1,N1

```

```

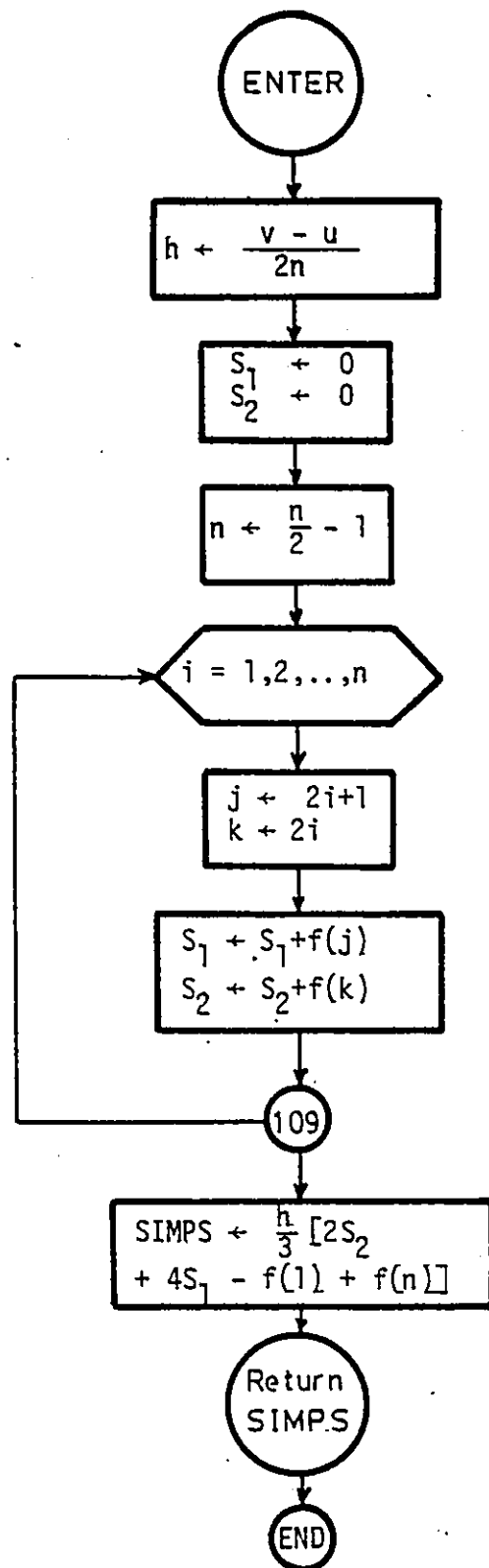
0231      DO 609 I=1,N1
0232          F61(I)=T1(I)/(1.-SIN(R(I))*SIN(R(J)))
0233          F62(I)=(ALOG(QH(I))-ALOG(QH(J)))/(SIN(R(I))-SIN(R(J)))
0234          F63(I)=ALOG(Q(I))/(SIN(S(I))-SIN(R(J)))
0235          F64(I)=T22(I)/(1.-SIN(S(I))*SIN(R(J)))
0236      609 CONTINUE
0237          F61INT=SIMPS(XLR,XHR,N1,F61)
0238          F62INT=SIMPS(XLR,XHR,N1,F62)
0239          F63INT=SIMPS(XLS,XHS,N1,F63)
0240          F64INT=SIMPS(XLS,XHS,N1,F64)
0241          ERR(J)=-F61INT+F62INT+F63INT+F64INT+ALOG(QH(J))
          $*TAN(XHS+R(J)/2.)
0242      610 CONTINUE
C
0243          WRITE(6,400) (X2(I),Q2(I),T22(I),Y2(I),X1(I),Q1(I),T1(I)
0244          $,Y3(I),ERR(I),I=1,N1)
          400 FORMAT(9F10.6)
0245          DO 800 I=1,N1
0246              Y2(I)=Y22(I)
0247              Y3(I)=Y1(I)
0248              Q1(I)=Q3(I)
0249              CP1(I)=1.+(2./F2)-QH(I)*QH(I)
0250              CP2(I)=1.-(2./F2)*((D/N1)*(I-1)-1.)
          $-Q(I)*Q(I)
0251      800 CONTINUE
0252      5 CONTINUE
0253          WRITE(6,500) D,(CP1(I),CP2(I),I=1,N1)
0254          500 FORMAT(/30X,'LENGTH OF B - C   =',F10.7//10X,
          $'PRESSURE DISTRIBUTION...'/2(F20.6))
C
C      ... PRINT OUTPUT ...
C
0255      1 FORMAT(I4,I4)
0256      2 FORMAT(/10X,'N   =',I4/10X,'F2   =',F10.5/10X,
          $'X0   =',F10.5/10X,'ALPHA =',F10.7)
0257          STOP
0258          END
C
C
0001      C
          FUNCTION SIMPS(U,V,N,F)
0002          REAL F(210)
0003          NN=N-1
0004          H=(V-U)/(6*FLOAT(NN))
0005          S11=0
0006          S22=0
0007          N2=NN/2
0008          DO 109 I=1,N2
0009              K=2*I
0010              IF(I.EQ.N2) GO TO 108
0011              J=2*I+1
0012              S11=S11+F(J)
0013          108 S22=S22+F(K)
0014          109 CONTINUE
0015          SIMPS=(2*S22+4*S11+F(1)+F(N))*H
0016          RETURN
0017          END

```

FUNCTION SIMPS

Program Symbol	Definition
H	stepsize, h .
N	number of increments, n .
S1	sum of all $f(i)$ for even i , S_1 .
S2	sum of all $f(i)$ for odd i , S_2 .
u	lower limit of integration
v	upper limit of integration.

Function SIMPS (Arguments: u,v,n,f)



Function of Lagrangian Interpolation

FORTRAN Implementation

List of Principal Variables

Program Symbol	Definition
FACTOR	The factor $c = \prod_{j=\min}^{\max} (\bar{x} - x_j)$
IDEG	Degree, d , of the interpolating polynomial.
MAX	Largest subscript for base points used to determine the interpolating polynomial, $\min + d$.
MIN	Smallest subscript for base points used to determine the interpolating polynomial, \min .
N	n , the number of paired values (x_i, y_i) .
TERM	t , a variable that assumes successively the values $L_i(\bar{x})y_i$, where $L_i(\bar{x}) = \prod_{\substack{j=\min \\ j \neq i}}^{\max} \frac{(\bar{x} - x_j)}{(x_i - x_j)}$
X	Vector of base points, x_i

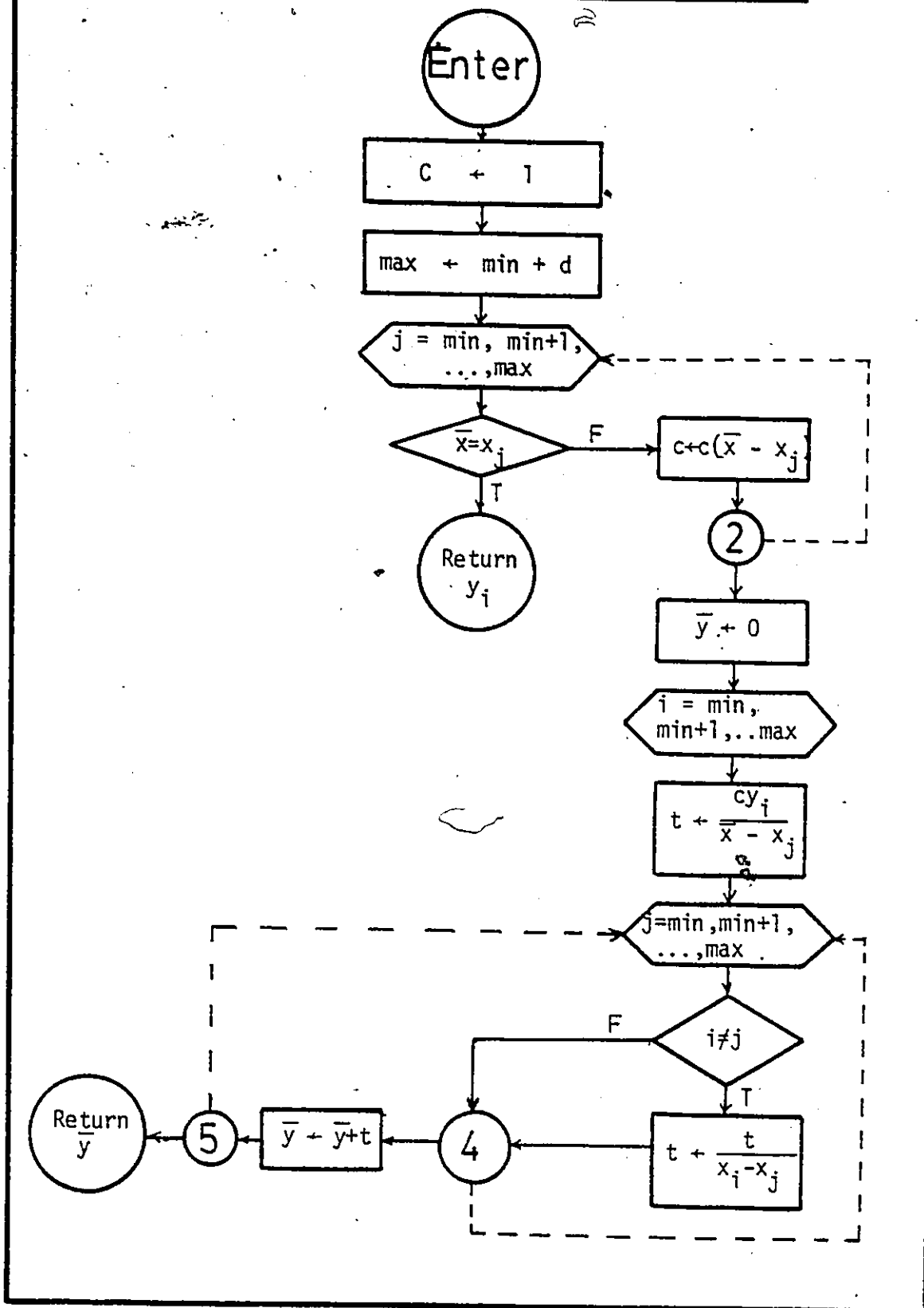
XARG

Interpolation argument, \bar{x} .

YEST

Interpolant value, $\overline{y(x)}$

Function FLAGR ($x, y, \bar{x}, d, \min, n$)



REFERENCES

- [1] Agrawal, K.M. Non-linear Theories in Two-Dimensional Fully and Partially-Cavitating Flow. Ph.D. Dissertation, University of Windsor, Windsor, Ontario, Canada, 1969.
- [2] Ames, W.F. Non-linear Partial Differential Equations in Engineering. Academic Press, New York, 1965.
- [3] Bakhmeteff, B.A. Hydraulics of Open Channels. McGraw-Hill, New York, 1932.
- [4] Bellman, R. Perturbation Techniques in Mathematics, Physics, and Engineering. Holt, Rinehart and Winston, Inc., New York, 1964.
- [5] Birkhoff, G. and Zarantonello, E.H. Jets, Wakes and Cavities. Academic Press, New York, 1957.
- [6] Blaisdell, F.W. Equation of the Free-Falling Nappe. Amer. Soc. Civil Engng., Proc., Vol. 80, No. 482, pp. 1-16, August 1954.
- [7] Brater, E.F. and King, H.W. Handbook of Hydraulics. 6th ed., McGraw-Hill, New York, 1976.
- [8] Carnahan, B., Luther, H.A. and Wilks, J.O. Applied Numerical Methods. John Wiley, New York, 1969.
- [9] Chow, V.T. Open Channel Hydraulics. McGraw-Hill, New York, 1959.
- [10] Chow, W.L. and Han, T. Inviscid Solution for the Problem of Free Overfall. J. Applied Mech., Vol. 46, No. 1, pp. 1-5, 1979.
- [11] Churchill, R.V. Complex Variables and Applications. McGraw-Hill, New York, 1960.
- [12] Clarke, N.S. On Two-Dimensional Inviscid Flow in a Waterfall. J. Fluid Mech., Vol. 22, Part 2, pp. 359-369, 1965.
- [13] Two-Dimensional Potential Flow Over a Sharp-Crested Weir. Hydraulics Research Station, Wallingford, Berkshire, England. Report No. INT 5], January 1966.

- [14] Two-Dimensional Flow Under Gravity in a Jet of Viscous Liquid. J. Fluid Mech., Vol. 31, Part 3, pp. 481-500, 1968.
- [15] Cole, J.D. Perturbation Methods in Applied Mathematics. Blaisdell Pub. Company, Toronto, 1968.
- [16] Creager, W.P., Justin, J.D. and Hinds, J. Engineering for Dams. Vol. 2, John Wiley, New York, 1917.
- [17] Creager, W.P. Engineering for Masonry Dams. 2nd ed., John Wiley, New York, 1929.
- [18] Cryer, C.W. A Bibliography of Free Boundary Problems. University of Wisconsin, Math. Res. Center, Tech. Summary Report, No. 1793, 1977.
- [19] Forsyth, A.R. Theory of Functions of a Complex Variable. Vol. 2, 3rd ed., Dover Pub., Inc., New York, 1965.
- [20] Geer, J. and Keller, J.B. Slender Streams. J. Fluid Mech., Vol. 93, Part 1, pp. 97-115, 1979.
- [21] Gilbarq, D. Jets and Cavities. Handbuch der Physik, Vol. 9, pp. 311-445, Springer-Verlag, Berlin, 1960.
- [22] Free Streamline Theory. Applied Mechanics Surveys, Spartan Books, Washington, D.C., 1966.
- [23] Ginzburg, I.P. Applied Fluid Dynamics. National Science Foundation, Washington, D.C., 1963.
- [24] Hauser, A.A. Complex Variables with Physical Applications. Simon and Schuster, New York, 1971.
- [25] Hay, N. and Markland, E. The Determination of the Discharge Over Weirs by the Electrolytic Tank. Institution of Civil Engng., London. Proc., Vol. 10, pp. 59-85, 1958.
- [26] Henderson, F.M. Open Channel Flow. MacMillan, New York, 1966.
- [27] Jaeger, C. Engineering Fluid Mechanics. Blackie and Son Ltd., London, 1956.
- [28] Keller, J.B. and Geer, J. Flows of Thin Streams with Free Boundaries. J. Fluid Mech., Vol. 59, Part 3, pp. 417-432, 1973.
- [29] Lamb, H. Hydrodynamics. 6th ed., Dover Pub., Inc., New York, 1945.

- [30] Larock, B.E. and Street, R.L. A Riemann-Hilbert Problem for Non-linear Fully Cavitating Flow. *J. Ship Research*, Vol. 9, No. 3, pp. 170-178, 1965.
- [31] _____ A Non-linear Theory for a Full Cavitating Hydrofoil in a Transverse Gravity Field. *J. Fluid Mech.*, Vol. 29, Part 2, pp. 317-336, 1967.
- [32] Larock, B.E. Gravity-Affected Flow from Planar Sluice Gates. *J. Hydraulics Division, Proc. Amer. Soc. Civil Engng.*, No. HY4, pp. 1211-1226, July 1969.
- [33] _____ Jets from Two-Dimensional Symmetric Nozzles of Arbitrary Shape. *J. Fluid Mech.*, Vol. 37, Part 3, pp. 479-489, 1969.
- [34] _____ A Theory of Free Outflow Beneath Radial Gates. *J. Fluid Mech.*, Vol. 41, Part 4, pp. 851-864, 1970.
- [35] Lim, T.H. Integral Equation Methods for the Numerical Solution of Free Surface Problems in Inviscid Flow. Ph.D. Dissertation, University of Windsor, Windsor, Ontario, Canada, 1978.
- [36] Mei, C.C. Steady Free Surface Flow Over Wavy Bed. *J. Engng. Mech. Division, Amer. Soc. Civil Engng.*, No. EM6, pp. 1393-1402, December 1969.
- [37] Mikhlin, S.G. Integral Equations. MacMillan, New York, 1964.
- [38] Milne-Thomson, L.M. Theoretical Hydrodynamics. 4th ed., MacMillan, New York, 1960.
- [39] Morris, H.M. Flow in Rough Conduits. *Amer. Soc. Civil Engineers, Trans.*, Vol. 120, pp. 373-398, 1955.
- [40] Muskhelishvili, N.I. Singular Integral Equations, Noordhoff-Groningen, 1953.
- [41] Nehari, Z. Conformal Mapping. McGraw-Hill, New York, 1952.
- [42] Rouse, H. Engineering Hydraulics. John Wiley, New York, 1950.
- [43] Rouse, H. and Ince, S. History of Hydraulics. Iowa Institute of Hydraulic Research, State University of Iowa, 1957.
- [44] Rouse, H. and Howe, J.W. Basic Mechanics of Fluids. 3rd ed., John Wiley, New York, 1958.
- [45] Scarborough, J.B. Numerical Mathematical Analysis, 6th ed., Johns Hopkins, Baltimore, 1966.

- [46] Smith, A.C. and Lim, T.H. The Steady Water Wave: A Numerical Solution Using the Riemann-Hilbert Method. Int. J. Engng. Sci., Vol. 18, pp. 139-152, 1980.
- [47] _____ A Riemann-Hilbert Solution for the Solitary Wave. To be published.
- [48] Song, S.C. A Quasi-linear and Linear for Non-Separated and Separated Two-Dimensional Irrotational Flow about Lifting Bodies. University of Minnesota, Min. SAF Lab. Tech. Paper B-43, 1963.
- [49] Southwell, R.V. Relaxation Methods in Theoretical Physics. Oxford University Press, London, 1946.
- [50] Southwell, R.V. and Vaisey, G. Relaxation Methods Applied to Engineering Problems. XII. Fluid Motions Characterized by "Free Stream-lines", Phil. Trans. Royal Soc., London, Series A, Vol. 240, pp. 117-161, 1946.
- [51] Streeter, V.L. Handbook of Fluid Dynamics. McGraw-Hill, New York, 1961.
- [52] Thomson, W. On Stationary Waves in Flowing Water. Part I - Part III, Phil. Mag. (5), Vol. 22, pp. 353-357, pp. 445-452, pp. 517-530, 1886. Part IV, Phil. Mag. (5), Vol. 23, pp. 52-58, 1887.
- [53] Tricomi, F.G. Integral Equations. Interscience, New York, 1957.
- [54] Van Dyke, M. Perturbation Methods in Fluid Mechanics. Annotated ed., The Parabolic Press, California, 1975.
- [55] Wehausen, J.V. and Laitone, E.V. Surface Waves. Handbuch der Physik, Vol. 9, pp. 446-814, Springer-Verlag, Berlin, 1960.
- [56] Michell, J. On the Theory of Free Streamlines. Phil. Trans. Roy. Soc. London, Ser. A 181, pp. 389-431, 1890.
- [57] Planck, M. Zur Theorie der Flüssigkeitsstrahlen. Wied. Ann (2) 21, pp. 499-509, 1884.

VITA AUCTORIS

- 1950 Born on the 14th of May in Alexandria, EGYPT.
- 1967 Matriculated from El-Abbasia High School,
Alexandria, EGYPT.
- 1972 Graduated with a B.Sc. degree in Electro-physics
Engineering, Faculty of Engineering, Alexandria
University, Alexandria, EGYPT.
- 1972 Appointed as an instructor in Mathematics and
Physics Department, Faculty of Engineering,
Alexandria University, Alexandria, EGYPT.
- 1974 Received a B.Sc. degree in Applied Mathematics,
Faculty of Science, Alexandria University,
Alexandria, EGYPT.
- 1975 Admitted to the program for Master of Art (Mathematics)
at York University, Downsview, Ontario, CANADA.
- 1976 Admitted to the program for Doctor of Philosophy
at University of Windsor, Windsor, Ontario, CANADA.
- 1978 Candidate for Doctor of Philosophy.